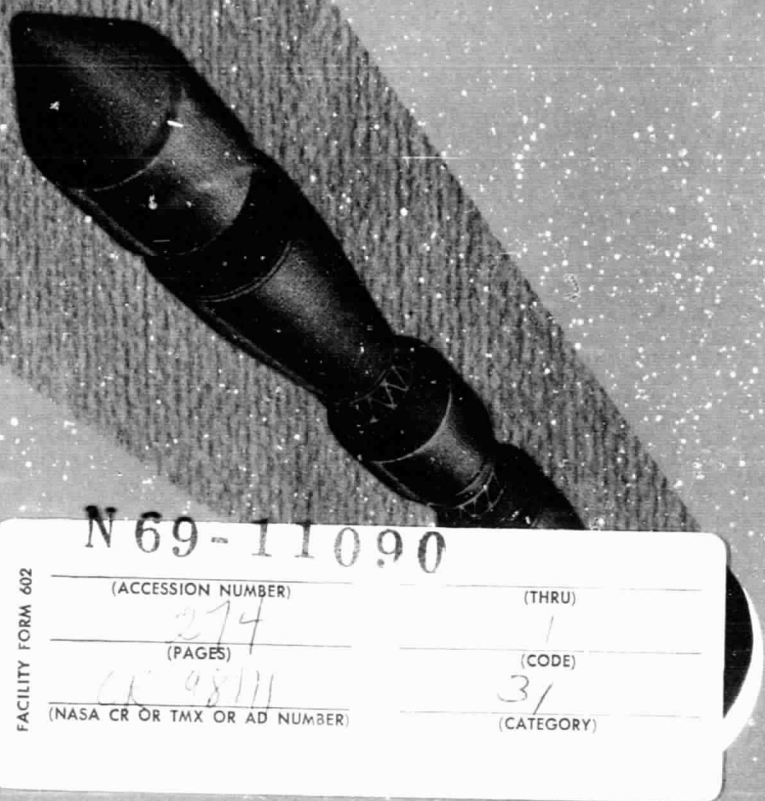


General Disclaimer

One or more of the Following Statements may affect this Document

- This document has been reproduced from the best copy furnished by the organizational source. It is being released in the interest of making available as much information as possible.
- This document may contain data, which exceeds the sheet parameters. It was furnished in this condition by the organizational source and is the best copy available.
- This document may contain tone-on-tone or color graphs, charts and/or pictures, which have been reproduced in black and white.
- This document is paginated as submitted by the original source.
- Portions of this document are not fully legible due to the historical nature of some of the material. However, it is the best reproduction available from the original submission.

FZA-434-1
31 Aug 1968
VOLUME 1



N 69-11090

FACILITY FORM 602	(ACCESSION NUMBER)	(THRU)
	274 (PAGES)	1 (CODE)
	CR 08111 (NASA CR OR TMX OR AD NUMBER)	31 (CATEGORY)

**PARAMETRIC STUDY of
OPTIMIZED LIQUID-HYDROGEN
THERMAL PROTECTION SYSTEMS
for NUCLEAR INTERPLANETARY
SPACECRAFT**



Results and Summary

GENERAL DYNAMICS
Fort Worth Division

GENERAL DYNAMICS
Fort Worth Division

FZA-434-1
31 August 1968

PARAMETRIC STUDY OF OPTIMIZED
LIQUID-HYDROGEN THERMAL PROTECTION SYSTEMS
FOR NUCLEAR INTERPLANETARY SPACECRAFT


Volume 1. Results and Summary

Prepared for the
George C. Marshall Space Flight Center
National Aeronautics and Space Administration
Huntsville, Alabama

under


Contract NAS8-21080

Prepared by:

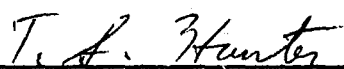


D. G. Barry
Sr. Aerothermodynamics Engineer

Approved by:



R. A. Stevens
Aerothermodynamics Group Engineer



T. S. Hunter
Aerothermodynamics Engineer

GENERAL DYNAMICS
Fort Worth Division

GENERAL DYNAMICS

Fort Worth Division

PRECEDING PAGE BLANK NOT FILMED.
F O R E W O R D

This document is Volume 1 of the final report on Contract NAS8-21080, "An Analytical Study of Storage of Liquid Hydrogen Propellant for Nuclear Interplanetary Spacecraft." The study was performed by the Fort Worth Division of General Dynamics Corporation for the George C. Marshall Space Flight Center of the National Aeronautics and Space Administration. The program was conducted under the technical direction of Mr. D. Price of the MSFC Propulsion and Vehicle Engineering Laboratory. His assistance in the performance of this study is gratefully acknowledged.

The final report comprises three volumes:

Volume 1. Results and Summary

Volume 2. Technical Details

Volume 3. Numerical Data

Volume 1 contains a complete presentation and discussion of the results, together with a summary of the important findings of the study. Volume 2 contains a description of the methods of analysis and the computer programs used in the study. Volume 3 contains a tabulation of the numerical data, including both the thermal protection system optimization results and the mass-buildup data.

The authors would like to acknowledge the contributions of K. A. Pinter and M. K. Fox in the mission analysis tasks and of L. E. Heyduck, Jr., in the structural and meteoroid protection analyses.

GENERAL DYNAMICS

Fort Worth Division

T A B L E O F C O N T E N T S

	<u>Page</u>
	PRECEDING PAGE BLANK NOT FILMED.
FOREWORD	iii
LIST OF FIGURES	vii
LIST OF TABLES	xix
1. INTRODUCTION	1
1.1 Study Objectives	2
1.2 Approach to the Study	2
1.3 Definitions	3
2. SUMMARY	5
3. MISSION AND VEHICLE DESCRIPTION	13
3.1 Mission Definition	14
3.2 Vehicle Configuration	18
3.3 Propellant Storage Modes	27
4. PARAMETRIC STUDY RESULTS AND DISCUSSION	29
4.1 Mars Vehicle Initial Mass	31
4.2 Earth Departure Stage Propellant Storage Penalty	66
4.3 Mars Braking Stage Propellant Storage Penalty	84
4.4 Mars Departure Stage Propellant Storage Penalty	120
4.5 Off-Optimum Data	157
5. SYSTEM PERFORMANCE CRITERIA	167
5.1 Vent System	169
5.2 Partial-Recondensation System	183
5.3 Combination System	203
5.4 Solar Shield Systems	213

GENERAL DYNAMICS
Fort Worth Division

T A B L E O F C O N T E N T S (Cont'd)

	<u>Page</u>
6. SUMMARY OF RESULTS AND CONCLUSIONS	227
6.1 Thermal Protection Findings	227
6.2 Mission Parameter Implications	237
6.3 Structural Implications	249
7. RECOMMENDATIONS	251
REFERENCES	253

GENERAL DYNAMICS
Fort Worth Division

L I S T O F F I G U R E S

<u>Figure</u>	<u>Title</u>	<u>Page</u>
3.1-1	Heliocentric Mission Geometry	16
3.1-2	Variation of Solar Distance with Flight Time	17
3.2-1	Nuclear Propulsion Module	23
3.2-2	Conjunction-Class Mars Vehicle	24
3.2-3	Mars Transfer Solar Shield-Vehicle Configuration	25
3.2-4	Mars Orbit Solar Shield-Vehicle Configuration	25
3.2-5	Variation of MEM Mass with Altitude	26
4.1-1	Effect of Ascent Shell Mass on IMIEO	44
4.1-2	IMIEO of the Unshielded Mars Vehicle vs Staytime: $h_{\text{Mars}} = 216 \text{ n.mi}$	45
4.1-3	IMIEO of the Unshielded Mars Vehicle vs Staytime: $h_{\text{Mars}} = 3238 \text{ n.mi}$	46
4.1-4	IMIEO of the Unshielded Mars Vehicle vs Staytime: $h_{\text{Mars}} = 9203 \text{ n.mi}$	47
4.1-5	IMIEO of the Shielded Mars Vehicle vs Staytime: $h_{\text{Mars}} = 216 \text{ n.mi}$	48
4.1-6	IMIEO of the Shielded Mars Vehicle vs Staytime: $h_{\text{Mars}} = 3238 \text{ n.mi}$	49
4.1-7	IMIEO of the Shielded Mars Vehicle vs Staytime: $h_{\text{Mars}} = 9203 \text{ n.mi}$	50
4.1-8	IMIEO Sensitivity to Insulation Thermal Performance: Vent Mode, Unshielded	51

GENERAL DYNAMICS
Fort Worth Division

L I S T O F F I G U R E S (Cont'd)

<u>Figure</u>	<u>Title</u>	<u>Page</u>
4.1-9	IMIEO Sensitivity to Insulation Thermal Performance: Partial Recondensation Mode, Unshielded	52
4.1-10	IMIEO Sensitivity to Insulation Thermal Performance: Nonvent Mode, Shielded	53
4.1-11	IMIEO Sensitivity to Insulation Thermal Performance: Partial Recondensation Mode, Shielded	54
4.1-12	Ratio of Penetration Heat Transfer to Total Propellant Heat Transfer	55
4.1-13	Effect of Altitude on Zero-Mass-Fraction IMIEO and Stage Masses	56
4.1-14	Effect of Altitude on Mars Vehicle IMIEO	57
4.1-15	Effect of Altitude on Mars Vehicle Propellant Storage Penalty	58
4.1-16	Effect of Propellant Storage Mode on IMIEO: Unshielded	59
4.1-17	Effect of Propellant Storage Mode on IMIEO: Shielded	60
4.1-18	Effect of Propellant Storage Mode on Mars Vehicle Propellant Storage Penalty	61
4.1-19	Mars Vehicle IMIEO vs Altitude: Vent and Partial Recondensation Modes	62
4.1-20	IMIEO Comparison of the Unshielded and Shielded Mars Vehicles: Vent Mode	63
4.1-21	IMIEO Comparison of the Unshielded and Shielded Mars Vehicles: Partial Recondensation Mode	64

GENERAL DYNAMICS
Fort Worth Division

L I S T O F F I G U R E S (Cont'd)

<u>Figure</u>	<u>Title</u>	<u>Page</u>
4.1-22	Effect of Solar Shield on Penetration Heat Transfer	65
4.2-1	Effect of Zero-Mass-Fraction Stage on Mars Vehicle IMIEO	72
4.2-2	Propellant Storage Penalty vs Staytime: Earth Departure Stage, $h_{\text{Mars}} = 216$ n.mi	73
4.2-3	Propellant Storage Penalty vs Staytime: Earth Departure Stage, $h_{\text{Mars}} = 3238$ n.mi	74
4.2-4	Propellant Storage Penalty vs Staytime: Earth Departure Stage, $h_{\text{Mars}} = 9203$ n.mi	75
4.2-5	Effect of Insulation Thermal Performance on Propellant Storage Penalty: Earth Departure Stage	76
4.2-6	Propellant Storage Penalty vs Altitude: Earth Departure Stage, $\theta/\theta_{\text{max}} = 1/3$	77
4.2-7	Propellant Storage Penalty vs Altitude: Earth Departure Stage, $\theta/\theta_{\text{max}} = 1$	78
4.2-8	Effect of Optimum Propellant Storage System on IMIEO vs Altitude: Earth Departure Stage	79
4.2-9	Effect of Propellant Storage Mode on Propellant Storage Penalty: Earth Departure Stage	80
4.2-10	Optimum Propellant Storage Component Mass Fractions: Earth Departure Stage, Nonvent Mode	81
4.2-11	Optimum Propellant Storage Component Mass Fractions: Earth Departure Stage, Vent Mode	82
4.2-12	Optimum Propellant Storage Component Mass Fractions: Earth Departure Stage, Partial Recondensation Mode	83

GENERAL DYNAMICS
Fort Worth Division

L I S T O F F I G U R E S (Cont'd)

<u>Figure</u>	<u>Title</u>	<u>Page</u>
4.3-1	Propellant Storage Penalty vs Staytime: Unshielded Mars Braking Stage, $h_{\text{Mars}} = 216 \text{ n.mi}$	94
4.3-2	Propellant Storage Penalty vs Staytime: Shielded Mars Braking Stage, $h_{\text{Mars}} = 216 \text{ n.mi}$	95
4.3-3	Propellant Storage Penalty vs Staytime: Unshielded Mars Braking Stage, $h_{\text{Mars}} = 3238 \text{ n.mi}$	96
4.3-4	Propellant Storage Penalty vs Staytime: Unshielded Mars Braking Stage, $h_{\text{Mars}} = 9203 \text{ n.mi}$	97
4.3-5	Propellant Storage Penalty vs Staytime: Shielded Mars Braking Stage, $h_{\text{Mars}} = 3238 \text{ n.mi}$	98
4.3-6	Propellant Storage Penalty vs Staytime: Shielded Mars Braking Stage, $h_{\text{Mars}} = 9203 \text{ n.mi}$	99
4.3-7	Comparison of Propellant Storage Penalties for Various Storage Modes: Unshielded Mars Braking Stage	100
4.3-8	Effect of Insulation Thermal Performance on Propellant Storage Penalty: Unshielded Mars Braking Stage	101
4.3-9	Effect of Insulation Thermal Performance on Propellant Storage Penalty: Shielded Mars Braking Stage	102
4.3-10	Propellant Storage Penalty vs Altitude: Shielded Mars Braking Stage	103
4.3-11	Effect of Optimum Propellant Storage System on IMIEO vs Altitude: Shielded Mars Braking Stage	104

GENERAL DYNAMICS
Fort Worth Division

L I S T O F F I G U R E S (Cont'd)

<u>Figure</u>	<u>Title</u>	<u>Page</u>
4.3-12	Propellant Storage Penalty vs Altitude: Unshielded Mars Braking Stage	105
4.3-13	Effect of Optimum Propellant Storage System on IMIEO vs Altitude: Unshielded Mars Braking Stage	106
4.3-14	Effect of Propellant Storage Mode on Pro- pellant Storage Penalty: Unshielded Mars Braking Stage	107
4.3-15	Effect of Propellant Storage Mode on Pro- pellant Storage Penalty: Shielded Mars Braking Stage	108
4.3-16	Optimum Propellant Storage Component Mass Fractions: Unshielded Mars Braking Stage, Nonvent Mode	109
4.3-17	Optimum Propellant Storage Component Mass Fractions: Unshielded Mars Braking Stage, Vent Mode	110
4.3-18	Optimum Propellant Storage Component Mass Fractions: Unshielded Mars Braking Stage, Partial Recondensation Mode	111
4.3-19	Optimum Propellant Storage Component Mass Fractions: Shielded Mars Braking Stage, Nonvent Mode	112
4.3-20	Comparison of Propellant Storage Penalties for the Combination and Nonvent Storage Modes: Unshielded Mars Braking Stage	113
4.3-21	Effect of Tanking on Propellant Storage Penalty: Unshielded Mars Braking Stage	114
4.3-22	Thermal Severity of the Mars Mission	115

GENERAL DYNAMICS

Fort Worth Division

L I S T O F F I G U R E S (Cont'd)

<u>Figure</u>	<u>Title</u>	<u>Page</u>
4.3-23	Effect of Solar Shield on Propellant Storage Penalty: Mars Braking Stage, Nonvent Mode	116
4.3-24	Effect of Solar Shield on Propellant Heat Transfer: Mars Braking Stage	117
4.3-25	Effect of Solar Shield on Propellant Storage Penalty: Mars Braking Stage, Vent and Partial Recondensation Modes	118
4.3-26	Difference in IMIEO between the Shielded and Unshielded Mars Braking Stages	119
4.4-1	Effect of Solar Shield on Propellant Heat Transfer: Mars Departure Stage	129
4.4-2	Propellant Storage Penalty vs Staytime: Unshielded Mars Departure Stage, $h_{\text{Mars}} = 3238$ n.mi	130
4.4-3	Propellant Storage Penalty vs Staytime: Shielded Mars Departure Stage, $h_{\text{Mars}} = 3238$ n.mi	131
4.4-4	Propellant Storage Penalty vs Staytime: Unshielded Mars Departure Stage, $h_{\text{Mars}} = 216$ n.mi	132
4.4-5	Propellant Storage Penalty vs Staytime: Shielded Mars Departure Stage, $h_{\text{Mars}} = 216$ n.mi	133
4.4-6	Propellant Storage Penalty vs Staytime: Unshielded Mars Departure Stage, $h_{\text{Mars}} = 9203$ n.mi	134
4.4-7	Propellant Storage Penalty vs Staytime: Shielded Mars Departure Stage, $h_{\text{Mars}} = 9203$ n.mi	135

GENERAL DYNAMICS

Fort Worth Division

L I S T O F F I G U R E S (Cont'd)

<u>Figure</u>	<u>Title</u>	<u>Page</u>
4.4-8	Comparison of Propellant Storage Penalties for the Vent and Vent-Tanking Modes	136
4.4-9	Comparison of Propellant Storage Penalties for the Combination and Nonvent Modes	137
4.4-10	Effect of Insulation Thermal Performance on Propellant Storage Penalty: Unshielded Mars Departure Stage	138
4.4-11	Effect of Insulation Thermal Performance on Propellant Storage Penalty: Shielded Mars Departure Stage	139
4.4-12	Effect of ΔV Variation with Altitude on Mars Departure Stage Propellant Storage Penalty	140
4.4-13	Propellant Storage Penalty vs Altitude: Unshielded Mars Departure Stage	141
4.4-14	Propellant Storage Penalty vs Altitude: Shielded Mars Departure Stage	142
4.4-15	Effect of Optimum Propellant Storage System on IMIEO vs Altitude: Unshielded Mars Departure Stage	143
4.4-16	Effect of Optimum Propellant Storage System on IMIEO vs Altitude: Shielded Mars Departure Stage	144
4.4-17	Effect of Propellant Storage Mode on Propellant Storage Penalty: Unshielded Mars Departure Stage	145
4.4-18	Effect of Propellant Storage Mode on Propellant Storage Penalty: Shielded Mars Departure Stage	146

GENERAL DYNAMICS
Fort Worth Division

L I S T O F F I G U R E S (Cont'd)

<u>Figure</u>	<u>Title</u>	<u>Page</u>
4.4-19	Optimum Propellant Storage Component Mass Fractions: Shielded Mars Departure Stage, Nonvent Mode	147
4.4-20	Optimum Propellant Storage Component Mass Fractions: Shielded Mars Departure Stage, Vent Mode	148
4.4-21	Optimum Propellant Storage Component Mass Fractions: Shielded Mars Departure Stage, Partial Recondensation Mode	149
4.4-22	Optimum Propellant Storage Component Mass Fractions: Unshielded Mars Departure Stage, Vent Mode	150
4.4-23	Effect of Tanking on Propellant Storage Penalty: Shielded Mars Departure Stage, Partial Recondensation Mode	151
4.4-24	Effect of Tanking on Propellant Storage Penalty: Shielded Mars Departure Stage, Vent Mode	152
4.4-25	Effect of Solar Shield on Penetration Heat Transfer Rate During Mars Orbit	153
4.4-26	Effect of Solar Shield on Propellant Storage Penalty: Mars Departure Stage, Vent Mode	154
4.4-27	Effect of Solar Shield on Propellant Storage Penalty: Mars Departure Stage, Partial Recondensation Mode	155
4.4-28	Relative Effect of Mars Transfer and Mars Orbit Solar Shields on Propellant Storage Penalty	156
4.5-1	Off-Optimum Propellant Storage System Mass Data: Earth Departure Stage	160

GENERAL DYNAMICS

Fort Worth Division

L I S T O F F I G U R E S (Cont'd)

<u>Figure</u>	<u>Title</u>	<u>Page</u>
4.5-2	Off-Optimum Propellant Storage System Mass Data: Mars Braking Stage	161
4.5-3	Comparison of Off-Optimum Mass Data for the Nonvent and Vent Modes: Mars Departure Stage	162
4.5-4	Location of the Optimum Insulation Thickness	163
4.5-5	Comparison of Off-Optimum Mass Data for the Nonvent and Vent Modes: Earth Departure Stage	164
4.5-6	Off-Optimum Mass Data for a Low-Pressure Condition	165
5.1-1	Vent System Allowable Mass: Earth Departure Stage	175
5.1-2	Vent System Boiloff Rates	176
5.1-3	Vent System Allowable Mass: Unshielded Mars Braking Stage	177
5.1-4	Vent System Allowable Mass: Shielded Mars Braking Stage	178
5.1-5	Vent System Allowable Mass With and Without Tanking: Mars Braking Stage	179
5.1-6	Effect of Tanking on Earth Orbit Staytime	180
5.1-7	Vent System Allowable Mass: Shielded Mars Departure Stage	181
5.1-8	Vent System Allowable Mass With and Without Tanking: Mars Departure Stage	182
5.2-1	Partial Recondensation System Allowable Mass: Earth Departure Stage	190

GENERAL DYNAMICS
Fort Worth Division

L I S T O F F I G U R E S (Cont'd)

<u>Figure</u>	<u>Title</u>	<u>Page</u>
5.2-2	Partial Recondensation System Allowable Specific Mass: Earth Departure Stage	191
5.2-3	Partial Recondensation System Allowable Mass: Unshielded Mars Braking Stage	192
5.2-4	Partial Recondensation System Allowable Specific Mass: Unshielded Mars Braking Stage	193
5.2-5	Effect of Mars Orbit Altitude on Partial Recondensation System Allowable Mass: Mars Braking Stage	194
5.2-6	Partial Recondensation System Allowable Mass: Shielded Mars Braking Stage	195
5.2-7	Partial Recondensation System Allowable Specific Mass: Shielded Mars Braking Stage	196
5.2-8	Effect of Tanking on Allowable Mass of the Partial Recondensation System: Mars Braking Stage	197
5.2-9	Partial Recondensation System Allowable Mass: Shielded Mars Departure Stage	198
5.2-10	Partial Recondensation System Allowable Specific Mass: Shielded Mars Departure Stage	199
5.2-11	Partial Recondensation System Allowable Mass Relative to the Vent System: Shielded Mars Departure Stage	200
5.2-12	Partial Recondensation System Allowable Mass Relative to the Vent System: Unshielded Mars Departure Stage	201
5.2-13	Effect of Tanking on Allowable Mass of the Partial Recondensation System: Mars Departure Stage	202

GENERAL DYNAMICS

Fort Worth Division

L I S T O F F I G U R E S (Cont'd)

<u>Figure</u>	<u>Title</u>	<u>Page</u>
5.3-1	IMIEO and System Allowable Mass for the Combination Mode: Mars Braking Stage, $k\rho = 1.5 \times 10^{-3} \frac{\text{Btu lb}_m}{\text{hr-ft}^4\text{-OR}}$	206
5.3-2	IMIEO and System Allowable Mass for the Combination Mode: Mars Braking Stage $k\rho = 7.5 \times 10^{-3} \frac{\text{Btu lb}_m}{\text{hr-ft}^4\text{-OR}}$	207
5.3-3	Range of Earth Orbit Staytime for the Combination Mode	208
5.3-4	Effect of Partial Recondensation on the Range of Earth Orbit Staytime for the Combination Mode	209
5.3-5	IMIEO and System Allowable Mass for the Combination Mode: Mars Departure Stage $k\rho = 1.5 \times 10^{-3} \frac{\text{Btu lb}_m}{\text{hr-ft}^4\text{-OR}}$	210
5.3-6	IMIEO and System Allowable Mass for the Combination Mode: Mars Departure Stage $k\rho = 7.5 \times 10^{-5} \frac{\text{Btu lb}_m}{\text{hr-ft}^4\text{-OR}}$	211
5.3-7	IMIEO and System Allowable Mass for the Combination Mode: Mars Departure Stage $k\rho = 5.0 \times 10^{-6} \frac{\text{Btu lb}_m}{\text{hr-ft}^4\text{-OR}}$	212
5.4-1	Mars Transfer Solar Shield Allowable Mass vs Altitude: Vent Mode	218
5.4-2	Mars Transfer Solar Shield Allowable Mass vs Altitude: Partial Recondensation Mode	219

GENERAL DYNAMICS
Fort Worth Division

L I S T O F F I G U R E S (Cont'd)

<u>Figure</u>	<u>Title</u>	<u>Page</u>
5.4-3	Mars Transfer Solar Shield Allowable Mass vs Staytime: Vent Mode	220
5.4-4	Mars Transfer Solar Shield Allowable Mass vs Staytime: Partial Recondensation Mode	221
5.4-5	Mars Transfer Solar Shield Allowable Mass vs Staytime: Nonvent Mode	222
5.4-6	Mars Orbit Solar Shield Allowable Mass vs Altitude: Vent Mode	223
5.4-7	Mars Orbit Solar Shield Allowable Mass vs Altitude: Partial Recondensation Mode	224
5.4-8	Effect of Earth Orbit Staytime on Mars Orbit Solar Shield Allowable Mass: Vent Mode	225
6.2-1	ΔV Requirements for Mars Braking and Departure vs Altitude	245
6.2-2	Mars Orbit Orientation History: $h_{\text{Mars}} = 3238$ n.mi	246
6.2-3	Effect of Mission Energy Requirements on IMIEO	247
6.2-4	Approximate Range of IMIEO with a Four-Module Earth Departure Stage	248

GENERAL DYNAMICS
Fort Worth Division

L I S T O F T A B L E S

<u>Table</u>	<u>Title</u>	<u>Page</u>
3.1-1	Mission Summary	15
4.1-1	IMIEO Difference Between the Shielded and Unshielded Vehicles: Vent Mode	42
4.1-2	IMIEO Difference Between the Shielded and Unshielded Vehicles: Partial Recondensation Mode	42
5.2-1	Heat Loads: Partial Recondensation Mode	185

GENERAL DYNAMICS
Fort Worth Division

S E C T I O N 1

I N T R O D U C T I O N

Successful long-term storage of liquid-hydrogen propellant, which is a requirement for manned planetary exploration, is completely dependent upon a highly effective thermal protection system. For the thermal designer to accomplish this goal, he must have the necessary data to make decisions regarding the insulation thermal performance requirements, appropriate propellant storage modes, and performance requirements of the associated thermal management system. Since solution of the thermal problem will be essential to the successful completion of the mission, it is necessary that thermal considerations enter into the mission planning and vehicle design activities at the earliest possible moment. Such consideration in the early planning phases may lessen the thermal problem and reduce the complexity of the thermal design task.

The study reported herein was conceived to provide guidelines and quantitative data concerning liquid-hydrogen thermal protection systems for both mission planning and thermal design with respect to a conjunction-class, manned, Mars stop-over mission. By quantitatively evaluating the influence of the various factors that affect the thermal protection system, the impact of these factors can be properly assessed. The intent is to provide useful data and to point out significant trends from the thermal protection standpoint in order that a successful total system design may be accomplished.

This volume is organized in such a manner that it may be easily used by persons desiring various degrees of detail concerning the study. Those interested in a general summary are referred to Sections 2, 6, and 7. Greater detail may be obtained by study of the mission and the vehicle descriptions in Section 3 and the Mars vehicle initial mass data in Subsection 4.1. The remainder of Section 4 treats the results pertaining to each stage of the vehicle separately; the section is concluded with a discussion of off-optimum performance. Performance criteria for the thermal management systems and the solar shield systems are discussed in Section 5.

GENERAL DYNAMICS
Fort Worth Division

1.1 STUDY OBJECTIVES

The primary purpose of this study is the assessment of the problems resulting from extended Earth orbital storage of liquid-hydrogen propellant. Secondary objectives are to investigate: (1) the sensitivity of the vehicle mass to insulation thermal performance, (2) the effect of Mars parking orbit altitude on thermally optimized vehicles, and (3) the reduction of penetration heat transfer by use of solar shields.

The scope of the study covers the investigation of the propellant storage modes listed below:

1. Nonvent storage with stratification reduction
2. Vent storage
3. Vent storage with partial recondensation (partial-recondensation mode)
4. Combination vent-nonvent and partial recondensation-nonvent storage.

In addition, the effect of orbital tanking on the vehicle mass will be determined.

1.2 APPROACH TO THE STUDY

A wide-ranging parametric study of optimized propellant storage systems was defined to achieve the objectives outlined above. Basic parameters were the Earth orbit staytime, the insulation performance (thermal conductivity-density product), and the Mars orbit altitude. In addition, several propellant storage modes were investigated and the interplanetary stages were studied both with and without solar shields. The optimum storage system is determined on the basis of minimum vehicle Initial Mass In Earth Orbit. Payload is fixed in each case, but the variation in Mars Excursion Module Mass with Mars orbit altitude is accounted for. Because of the large number of parameters, only one mission could be studied. The 1984 conjunction-class, manned, Mars stopover mission was selected, which is characterized by low energy requirements and a long mission duration. The Mars vehicle configuration was developed from the modular nuclear vehicle concept.

GENERAL DYNAMICS

Fort Worth Division

The study was divided into two phases. In the initial phase, simplified optimization techniques were used to investigate a wide range of parameters and storage modes in order to determine the importance of these parameters and modes. The final phase was accomplished utilizing a computerized and more complex optimization procedure involving an iterative scheme of vehicle mass buildup and propellant storage system optimization.

In investigating the effect of propellant storage mode, the mass of the particular thermal management system was not included in the analysis. This approach was adopted for two reasons. First, parametric mass data for the various systems are not readily available. Second, these systems are in development, and the limited mass data presently available are subject to change. The approach taken here allows performance criteria for the various systems to be generated by comparison of the results for different storage modes. This same approach was taken with respect to solar shield systems.

1.3 DEFINITIONS

Certain phrases and terms require definition to orient the reader properly. These definitions are provided below.

Propellant storage system - A set of subsystems that contain the propellant, offer protection against the natural environment, or reduce the propellant heat transfer. The set comprises the tank and associated structure, whose mass is proportional to the tank mass; the insulation; the pressurant; the boiloff; and the meteoroid protection.

Thermal management system - A system that acts to alleviate the problems caused by heat transfer to the propellant. These systems include vent, partial recondensation, and stratification reduction systems.

Thermal protection system - A system that comprises the propellant storage system and the thermal management system.

IMIEO - The initial mass in Earth orbit of the Mars vehicle.

GENERAL DYNAMICS

Fort Worth Division

Propellant-storage-system effective mass fraction - The ratio of the stage propellant-storage-system effective mass to the total propellant loading. The term "effective" denotes that the mass of each propellant-storage-system component that is jettisoned (propellant boiloff and meteoroid protection) has been multiplied by the appropriate weighting factor to adjust the masses of these components to the same basis as the mass of nonjettisoned components (tank, insulation, and pressurant). Jettisoned items are not carried through the total number of velocity changes and thus affect the IMIEO differently from nonjettisoned items. For example, insulation on the Mars Departure Stage is carried through three propulsive maneuvers (Earth departure, Mars braking, and Mars departure) and thus a certain portion of the propellant loading is directly attributable to accelerating the insulation through the velocity changes. On the other hand, boiloff from the Mars Departure Stage that occurs during Earth orbit is not carried through any of the above propulsive maneuvers. Thus, no portion of the propellant loading can be directly attributable to accelerating this boiloff. However, additional propellant is required to accelerate those added portions of the tank and insulation masses, etc., that are related to the boiloff mass. For a mathematical definition of this term, the reader is referred to Section 6 of Volume 2.

Zero-mass-fraction vehicle - A vehicle with a propellant storage system mass fraction of zero for at least one of the vehicle stages.

Propellant storage penalty - The additional mass required at the start of the mission that is directly attributable to the propellant storage system. This penalty includes the additional stage propellant requirements due to the mass of the propellant storage system. Also included are the additional masses of propellant, tank, insulation, etc., required on all lower stages. The penalty is generally expressed as a percentage of the zero-mass-fraction vehicle IMIEO.

Propellant initial condition - In all cases, the initial propellant thermodynamic state is triple-point saturated liquid.

Vent pressure - The vent pressure for the vent and partial recondensation modes is 14.7 psia.

GENERAL DYNAMICS

Fort Worth Division

S E C T I O N 2

S U M M A R Y

Space storage of liquid-hydrogen propellant for time periods associated with manned, planetary, exploration missions requires highly effective thermal protection systems. This report presents the results of a parametric study of optimized liquid-hydrogen propellant storage systems for a conjunction-class, manned, Mars mission. The factors considered are (1) the basic parameters of Earth orbit staytime, insulation thermal performance, and Mars orbit altitude; (2) the mode of propellant storage; (3) the use of solar shields during Mars transfer and Mars orbit; and (4) orbital tanking. Propellant storage modes considered in this study are:

1. Nonvent (with stratification reduction)
2. Vent
3. Partial recondensation
4. Combination vent-nonvent and partial recondensation-nonvent

The objective of the study is to determine the effects of the above-mentioned variables upon the stage thermal protection systems and the vehicle Initial Mass In Earth Orbit (IMIEO).

The mission is a 1984 conjunction-class, manned, Mars stopover mission with a total duration beyond Earth orbit of 930 days, of which 510 days are spent in Mars orbit. Earth orbit staytime, one of the basic study parameters, ranges from 90 to 270 days. The Mars vehicle is built up from seven nuclear propulsion and propellant modules and the mission payload modules. This configuration is constant, although the module sizes are variable; the propellant tank length is a function of the variables of the study. For the multi-tank Earth Departure and Mars Braking stages, all tanks of a particular stage are considered to be identical in all aspects. In all cases, the initial propellant thermodynamic state is triple-point saturated liquid. The vent pressure for the vent and partial recondensation modes is 14.7 psia.

GENERAL DYNAMICS

Fort Worth Division

Optimum propellant storage systems were determined using the Thermal Protection System Optimization computer program. This program combines a rocket-vehicle mass buildup-sensitivity analysis with a propellant-storage-system optimization analysis to define the propellant storage system for one stage of the vehicle that yields the minimum vehicle IMIEO. The remaining two stages of the vehicle are defined in terms of nominal mass fractions. The propellant loadings and subsystem masses for these stages will vary, but the mass fractions remain constant. This approach was used to generate the bulk of the data presented in this report. Additional IMIEO data were obtained by using the optimum mass fractions for all stages simultaneously in conjunction with a rocket vehicle mass-buildup program. The vehicle defined in this manner is loosely referred to as an "optimized" vehicle.

The IMIEO data do not include the mass of the thermal management system required for the particular storage mode. For example, the IMIEO values for the partial-recondensation mode do not account for the mass of the system necessary to reliquify a portion of the gross propellant boiloff. With this approach, the data for the various modes can be compared to determine relative performance criteria for the thermal management systems.

Each of the study variables has been found to have a significant effect on the stage propellant storage systems and on the vehicle IMIEO. The thermal performance of the insulation system is the key item, however, since it has a strong effect in itself and determines to a great extent the influence of the other study variables. For example, with high-performance insulation, the propellant heat transfer in many cases is less than that required to raise the propellant pressure from the initial triple-point pressure of 1.02 psia (0.70 N/cm²) to the vent pressure of 14.7 psia (10.1 N/cm²). Under these conditions, no propellant boiloff occurs and the vent and partial-recondensation storage modes yield the same results as the nonvent mode. With respect to the "optimized" vehicle, the insulation thermal performance has a substantial impact on the vehicle IMIEO. Percentage increases in IMIEO over the range of performance reach a maximum of 49%. Of special significance is the fact that for the case mentioned above, the bulk of the increase, 42%, occurs in the range of $k\rho$ values above the intermediate value of 7.5×10^{-5} Btu lb_m/hr-ft⁴-°R (2.08×10^{-3} W kg/m⁴-°K). This trend was noted throughout the study; the benefits associated with improving

GENERAL DYNAMICS

Fort Worth Division

the insulation performance beyond the intermediate $k\rho$ value are limited.

In many of the cases with low-performance insulation, the vehicle IMIEO is of such magnitude that it exceeds the maximum associated with the four-module Earth Departure Stage configuration assumed in this study (the maximum is determined on the basis of a 330,000-lb_m (149,700 kg) payload capability for an uprated Saturn V launch vehicle). Therefore, at least one additional module would be required in the first stage to meet the propellant requirements.

The effect of Earth orbit staytime on the vehicle IMIEO is strongly dependent upon the insulation thermal performance. With low-performance insulation, IMIEO increases as much as 26% as the staytime increases from 90 to 270 days. This increase is reduced to less than 6% at the intermediate $k\rho$ value. In terms of the vehicle propellant storage penalty, an extended staytime in Earth orbit can result in significant increases in the penalty. With low-performance insulation, the penalty to IMIEO in one case increases by 444,500 lb_m (201,600 kg) as the staytime increases from 90 to 270 days. Again, solely by improving the insulation performance to the intermediate $k\rho$ value, the increase in penalty is reduced to 108,600 lb_m (49,250 kg).

Earth orbit staytime affects the Earth Departure Stage to a greater extent than it does the interplanetary stages because the mission of this stage is restricted to Earth orbit. However, data for the shielded Mars Braking Stage are similar to that of the first stage since its heating history is dominated by the Earth orbit mission phase. The Mars Departure Stage, on the other hand, shows little effect of staytime for the range of staytime investigated, even in the shielded case. The heating history of this stage is dominated by the 510-day period spent in Mars orbit.

Two methods of mitigating the effects of extended Earth orbital storage were investigated during this study: orbital tanking and the combination vent-nonvent (or partial recondensation-nonvent) storage mode. Preliminary analyses indicated that tanking is beneficial only with low-performance insulation. Consequently, optimized propellant storage system data were obtained only at the high $k\rho$ value. For the unshielded Mars Braking Stage, tanking results in propellant storage penalty reductions of 4.4% and 2.6% of the zero-mass-fraction

GENERAL DYNAMICS

Fort Worth Division

IMIEO for the vent and partial-recondensation modes, respectively (180-day staytime). Maximum staytimes, which correspond to tanking of the total propellant loading, are of the order of 1000 days. In the shielded Mars Departure Stage case, the penalty reduction is less than 1% of the zero-mass-fraction IMIEO in all cases (staytimes less than 90 days). However, tanking increases the maximum staytime beyond 500 days. Tanking is not feasible for the shielded Mars Braking Stage or the unshielded Mars Departure Stage.

The combination mode yields a greater reduction in the storage penalty than does orbital tanking, but the increase in Earth orbit staytime is much less. In this mode, the expansion volume required by nonvent operation during mission phases beyond Earth orbit is used to store excess propellant. This excess propellant is then boiled off during Earth orbit. For the unshielded Mars Braking Stage with low-performance insulation, the propellant storage penalty is reduced 23% (110,300 lb_m or 50,000 kg) with no extension of Earth orbit staytime. In the shielded Mars Departure Stage case, the penalty is reduced 22% (40,300 lb_m or 18,300 kg) at the high $k\rho$ value. Only a few additional days staytime are gained. As in the case of tanking, the combination mode is not feasible for the shielded Mars Braking Stage or the unshielded Mars Departure Stage.

Mars orbit altitude affects the vehicle in three ways: Mars Excursion Module mass requirements, thermal environment of the Mars Departure Stage, and energy requirements for the Mars braking and departure maneuvers. Results of this study show that the Mars Excursion Module mass variation with altitude is, by far, the most important of the three factors with respect to the vehicle IMIEO. This results in the general increase in IMIEO as the altitude increases; percentage increases in IMIEO reach 22% as the altitude increases from 216 n.mi (400 km) to the synchronous altitude of 9203 n.mi (17,053 km).

Relative to the individual stages, higher Mars orbit altitudes result in larger Earth Departure and Mars Braking Stages. The increased propellant loadings are caused by the larger mass of the Mars Excursion Module. Since this module is left at Mars, it does not affect the Mars Departure Stage. The initial mass of this stage decreases as the altitude increases, reflecting the less severe thermal environment at the higher altitudes.

GENERAL DYNAMICS

Fort Worth Division

The importance of the propellant storage mode increases with increasing stage number and, for a particular stage, as the propellant heat transfer increases. In terms of the parameters investigated, the heat transfer increases as a result of poorer insulation thermal performance, a more severe thermal environment, and increased Earth orbit staytime. The influence of propellant storage mode is a maximum for the condition of maximum Earth orbit staytime and low Mars orbit altitude with low-performance insulation (unshielded vehicle). The difference in IMIEO between the vent and partial-recondensation modes for this case is 519,300 lb_m (235,500 kg), or 22.3% of the partial-recondensation-mode value.

In all cases where the vent and partial-recondensation modes can be defined, both of these modes result in mass savings relative to the nonvent mode. At the synchronous altitude, the difference in IMIEO due to propellant storage mode reaches a maximum of 509,200 lb_m (230,900 kg) between the nonvent and partial-recondensation modes for the shielded vehicle. At this condition, the difference in IMIEO between the nonvent and vent modes is 231,800 lb_m (105,100 kg). The IMIEO difference is reduced as the insulation performance improves. At the intermediate $k\rho$ value, with all other conditions the same as above, the IMIEO difference is 49,700 lb_m (22,500 kg) between the nonvent and partial-recondensation modes.

The influence of propellant storage mode varies between stages. For the Earth Departure Stage, the vent and partial-recondensation modes begin to yield mass savings at the intermediate $k\rho$ value at staytimes beyond 180 days. With the highest performance insulation, the vent pressure is not reached at any staytime, and results for the vent and partial-recondensation modes cannot be defined. The above remarks also apply to the shielded Mars Braking Stage, where the vent and partial-recondensation modes become definable only at the longer staytimes for the intermediate $k\rho$ value. For the unshielded Mars Braking Stage, the modes associated with propellant boiloff become definable near the maximum staytime at the lowest $k\rho$ value.

Propellant storage mode is most important for the Mars Departure Stage. The long mission time of this stage precludes use of the nonvent mode; under the most favorable

GENERAL DYNAMICS

Fort Worth Division

conditions, the tank pressure reaches 37 psia. Thus, either a vent or partial-recondensation thermal management system is required on this stage. For the unshielded stage, the partial-recondensation mode yields a percentage reduction in storage penalty of roughly 45% in all cases. This reduction is less in the shielded case, ranging from 28% to 38% as the $k\rho$ value increases.

The use of solar shields to reduce the radiant energy incident upon the vehicle was investigated for the Mars transfer and Mars orbit mission phases. Shielding yields substantial reduction in the vehicle IMIEO, especially with low-performance insulation. Savings in IMIEO reach 346,200 lb_m (157,000 kg) with the lowest performance insulation. With higher performance insulation, the savings are an order of magnitude less. Propellant storage mode affects the IMIEO difference between the unshielded and shielded vehicles; IMIEO differences for the partial-recondensation mode are less than one-half those for the vent mode.

The relative effectiveness of the Mars transfer and Mars orbit solar shields is dependent upon the Mars orbit altitude. At low altitudes, the planetary-emitted and albedo radiation are dominant, thereby reducing the effectiveness of the Mars orbit shield with respect to the total incident energy. Thus, at low altitudes, the major portion of the IMIEO reduction associated with a shielded Mars Departure Stage is attributable to the Mars transfer solar shield. At the synchronous altitude (9203 n.mi or 17,053 km), however, more than one-half of the IMIEO reduction is attributable to the Mars orbit shield.

A significant aspect of the solar shield is its effect on the penetration heat transfer. During Mars transfer, the shield reduces the incident radiation, and thus the penetration heat transfer, to a negligible value, except during the periods of guidance correction. In Mars orbit, the orbit altitude influences the amount of reduction in the penetration heat transfer. The percentage reduction increases from 7% to 57% as the altitude increases.

Estimates of the system masses for the Mars transfer shield and the Mars orbit shield show little variation over the wide ranges of the variables investigated. These system masses, which include the basic shield mass, the canister,

GENERAL DYNAMICS

Fort Worth Division

and the associated subsystems, can be considered constant for most purposes with little error. For the Mars transfer shield, the total system mass is 950 lb_m (430 kg); the Mars orbit shield system mass is 495 lb_m (225 kg).

PRECEDING PAGE BLANK NOT FILMED.

GENERAL DYNAMICS

Fort Worth Division

S E C T I O N 3

M I S S I O N A N D V E H I C L E
D E S C R I P T I O N

In a broad parametric study of the type discussed here, it is necessary to restrict the scope of the study to a single mission and vehicle. To aid the reader in understanding and interpreting the results presented in later sections of this report, a brief summary of the mission and a short description of the vehicle are presented in this section. Additional information concerning the mission analyses performed during the study and the vehicle itself are contained in Sections 2 and 3 of Volume 2, respectively. The section is concluded with a description of the characteristics of each of the propellant storage modes investigated in this study.

GENERAL DYNAMICS

Fort Worth Division

3.1 MISSION DEFINITION

The reference mission for this study is a conjunction-class, manned, Mars stopover mission. This class of mission is characterized by long mission durations (about 2½ years from Earth departure to Earth return), long staytimes at Mars (about 1½ years), relatively low energy requirements, and relatively small variations in energy requirements from year to year.

The selected mission departs Earth on 1 March 1984 and returns to Earth on 17 September 1986. Mission duration following departure from Earth orbit is 930 days, and the total duration varies from 1020 to 1200 days, depending upon the Earth orbit staytime. The heliocentric geometry for the mission is presented in Figure 3.1-1; the polar plot relates solar distance, heliocentric longitude, and time. Variation of solar distance with flight time is presented in Figure 3.1-2, and additional mission data are tabulated in Table 3.1-1. The data in the table are standard trajectory data and are self-explanatory.

The three Mars circular-orbit altitudes selected for the study are 216 n.mi (400 km), 3238 n.mi (6000 km), and 9203 n.mi (17,053 km). The highest altitude is for a synchronous orbit (orbit period is equal to the period of rotation of Mars about its axis), while the lowest altitude is an estimate of the lowest altitude considered feasible for a 510-day duration in Mars orbit - based on estimated orbit decay rates. This altitude is considered approximate because of the large uncertainty concerning the density of the Martian atmosphere. The intermediate orbit altitude was selected from considerations of the variation of the total energy (ΔV) requirements for Mars braking and Mars departure, the reconnaissance capability, and landing-site accessibility. The selected altitude yields a near-minimum total ΔV and allows a high-inclination orbit, which is desirable for more complete planet coverage and access to landing sites over a wide range of latitudes.

Equatorial inclinations of the Mars orbits were selected by the requirement that the resulting orbit precession yields the correct orientation for a coplanar departure from orbit. Only posigrade orbits were considered. The selected inclinations are listed in Table 3.1-1.

GENERAL DYNAMICS

Fort Worth Division

TABLE 3.1-1

MISSION SUMMARY

	Civil Date	Julian Date									
Depart Earth:	1.0 March 1984	244 5760.5									
Arrive Mars:	27.0 September 1984	244 5970.5									
Depart Mars:	19.0 February 1986	244 6480.5									
Return Earth:	17.0 September 1986	244 6690.5									
<table style="width: 100%; border-collapse: collapse;"> <tr> <td style="width: 40%;">Outbound Flight Time:</td> <td style="width: 30%;">210 days</td> <td style="width: 30%;"></td> </tr> <tr> <td>Mars Staytime:</td> <td>510 days</td> <td></td> </tr> <tr> <td>Inbound Flight Time:</td> <td>210 days</td> <td></td> </tr> </table>			Outbound Flight Time:	210 days		Mars Staytime:	510 days		Inbound Flight Time:	210 days	
Outbound Flight Time:	210 days										
Mars Staytime:	510 days										
Inbound Flight Time:	210 days										
	<u>Planetocentric (Earth) Departure Phase</u>	<u>Planetocentric (Mars) Departure Phase</u>									
Parking Orbit Altitude:	262 n.mi (485 km)	Selected*									
Hyperbolic Excess Speed:	0.1270 EMOS	0.0813 EMOS									
Declination of Departure Asymptote:	-35.71°	9.62°									
Right Ascension of Departure Asymptote:	182.43°	212.72°									
Parking Orbit Inclination:	36.0°	Selected*									
	<u>Heliocentric Phase (Outbound Leg)</u>	<u>Heliocentric Phase (Inbound Leg)</u>									
Heliocentric Transfer Angle:	148.89°	141.77°									
Inclination of Transfer Orbit:	3.53°	0.894°									
Eccentricity of Transfer Orbit:	0.1835	0.2396									
Perihelion Distance:	0.9621 AU (no transit)	0.9948 AU (no transit)									
Aphelion Distance:	1.3946 AU	1.618 AU (no transit)									
	<u>Planetocentric (Mars) Arrival Phase</u>	<u>Planetocentric (Earth) Return Phase</u>									
Parking Orbit Altitude:	Selected*	Direct Reentry									
Unbraked Entry Speed:	--	38,321 ft/sec (11,6801 km/sec)									
Hyperbolic Excess Speed:	0.1272 EMOS	0.1235 EMOS									
Declination of Arrival Asymptote:	4.51°	14.03°									
Right Ascension of Arrival Asymptote:	316.53°	110.25°									
Parking Orbit Inclination:	Selected*	-									

* The selected circular orbit altitudes and inclinations are:

<u>Altitude</u>	<u>Inclination</u>
9203 n.mi (17,053 km)	10.7 deg
3238 n.mi (6000 km)	63.0 deg
216 n.mi (400 km)	75.2 deg

GENERAL DYNAMICS
Fort Worth Division

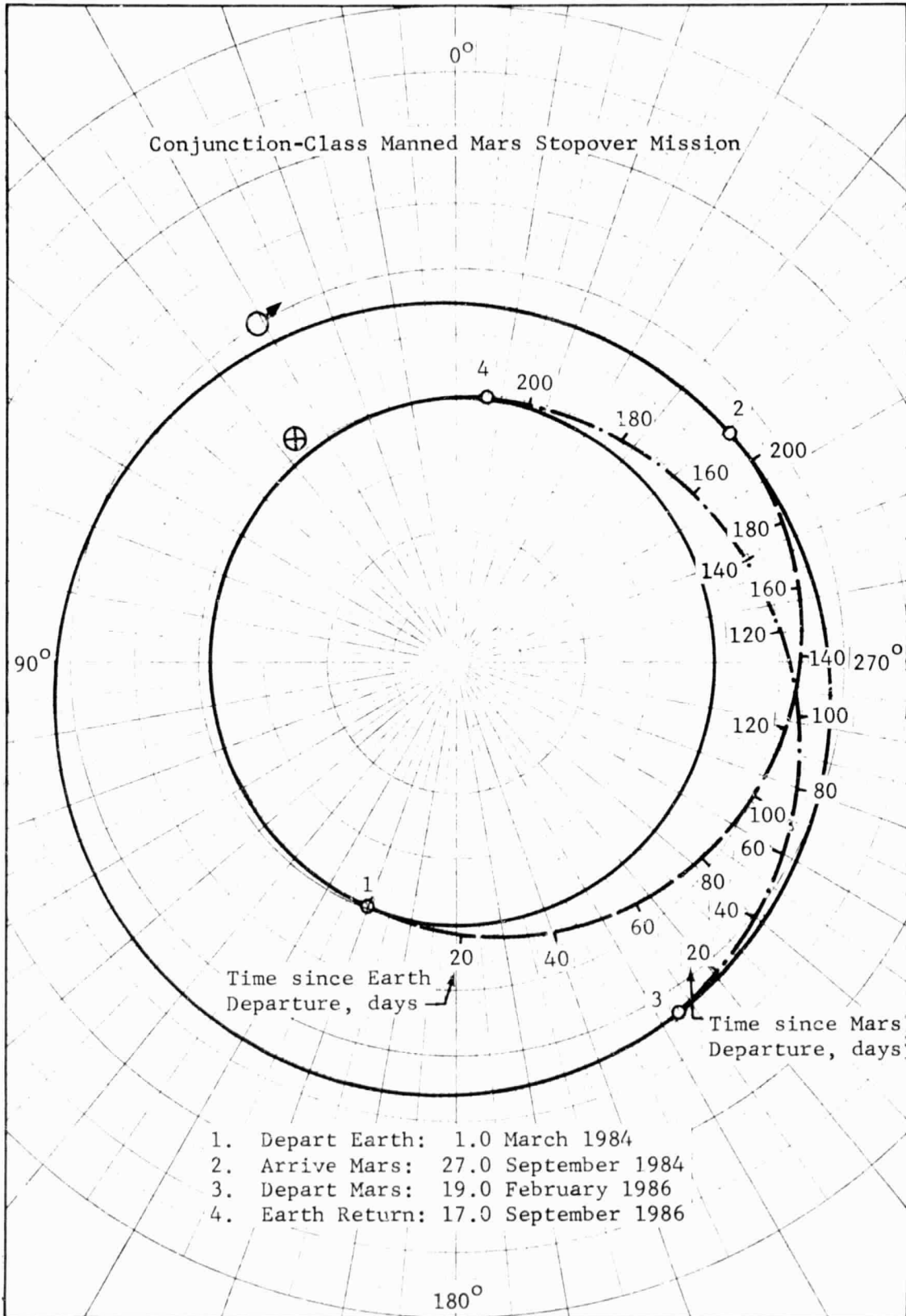


Figure 3.1-1 Heliocentric Mission Geometry

GENERAL DYNAMICS
Fort Worth Division

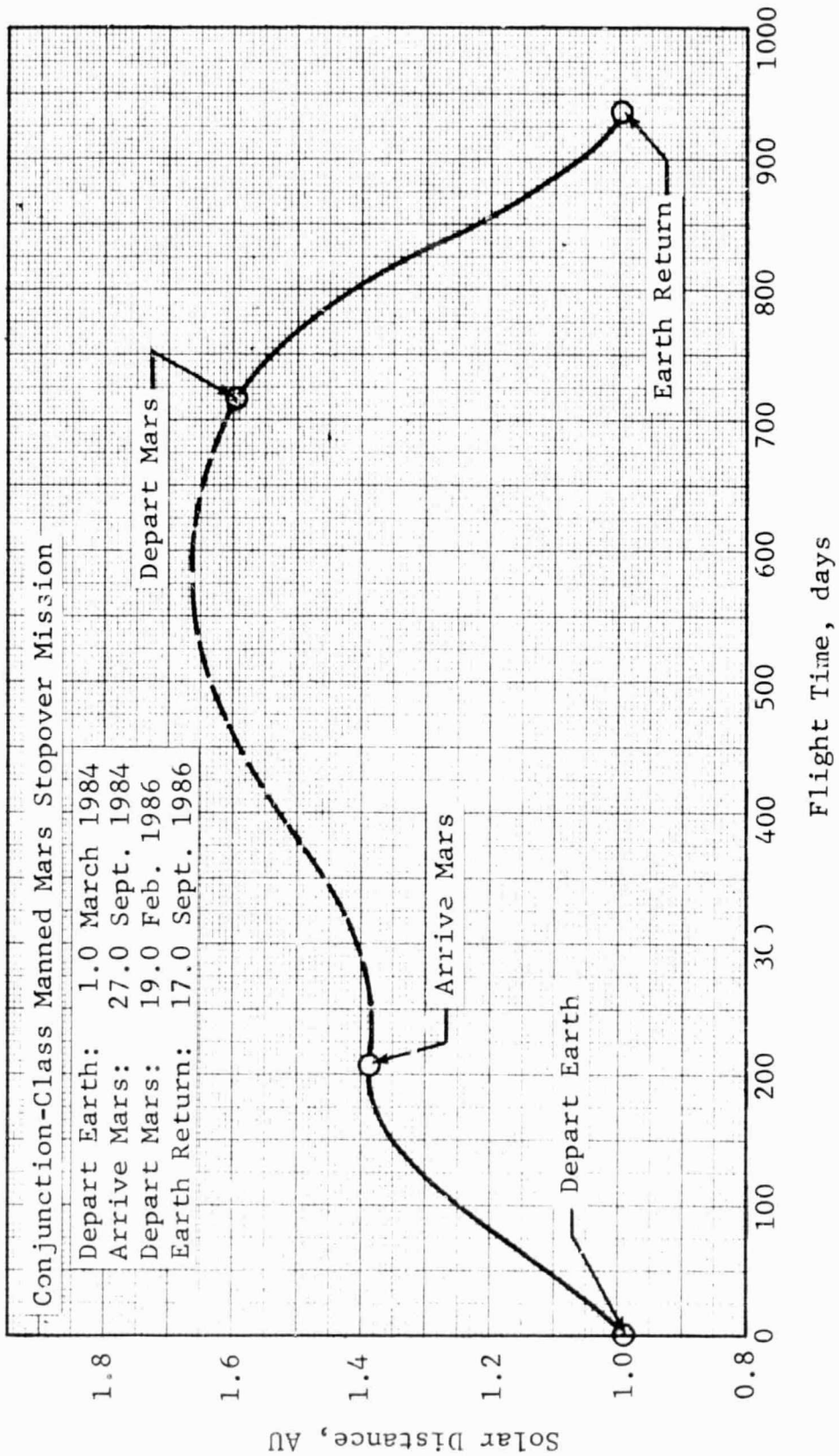


Figure 3.1-2 Variation of Solar Distance with Flight Time

GENERAL DYNAMICS
Fort Worth Division

3.2 VEHICLE CONFIGURATION

The vehicle configuration upon which the study is based was developed using the modular approach. The basic propulsion unit is the nuclear propulsion module, which has been under study for several years. Individual stages of the vehicle comprise one or more of the basic modules, either as propellant or propulsion modules. The propellant module is identical to the propulsion unit with the exception of the engine and related structure. Important features of the nuclear module, with respect to this study, are described in Subsection 3.2.1. The configuration of the complete conjunction-class Mars vehicle is discussed in Subsection 3.2.2, including the considerations that led to its selection.

An important aspect of this study concerned the variation of the Mars Excursion Module (MEM) mass with Mars orbit altitude. (The MEM is part of the payload on the Mars Braking Stage and has chemical, rather than nuclear, propulsion systems.) A brief description of the MEM and the variation with altitude of the MEM mass is presented in Subsection 3.2.3.

3.2.1 Nuclear Propulsion Module

The nuclear propulsion module, shown in Figure 3.2-1, is powered by the 230,000-lb-thrust (1,023,000 N) NERVA engine (Reference 3-1). Liquid-hydrogen propellant is contained in the 384-in.-diameter (9.75 m) aluminum cylindrical tank, which is closed with ellipsoidal heads. Propellant tank length is variable according to the propellant requirements of the particular stage. Within a stage, however, all tanks are identical.

The basic structural concept is the pressure-stabilized, membrane-type tank, which is suspended by a stiffened titanium cone within the ascent shell. This shell carries the high-g inertial loads experienced during Earth launch and is retained during the Earth orbit assembly period for meteoroid protection. It is jettisoned just prior to departure from Earth orbit. During the low-g propulsion maneuvers of the Mars vehicle, the loads are carried by the tank wall. An orbital-assembly interstage is attached to the aft end of the tank by means of a titanium skirt. This interstage transmits loads from lower stages during the low-g propulsive maneuvers,

GENERAL DYNAMICS
Fort Worth Division

supports the docking cone, and furnishes meteoroid protection to the engine and the aft-end of the tank.

Meteoroid protection is furnished by a system comprising the tank wall, the jettisonable foam-filled meteoroid bumper, the orbital-assembly interstage and docking cone, the forward thrust structure, and the ascent shell. The tank wall furnishes protection during the period between the jettisoning of the meteoroid bumper and the engine ignition. The combination of the foam-filled bumper and the tank wall provides protection during the interplanetary mission phase, with the bumper sized by the interplanetary meteoroid protection requirements. The addition of the ascent shell to the bumper and tank-wall combination furnishes the additional protection required during Earth orbit.

3.2.2 Total Mars Vehicle

3.2.2.1 Vehicle Stages

The complete Mars vehicle, shown in Figure 3.2-2, comprises a four-module Earth Departure Stage, a two-module Mars Braking Stage, a single-module Mars Departure Stage, and the mission payload. An in-line configuration was selected since it is well adapted to the modular approach and allows the ascent shells to be jettisoned easily.

The Earth Departure Stage is made up of three propulsion modules and a single propellant module stacked above the central propulsion module. The additional propellant module was necessary to meet the stage propellant requirements while keeping the individual module mass within the payload capability of an uprated Saturn V launch vehicle. While three modules would be adequate at some of the conditions investigated in this study, the majority requires four modules, and a common configuration with respect to the number of modules was deemed necessary to preclude discontinuities in the data presentations.

The Mars Braking Stage is made up of a propellant module and a propulsion module stacked above the propellant module of the Earth Departure Stage. The Mars Departure Stage is the smallest of the three stages and consists of a single propulsion module. Module size is variable in terms of the tank length and is dependent upon the study variables and

GENERAL DYNAMICS
Fort Worth Division

the stage number. All propellant tanks for a particular stage are identical, however.

Payload for the vehicle includes the Mission Module, the Mars Excursion Module, and the Earth Entry Vehicle. The Mission Module mass is 116,000 lb_m (52,600 kg), including the solar-flare shield mass of 16,000 lb_m (7260 kg), and the Earth Entry Vehicle mass is 15,000 lb_m (6800 kg). The Mars Excursion Module mass is dependent upon the Mars orbit altitude, as discussed in Subsection 3.2.3. An additional payload of 1500 lb_m (680 kg) consists of scientific payload returned from Mars, such as soil samples.

Just prior to the Earth departure maneuver, the ascent shells are jettisoned from all of the modules. The Earth Departure Stage engines are fired and the vehicle leaves Earth orbit and enters the Mars transfer trajectory. The Earth Departure Stage is then separated. Prior to the braking maneuver at Mars, the orbital-assembly interstage and the meteoroid bumpers from both modules are jettisoned from the Mars Braking Stage. The vehicle achieves orbit and the Braking Stage is separated. The orbital-assembly interstage and meteoroid bumper of the Mars Departure Stage are jettisoned just prior to the Mars Departure maneuver and the vehicle enters the Earth transfer trajectory, where separation of the spent Mars Departure Stage occurs. The mission is completed with an atmospheric-braking re-entry into Earth orbit and finally to the Earth's surface.

3.2.2.2 Solar Shields

One objective of the study is to investigate the effectiveness of inflatable solar shields during the interplanetary phases of the mission. In cases where these shields are utilized, the vehicle is said to be "shielded." Two shields are used during the mission. The first, the Mars transfer shield, is deployed early in the Mars transfer phase and shields the Mars Braking and Departure Stages from direct solar radiation. This configuration is shown in Figure 3.2-3 with the spherical shield deployed from the aft end of the Braking Stage. It is required that the vehicle longitudinal axis be aligned with the solar vector except during the guidance correction periods at the beginning and end of the outbound leg. This shield is jettisoned just prior to Mars braking.

GENERAL DYNAMICS
Fort Worth Division

The second solar shield, the Mars orbit shield, is deployed upon achieving Mars orbit and shields the Mars Departure Stage from direct solar radiation. The vehicle-shield configuration is shown in Figure 3.2-4 with the spherical solar shield deployed from the aft end of the Mars Departure Stage. Again, the vehicle longitudinal axis must be aligned with the solar vector. This shield is jettisoned prior to Mars departure.

For the unshielded case, the vehicle orientation during Mars transfer is such that the vehicle longitudinal axis is broadside to the sun. In the Mars orbit mission phase, the vehicle axis is oriented along the velocity vector.

3.2.3 Mars Excursion Module

The Mars Excursion Module (MEM) is used to descend from the parking orbit at Mars to the surface of Mars and to ascend from the surface back to orbit. The major components of the MEM are a descent vehicle, a surface payload, an ascent vehicle, and an ascent payload. The MEM used in this study is based on the concept given in Reference 3-2. The reference MEM was designed for a crew size of six men and a nominal stay time of 500 days. The most important deviation from the reference MEM was the choice of propellant; storable propellants were assumed rather than cryogenic propellants because of the long staytime on the planet. Specific impulse of both the ascent and the descent vehicle propulsion systems was assumed to be $360 \text{ lb}_f\text{-sec}/\text{lb}_m$ ($3530 \text{ N-sec}/\text{kg}$).

A two-stage ascent vehicle was defined. The first stage is used for a direct ascent to a 100-n.mi (185 km) circular orbit and the second stage is used for a transfer to the parking orbit. The mass of the ascent payload is $11,310 \text{ lb}_m$ (5140 kg). Included in the ascent payload are the crew and associated equipment; control, tracking and computer equipment for piloting the stage; and the scientific payload and samples brought from the surface. The structural mass of each stage is based on a propellant mass fraction (propellant mass divided by the sum of propellant mass and structure mass) of 0.9.

A single-stage descent vehicle was defined. The propulsion system of the stage is used for de-orbit, propulsive braking, hover, and translation prior to landing. In

GENERAL DYNAMICS

Fort Worth Division

addition to the normal structure based on a propellant mass fraction of 0.85, allowances are included for a landing gear and a heat shield. Payload of the descent vehicle consists of the ascent stage and the surface payload. Included in the surface payload of 62,660 lb_m (28,420 kg) are two roving vehicles, life-support equipment and supplies, experimental equipment, power supply, and other items to maintain a base on the surface.

The ΔV requirements for the MEM were determined for each selected Mars orbit altitude. The effect of altitude on the total ΔV requirements is reflected in the transfer ΔV requirements of the second stage of the ascent vehicle and the descent de-orbit ΔV requirements.

The total mass of the MEM is presented as a function of orbit altitude in Figure 3.2-5. The large increase of MEM mass with increasing altitude results from the increase of the ΔV requirements with altitude. Increased ΔV requirements result in larger propellant and propulsion system mass requirements and, therefore, larger total MEM mass.

GENERAL DYNAMICS
Fort Worth Division

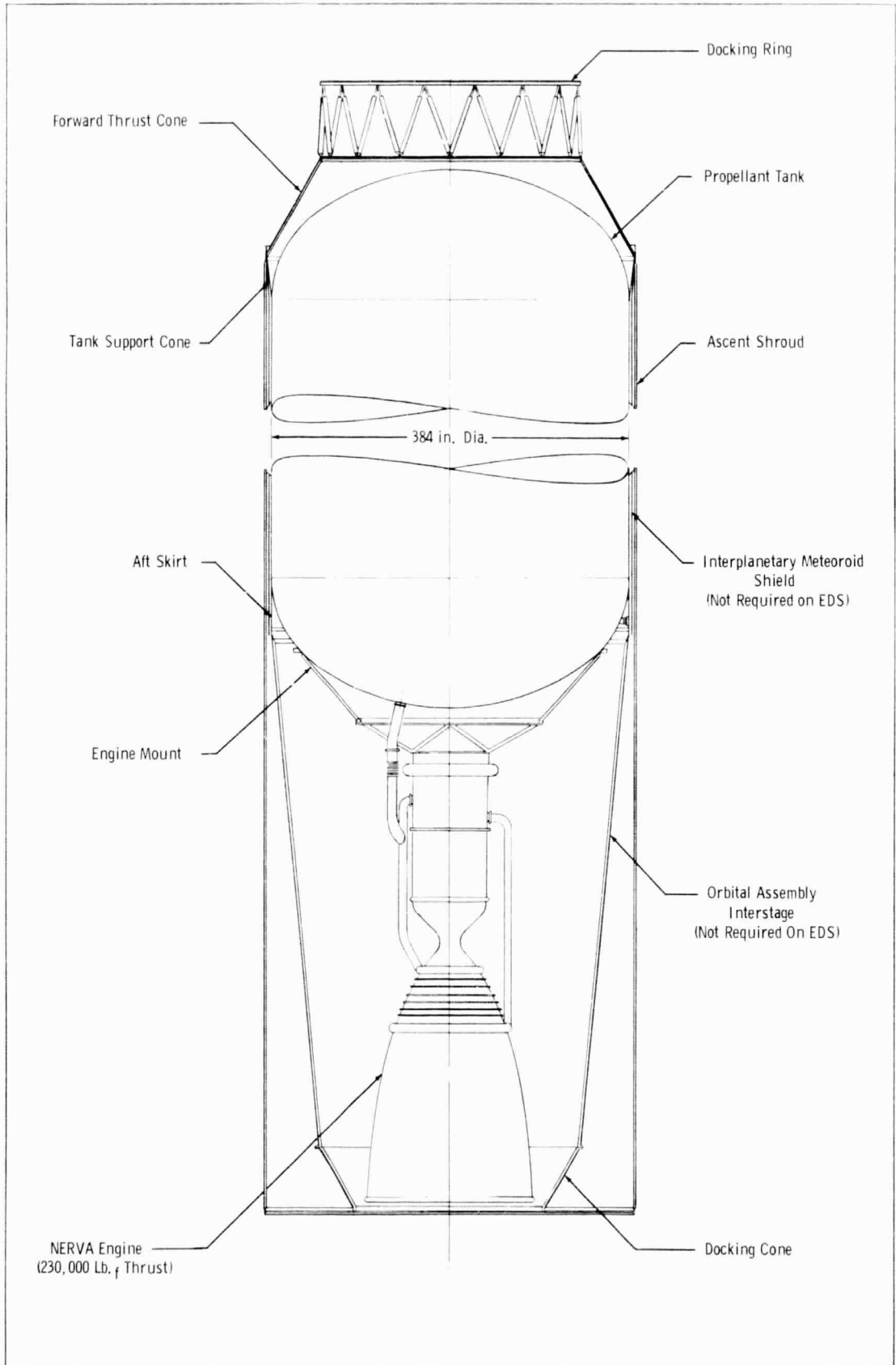


Figure 3.2-1 Nuclear Propulsion Module

GENERAL DYNAMICS
Fort Worth Division

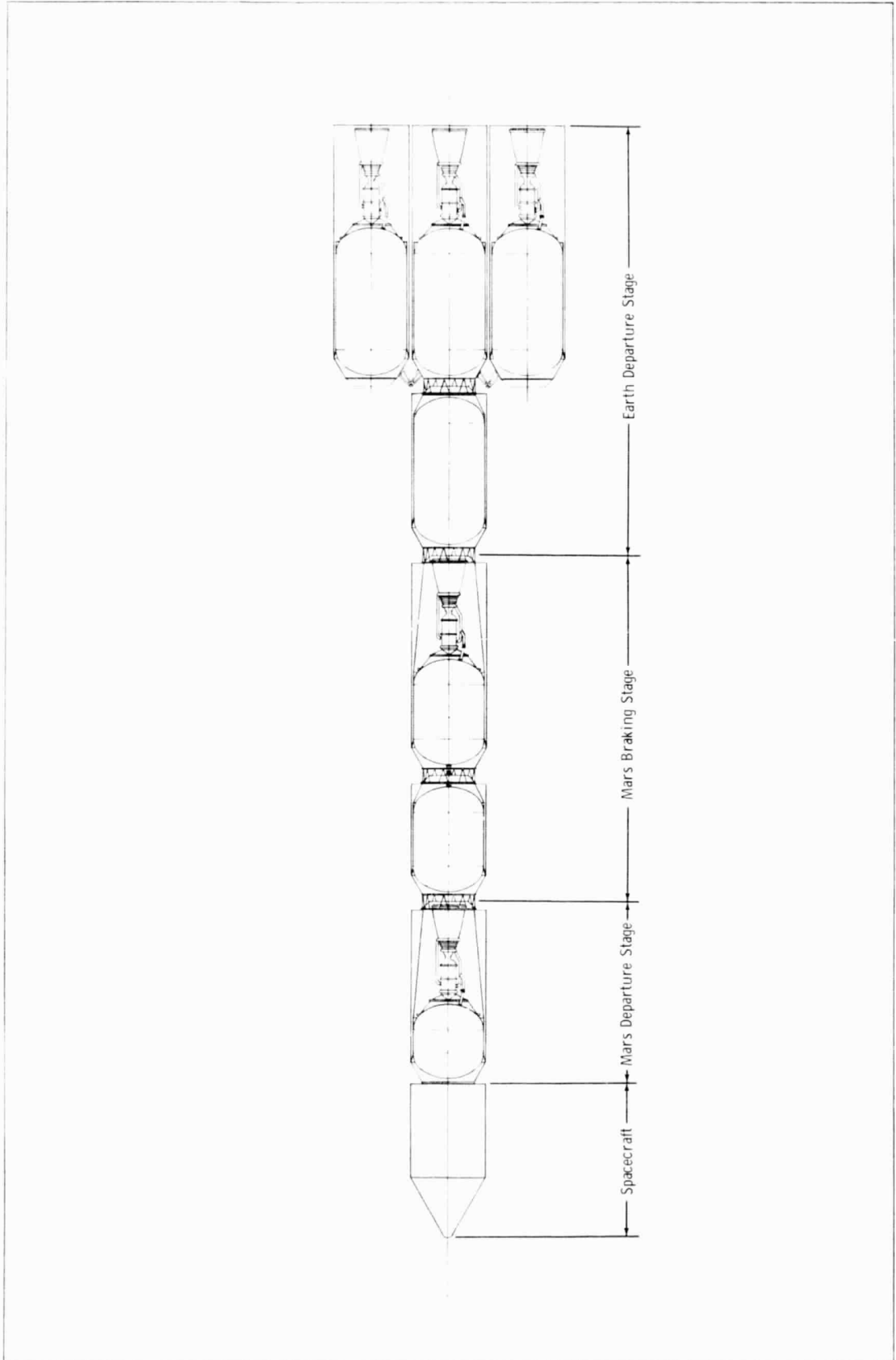


Figure 3.2-2 Conjunction-Class Mars Vehicle

GENERAL DYNAMICS
Fort Worth Division

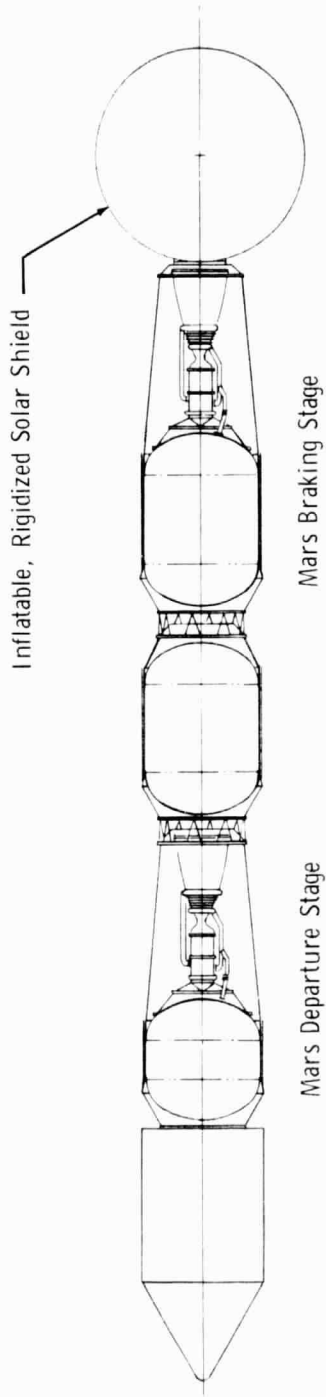


Figure 3.2-3 Mars Transfer Solar Shield-Vehicle Configuration

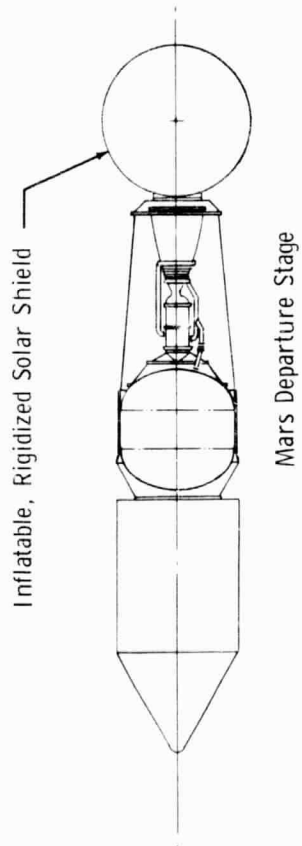


Figure 3.2-4 Mars Orbit Solar Shield-Vehicle Configuration

GENERAL DYNAMICS

Fort Worth Division

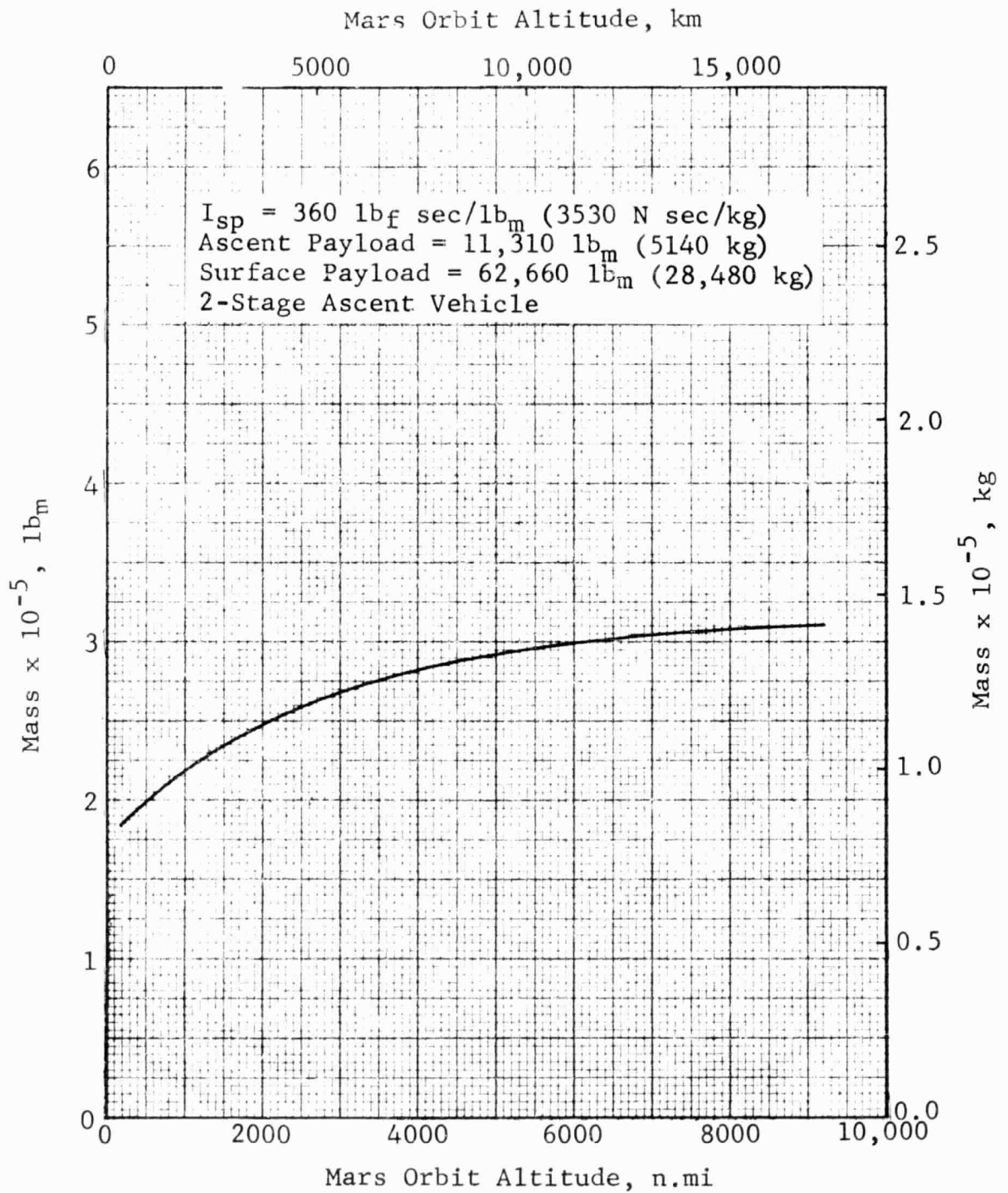


Figure 3.2-5 Variation of MEM Mass with Altitude

GENERAL DYNAMICS
Fort Worth Division

3.3 PROPELLANT STORAGE MODES

Five modes of propellant storage are treated in this study: nonvent, vent, partial-recondensation, combination, and tanking. The latter is not a storage mode as such, but rather a variation of the vent or partial-recondensation modes. The initial thermodynamic state of the propellant (triple-point saturated liquid) is the same in all cases, and the mission time history begins at the start of the Earth orbit assembly period.

In the nonvent storage mode, the tank is a closed container throughout the mission and the heat transfer to the propellant is accepted as an increase in the propellant internal energy. Accompanying the increase of internal energy are the associated increases in pressure and temperature and a reduced propellant density. Because of the density change over the mission, there is necessarily a large initial ullage fraction. As the propellant expands during the mission, this ullage volume is reduced; the tank is sized by a 5% ullage volume fraction at the end of the mission. Typically, in the nonvent mode, the tank and insulation masses are the dominant components of the propellant storage system mass.

The vent mode is characterized by boiloff of the propellant at a constant pressure which, in this study, is 14.7 psia in all vent-mode cases. Since the propellant initial thermodynamic state is triple-point saturated liquid, there is an initial nonvent period associated with the vent storage mode. In many of the cases studied the vent pressure was not reached, with the result that a vent-mode case for the particular set of parameters could not be defined. Typically, in the vent mode, the boiloff, insulation, and tank masses are the dominant components of the propellant storage system mass. The tank is sized to contain the total propellant loading including the boiloff with a 5% ullage volume fraction.

The partial-recondensation mode is similar to the vent mode in that a portion of the heat load is removed by propellant boiloff. However, in the partial recondensation mode, a fraction of the boiloff is reliquified and retained as useful propellant; the remainder is super-heated before being vented to the surroundings. As in the vent mode, the vent pressure is 14.7 psia in all cases and the tank is

GENERAL DYNAMICS
Fort Worth Division

sized with a 5% ullage volume fraction. Dominant components of the propellant storage system are the boiloff, the insulation, and the tank.

A variation of the nonvent mode, which utilizes the large initial ullage volume characteristic of that mode, is termed the combination mode. The basic concept is to utilize the tank volume required for propellant expansion during nonvent operation to load excess propellant that is subsequently boiled off during Earth orbit. This concept will reduce the propellant storage system mass and allow some extension of the Earth orbit staytime. The vent is closed at the beginning of the Mars transfer trajectory and the remainder of the mission is completed in the nonvent mode. Sizing of the tank is based on the interplanetary mission phases alone, with a 5% ullage volume fraction requirement at the end of the mission. Propellant expansion during the interplanetary mission phases then determines the initial ullage required at the start of the Mars transfer trajectory, and the maximum additional propellant loading is set by that ullage volume. Actual propellant loading could be tailored to the desired Earth orbit staytime. To maximize the range of staytime, the vent pressure during Earth orbit was set at 8 psia (5.5 N/cm^2) for the combination mode.

The tanking mode can be considered as a variation on either the vent or the partial-recondensation modes. Tanking implies the replenishing of the propellant boiled off during Earth orbit; the additional propellant is furnished by an orbital tanker. Vent pressure during Earth orbit is set at 8 psia to achieve maximum utility from the tanking mode. Beyond Earth orbit, the vent pressure is the usual 14.7 psia (10.1 N/cm^2), and a nonvent period will occur subsequent to Earth orbit as the tank pressure increases from 8 to 14.7 psia.

GENERAL DYNAMICS

Fort Worth Division

S E C T I O N 4

P A R A M E T R I C S T U D Y R E S U L T S A N D D I S C U S S I O N

In this section, the results of the parametric study are presented and basic trends in the data are pointed out and discussed. The discussion is organized to present results applicable to the total Mars vehicle first, followed by separate discussions of the effects of the various parameters and systems upon the individual stages. The section is concluded with a discussion of off-optimum data.

The basic parameters in this study are the Earth orbit staytime, the insulation performance (thermal conductivity-density product), and the Mars orbit altitude. The importance of the Earth orbital storage period as a parameter, from the thermal standpoint, rests principally on two facts: (1) for a Mars mission, the Earth orbital environment is likely to be the most severe thermal environment of the mission; and (2) for manned Mars vehicles, the long orbital assembly times presently envisioned may be a significant fraction of the total storage period and may dominate the propellant heating history of the first two stages. In this study, the total Earth orbit staytime ranges from 90 to 270 days. The Earth Departure Stage is assumed to be in orbit for the full staytime, while the Mars Braking Stage and the Mars Departure Stage have staytimes of two-thirds and one-third of the total, respectively.

Insulation thermal performance is an extremely important parameter for study, since the effective thermal conductivity values for multilayer insulation quoted in the literature cover a wide range (Refs. 4-1, 4-2, and 4-3). This parameter assumes added importance since the installed performance may be less than that measured under more ideal conditions in the laboratory. The measure of insulation performance is the product of effective thermal conductivity and density. Although the effective thermal conductivity varies with insulation thickness and temperature level, it was necessary in this study to neglect such effects.

GENERAL DYNAMICS

Fort Worth Division

The third basic parameter, Mars parking-orbit altitude, is important from a thermal standpoint since the planetary emitted and albedo radiation vary with orbit altitude. Another related aspect of thermal effects is the change in solar shield effectiveness with altitude. At lower altitudes, the planetary components of the incident radiation degrade the performance, since the shield is designed to intercept only the direct solar radiation. Mars orbit altitude is also important with respect to variations in the velocity increments for the Mars Braking and Mars Departure Stages and in the mass of the Mars Excursion Module.

In addition to variation of the basic parameters, the propellant storage mode was also varied. The five different modes investigated (nonvent, vent, partial-recondensation, combination, and tanking) are described in Subsection 3.3. Finally, the effectiveness of solar shields for reducing the incident radiation during the interplanetary portions of the mission was investigated.

As mentioned in Section 1, the study was conducted in two phases. The results presented here were obtained during the final phase of the study. It will be noted that data are not presented for certain combinations of parameters, propellant storage modes, and stages. These combinations were not investigated during the final phase because results of the preliminary study indicated that such combinations were either not feasible or not of interest. For example, it was found during the preliminary analysis that the high heat transfer to the unshielded Mars Departure Stage resulted in extremely high pressures in the nonvent mode. Even with the solar shield, the pressures were beyond the range of interest for practical tank design, except at the synchronous altitude.

GENERAL DYNAMICS

Fort Worth Division

4.1 MARS VEHICLE INITIAL MASS

The basic approach in this study was to generate optimized propellant-storage-system and mass-buildup data, with the propellant storage system of only one stage of the Mars vehicle optimized at a time. Nominal mass fractions, evaluated from the preliminary analysis results, were used to define the remaining stages in order to determine the Initial Mass In Earth Orbit (IMIEO) of the entire vehicle. However, once the single-stage optimizations were obtained, it became possible to obtain mass-buildup data for a vehicle using the optimum-mass-fraction data for each stage simultaneously. In this section, data for such an "optimized" vehicle are presented. The limitations are recognized, since the thermal protection system of each stage of the vehicle should be optimized simultaneously for a truly optimized vehicle. However, the general trends should be similar. In each case the insulation performance, Mars orbit altitude, and fractional Earth orbit staytime were common to all three stages.

Propellant storage mode was also common to all three stages, and the graphs are labelled as such. However, under conditions that result in low propellant heat transfer (high insulation performance, short staytime, high altitude), the vent pressure may not be reached in the Earth Departure and Mars Braking Stages because of the larger propellant loading and shorter mission time relative to the Mars Departure Stage. Thus, in some of the figures presented in this section, the labels "vent mode" and "partial-recondensation mode" may not describe the actual storage mode in the lower stages. The actual mode may be the nonvent mode in the first stage or the first and second stages (refer to stage data sheet in Volume 3). This situation actually makes the data more useful for the following reason. The assumption of a common storage mode for all three stages relates to the modular approach to the Mars vehicle. Assume that each stage has a partial-recondensation thermal management system and assume further that the vent pressure level is not reached in the Earth Departure Stage. The data presented here are applicable to this case because the thermal management system mass has not been included. Now, assume that the common-storage-mode requirement is waived and the non-vent mode is assumed for the Earth Departure Stage. The data for the common-mode case are also applicable to this case of mixed nonvent and partial-recondensation modes

GENERAL DYNAMICS

Fort Worth Division

between the stages. The only difference is that there are fewer partial-recondensation systems required and thus a smaller mass penalty to be added to the IMIEO value presented here (partial-recondensation mode) to obtain the actual value of IMIEO.

The bulk of the data presented in this section is for the vent and partial-recondensation propellant storage modes. For the shielded vehicle at the synchronous (9203 n.mi or 17,053 km) Mars orbit altitude, the nonvent mode results are also presented. The reason for the lack of nonvent mode data is that this mode was not considered feasible for the Mars Departure Stage except for the specific condition mentioned above. During the preliminary analysis, it was found that the nonvent mode resulted in extremely high pressures for the unshielded Mars Departure Stage at all orbit altitudes. Even in the shielded case, the pressures were beyond reasonable values at the lower altitudes.

Data in this section are presented in terms of the IMIEO or the propellant storage penalty. Propellant storage penalties are referenced to the zero-mass-fraction vehicle and, if expressed in fractional form, are normalized by the IMIEO of the zero-mass-fraction vehicle.

The mass of the ascent shell was not included in the optimization analyses since it would have little effect on the optimum insulation thickness. The effect of this mass on the IMIEO is shown in Figure 4.1-1 for the vent mode with low-performance insulation. This condition would tend to yield the largest ascent shell mass. With the shell mass included, the IMIEO is increased approximately 6% across the entire range of staytime. At less extreme conditions, higher insulation performance for example, the increment in IMIEO would be reduced.

4.1.1 Sensitivity to Parameters

In this subsection, the sensitivity of the Mars vehicle IMIEO with respect to the basic study parameters (Earth orbit staytime, insulation performance, and Mars orbit altitude) is discussed.

GENERAL DYNAMICS
Fort Worth Division

4.1.1.1 Earth Orbit Staytime

Earth orbit presents the most severe thermal environment that the vehicle experiences during the conjunction-class Mars mission. The influence of Earth orbit staytime is greatest, of course, on the Earth Departure Stage because Earth orbit encompasses the total mission time of that stage. For the interplanetary stages, the influence of Earth orbit staytime is lessened because these stages spend only a fraction of their total mission time in Earth orbit. The effect of the Earth orbital storage period on the IMIEO for the unshielded Mars vehicle is shown in Figures 4.1-2, 4.1-3, and 4.1-4 for the three Mars orbit altitudes investigated. Data are shown for both the vent mode and the partial-recondensation mode. The independent variable is the fraction of the maximum staytime since the absolute staytime is not the same for the three stages of the vehicle. Maximum values are 270 days for the Earth Departure Stage, 180 days for the Mars Braking Stage, and 90 days for the Mars Departure Stage. Included in each figure is the IMIEO of a vehicle with adiabatic tank walls; this IMIEO represents the lower limit on the initial mass.

In all cases, the IMIEO increases with staytime because of a larger total propellant heat transfer to all stages. However, the magnitude of the increase is greatly dependent upon the insulation performance and the propellant storage mode. With low-performance insulation, the influence of staytime is amplified because the heat transfer rate is increased. For the low-altitude case (Fig. 4.1-2), the IMIEO increases 18.5% from 2.40 to 2.84 million lb_m (1.09 to 1.29 million kg) in the vent mode with the lowest-performance insulation (highest $k\rho^4$ value): 15.3% of the increase occurs in the Earth Departure Stage, 2.8% in the Mars Braking Stage and 0.4% in the Mars Departure Stage. This distribution between stages is expected since the stage size and the ratio of Earth orbit staytime to total mission time decrease with increasing stage number. With the same insulation performance but with the partial-recondensation storage mode, the percentage increase is reduced by roughly one-half to 9.3% and the absolute IMIEO values are also reduced. Again, the bulk of the increase, 7.6%, occurs in the Earth Departure Stage mass.

At the intermediate $k\rho^4$ value of 7.5×10^{-5} Btu lb_m /hr-ft⁴-°R (2.08×10^{-3} W kg/m⁴-°K), the influence of staytime

GENERAL DYNAMICS

Fort Worth Division

is greatly reduced. The percentage increase in IMIEO over the range of staytime for the vent mode is 5.6% or 108,700 lb_m (49,300 kg). The Earth Departure Stage accounts for 80,800 lb_m (36,650 kg) of the increase; the Mars Braking Stage, 22,800 lb_m (10,340 kg); and the Mars Departure Stage, 5100 lb_m (2310 kg). The percentage increase is reduced to 3.2% for the partial-recondensation mode. A further improvement in insulation performance to the lowest $k\rho$ value investigated reduces the influence of staytime even further.

Similar trends can be noted for the higher altitudes (Figs. 4.1-3 and 4.1-4) together with a general shift to larger values of the IMIEO. The effects of Mars orbit altitude will be discussed in Subsection 4.1.1.3.

The effect of reducing the propellant heat transfer by deploying solar shields during Mars transfer and Mars orbit should be to increase the influence of Earth orbit staytime, since Earth orbit heat transfer is then a larger fraction of the total. Figures 4.1-5, 4.1-6, and 4.1-7 present the variation of the IMIEO with Earth orbit staytime for the shielded vehicle for the three Mars orbit altitudes. A comparison of the shielded and unshielded vehicles at a given altitude for similar conditions shows that the influence of staytime as measured by the percentage increase of IMIEO depends upon insulation performance. With low-performance insulation, the percentage increase in IMIEO is greater for the shielded case. At the intermediate and low $k\rho$ values, however, the percentage increase in IMIEO is greater for the unshielded vehicle. The reason for the change in trend involves the Mars Braking Stage propellant storage mode. In the unshielded case, the vent pressure is reached at the intermediate and low $k\rho$ values for all staytimes other than the minimum. In the shielded case, the vent pressure is reached at the highest $k\rho$ value, but the mode is nonvent at all staytimes at the intermediate and low $k\rho$ values. This reduces the influence of staytime for that stage because the minimum tank design pressure is not exceeded and the effect is carried through to the entire vehicle.

For the 9203-n.mi (17,053 km) altitude, the IMIEO increases 25.7% from 2.50 to 3.14 million lb_m (1.13 to 1.42 million kg) for the nonvent mode at the high $k\rho$ value. This is an increase of 642,000 lb_m (291,200 kg) of which 522,900 lb_m (237,100 kg) occurs in the Earth Departure Stage. The

GENERAL DYNAMICS

Fort Worth Division

Mars Braking and Mars Departure Stages contribute 101,900 lb_m (46,210 kg) and 17,000 lb_m (7710 kg) to the increase, respectively. For the vent and partial-recondensation modes, the corresponding percentage increases are 17.7 and 9.5%. As the insulation performance improves, these percentage increases drop rapidly to values less than 4%.

4.1.1.2 Insulation Thermal Performance

Results presented in the previous subsection show that the insulation thermal performance has a strong influence on the IMIEO of the Mars vehicle. The range of thermal performance investigated here is large - approximately three orders of magnitude as measured by the $k\rho$ product. Commonly-quoted values for the best multilayer insulation systems fall just below the middle of the range at a $k\rho$ value of approximately 7.5×10^{-5} Btu lb_m/hr-ft⁴-°R (2.08×10^{-3} W kg/m⁴-°K). Sensitivity of the IMIEO to insulation performance is shown in Figure 4.1-8 for the unshielded vehicle in the vent mode at the low Mars orbit altitude. This is a severe case from the thermal standpoint, and this fact is reflected in the IMIEO variation. For the maximum staytime, the IMIEO increases 935,000 lb_m (424,000 kg), or 49%, over the range of insulation performance. It is especially important to note that the bulk of the increase, 42.5%, occurs in the range of $k\rho$ values above 7.5×10^{-5} Btu lb_m/hr-ft⁴-°R (2.08×10^{-3} W kg/m⁴-°K). For the minimum staytime case, the variation is reduced, with the IMIEO ranging from 1.86 to 2.40 million lb_m (0.84 to 1.09 million kg), a percentage increase of 29.0%. Again, the major portion of the increase, 24.7%, occurs in the range above the intermediate value. Figure 4.1-9 presents the IMIEO variation for the partial-recondensation mode at the synchronous altitude. The more effective thermal management system and the less severe thermal environment for the Mars Departure Stage reduce the influence of insulation performance. At the maximum staytime, the IMIEO increases from 2.25 to 2.80 million lb_m (1.02 to 1.27 million kg), a percentage increase of 24.3%. The percentage increase is reduced further at the minimum staytime to 15.2%.

The influence of insulation performance on IMIEO for the shielded vehicle is shown in Figure 4.1-10 for the non-vent storage mode. The IMIEO increases from 2.25 to 3.14 million lb_m (1.02 to 1.42 million kg), or 39.7% for the maximum staytime case. Even though the thermal environment

GENERAL DYNAMICS

Fort Worth Division

is effectively reduced by the solar shields, the IMIEO variation is still very large as a result of the nonvent propellant storage mode. At the minimum staytime, the percentage increase is only 12.6%. The increased efficiency of the partial-recondensation mode as compared to the nonvent mode can be seen by comparing Figures 4.1-11 and 4.1-10. For the partial-recondensation mode, the IMIEO varies from 2.22 to 2.63 million lb_m (1.01 to 1.19 million kg) over the range of insulation performance. This is an increase of 18.5% as compared to 39.7% for the nonvent mode. At the minimum staytime, the increase is only 8.6% for the partial-recondensation mode.

An interesting aspect of the effects of insulation performance is the relationship between the total propellant heat transfer and the penetration heat transfer. The latter encompasses the energy transferred by conduction through the tank support cone, the engine mount, the aft skirt, and the piping. Since the penetration heat transfer is independent of insulation performance, it can become the dominant mode of heat transfer when high-performance insulation is used on the tank wall. The ratio of penetration to total heat transfer is presented as a function of insulation thermal performance in Figure 4.1-12 for each of the vehicle stages. Even with the lowest-performance insulation, more than 30% of the heat transfer occurs through penetrations under the conditions given in the figure. With improved insulation performance, the percentage increases. For the Mars Departure Stage at the lowest $k\rho$ value, 96% of the total heat transfer is due to penetration.

4.1.1.3 Mars Orbit Altitude

The Mars orbit altitude influences the Mars vehicle from three different aspects. Most important of these is the variation of the mass of the Mars Excursion Module (MEM). As the altitude increases, the ΔV requirements for both descent and ascent increase, yielding the large variation in mass shown in Figure 3.2-5. Thermal environment variation ranks second in importance to the MEM mass variation. The planetary components of the incident thermal radiation, planet emission and albedo, decrease as the altitude increases while the solar component remains constant. This lessening of the intensity of the thermal environment results in reduced heat transfer to the Mars Departure Stage. The third, and least important aspect,

GENERAL DYNAMICS

Fort Worth Division

is the variation of the propulsive ΔV requirements for both the Mars braking maneuver and the Mars departure maneuver.

The influence of the MEM mass variation on the total vehicle IMIEO can be seen in Figure 4.1-13, where the zero-mass-fraction IMIEO and stage masses are presented as a function of altitude. These zero-mass-fraction data include only the propellant, payload, engine, and interstage masses. All propellant storage components (tanks, insulation, etc.) and heat transfer effects are neglected. The effect of ΔV variation for the Mars Braking and Mars Departure Stages is included. However, the increase of IMIEO with increasing altitude shown in Figure 4.1-13 demonstrates the dominance of the MEM mass, since the ΔV effects on both the Mars Braking and Departure Stages would be to decrease the IMIEO. The initial mass varies from 1.59 to 1.98 million lb_m (0.72 to 0.90 million kg), an increase of 390,000 lb_m (176,900 kg), while the MEM mass increase is only 128,000 lb_m (58,050 kg). The difference is the additional propellant required for the Earth Departure and Mars Braking Stages. The propellant requirement for the Mars Departure Stage follows the trend of the ΔV variation (Figure 6.2-1), decreasing initially at the low altitudes and then increasing slightly at the higher altitudes.

Variation of the Mars vehicle IMIEO with altitude is shown in Figure 4.1-14 for the vent mode. Note that the generally increasing trend is similar to that of the zero-mass-fraction vehicle. This trend is indicative of the dominance of the MEM mass variation over heat transfer effects. With low-performance insulation, the IMIEO rises from 2.63 to 3.05 million lb_m (1.19 to 1.38 million kg), an increase of 15.8%. With the highest-performance insulation, the initial mass increases by 21.5%, compared to 24.5% for the zero-mass-fraction vehicle.

The effects of heat transfer and propellant storage requirements can be isolated by examining the difference between the IMIEO for a given set of parameters and the zero-mass-fraction vehicle IMIEO. This difference is the propellant storage system penalty since it encompasses the propellant storage system components for all of the stages as well as the additional propellant requirements resulting from these items. This penalty is presented in Figure 4.1-15 as a percentage of the zero-mass-fraction IMIEO for the same conditions as in Figure 4.1-14. Also shown are the data for

GENERAL DYNAMICS

Fort Worth Division

the adiabatic tank wall case. The effects of heat transfer can be further isolated by comparing the propellant storage penalty for the vent mode with that for the adiabatic case. At the high $k\rho$ value (low insulation performance), the propellant storage system penalty decreases from 65.5% to 54.0% of the zero-mass-fraction IMIEO as the altitude increases from 216 n.mi (400 km) to the synchronous altitude of 9203 n.mi (17,053 km). Of this total penalty, approximately 9% would be incurred even if there were no heat transfer; the difference is then attributable solely to heat transfer. As the insulation performance improves, the propellant storage penalty is significantly reduced and the effect of altitude is also reduced. With the highest performance insulation studied, the propellant storage system penalty decreases from 18.3% to 15.6% over the altitude range. The decrease in storage penalty with altitude is due mainly to the less-severe thermal environment for the Mars Departure Stage at the higher altitudes. Increasing propellant loadings on the Earth Departure and Mars Braking Stages have some effect at the lower altitudes.

4.1.2 Influence of Propellant Storage Mode

From the data presented in Subsection 4.1.1, it is evident that propellant storage mode becomes an increasingly important factor as the propellant heat transfer increases. In terms of the parameters investigated in this study, the propellant heat transfer increases as a result of poorer insulation thermal performance, a more severe thermal environment, or increased Earth orbit staytime. The discussion in this subsection will be limited to the influence on the Mars vehicle IMIEO as a unit. More detailed discussion of the influence of storage mode will be presented in the subsections devoted to the individual stages.

The influence of propellant storage mode reaches a maximum for the condition of maximum Earth orbit staytime and minimum Mars orbit altitude for the unshielded vehicle. In Figure 4.1-16, the IMIEO for the vent and the partial-recondensation storage modes is compared at these conditions. The nonvent mode was not examined for these conditions, as explained earlier in this section. With the highest insulation performance, the difference in IMIEO between the modes is 4.1%. All three stages benefit from the partial-recondensation mode; the Mars Departure Stage

GENERAL DYNAMICS

Fort Worth Division

shows the greatest benefit in terms of the percentage reduction in initial stage mass. As the insulation performance worsens, the IMIEO percentage difference rises to 22.3% at the lowest insulation performance. This represents a mass difference of 519,000 lb_m (235,400 kg). At this condition, the Earth Departure Stage exhibits the largest percentage change in stage size. Note that the bulk of the change in IMIEO occurs in the upper range of $k\rho$ values. At the intermediate value of 7.5×10^{-5} Btu lb_m/hr-ft⁴-°R (2.08×10^{-3} W kg/m⁴-°K), the percentage difference in the IMIEO is 6.5%.

The only condition at which the nonvent mode was analyzed for all three stages is the high-altitude, shielded-vehicle case. Effect of propellant storage mode on the IMIEO at this condition is shown in Figure 4.1-17 for all three basic modes. Again, the insulation thermal performance is a determining factor in the storage mode effect. With high-performance insulation, the IMIEO difference between modes is small: at the lowest $k\rho$ value the percent difference is 1.3% between the nonvent and partial-recondensation modes. At the other extreme, the highest $k\rho$ value, the difference in IMIEO is 16.2% of the value for the nonvent mode. As before, the bulk of the increase in percentage difference occurs in the upper range of $k\rho$ values.

Thermal environment influences propellant storage mode effects to a small extent, as shown in Figure 4.1-18 where the vehicle propellant storage penalty to IMIEO is presented as a function of Mars orbit altitude. The decrease with altitude is mainly due to the Mars Departure Stage; there is little influence of altitude on propellant storage penalty for the Earth Departure and the Mars Braking Stages. Note that the effect is more pronounced for the vent mode than for the partial-recondensation mode. At the high $k\rho$ value, the penalty decreases from 65.5 to 54.1% over the altitude range for the vent mode. For the partial-recondensation mode, the penalty decreases from 40.4 to 36.2%. In addition, poorer insulation performance tends to amplify the environmental effects. The IMIEO variation for the same conditions is shown in Figure 4.1-19. Although the propellant storage penalty decreases with increased altitude, the IMIEO increases with altitude. This indicates again the dominance of the Mars Excursion Module mass variation with altitude over the thermal environment variation.

GENERAL DYNAMICS

Fort Worth Division

An increase in the length of the Earth orbital storage period also tends to increase the influence of storage mode. This is shown in Figure 4.1-7 for the shielded vehicle at the synchronous altitude. At the highest insulation performance, the IMIEO differences due to propellant storage mode are small, ranging from 0.5 to 1.25% over the range of staytimes. With the poorest insulation performance studied, the difference between the nonvent and the partial-recondensation modes increases from 4.0 to 19.3%.

4.1.3 Comparison of Shielded and Unshielded Vehicles

The purpose of deploying an inflatable solar shield is to reflect and reradiate a large portion of the radiant energy that would otherwise be incident upon the vehicle. This reduction of propellant heat transfer accomplishes mass savings in the propellant storage system of the stages involved and also in the propellant requirements of lower stages. As long as these savings exceed the IMIEO increase due to the solar shield system, the shield can be said to be effective. There are two general avenues by which thermal energy reaches the propellant. First, energy can travel by a complex heat transfer process involving conduction and radiation through the multilayer insulation to the tank wall and the propellant. Second, the energy can be conducted to the tank wall and propellant along solid conduction paths generally referred to as "penetrations." The solar shield affects both modes of energy transfer since it reduces the radiant energy incident upon the vehicle.

As used in this report, the term "shielded vehicle" refers to a vehicle which utilizes inflatable solar shields during the Mars transfer and the Mars orbit mission phases. A separate shield is required for each of the mission phases, since the shield cannot withstand the loads experienced during the Mars braking maneuver. Reference to the shielded vehicle also implies an orientation requirement different from the unshielded vehicle. During Mars transfer the vehicle longitudinal axis is oriented along the solar vector with the shield deployed from the aft end of the Mars Braking Stage (see Figure 3.2-3). This orientation is maintained except for two hours of guidance-correction during which a broadside orientation with full exposure to solar radiation is assumed. For the Mars orbit period, the vehicle

GENERAL DYNAMICS

Fort Worth Division

longitudinal axis is oriented along the solar vector with the shield deployed from the aft end of the Mars Departure Stage (see Figure 3.2-4).

In the unshielded case, the vehicle orientation is broadside to the sun during the entire Mars transfer period. During Mars orbit, the longitudinal axis is oriented along the velocity vector. In comparing the shielded and unshielded vehicles in this section, neither the shield system mass nor any additional attitude control system mass have been included in the shielded-vehicle mass data. Thus the beneficial differences in IMIEO indicated here will be offset to an extent determined by the mass of the solar shield system.

In this section, the shielded and unshielded vehicles will be compared with respect to overall effects on the Mars vehicle. Discussion of the effects on the Mars Braking and Mars Departure Stages individually is presented in Subsections 4.3 and 4.4, respectively. Performance criteria for the solar shield systems are discussed in Subsection 5.4.

The IMIEO of the shielded and unshielded vehicles is compared in Figures 4.1-20 and 4.1-21 for the vent and the partial-recondensation storage modes, respectively. Shielding yields significant reductions in IMIEO, especially with low-performance insulation. It also reduces slightly the variation of IMIEO with altitude. The actual differences in IMIEO are tabulated in Tables 4.1-1 and 4.1-2 for the vent and the partial recondensation modes, respectively. For the vent mode, the IMIEO difference at the high $k\rho$ value increases from 262,900 lb_m (119,200 kg) to 346,200 lb_m (157,000 kg), as the altitude increases. This increase is due mainly to the increased effectiveness of the Mars orbit shield in reducing the incident thermal radiation at the higher altitudes. At the lower altitudes, the planet-emitted thermal radiation is the dominant component of the incident radiation and the shield configuration is not effective in intercepting this component. As the altitude increases, the intensity of this component decreases and the direct solar component becomes dominant.

Although the Earth Departure Stage is not shielded, it furnishes the largest contribution to the IMIEO reduction, approximately 58%. The Mars Braking Stage accounts for roughly 30% of the difference, with the remaining 12%

GENERAL DYNAMICS

Fort Worth Division

Table 4.1-1 IMIEO DIFFERENCE BETWEEN THE SHIELDED
AND UNSHIELDED VEHICLES: VENT MODE

[1b_m]
[(kg)]

kρ , $\frac{\text{Btu lb}_m}{\text{hr-ft}^4 \cdot \text{°R}} \left(\frac{\text{W kg}}{\text{m}^4 \cdot \text{°K}} \right)$	Mars Orbit Altitude		
	216 n.mi (400 km)	3238 n.mi (6000 km)	9203 n.mi (17,053 km)
1.5x10 ⁻³ (4.16x10 ⁻²)	262,900 (119,200)	295,800 (134,100)	346,200 (157,000)
7.5x10 ⁻⁵ (2.08x10 ⁻³)	75,440 (34,210)	83,960 (38,080)	94,220 (42,730)
5.0x10 ⁻⁶ (1.39x10 ⁻⁴)	42,210 (19,140)	49,140 (22,290)	61,980 (28,110)

Table 4.1-2 IMIEO DIFFERENCE BETWEEN THE SHIELDED
AND UNSHIELDED VEHICLES: PARTIAL
RECONDENSATION MODE

[1b_m]
[(kg)]

kρ , $\frac{\text{Btu lb}_m}{\text{hr-ft}^4 \cdot \text{°R}} \left(\frac{\text{W kg}}{\text{m}^4 \cdot \text{°K}} \right)$	Mars Orbit Altitude		
	216 n.mi (400 km)	3238 n.mi (6000 km)	9203 n.mi (17,053 km)
1.5x10 ⁻³ (4.16x10 ⁻²)	116,300 (52,730)	137,400 (62,330)	165,900 (75,240)
7.5x10 ⁻⁵ (2.08x10 ⁻³)	36,490 (16,550)	43,000 (19,490)	49,560 (22,480)
5.0x10 ⁻⁶ (1.39x10 ⁻⁴)	20,440 (9270)	23,560 (10,680)	29,130 (13,210)

GENERAL DYNAMICS

Fort Worth Division

from the Mars Departure Stage. These percentages change only slightly with altitude. With higher-performance insulation, the difference in IMIEO drops substantially. At the intermediate $k\rho$ value, the IMIEO difference varies from 75,430 lb_m (34,200 kg) to 94,200 lb_m (42,700 kg) over the range of altitude. The percentage contributions to the IMIEO difference also change with insulation performance. The Earth Departure Stage now accounts for 49% of the IMIEO difference; the Mars Braking Stage, 29%; and the Mars Departure Stage, 22%. A further improvement in insulation performance reduces the IMIEO difference even further; the range of values is then 42,200 to 62,000 lb_m (19,140 to 28,120 kg). The Earth Departure Stage percentage contribution remains at 49%, while the Mars Braking Stage now accounts for only 20%, and the Mars Departure Stage contribution is roughly 30%. Note that as the insulation performance improves, the contribution of the Mars Departure Stage to the IMIEO difference between the unshielded and shielded vehicle increases. This is due to the long mission time of the Mars Departure Stage and the resulting high penetration heat transfer which is independent of insulation performance. The shields' effectiveness in reducing the penetration heat transfer becomes more noticeable as the insulation performance improves.

Influence of the solar shields on penetration heat transfer is presented in Figure 4.1-22. These values are total values (on a per-tank basis) and include the penetration heat transfer during Earth orbit where shields are not utilized. In the Mars Braking Stage case, the penetration heat transfer is reduced 41.5% by the shield and Mars orbit altitude has no effect on this quantity. For the Mars Departure Stage, however, orbit altitude plays a significant role. At the 216-n.mi altitude, the percentage reduction is 25.6%. As the altitude increases, the penetration heat transfer decreases, reflecting reductions in the amounts of planetary-emitted and albedo radiation incident upon the vehicle. The effectiveness of the shield also increases with increasing altitude, resulting in larger percentage reductions in penetration heat transfer at the higher altitudes. At the 3238-n.mi altitude, the reduction is 43.3%, while the reduction at the synchronous altitude is 57.7%. All of these values are based on the maximum Earth orbit staytime. The percentage reductions would be even higher at shorter staytimes.

GENERAL DYNAMICS
Fort Worth Division

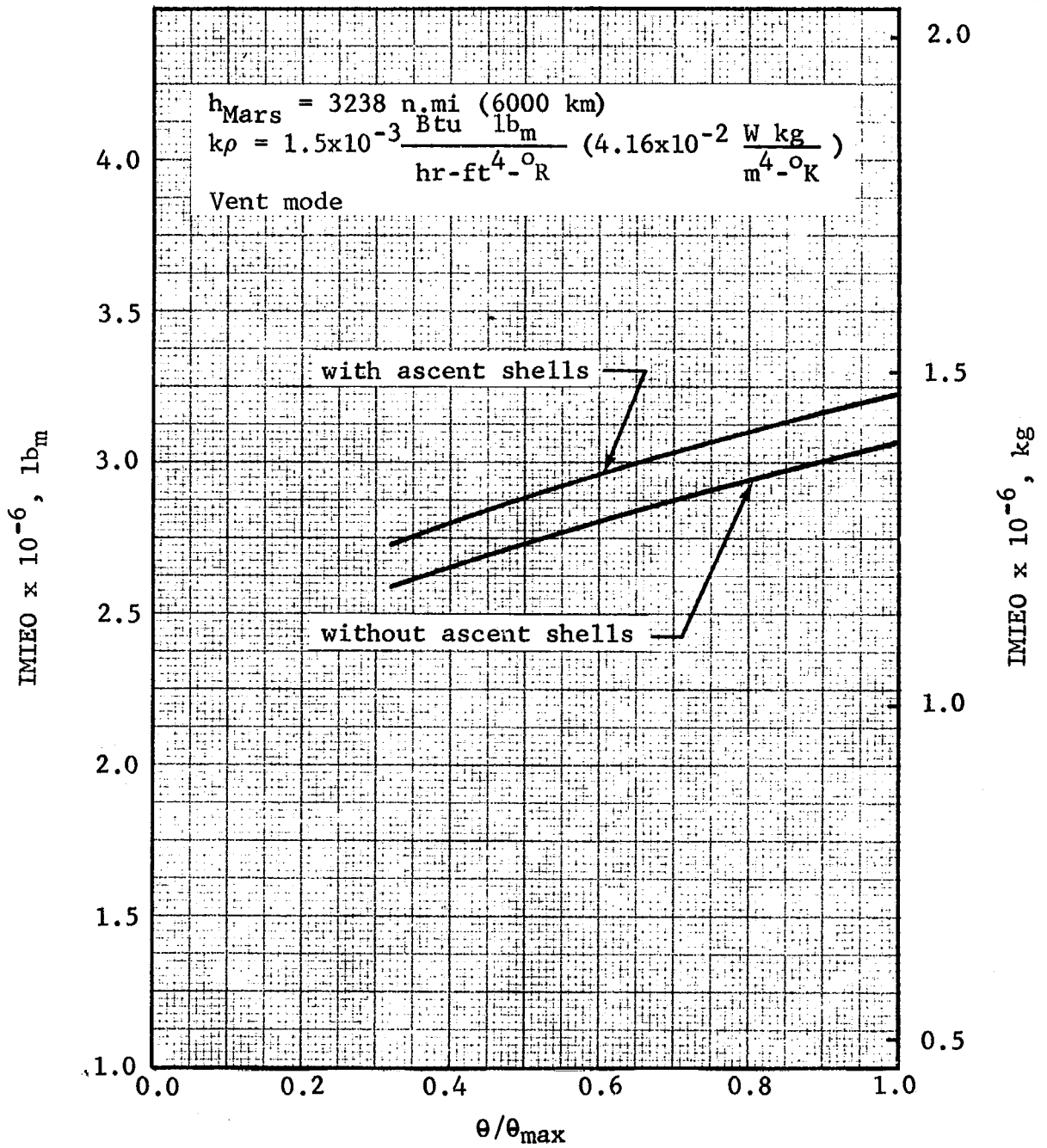


Figure 4.1-1 Effect of Ascent Shell Mass on IMIEO

GENERAL DYNAMICS
Fort Worth Division

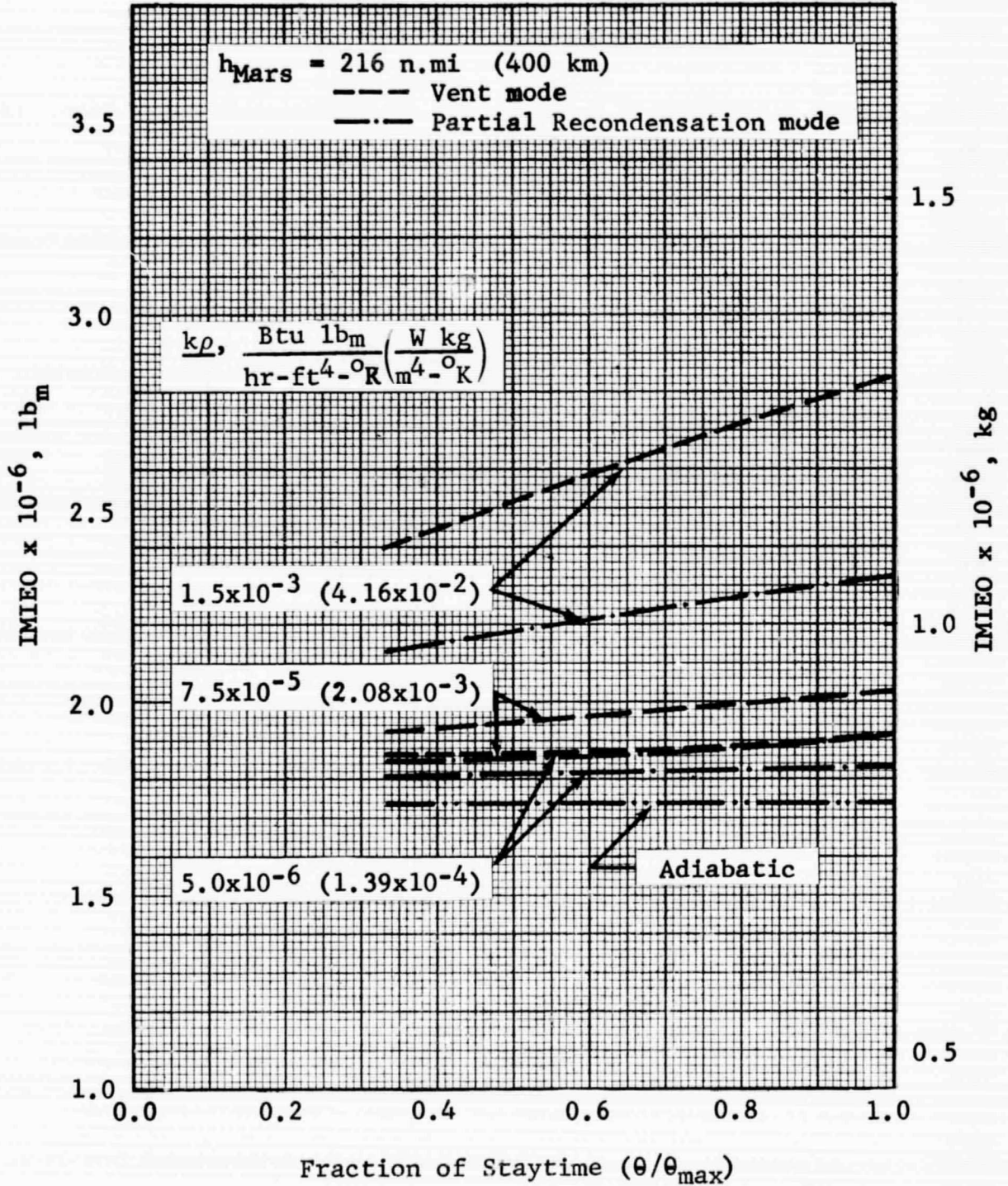


Figure 4.1-2 IMIEO of the Unshielded Mars Vehicle vs Staytime: $h_{Mars} = 216 \text{ n.mi}$

GENERAL DYNAMICS
Fort Worth Division

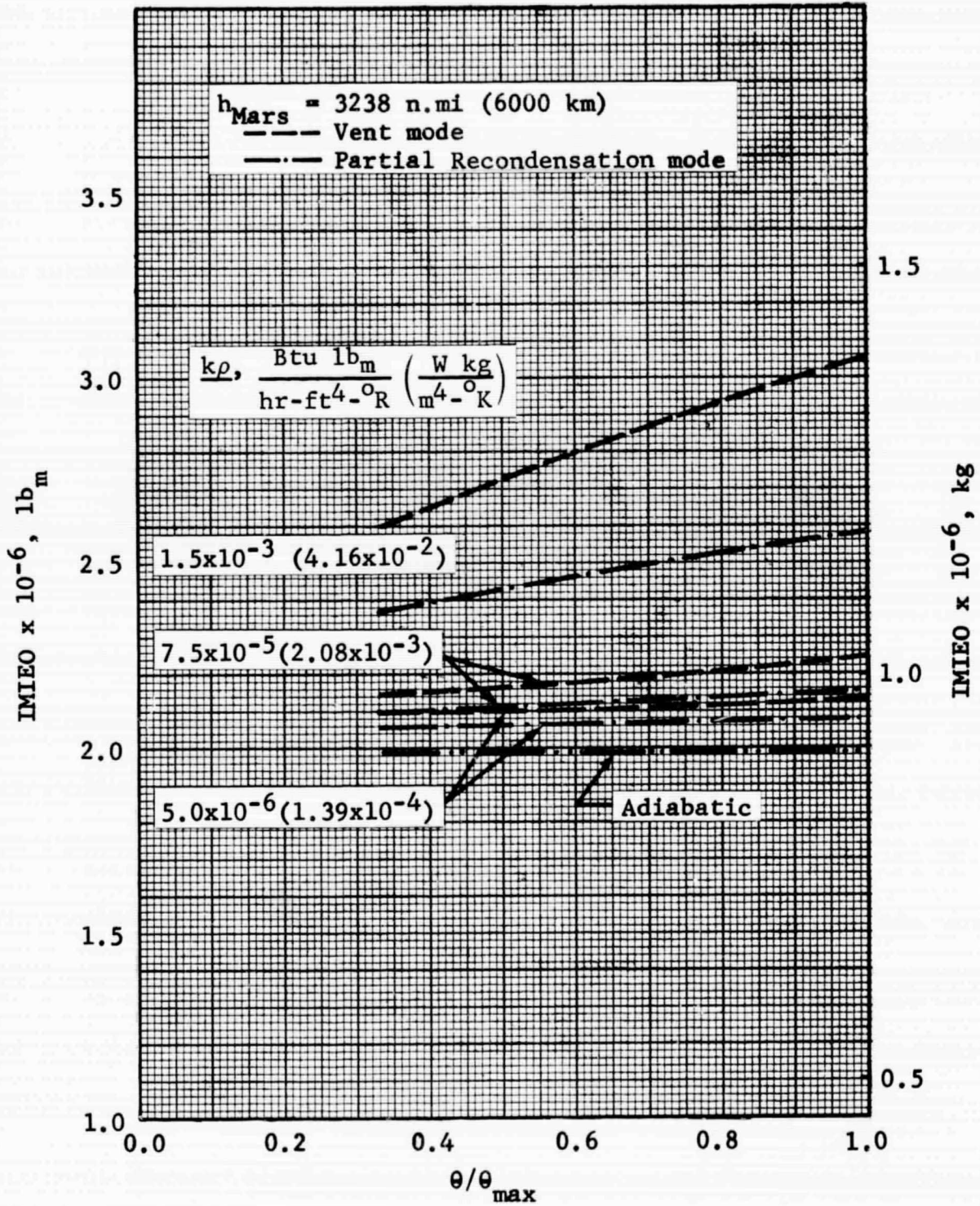


Figure 4.1-3 IMIEO of the Unshielded Mars Vehicle vs Staytime: $h_{Mars} = 3238 \text{ n.mi}$

GENERAL DYNAMICS
Fort Worth Division

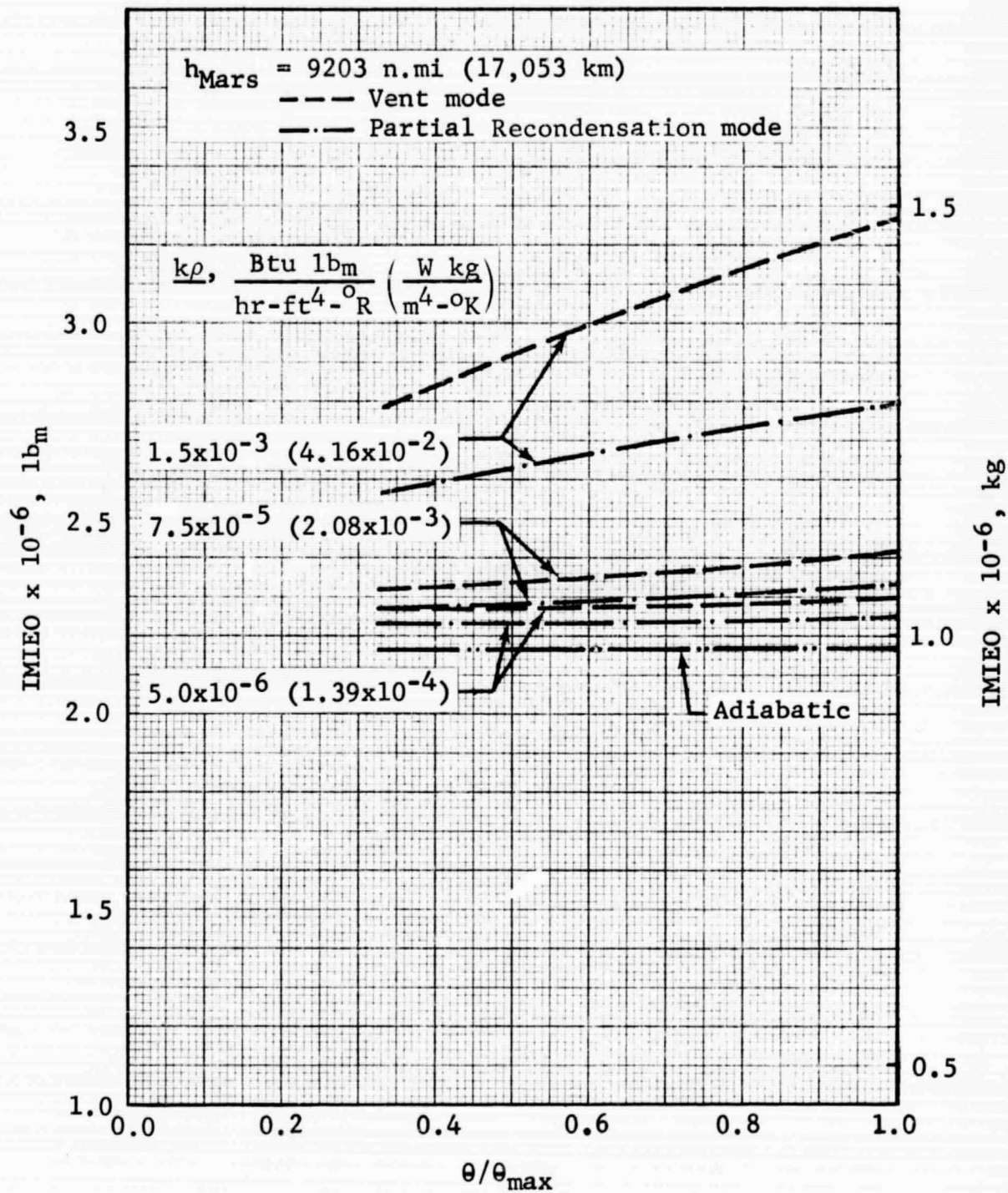


Figure 4.1-4 IMIEO of the Unshielded Mars Vehicle vs Staytime: $h_{\text{Mars}} = 9203 \text{ n.mi}$

GENERAL DYNAMICS

Fort Worth Division

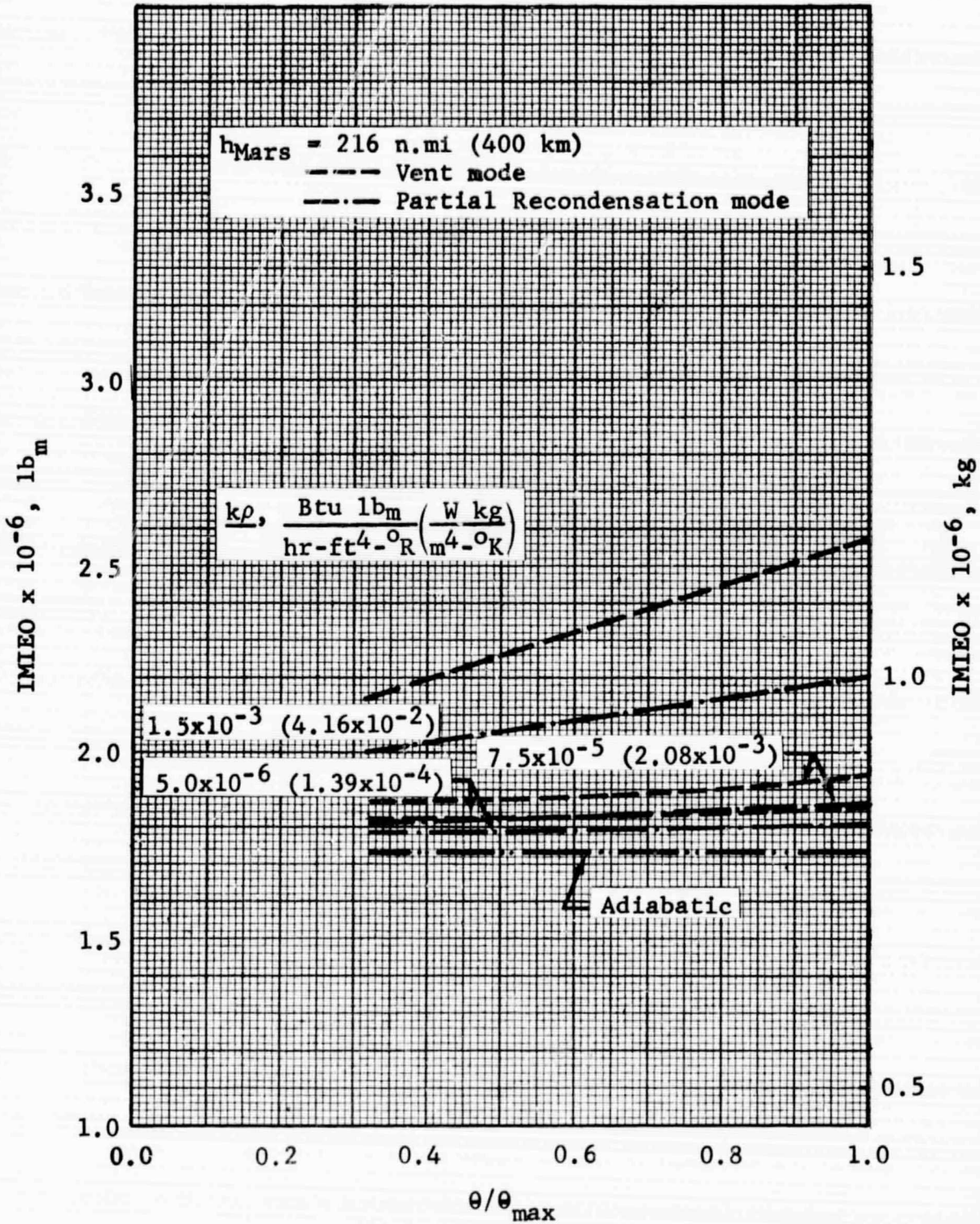


Figure 4.1-5 IMIEO of the Shielded Mars Vehicle vs Staytime: $h_{Mars} = 216 \text{ n.mi}$

GENERAL DYNAMICS
Fort Worth Division

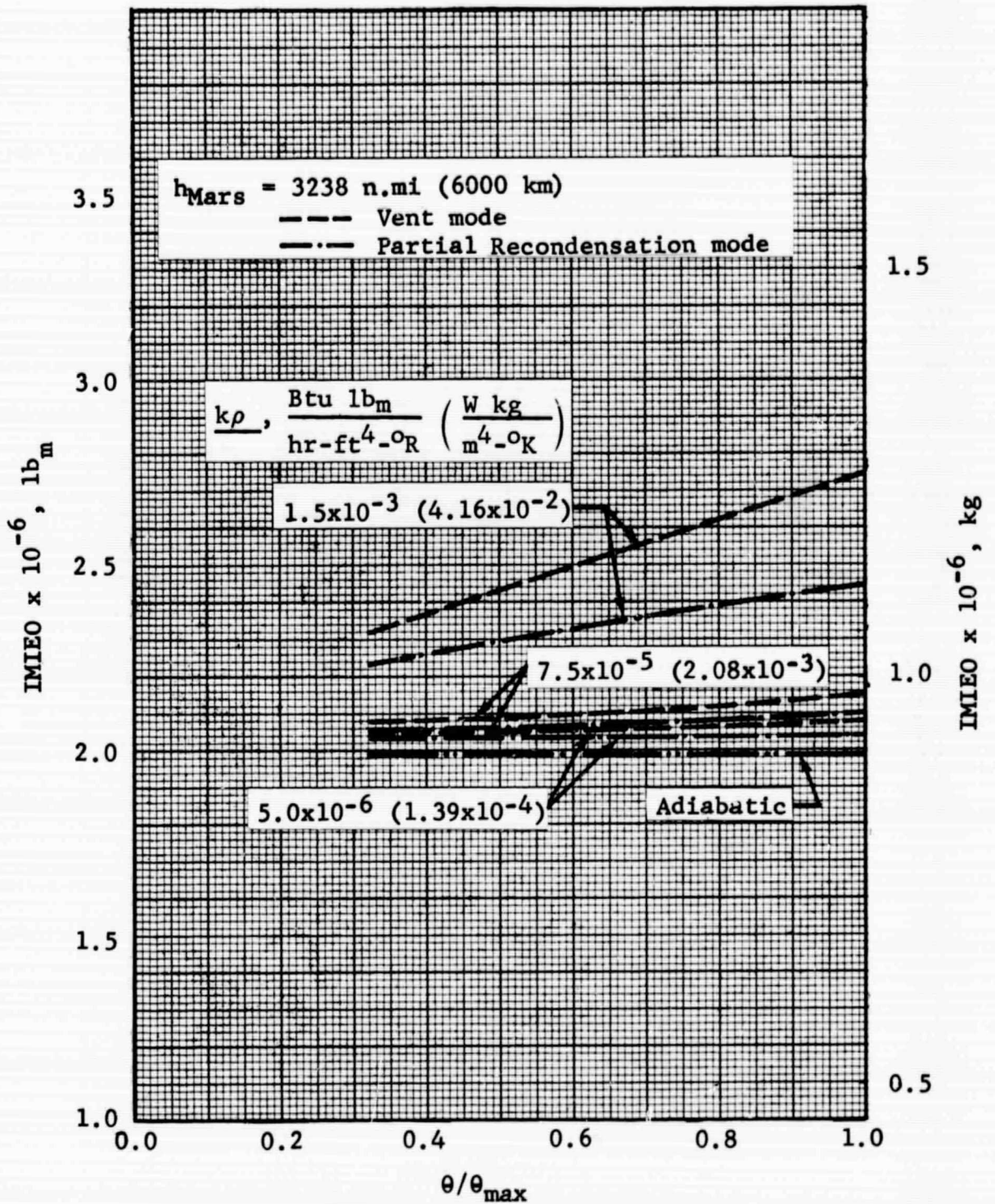


Figure 4.1-6 IMIEO of the Shielded Mars Vehicle vs Staytime: $h_{Mars} = 3238 \text{ n.mi}$

GENERAL DYNAMICS
Fort Worth Division

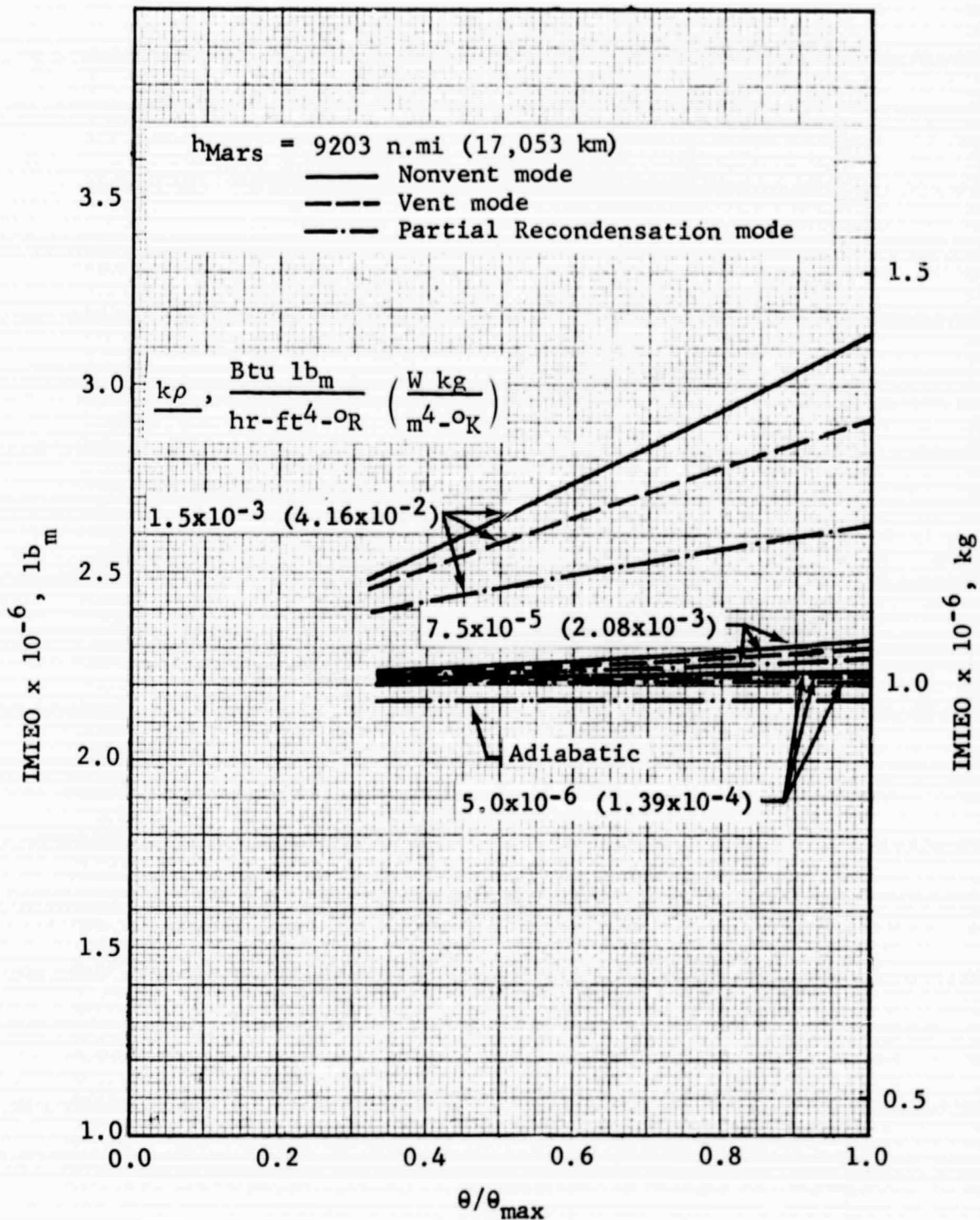


Figure 4.1-7 IMIEO of the Shielded Mars Vehicle vs Staytime: $h_{\text{Mars}} = 9203 \text{ n.mi}$

GENERAL DYNAMICS
Fort Worth Division

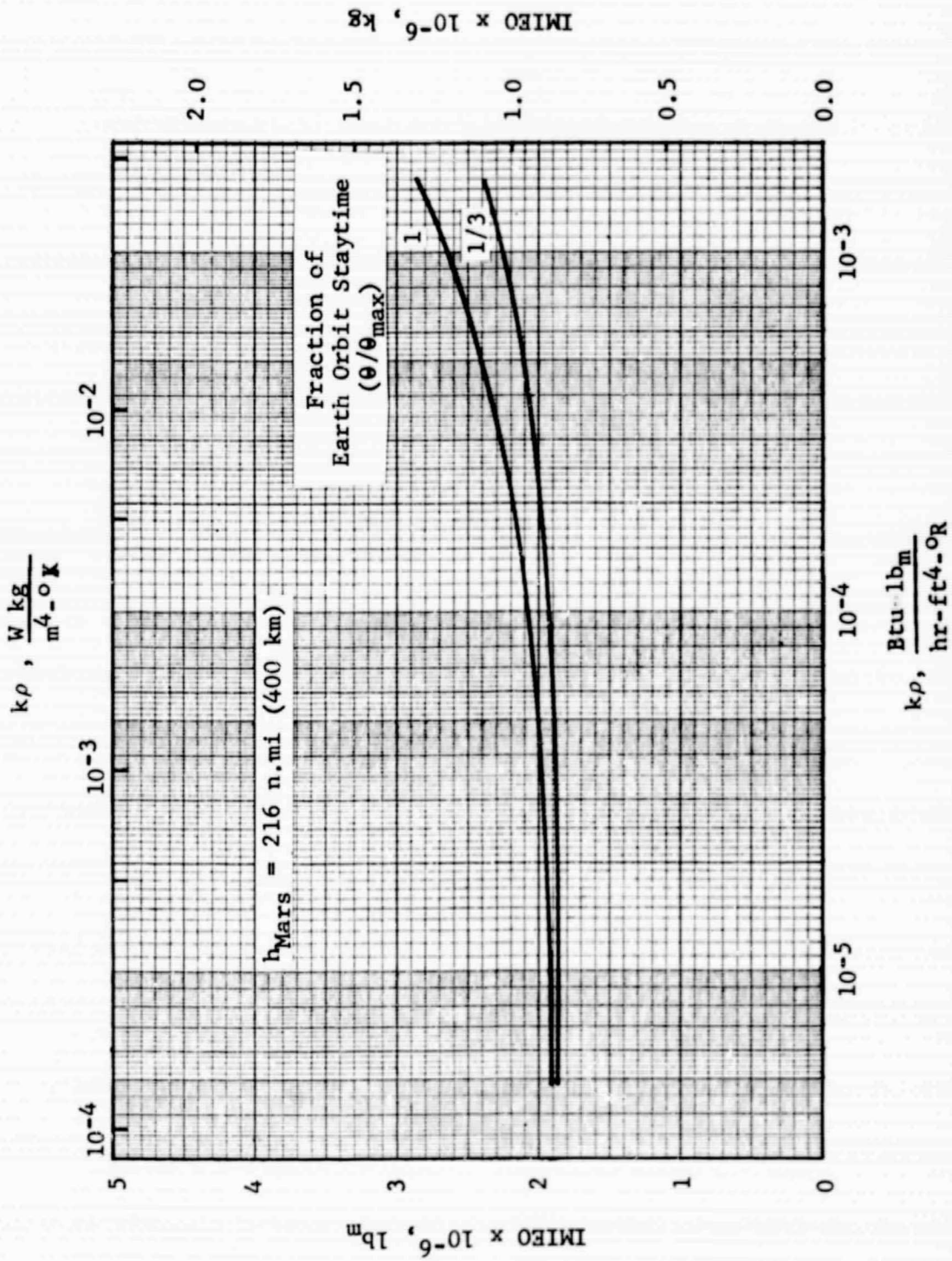


Figure 4.1-8 IMIEO Sensitivity to Insulation Thermal Performance: Vent Mode, Unshielded

GENERAL DYNAMICS
Fort Worth Division

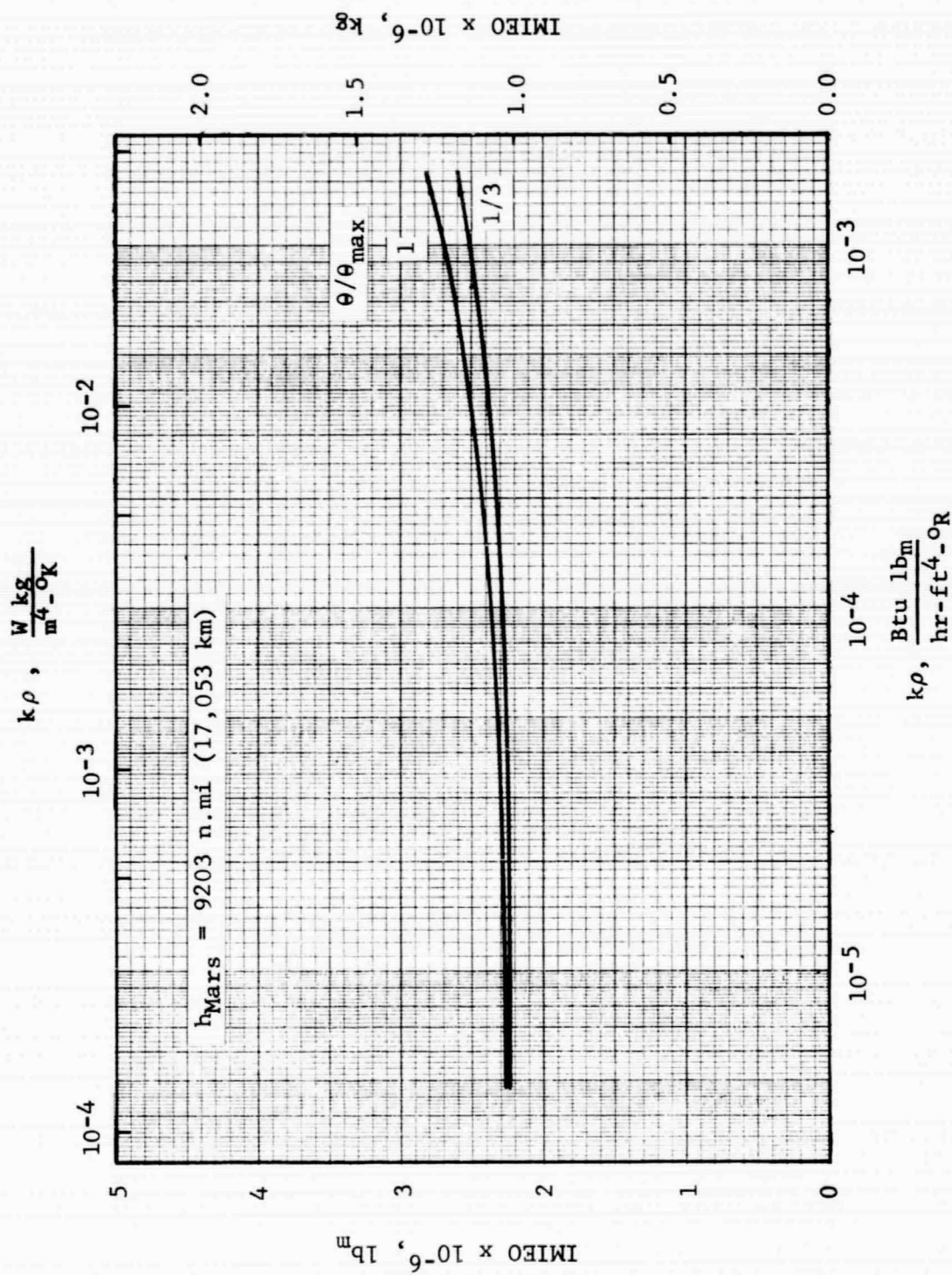


Figure 4.1-9 IMIEO Sensitivity to Insulation Thermal Performance:
Partial Recondensation Mode, Unshielded

GENERAL DYNAMICS
Fort Worth Division

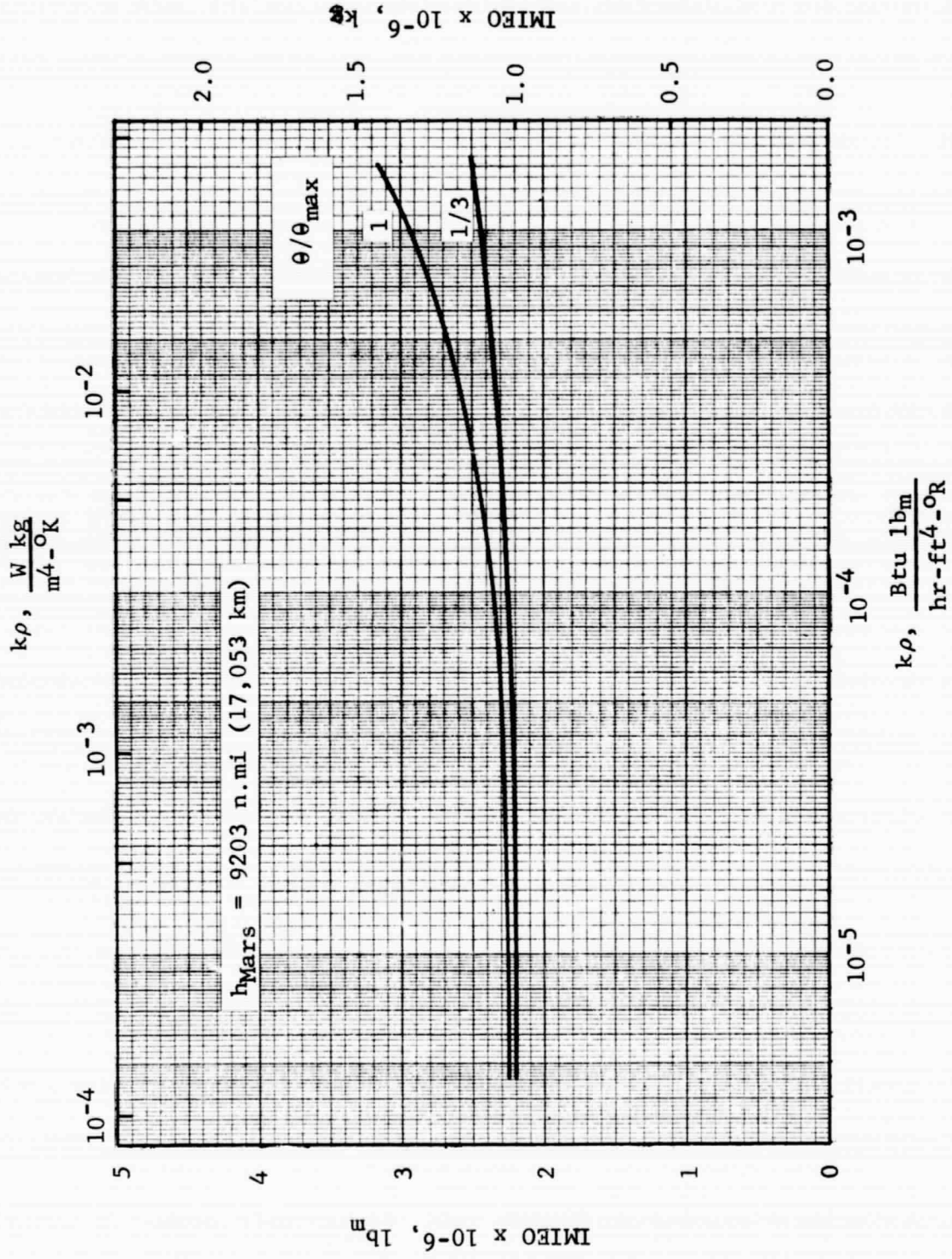


Figure 4.1-10 IMIEO Sensitivity to Insulation Thermal Performance: Nonvent Mode, Shielded

GENERAL DYNAMICS
Fort Worth Division

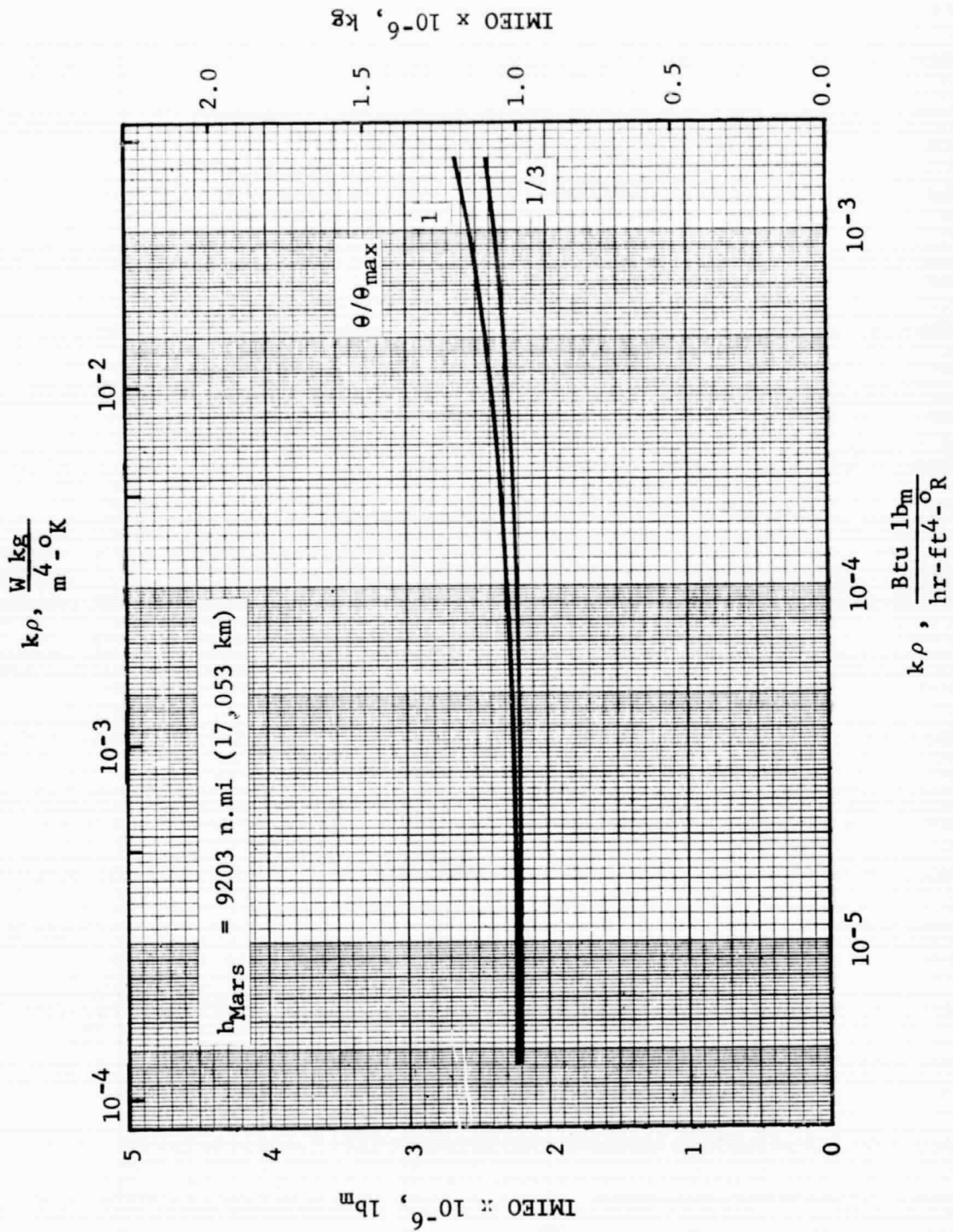


Figure 4.1-11 IMIEO Sensitivity to Insulation Thermal Performance:
Partial Recondensation Mode, Shielded

GENERAL DYNAMICS
Fort Worth Division

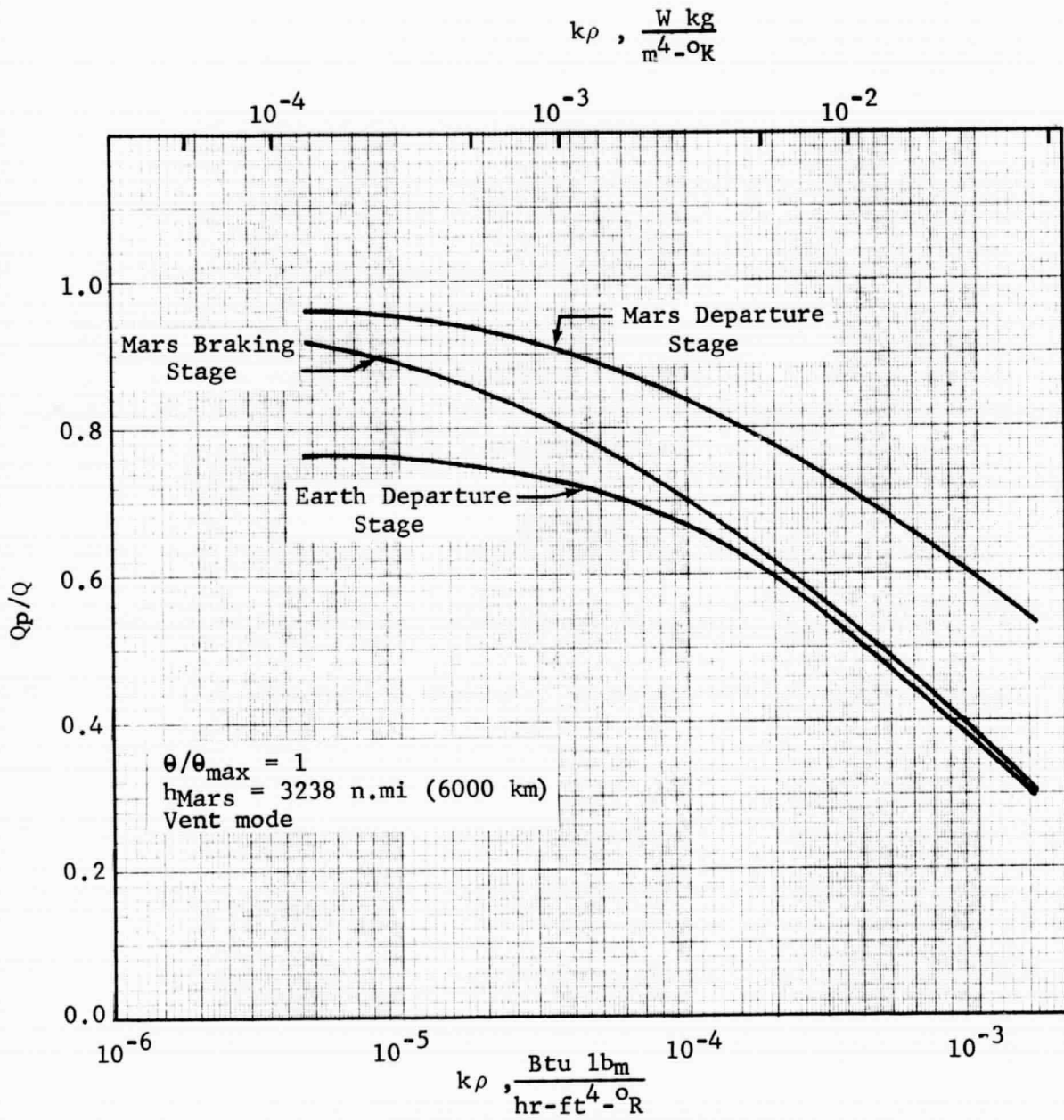


Figure 4.1-12 Ratio of Penetration Heat Transfer to Total Propellant Heat Transfer

GENERAL DYNAMICS

Fort Worth Division

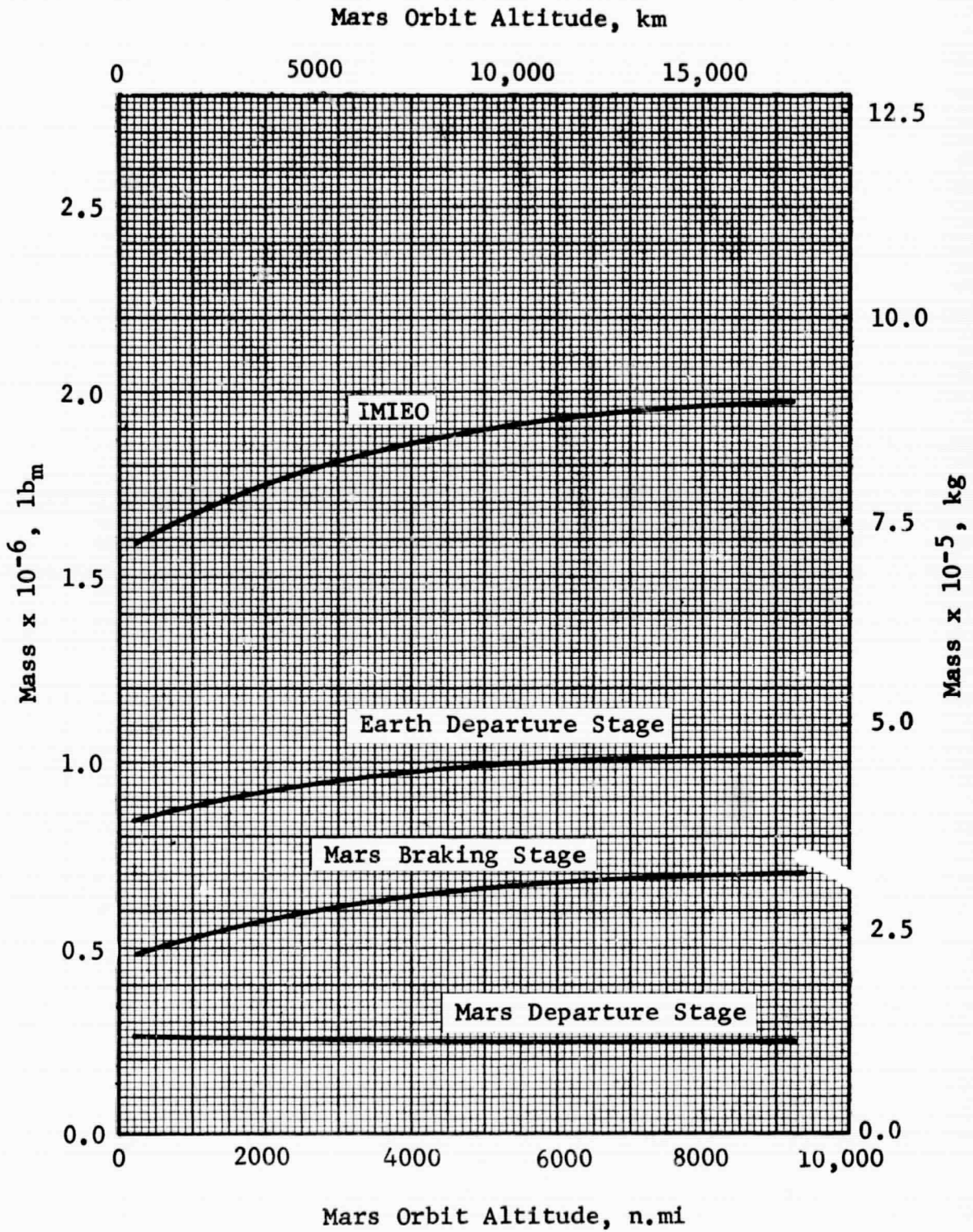


Figure 4.1-13 Effect of Altitude on Zero-Mass-Fraction IMIEO and Stage Masses

GENERAL DYNAMICS

Fort Worth Division

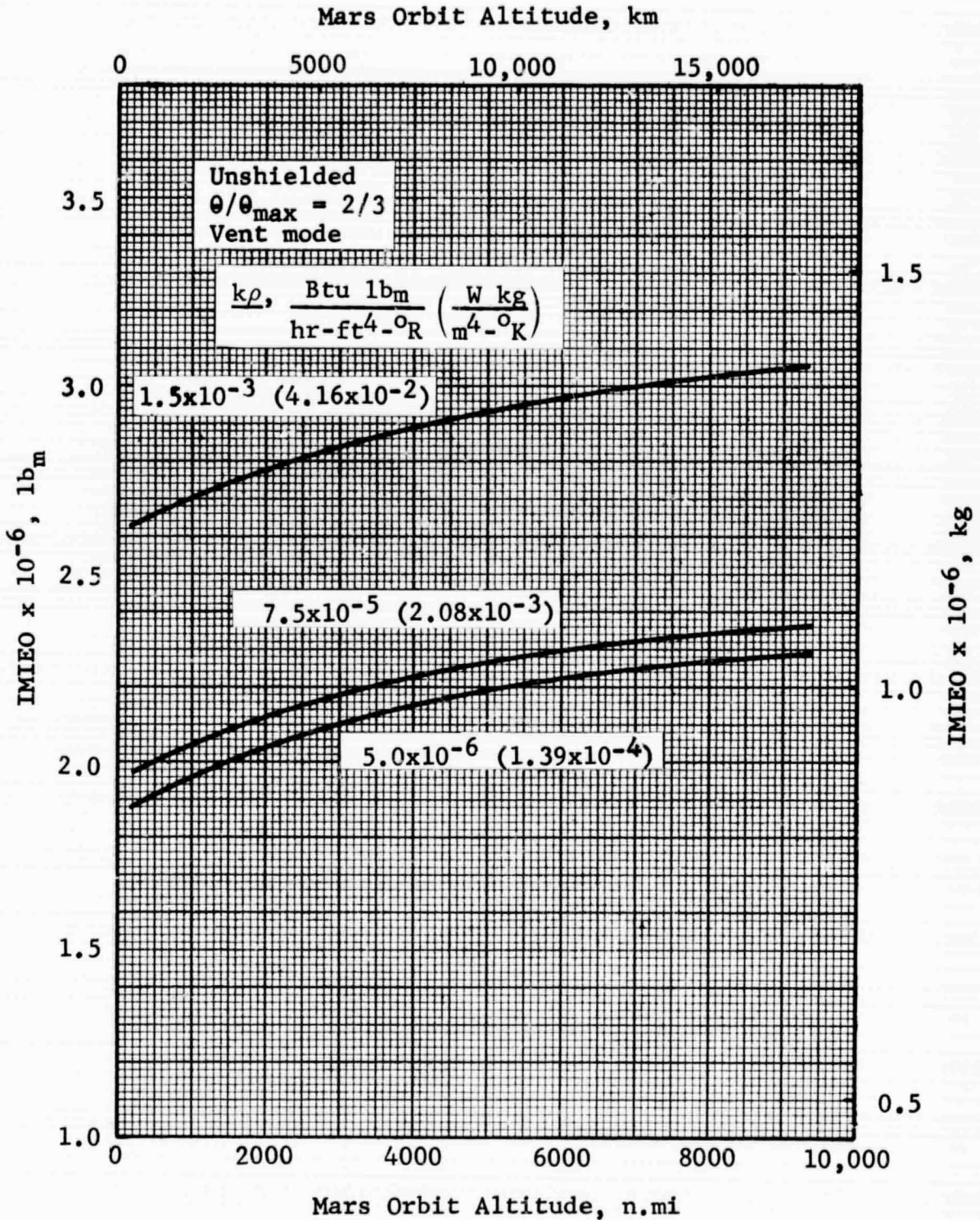


Figure 4.1-14 Effect of Altitude on Mars Vehicle IMIEO

GENERAL DYNAMICS

Fort Worth Division

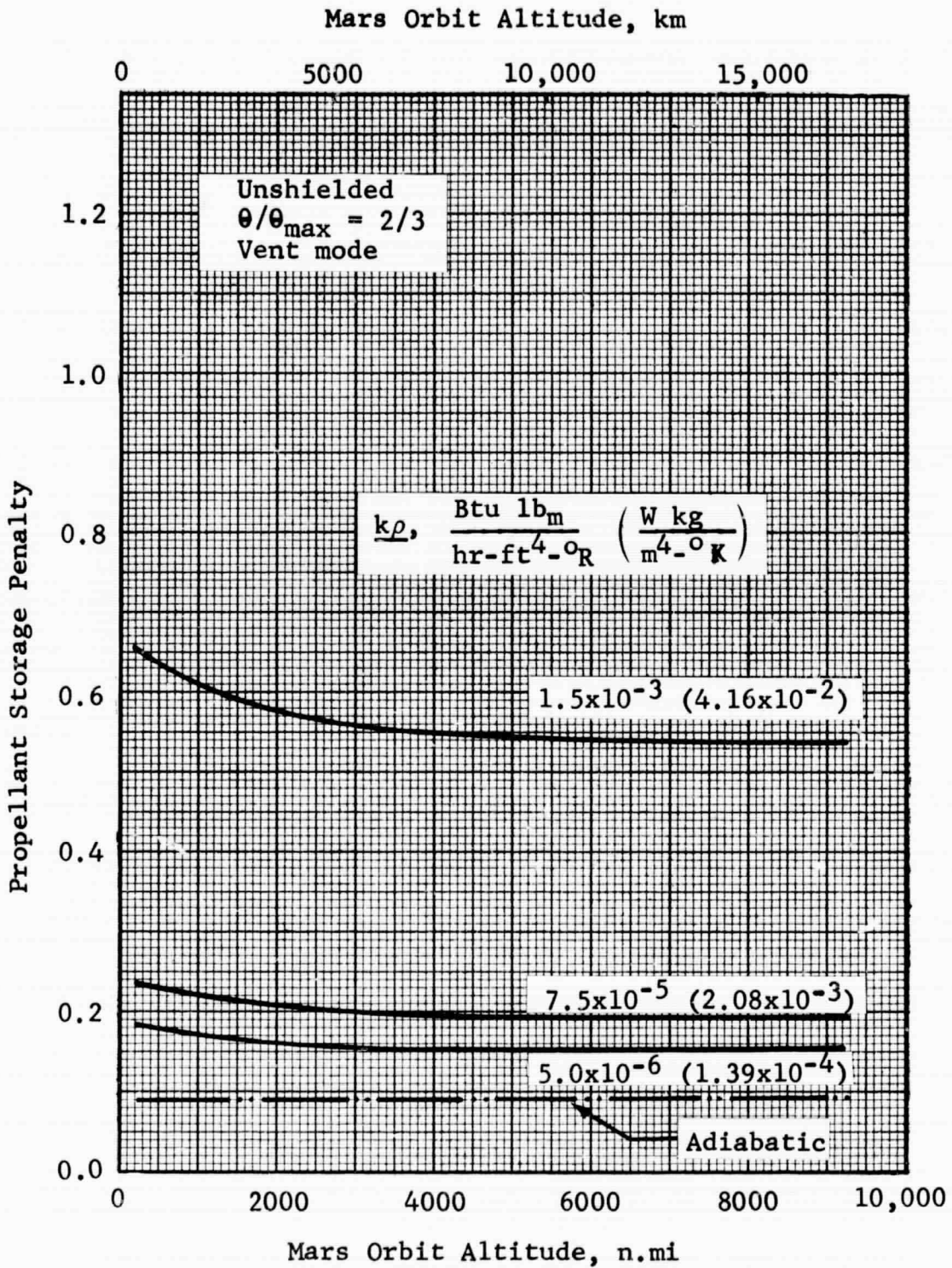


Figure 4.1-15 Effect of Altitude on Mars Vehicle Propellant Storage Penalty

GENERAL DYNAMICS
Fort Worth Division

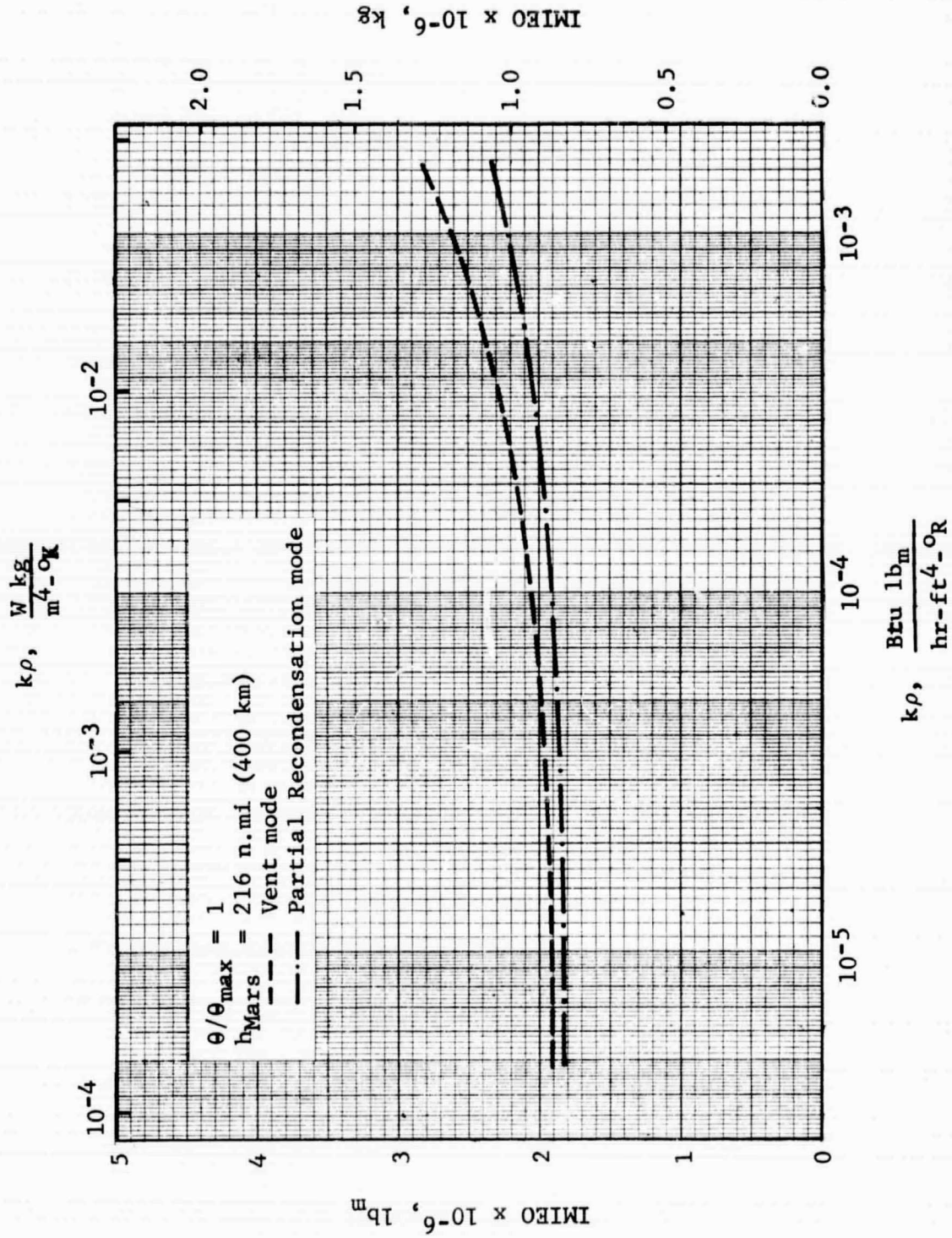


Figure 4.1-16 Effect of Propellant Storage Mode on IMIEO: Unshielded

GENERAL DYNAMICS
Fort Worth Division

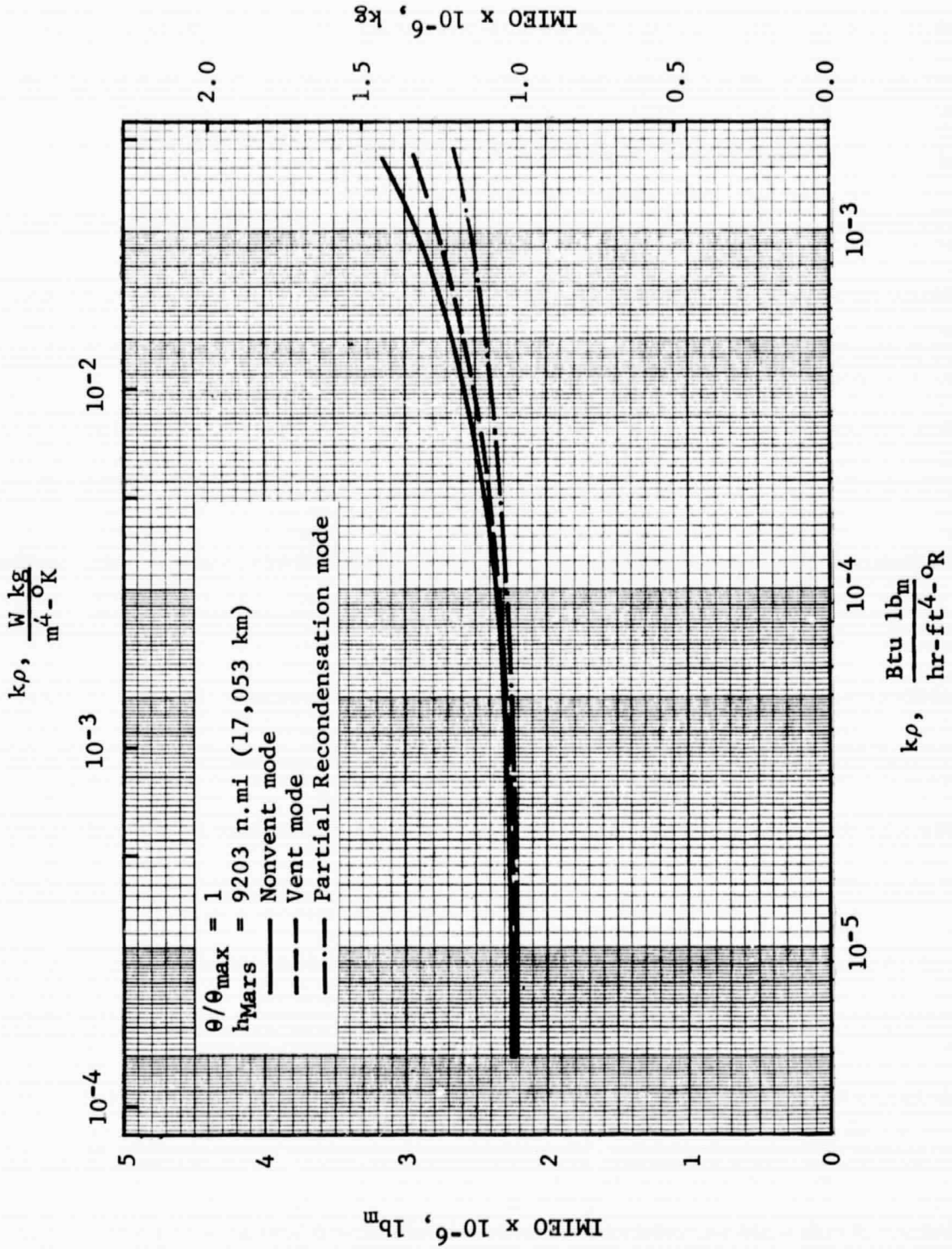


Figure 4.1-17 Effect of Propellant Storage Mode on IMIEO: Shielded

GENERAL DYNAMICS

Fort Worth Division

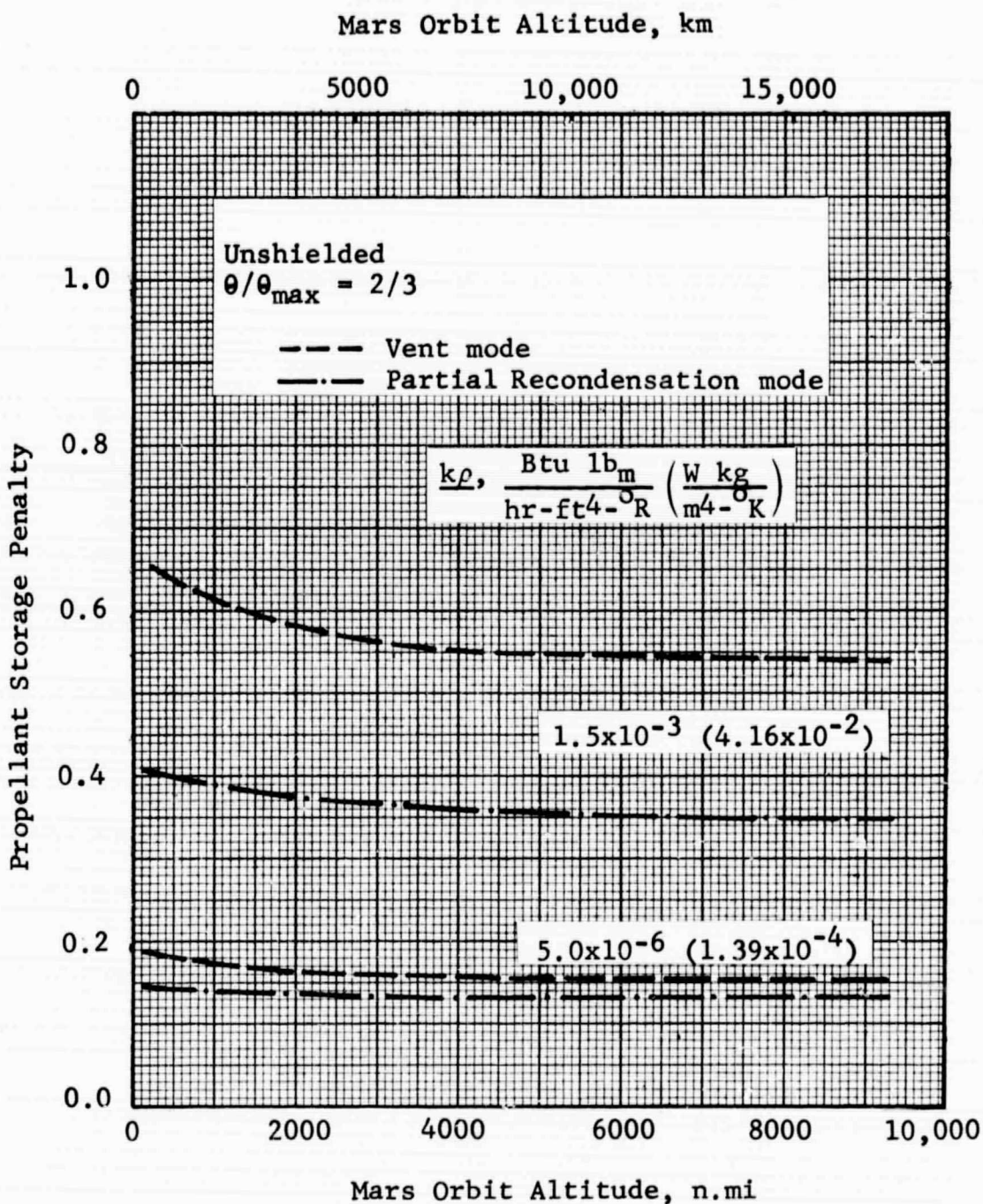


Figure 4.1-18 Effect of Propellant Storage Mode on Mars Vehicle Propellant Storage Penalty

GENERAL DYNAMICS
Fort Worth Division

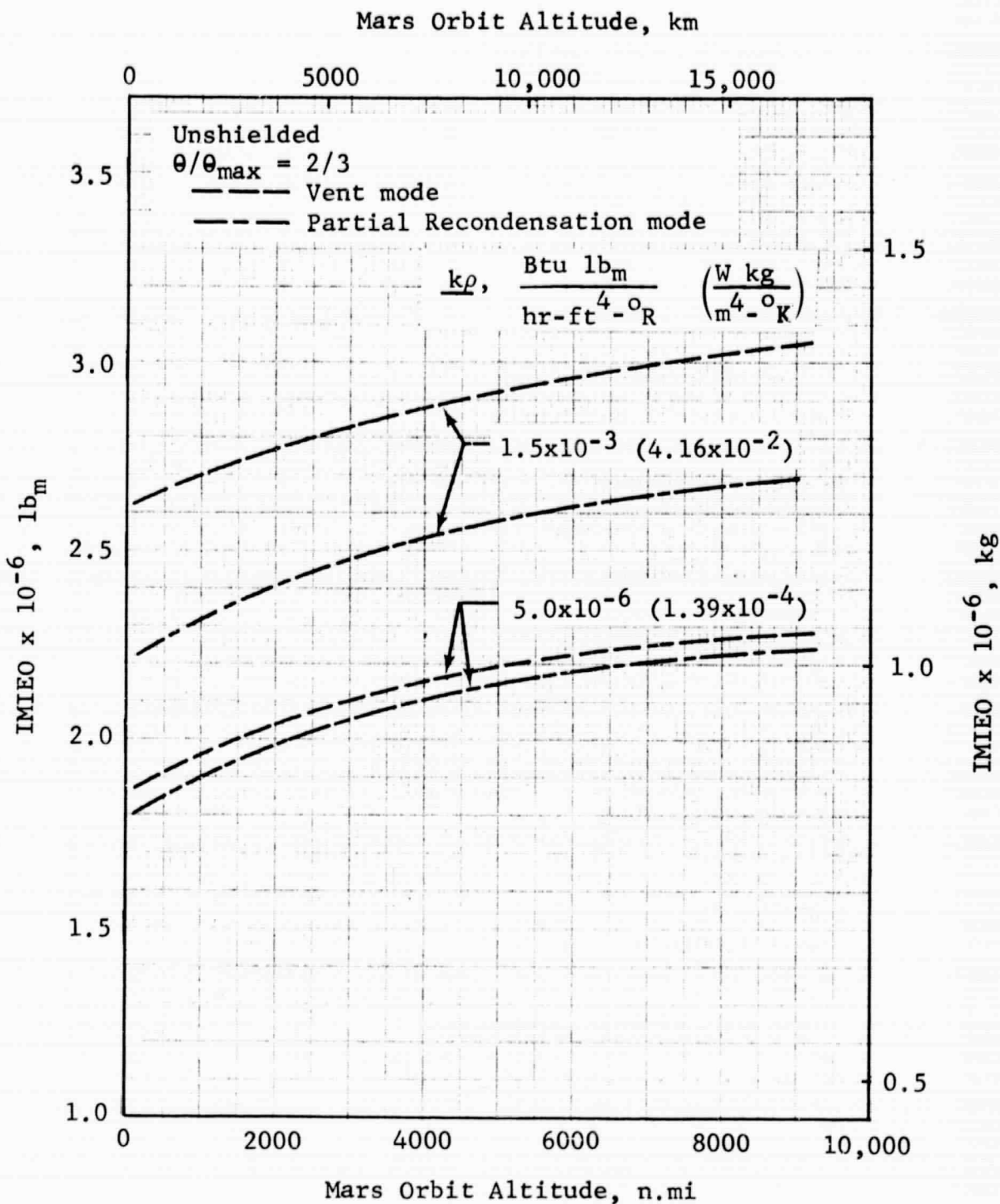


Figure 4.1-19 Mars Vehicle IMIEO vs Altitude: Vent and Partial Recondensation Modes

GENERAL DYNAMICS

Fort Worth Division

Mars Orbit Altitude, km

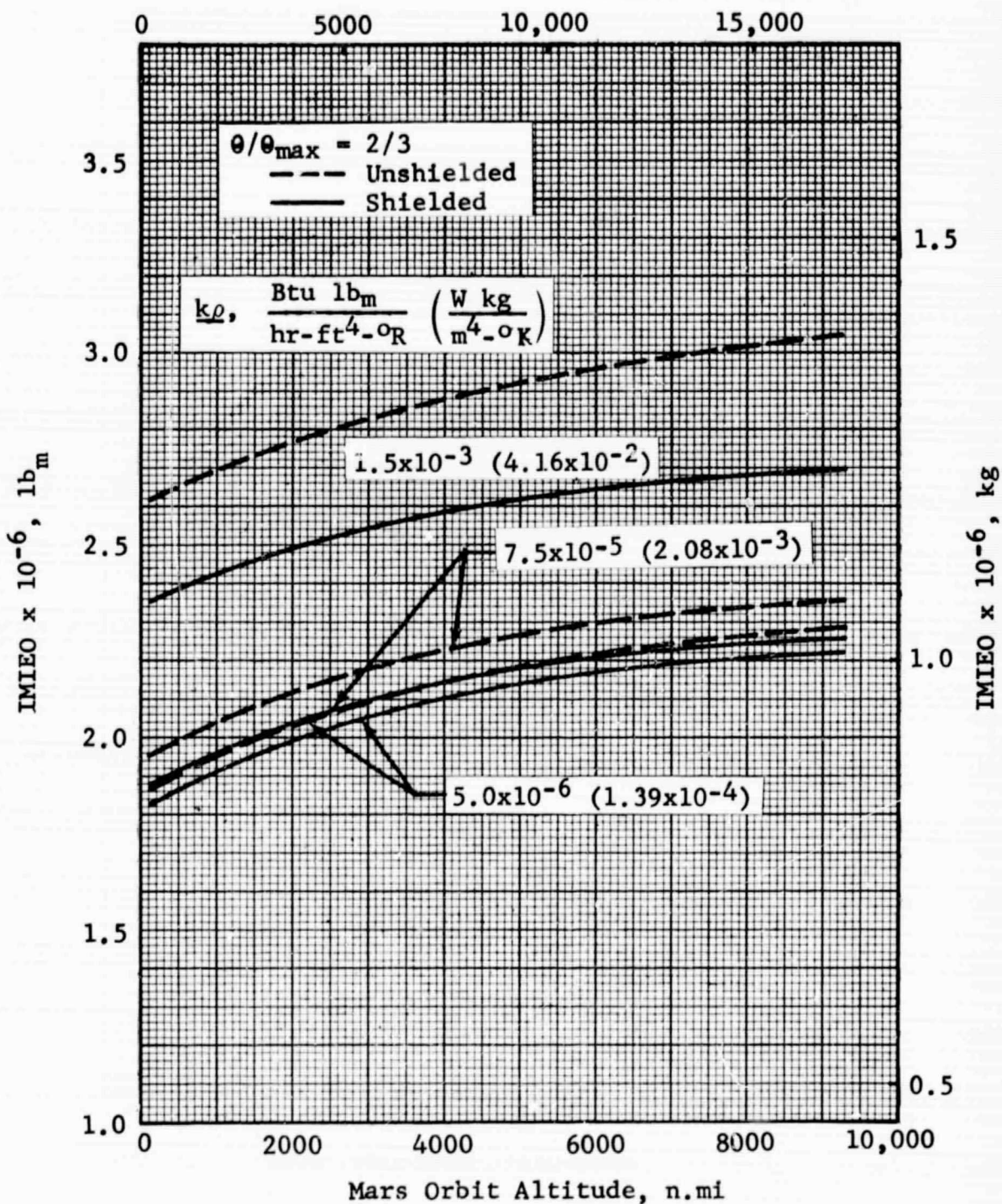


Figure 4.1-20 IMIEO Comparison of the Unshielded and Shielded Mars Vehicles: Vent Mode

GENERAL DYNAMICS
Fort Worth Division

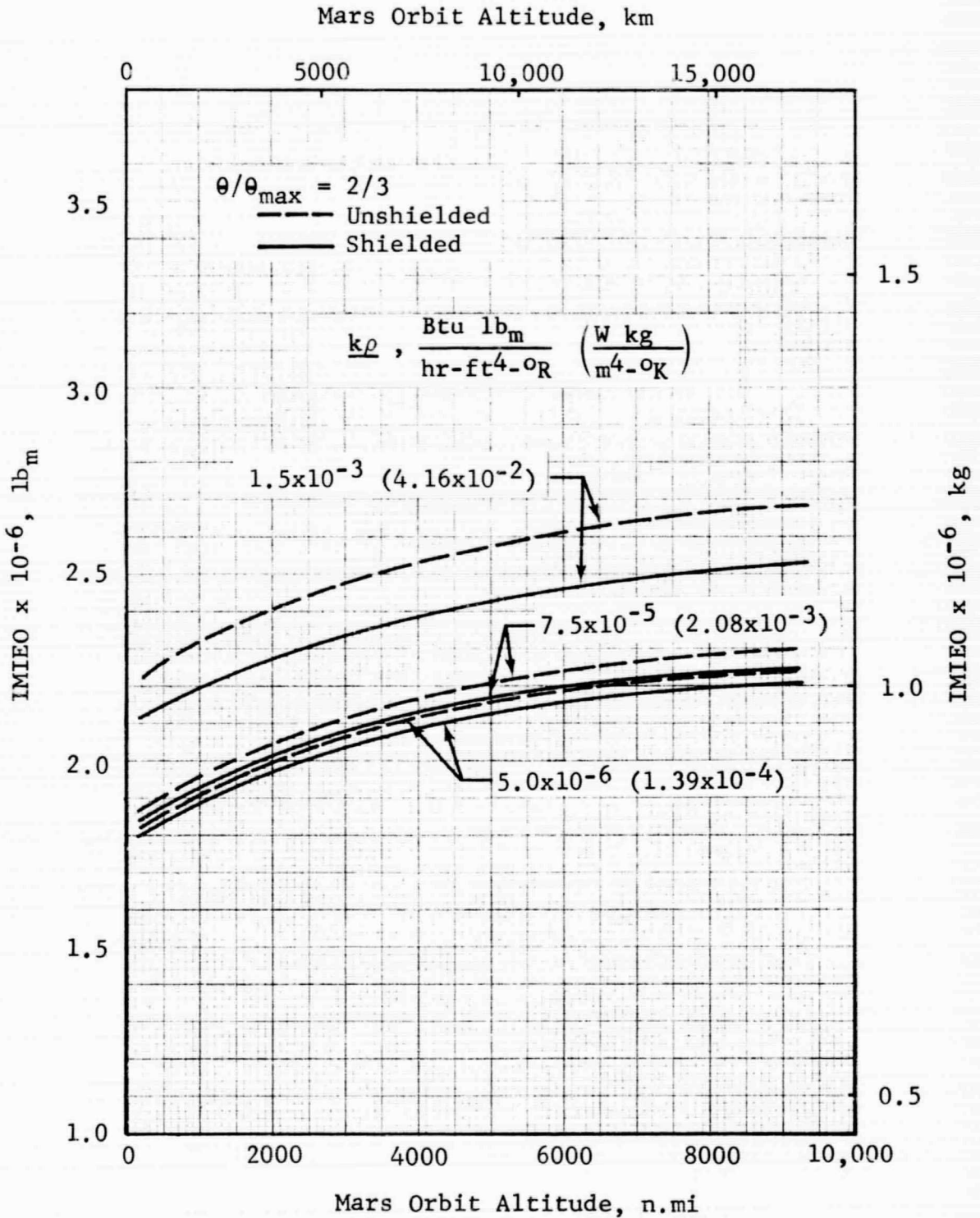


Figure 4.1-21 IMIEO Comparison of the Unshielded and Shielded Mars Vehicles: Partial Recondensation Mode

GENERAL DYNAMICS
Fort Worth Division

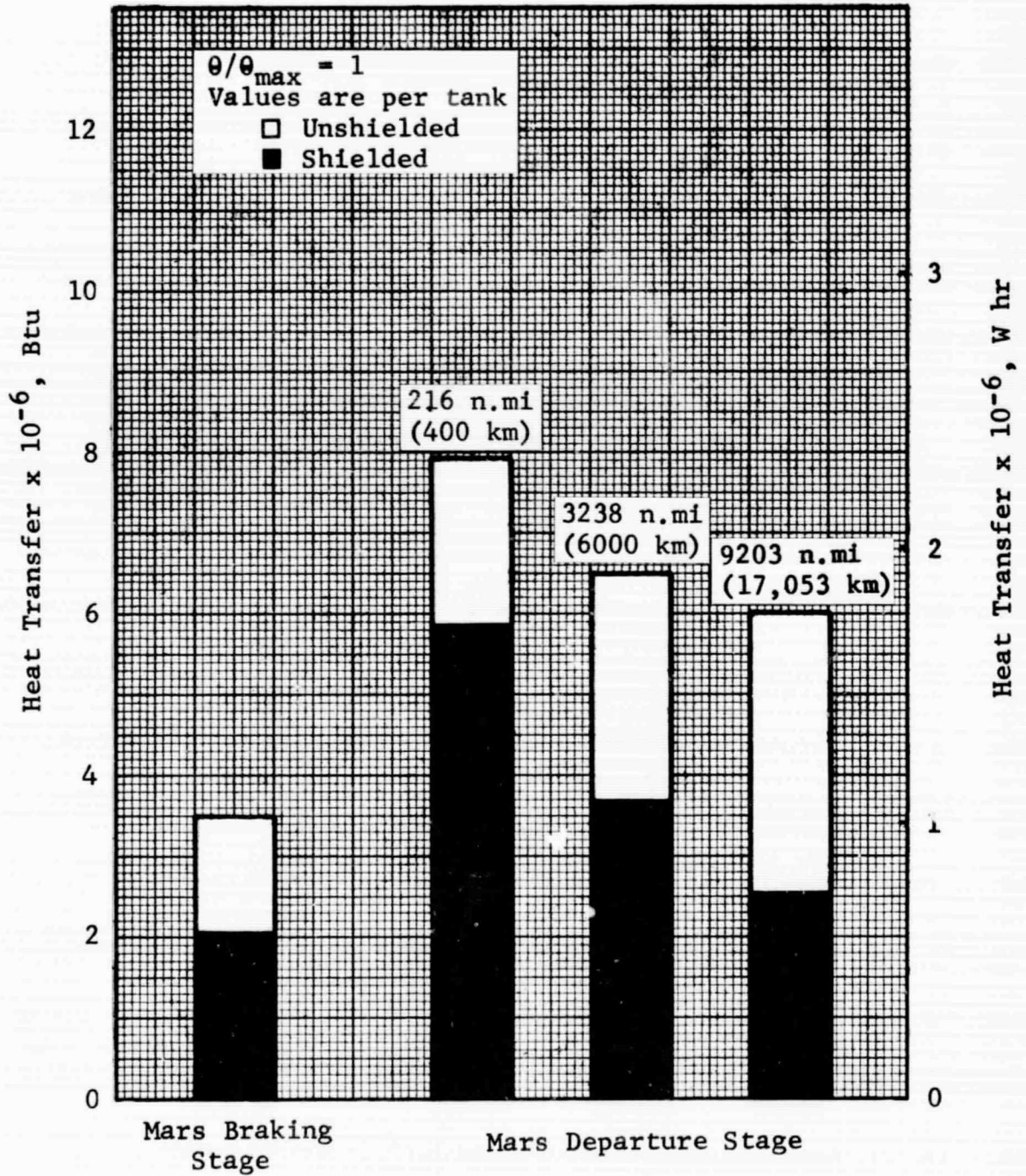


Figure 4.1-22 Effect of Solar Shield on Penetration Heat Transfer

GENERAL DYNAMICS

Fort Worth Division

4.2 EARTH DEPARTURE STAGE PROPELLANT STORAGE PENALTY

In this and the following two subsections, the discussion shifts from the total Mars vehicle to the individual stages; the discussion in this subsection is focused on the Earth Departure Stage. The effect of the various parameters and storage modes on the propellant storage penalty and the vehicle IMIEO is examined with respect to optimized propellant storage systems for the first or Earth Departure Stage. To isolate the effects of the Earth Departure Stage and still obtain IMIEO data, the Mars Braking and Departure Stages are treated in terms of nominal, constant mass fractions. Since variations in the Earth Departure Stage have no influence on the upper stages, the component masses of these stages actually remain constant through all of the parameter variations, with the exception of Mars orbit altitude. The effect of altitude on the Earth Departure Stage manifests itself only through the upper stages and the Mars Excursion Module; the ΔV requirements and the thermal environment of the Earth Departure Stage are independent of Mars orbit altitude. Thus, with respect to the first stage, altitude acts only to change the payload.

The propellant storage system of the Earth Departure Stage differs in one respect from that of the other stages in that an interplanetary meteoroid shield is not required. The mission of the Earth Departure Stage is of course limited to Earth orbit and the meteoroid protection requirements are met by the combination of the ascent shell and the tank wall. The ascent shell was not included in the optimization analysis since it would have little effect on the optimum insulation thickness. Therefore, the numerical results for the Earth Departure Stage presented in Volume 3 indicate a meteoroid protection mass of zero.

Propellant storage penalties in this subsection are referenced to a vehicle with a zero-mass-fraction Earth Departure Stage. The Mars Braking and the Mars Departure Stages of the reference vehicle are defined in terms of the same nominal mass fractions used to obtain the parametric data. The IMIEO variation with Mars orbit altitude for this vehicle is shown in Figure 4.2-1 as the curve labeled EDS. Also shown in the figure are the IMIEO variations for the cases where the Mars Braking Stage (MBS) and the Mars Departure Stage (MDS) are defined with a propellant storage

GENERAL DYNAMICS

Fort Worth Division

mass fraction of zero. In each case, the remaining two stages are defined with nominal mass fractions. The remaining curve in Figure 4.2-1 is the IMIEO variation when all stages are defined with zero mass fractions. This curve is identical to the IMIEO variation shown in Figure 4.1-13.

4.2.1 Sensitivity to Parameters

4.2.1.1 Earth Orbit Staytime

The propellant storage system of the Earth Departure Stage is more sensitive to Earth orbit staytime variations than that of any of the three stages. This is to be expected since the propellant heating history of this stage is limited to the Earth orbit mission phase. Propellant storage penalty to IMIEO for the Earth Departure Stage is presented in Figure 4.2-2 as a function of staytime for the 216-n.mi (400 km) Mars orbit altitude. The influence of staytime is seen to be strongly dependent upon the insulation performance and the propellant storage mode. With the highest performance insulation, the penalty ranges from 5.5 to 6.1% for the nonvent mode as the staytime increases from 90 to 270 days. This represents an increase of 11.4% attributable to an extended staytime. However, the curve for the adiabatic tank wall case indicates that a 5.1% penalty would be incurred regardless of staytime; this penalty represents the tank mass necessary to contain the propellant and the pressurant mass required to maintain a 5-psig (3.45 N/cm^2) net positive suction pressure during engine operation.

At the intermediate $k\rho$ value, the penalty for the nonvent mode rises from 6.0 to 9.3 percent, an increase of 54.5 percent. With this insulation performance, the vent and the partial-recondensation modes become definable at the longer staytimes and yield some reduction in penalty.

With the lowest performance insulation, the effect of staytime is greatly amplified; the penalty for the nonvent mode increases 143% from 12.6 to 30.6% over the range of staytime. Propellant storage mode also becomes an important factor at this condition. For the 270-day staytime, the penalty to IMIEO varies from 18.4% for the partial-recondensation mode to 26.2% for the vent mode and 30.6% for the

GENERAL DYNAMICS
Fort Worth Division

nonvent mode. Again, a 5.1% penalty would be incurred independent of staytime for the adiabatic case. The difference between this penalty and the values quoted above is then directly attributable to propellant heat transfer. Similar data are shown in Figures 4.2-3 and 4.2-4 for the Earth Departure Stage at the 3238-n.mi (6000 km) and 9203-n.mi (17,053 km) Mars orbital altitudes, respectively. The general trends with staytime are seen to be the same as in the low-altitude case. The effect of altitude will be discussed further in Subsection 4.2.1.3.

4.2.1.2 Insulation Thermal Performance

It was seen above that the insulation thermal performance strongly affects the propellant storage system penalty to IMIEO. This effect is shown more directly in Figure 4.2-5, where the propellant storage penalty is plotted as a function of insulation thermal performance for the nonvent mode. For the 90-day staytime, the penalty increases 121% over the range of insulation performance investigated. At the 270-day staytime, the percentage increase is more than three times the 90-day staytime value, reaching 382%. Note that the propellant storage penalty increases faster as the $k\rho$ value rises. Of the 382% increase in penalty at the 270-day staytime, only 42% occurs below the intermediate $k\rho$ value that is representative of the highest currently quoted multilayer insulation performance. This same trend is noticeable at the shorter staytimes.

The propellant storage penalty for the adiabatic tank wall condition, which represents the lower limit, is also shown in Figure 4.2-5. At the lower $k\rho$ values, this limit is closely approached, especially at the shorter staytimes. The figure also demonstrates that the Earth orbit staytime plays a strong role in determining the required insulation performance. For example, assuming an 8% propellant storage penalty is tolerable, the required insulation performance ranges from 5.8×10^{-5} to 3.3×10^{-4} Btu lb_m/hr-ft²-°R (1.6×10^{-3} to 9.15×10^{-3} W kg/m²-°K), depending upon the staytime. This can also be interpreted as a safety factor for the low-staytime case in that degradation of the insulation performance by a factor of 6 can be absorbed within the same 8% penalty.

Similar trends were found for the vent and partial-recondensation modes. The effect of propellant mode will be discussed in Subsection 4.2.2.

GENERAL DYNAMICS
Fort Worth Division

4.2.1.3 Mars Orbit Altitude

As mentioned earlier, Mars orbit altitude affects the Earth Departure Stage only through the upper stages and the vehicle payload. The propellant storage penalty to IMIEO is shown in Figure 4.2-6 as a function of the altitude for the 90-day staytime. At the low and intermediate $k\rho$ values, the penalty increases slightly with altitude. Under these conditions, the minimum tank design pressure of 19.7 psia is not exceeded and the increased penalty is due to a larger propellant loading at the higher altitudes. With low-performance insulation, the trend is reversed. In the nonvent mode, the minimum pressure is exceeded at the low altitudes and the tank mass fraction is therefore higher. As the altitude increases, the propellant loading increases, reducing the heat transfer per pound of propellant, and the tank pressure falls below the minimum design value. In the vent and the partial-recondensation modes, the variation in propellant loading affects the boiloff mass fraction, which decreases as the altitude increases, leading to a general decrease in propellant storage penalty.

With increased staytime, the total propellant heat transfer rises, causing some changes in the trends with the altitude. Figure 4.2-7 presents the propellant storage penalty as a function of altitude for the maximum staytime of 270 days. Note that the penalty now decreases or remains constant at all $k\rho$ values. The tank pressure exceeds the minimum design value at all conditions with the exception of the low- $k\rho$ -value, high-altitude combination where it is only slightly lower. In addition, the larger heat transfer results in the vent and the partial-recondensation modes being defined at the intermediate $k\rho$ value. At the high $k\rho$ value, the difference in penalty between storage modes is much increased.

The propellant storage penalties presented in Figures 4.2-6 and 4.2-7 show that the effect of Mars orbit altitude upon the propellant storage penalty of the Earth Departure Stage is relatively minor. Under some conditions the penalty rises slightly, while in other cases it decreases slightly. This is not to say that the total vehicle IMIEO follows the same trend. In fact, the IMIEO increases as the altitude increases in all cases, as shown in Figure 4.2-8 for the 270-day staytime. The trend is, of course, similar at the shorter staytime. The upward trend indicates that the Mars

GENERAL DYNAMICS
Fort Worth Division

Excursion Module is the dominant factor in the altitude variation.

4.2.2 Influence of Propellant
Storage Mode

The influence of propellant storage mode on the storage penalty is dependent upon the heat transfer to the propellant. As shown in Subsection 4.2.1.1, the differences in propellant storage penalty between modes grows larger as the insulation performance worsens and the staytime lengthens. Propellant storage penalties for the three basic storage modes are compared in Figure 4.2-9. The low-altitude, maximum-staytime condition is the worst case thermally, resulting in the maximum differences between modes. Only in the range of $k\rho$ values above the intermediate value does the effect of storage mode become significant. At the intermediate $k\rho$ value, the penalty ranges from 8.0% for the partial-recondensation mode to 9.3% for the nonvent mode. At the highest $k\rho$ value, the penalty ranges from 18.4% for the partial-recondensation mode to 26.2% for the vent mode and 30.6% for the nonvent mode.

At the higher altitudes, the differences between modes decrease. The vent and the partial-recondensation modes cannot be defined for the low $k\rho$ value and only at the maximum staytime for the intermediate $k\rho$ value. Increased propellant loadings provide a larger heat sink so that the vent pressure is not reached at the above conditions.

In comparing the propellant storage penalties for the basic storage modes, it is of interest to examine the contributions of the individual components of the propellant storage system. For the Earth Departure Stage, this system comprises the tank (including related structural mass that is proportional to tank mass), the insulation, the pressurant, and the propellant boiloff (vent and partial-recondensation modes only). The relation of the various component masses to the total propellant storage system mass is presented in Figures 4.2-10, 4.2-11, and 4.2-12 for the nonvent, vent, and partial-recondensation modes, respectively. The data are presented in the mass-fraction form, the particular component mass divided by the propellant loading. Since all tanks of a particular stage are identical, these mass fractions apply on either a stage basis or a tank basis. For the non-

GENERAL DYNAMICS
Fort Worth Division

vent mode (Fig. 4.2-10), the tank mass is the largest component mass over most of the range of $k\rho$ values. Insulation mass fraction is small at low $k\rho$ values, but increases rapidly and exceeds the tank mass fraction at the highest $k\rho$ value. The pressurant mass fraction is of the same order as the insulation mass fraction at low $k\rho$ values and rises slowly as the $k\rho$ value increases.

Tank mass is also the dominant component mass at low $k\rho$ values in the vent mode (Fig. 4.2-11) and the tank mass fraction remains approximately constant over the entire range of insulation performance. The insulation and boiloff fractions are small at the low $k\rho$ values, rise rapidly as the $k\rho$ value increases, and exceed the tank mass fraction at the highest $k\rho$ value. The insulation mass fraction exceeds the boiloff mass fraction except at the higher $k\rho$ values. The pressurant mass fraction is small and remains approximately constant. In the partial-recondensation mode (Fig. 4.2-12), the relationship between the component masses is similar to that of vent mode. However, the crossover point where the boiloff fraction begins to exceed the insulation mass fraction occurs at a lower value of the $k\rho$ product.

The tanking and combination propellant storage modes were not considered to be applicable to the Earth Departure Stage. In the tanking mode, the optimum insulation thickness cannot be defined since there is no heating period beyond Earth orbit upon which to base the optimization. Perhaps the optimum solution would be to launch dry tanks with very little insulation and provide the total propellant loading from an orbital tanker just prior to Earth departure. However, this is not considered to be feasible with pressure-stabilized tanks at present. The combination mode with respect to the Earth Departure Stage is functionally identical to the vent mode since the mission is limited to Earth orbit. However, as in the tanking mode case, the optimum insulation thickness cannot be defined.

GENERAL DYNAMICS
Fort Worth Division

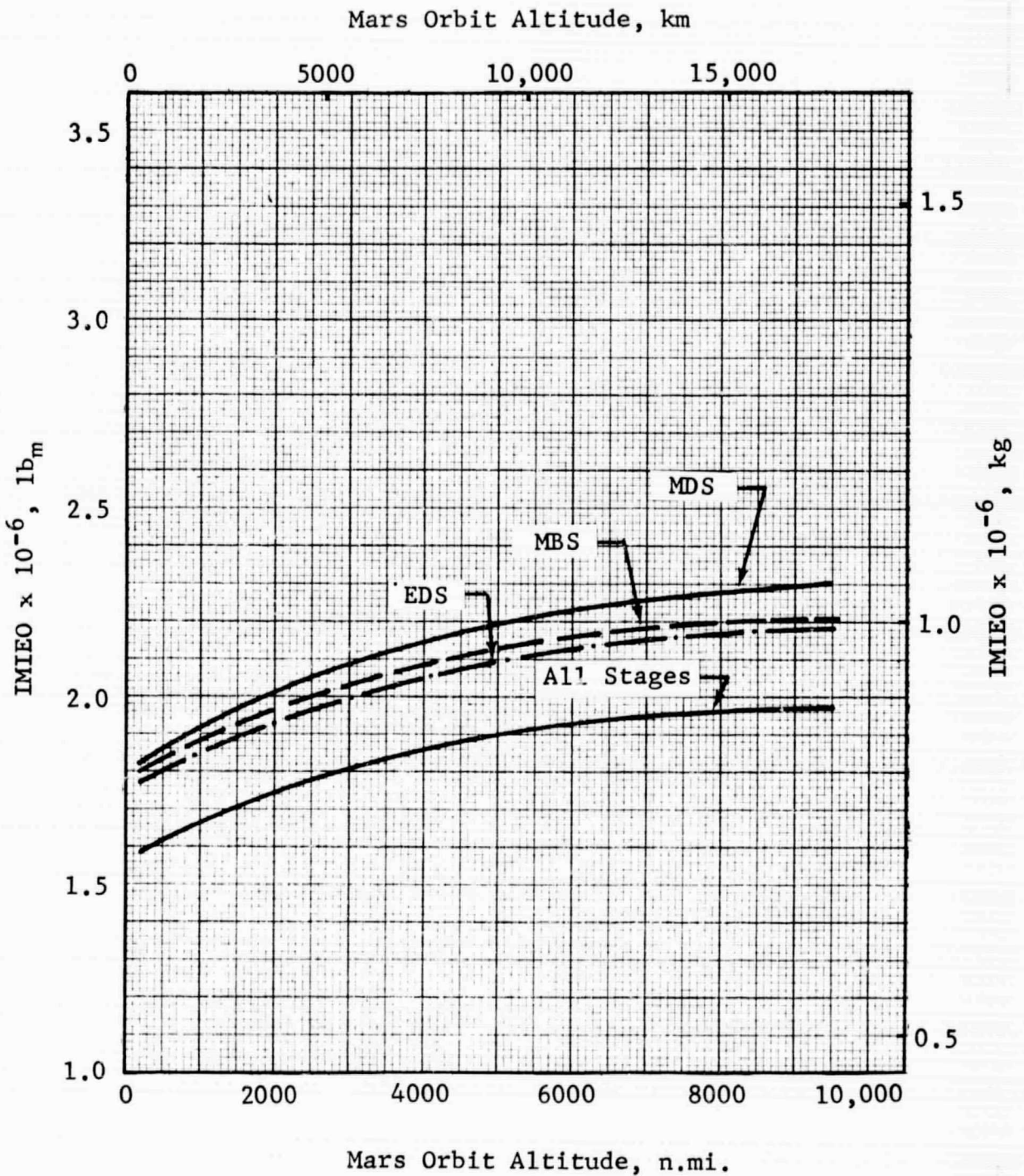


Figure 4.2-1 Effect of Zero-Mass-Fraction Stage on Mars Vehicle IMIEO

GENERAL DYNAMICS
Fort Worth Division

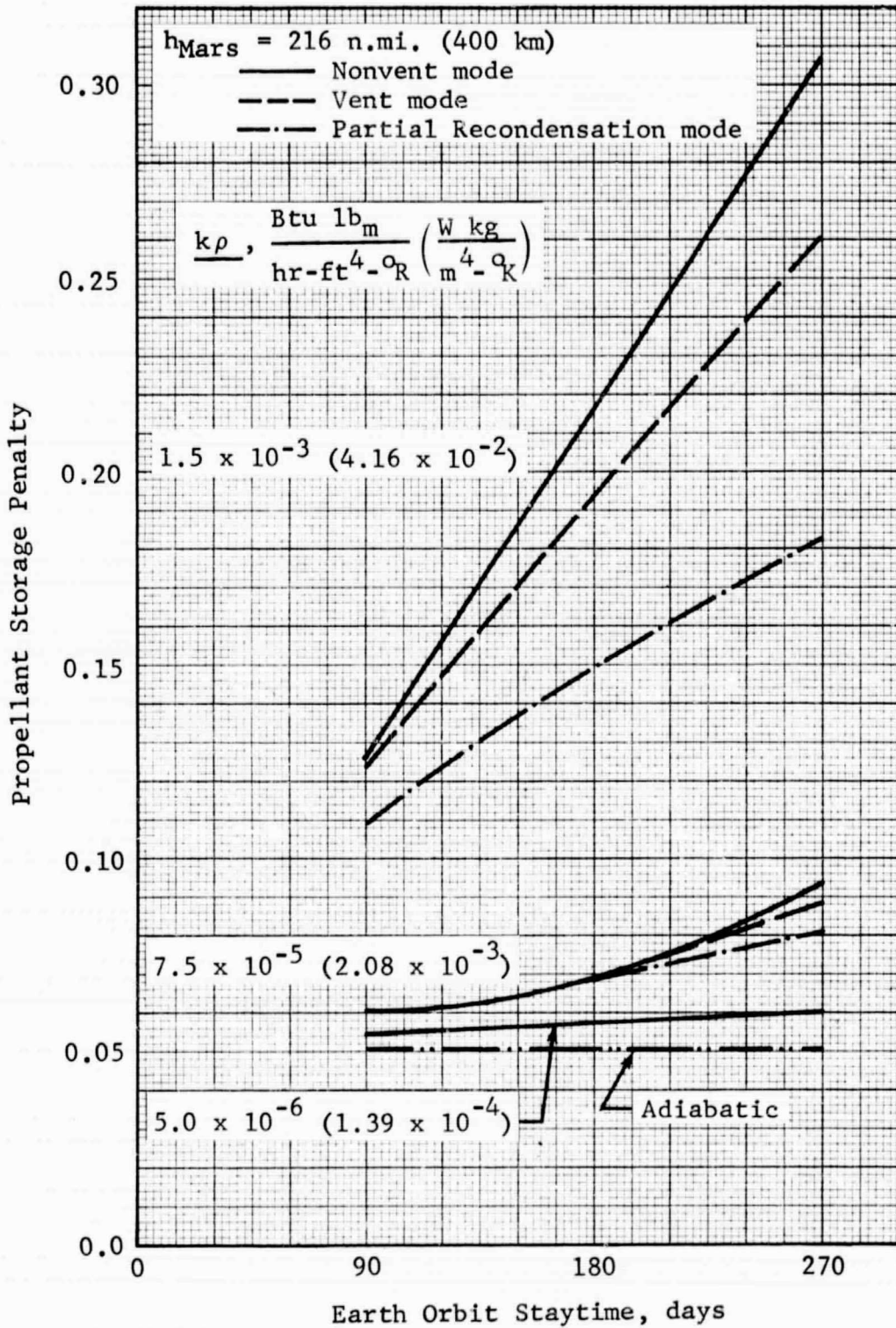


Figure 4.2-2 Propellant Storage Penalty vs Staytime: Earth Departure Stage, $h_{\text{Mars}} = 216 \text{ n.mi.}$

GENERAL DYNAMICS
Fort Worth Division

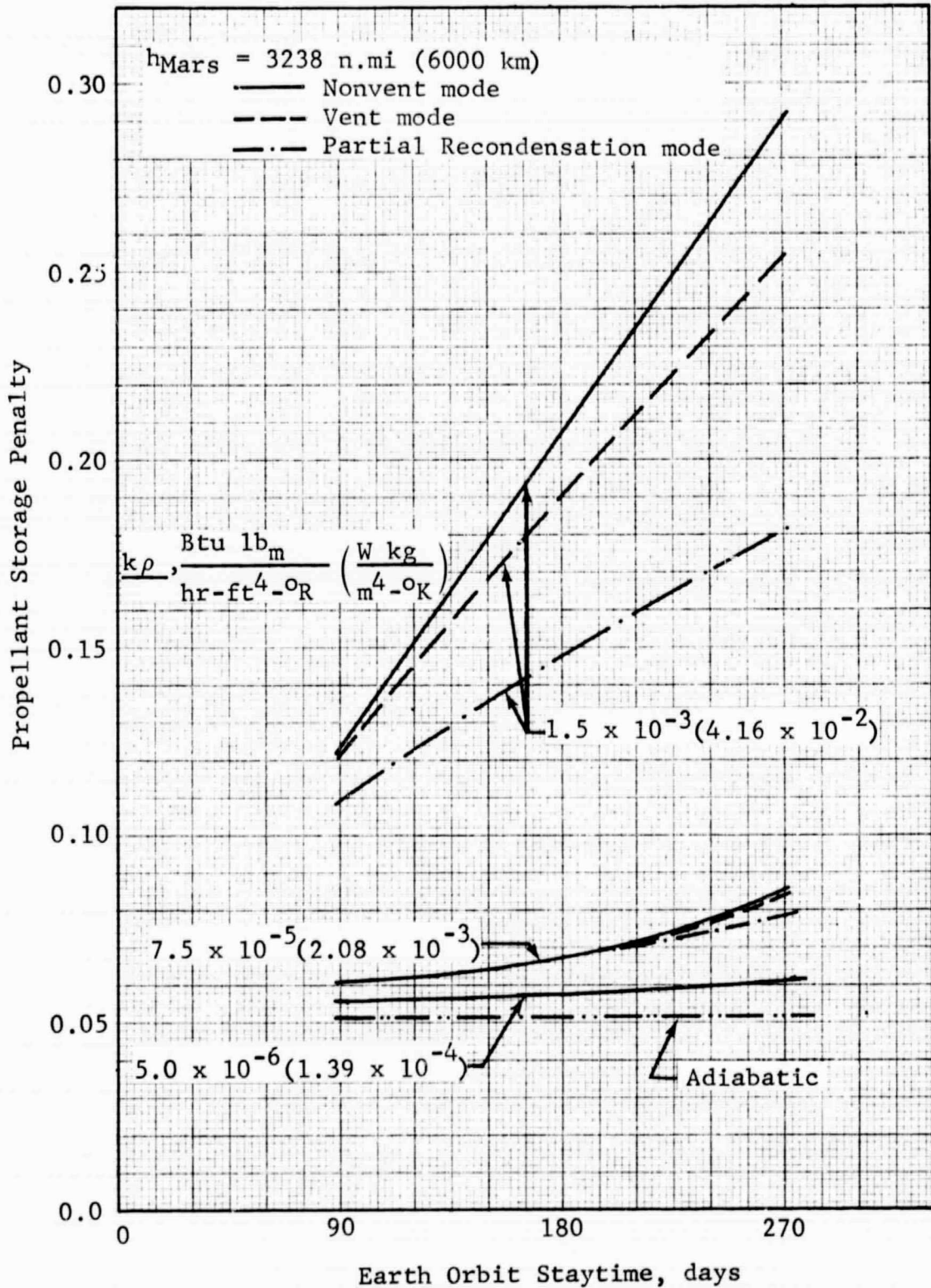


Figure 4.2-3 Propellant Storage Penalty vs Staytime: Earth Departure Stage, $h_{Mars} = 3238 \text{ n.mi}$

GENERAL DYNAMICS
Fort Worth Division

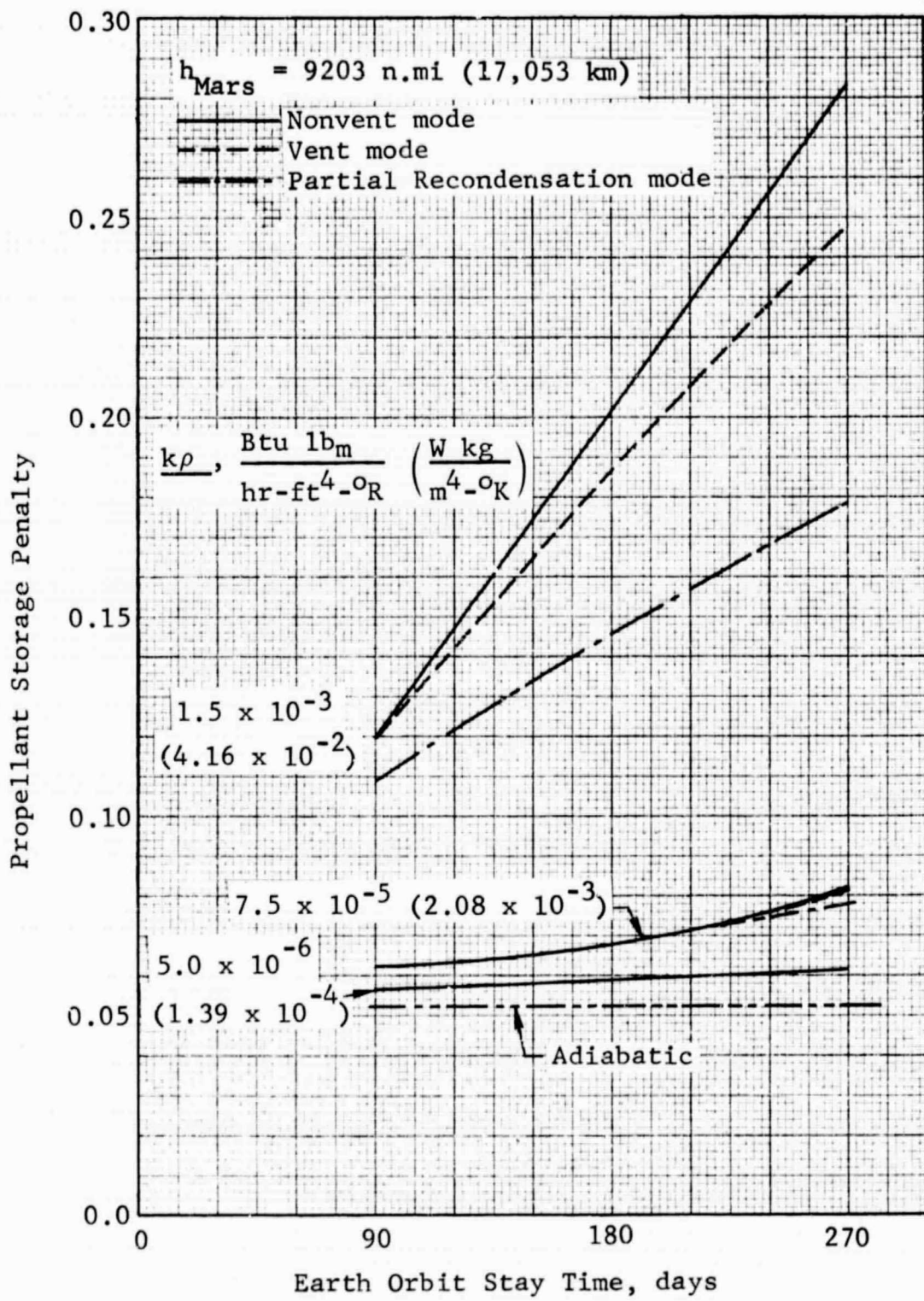


Figure 4.2-4 Propellant Storage Penalty vs Staytime: Earth Departure Stage, $h_{\text{Mars}} = 9203 \text{ n.mi}$

GENERAL DYNAMICS
Fort Worth Division

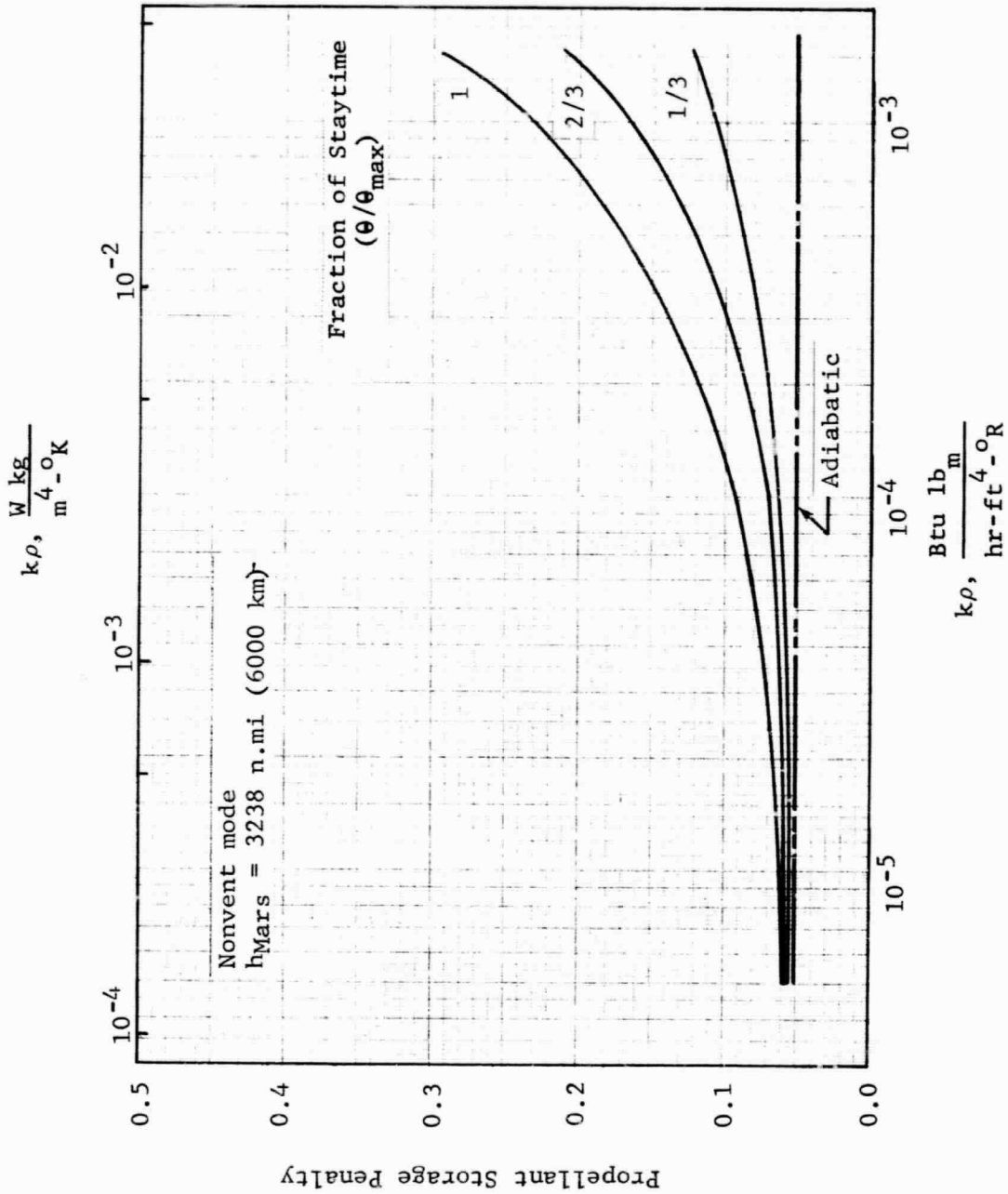


Figure 4.2-5 Effect of Insulation Thermal Performance on Propellant Storage Penalty: Earth Departure Stage

GENERAL DYNAMICS
Fort Worth Division

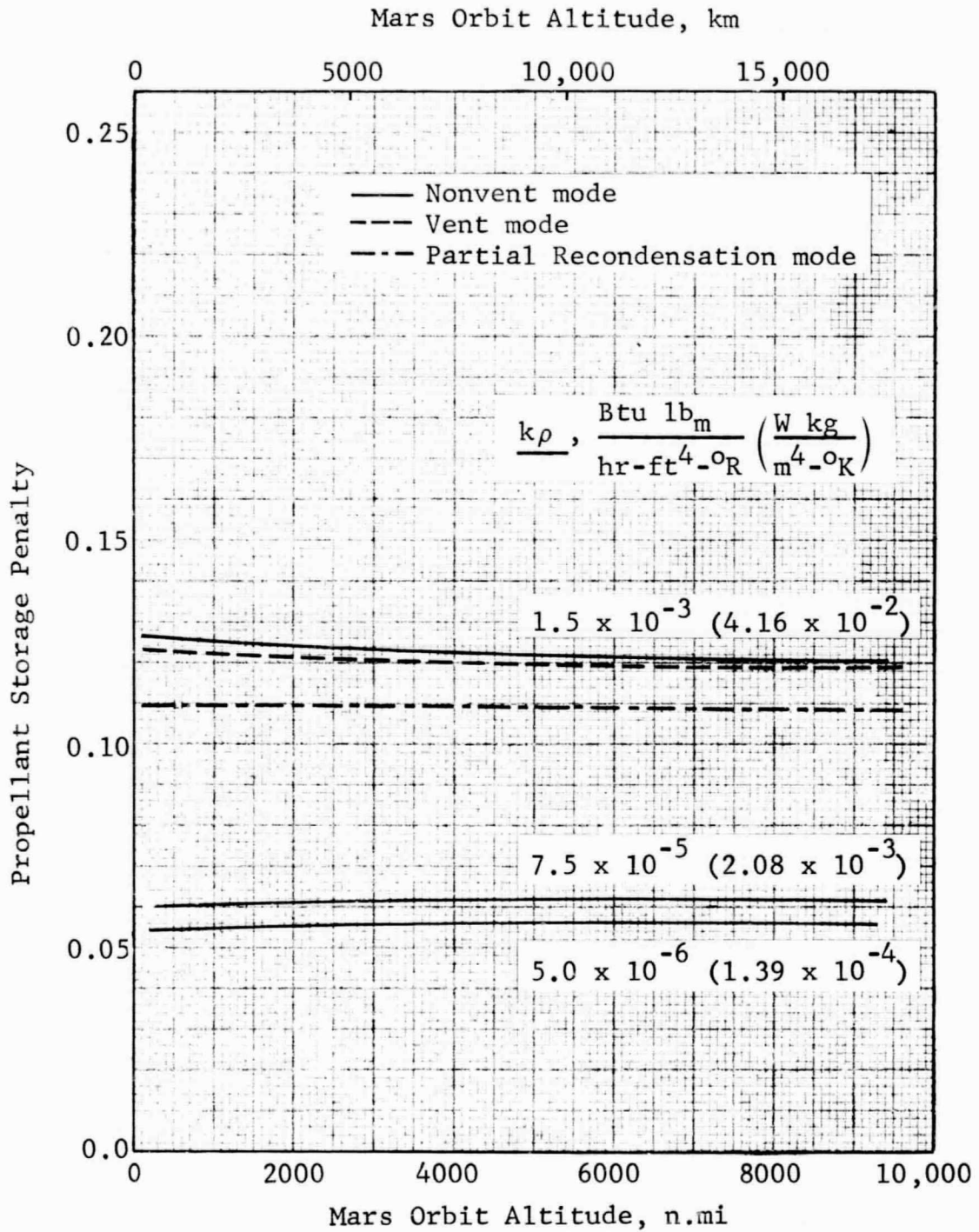


Figure 4.2-6 Propellant Storage Penalty vs. Altitude: Earth Departure Stage, $\theta/\theta_{\max} = 1/3$

GENERAL DYNAMICS
Fort Worth Division

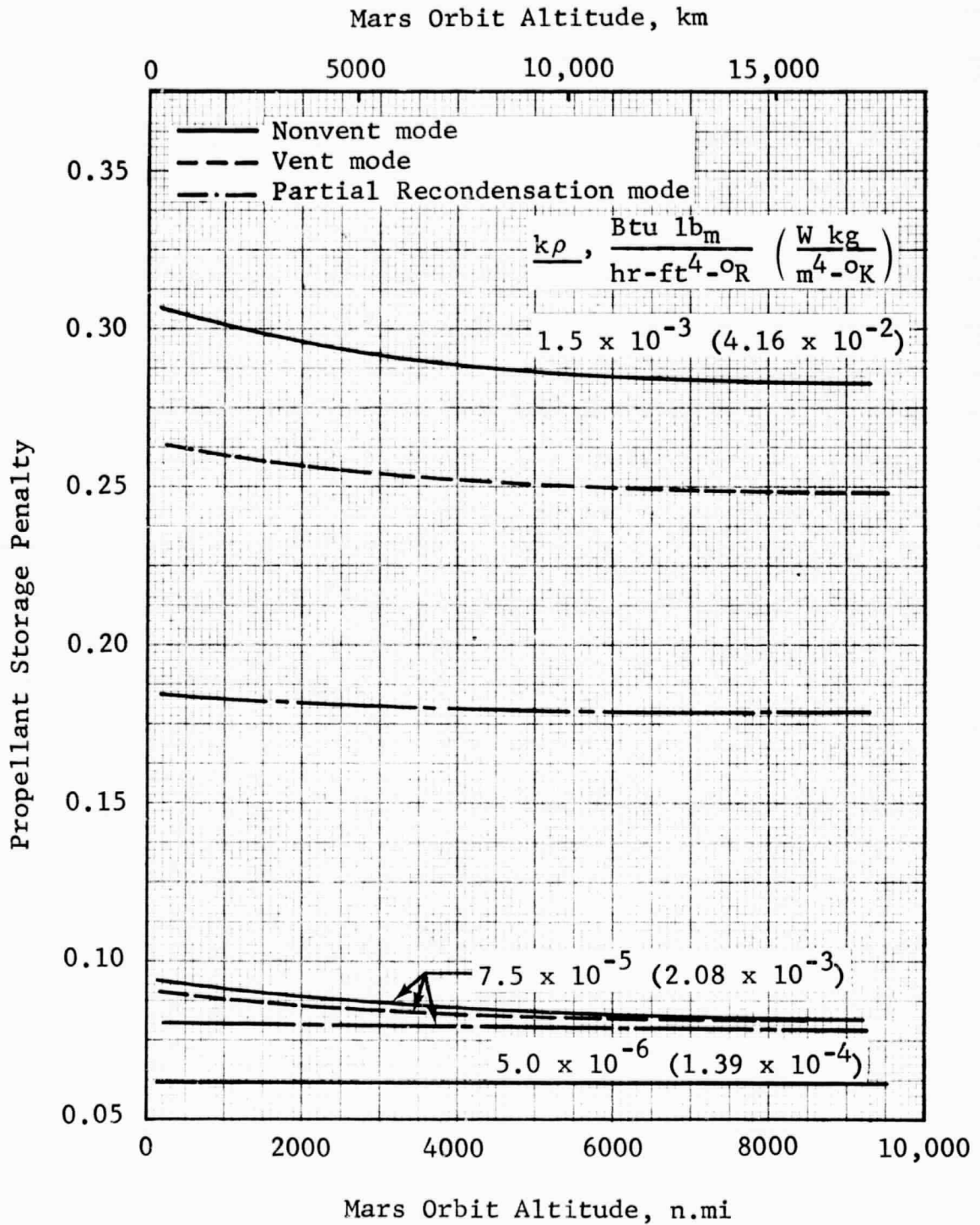


Figure 4.2-7 Propellant Storage Penalty vs Altitude: Earth Departure Stage, $\theta/\theta_{\max} = 1$

GENERAL DYNAMICS
Fort Worth Division

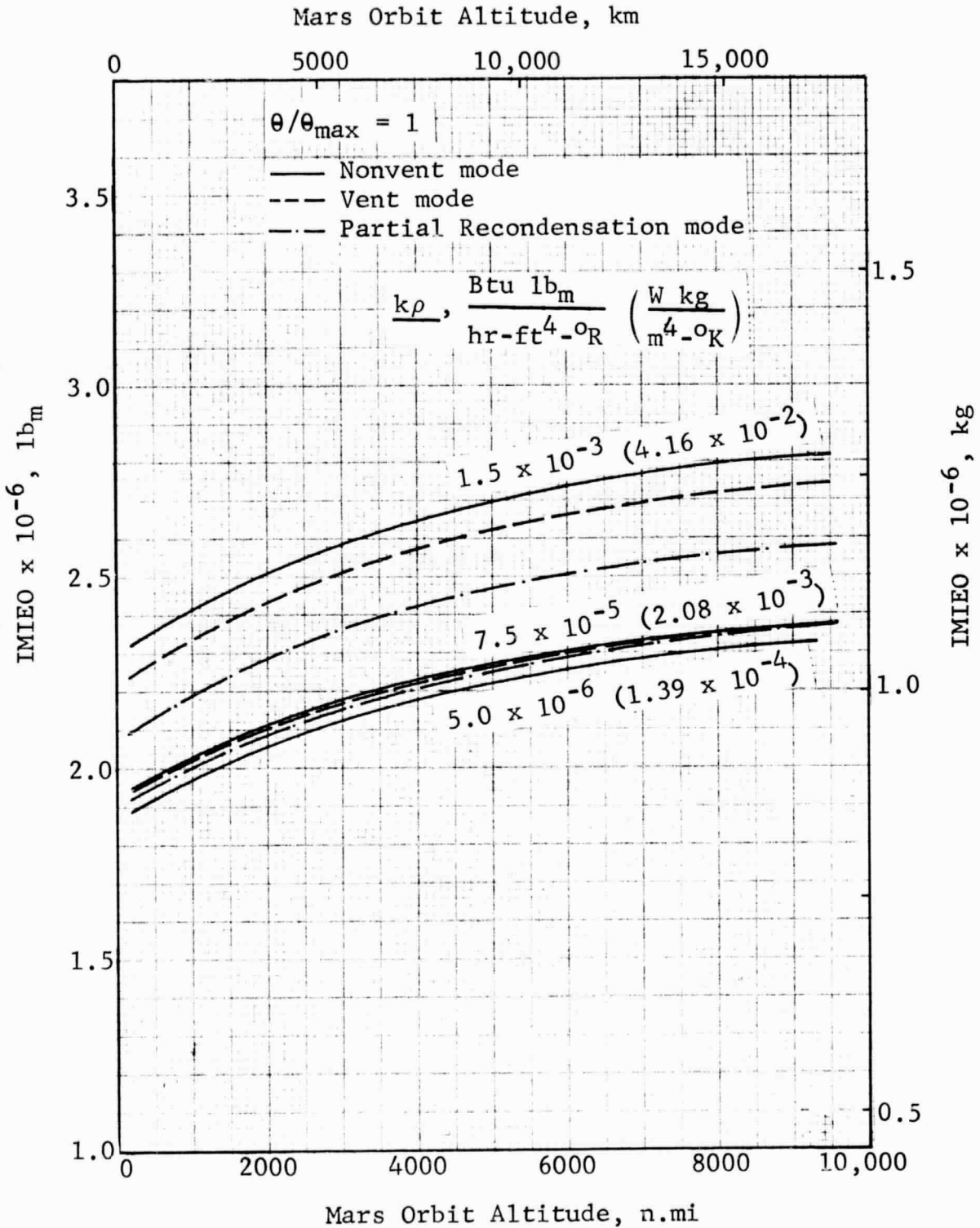


Figure 4.2-8 Effect of Optimum Propellant Storage System on IMIEO vs. Altitude: Earth Departure Stage

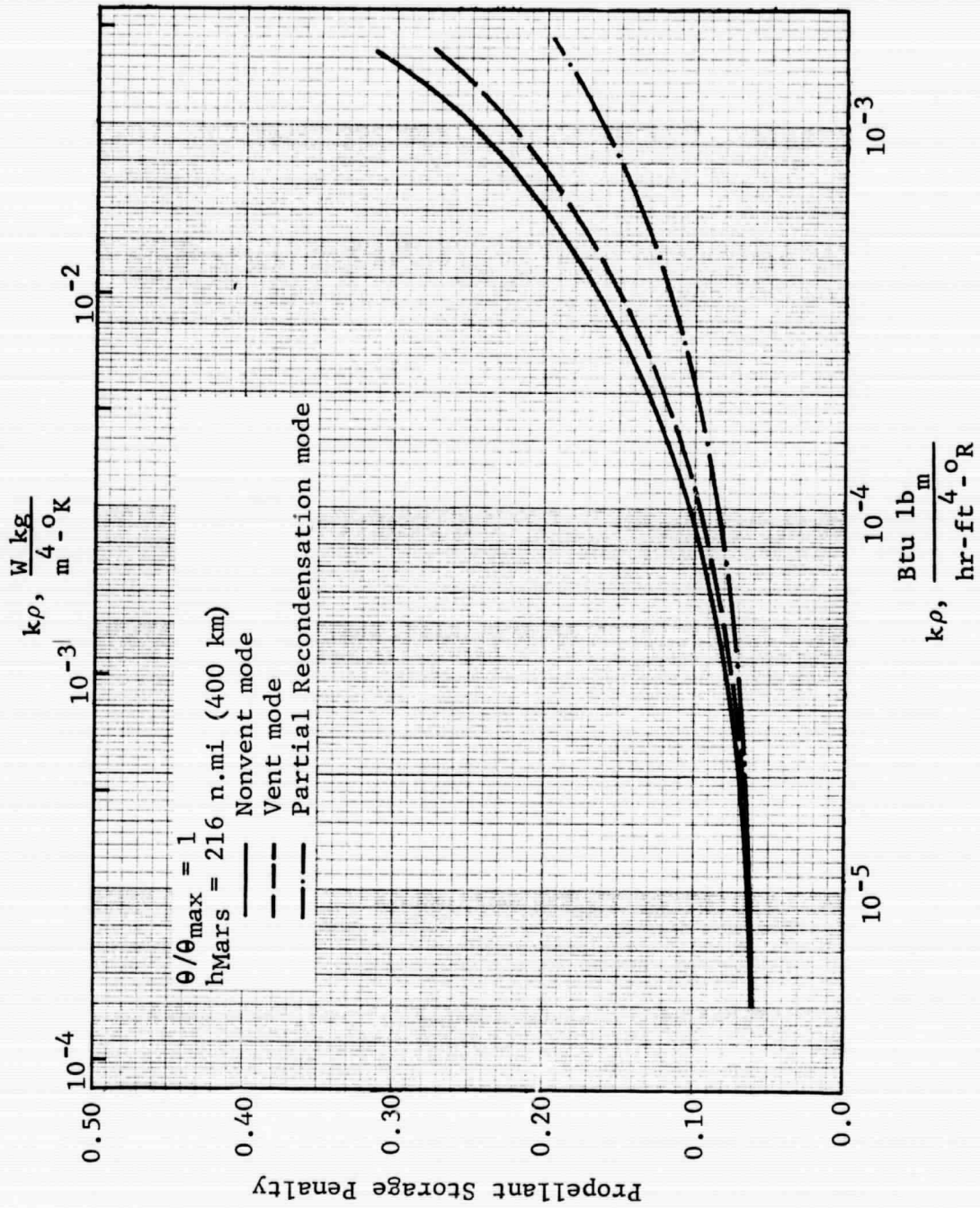
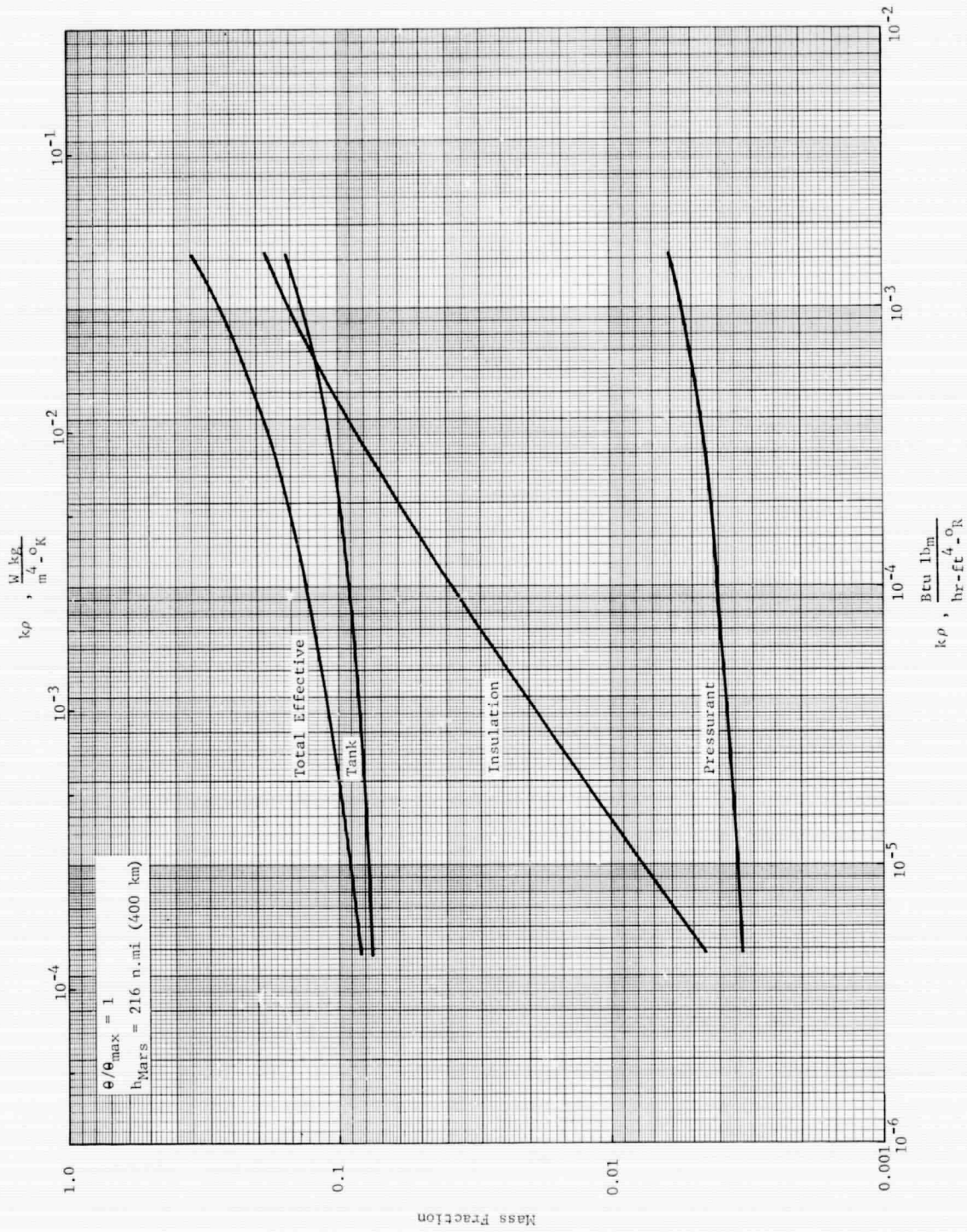


Figure 4.2-9 Effect of Propellant Storage Mode on Propellant Storage Penalty: Earth Departure Stage

GENERAL DYNAMICS
Fort Worth Division



4.2-10 Optimum Propellant Storage Component Mass Fractions:
Earth Departure Stage, Nonvent Mode

GENERAL DYNAMICS
Fort Worth Division

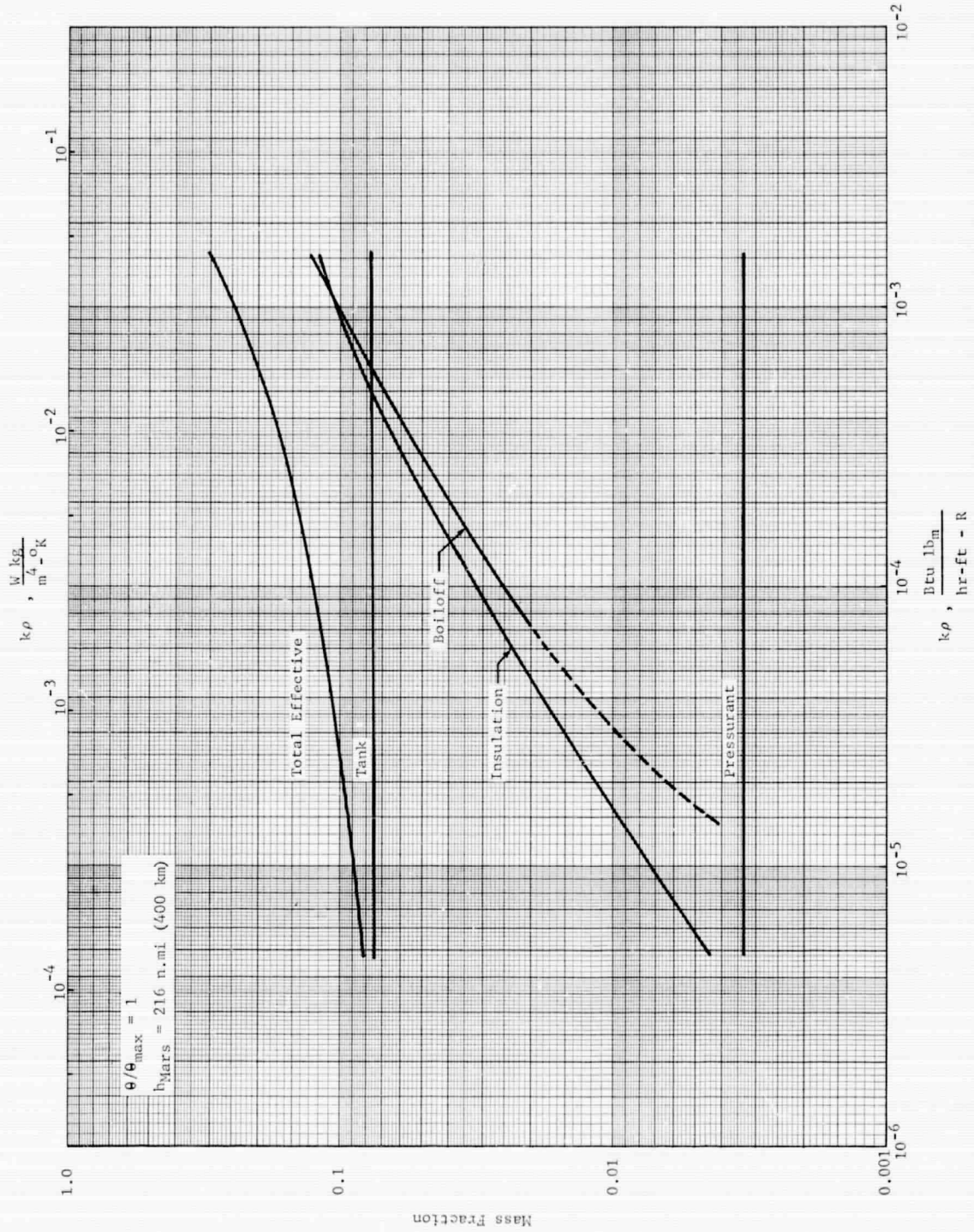
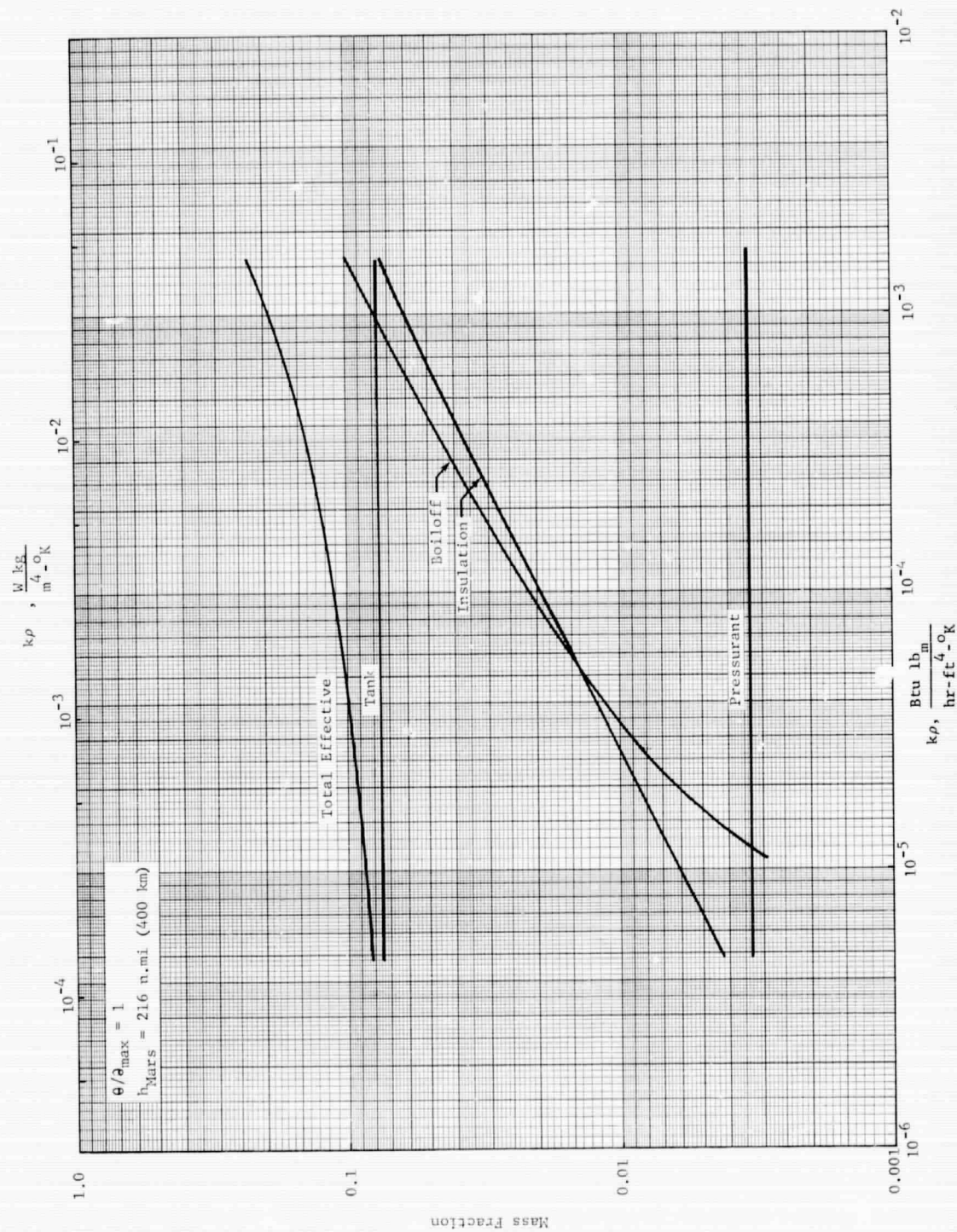


Figure 4.2-11 Optimum Propellant Storage Component Mass
Fractions: Earth Departure Stage, Vent Mode

GENERAL DYNAMICS
Fort Worth Division



4.2-12 Optimum Propellant Storage Component Mass Fractions: Earth Departure Stage, Partial Recondensation Mode

GENERAL DYNAMICS
Fort Worth Division

4.3 MARS BRAKING STAGE
PROPELLANT STORAGE PENALTY

Effects of the basic parameters and the propellant storage modes on the stage propellant storage penalty and on the vehicle IMIEO are examined with respect to optimized propellant storage systems. In addition, the effect of utilizing a solar shield during the Mars transfer period is also presented. Nominal mass fractions are employed to define the Earth Departure and the Mars Departure Stages in order to obtain the vehicle IMIEO. With this approach, the mass of the Mars Departure Stage remains constant with respect to all parameters save Mars orbit altitude since this stage is not affected by variations in the Braking Stage. The Earth Departure Stage mass will reflect changes in the Braking Stage because it must accelerate the Braking Stage through the Earth Departure maneuver and the propellant requirements will vary accordingly. However, the mass fractions are held constant in order to isolate the effects of variations in the Braking Stage.

The results presented in this section are given on a per-tank basis where appropriate; IMIEO data reflect the fact that the Braking Stage comprises two modules. Propellant storage penalties are referenced to a vehicle with a Mars Braking Stage propellant-storage-system mass fraction of zero. The IMIEO variation with altitude of this vehicle is shown in Figure 4.2-1 as the curve labelled MBS.

4.3.1 Sensitivity to Parameters

4.3.1.1 Earth Orbit Staytime

Since the Mars Braking Stage mission history includes a 210-day Mars transfer phase in addition to the Earth orbit period, it is expected that Earth orbit staytime would have less influence on the propellant storage penalty than it does on the Earth Departure Stage. In general, this expected result is found to be the case, as shown in Figure 4.3-1, where the propellant storage penalty for the unshielded Mars Braking Stage at the 216-n.mi (400 km) altitude is presented (compare with Earth Departure Stage data of Figure 4.2-2). For example, at the high $k\rho$ value, the propellant storage penalty in the nonvent mode increases 55.3% over the range of staytime for the Braking Stage. The corresponding

GENERAL DYNAMICS
Fort Worth Division

percentage increase for the Earth Departure Stage is 143.7%. A similar relationship is found for the vent and the partial-recondensation storage modes. However, at the lowest $k\rho$ value, the relationship is reversed for the nonvent mode - the percentage increase with staytime is greater for the Braking Stage. The reversal occurs because the tank pressure in the Earth Departure Stage case remains below the minimum tank design pressure, even at the maximum staytime. Note also from the comparison that the magnitude of the propellant storage penalty is generally lower for the Braking Stage as compared to the Earth Departure Stage. This is to be expected since the Braking Stage is smaller than the Earth Departure Stage.

Again, the insulation performance is a dominant factor in determining the magnitude of the propellant storage penalty. The penalty ranges from 10% to 24% at the high $k\rho$ value, depending upon the storage mode and the staytime. For the intermediate $k\rho$ value, both the magnitude of the penalty and the range is reduced to the 5-8% interval. With a further improvement in insulation performance, the penalty is reduced somewhat further, ranging from 3.8 to 5.5%. However, it is interesting to note that a 3.3% penalty would be incurred even under the ideal condition of an adiabatic wall. Thus, the minimum penalty can be approached with presently quoted values of multilayer insulation performance.

For the shielded stage, the reduction in heat transfer during the Mars transfer phase results in a correspondingly greater influence of the Earth orbit heat transfer and, thus, of Earth orbit staytime. This is shown in the data presented in Figure 4.3-2 for the low Mars orbit altitude. Note the similarity to the Earth Departure Stage data at all $k\rho$ values; the only difference is in the magnitude of the propellant storage penalty. At the high $k\rho$ value, the percentage increase in penalty ranges from 47.0% for the partial-recondensation mode to 119% for the nonvent mode. With improved insulation performance, the percentage increase with staytime is reduced; at the low $k\rho$ value, the increase is only 6.9% for the nonvent mode while the vent and partial-recondensation modes are undefined. As in the unshielded case, a 3.3% penalty would be incurred under the ideal adiabatic condition.

It is noted that in some cases data have not been included for the vent mode and the partial-recondensation mode,

GENERAL DYNAMICS

Fort Worth Division

particularly at the lowest value of the $k\rho$ product. This is because the optimum system does not reach the vent pressure, so that the results are identical to those for the nonvent mode.

Figures 4.3-3 through 4.3-6 show the propellant storage penalties for vehicles with optimized propellant storage systems on the Mars Braking Stage at the 3238-n.mi (6000 km) and 9203-n.mi (17,053 km) altitudes, including both unshielded and shielded stages. The effect of the Mars orbit altitude on the propellant storage system of the Mars Braking Stage is discussed in Subsection 4.3.1.3; it is significant to note here that the general trends with Earth orbit staytime are similar at all altitudes.

Two methods of reducing the thermal effects of Earth orbit staytime, or of extending the time which may be spent in Earth orbit, are to use tanking or the combination vent-nonvent mode. These methods are compared to the basic propellant storage modes in Figure 4.3-7 in terms of propellant storage penalty. Tanking is feasible only at the high $k\rho$ value and completely removes the effect of Earth orbit staytime since increased boiloff is replenished during the tanking operation. Note that the maximum staytimes are well beyond the range treated in this study. However, these maximum staytimes correspond to replenishing the total propellant loading or, in other words, the tanks becoming empty. Whether or not this is practicable for a membrane-type tank has yet to be established.

For the combination vent-nonvent mode, the penalty increases with staytime since the excess propellant loading which is boiled off during Earth orbit represents a direct penalty to the IMIEO. However, the variation of storage penalty with staytime is much reduced as compared to the nonvent mode. Note that the maximum staytimes are much lower than in the tanking mode, even at the intermediate $k\rho$ value. Further discussion of these storage modes is given in Subsection 4.3.2.

4.3.1.2 Insulation Thermal Performance

As shown in the previous subsection, the thermal performance of the insulation has a dominant effect on the propellant storage system penalty. The penalty for the unshielded Mars Braking Stage is shown directly as a function

GENERAL DYNAMICS

Fort Worth Division

of insulation thermal performance in Figure 4.3-8. For the 120-day staytime, the penalty to IMIEO increases 345% over the range of insulation performance (from 4.2% to 18.7%). Note that the bulk of the increase occurs in the upper range of the $k\rho$ product. Between the low and intermediate $k\rho$ values, the penalty increases 45%; the remaining 300% of the total increase takes place above the intermediate value. As shown in the figure, the trends are similar at the other staytimes. Also shown is the propellant storage penalty for a Braking Stage with adiabatic tank walls. The difference in penalty between the nonvent mode and the adiabatic case illustrates the impact of heat transfer on the IMIEO. At the low staytime and low $k\rho$ value, the curves flatten out, but the adiabatic limit is not reached because of the penetration heat transfer that is independent of insulation performance.

When the solar shield is used to intercept the incident radiation, the demands on the insulation system are reduced and the effect of insulation performance on the propellant storage system penalty is lessened. Figure 4.3-9 presents the penalty for the shielded Braking Stage for the same conditions as shown in Figure 4.3-8. For the 120-day staytime, the mass penalty increases from 3.9% to 10.5% of the zero-mass-fraction-vehicle IMIEO, a percentage increase of 167% (compared to a 345% increase in the unshielded case). Again, the bulk of the increase, 156%, occurs above the intermediate $k\rho$ value. Also, the penalty tends closer to the adiabatic limit at the low $k\rho$ value, which indicates the effectiveness of the solar shield in reducing the penetration heat transfer.

4.3.1.3 Mars Orbit Altitude

Mars orbit altitude affects the Mars Braking Stage propellant storage system through the Mars Excursion Module (MEM) mass, the ΔV requirement for the braking maneuver, and the mass of the Mars Departure Stage. The MEM mass is the dominant factor, increasing 70% as the altitude increases, while the velocity requirement increases by only 8%. The nominal Mars Departure Stage mass used in this analysis varies by only 5.3% over the altitude range. The influence of altitude, neglecting thermal effects, on the Braking Stage mass can be seen in Figure 4.2-1, where the zero-mass-fraction data is presented as a function of Mars orbit altitude. The Braking Stage initial mass increases from 485,000 lb_m

GENERAL DYNAMICS

Fort Worth Division

(220,000 kg) to 703,600 lb_m (319,000 kg), an increase of 45% over the range of altitude.

The propellant storage penalty to IMIEO for the shielded Mars Braking Stage is presented in Figure 4.3-10 as a function of Mars orbit altitude. In discussing this figure, it is important to note that the zero-mass-fraction IMIEO varies with altitude, as shown in Figure 4.2-1. The dominant effect of altitude is that of stage size increasing with altitude. This produces a steady increase in the propellant storage penalty to IMIEO, amounting to a 15.9% increase at the low $k\rho$ value (nonvent mode) and a somewhat lower percentage increase for the other cases. The combination of the high $k\rho$ value and the nonvent mode shows a slight decreasing trend at lower altitudes. This is caused by the lower propellant loading and higher heat transfer per pound of propellant, which results in a higher tank mass fraction. Note that this does not mean that the value of IMIEO is lower at an intermediate altitude, but that the difference in the IMIEO with respect to the vehicle with a zero-mass-fraction Mars Braking Stage is less at that altitude. The IMIEO is still dominated by the MEM mass and increases with altitude, as shown in Figure 4.3-11. Significantly, for a vehicle with a shielded Mars Braking Stage at $k\rho$ values of 1.5×10^{-3} and 5.0×10^{-6} Btu lb_m/hr-ft⁴-°R (4.16×10^{-2} and 1.39×10^{-4} W kg/m⁴-°K) the increases in the value of IMIEO for the nonvent mode are 447,900 lb_m (203,200 kg) or 22.3% and 426,000 lb_m (193,200 kg) or 22.6%, respectively. With the zero-mass-fraction Mars Braking Stage, the increase is 398,000 lb_m (180,600 kg) or 21.9% (Fig. 4.2-1). Thus, the results give percent changes of IMIEO with altitude that are within 0.7% of those for the zero-mass-fraction case, clearly showing that the MEM mass influences the shielded Mars Braking Stage more strongly than any of the other aspects of Mars orbit altitude.

The case with the unshielded Mars Braking Stage yields different trends because of the greater heat transfer. The propellant storage penalty curves for a vehicle with an optimized propellant storage system on an unshielded Mars Braking Stage are presented in Figure 4.3-12. In this case, a minimum occurs in most of the curves because of the more severe thermal conditions. For the nonvent mode, the reason for the minima is the same as in the shielded case: the smaller propellant loadings at the lower altitude result in a relatively higher penalty due to larger tank and insulation

GENERAL DYNAMICS

Fort Worth Division

mass fractions. At the higher altitudes, the effect of increasing stage size dominates. For the vent and partial-recondensation modes, the higher penalty at the lower altitudes is due to higher boiloff fractions.

As before, the IMIEO increases monotonically with altitude, as shown in Figure 4.3-13, reflecting the dominance of the MEM mass variation with altitude. The increases in IMIEO between the 216-n.mi (400 km) and the 9203-n.mi (17,053 km) Mars orbit altitude for the nonvent mode at $k\rho$ values of 1.5×10^{-3} and 5×10^{-6} Btu $lb_m/hr-ft^4-^{\circ}R$ are 468,600 lb_m (212,500 kg) or 21.6% and 419,900 lb_m (190,500 kg) or 22.1%, respectively. Thus, although the increased heat transfer translates the entire curve, the shape of the curve is determined almost entirely by the increase of the MEM mass with altitude.

4.3.2 Influence of Propellant Storage Mode

The effect of propellant storage mode on the Mars Braking Stage propellant storage penalty is strongly dependent upon the insulation thermal performance and whether or not the solar shield is used during Mars transfer. Figure 4.3-14 presents a comparison of the propellant storage penalties for the basic storage modes for the maximum-staytime, low-altitude condition. The vent and partial-recondensation modes offer a lower penalty at all values of the insulation performance, with the differences between modes increasing as the $k\rho$ value increases. At the lowest $k\rho$ value, the propellant storage penalty varies from 5.5% for the nonvent mode to 5.2% for the vent mode and 4.6% for the partial-recondensation mode. At the highest $k\rho$ value, the corresponding penalties are 23.7%, 18.8%, and 12.5%. In terms of the initial mass, the vent mode yields a 89,400 lb_m (40,500 kg) reduction in the IMIEO at the high $k\rho$ value. The partial-recondensation mode yields an even greater reduction, amounting to 202,900 lb_m (92,000 kg). The penalties at the higher altitudes are little changed from the values shown in the figure. Shorter staytimes reduce the differences between modes, and at the lower $k\rho$ values the vent and partial-recondensation modes may not be definable. These effects of staytime were pointed out in Subsection 4.3.1.1.

GENERAL DYNAMICS

Fort Worth Division

For the shielded stage, the effect of storage mode on the propellant storage penalty is shown in Figure 4.3-15 for the maximum staytime and the 216-n.mi (400 km) altitude. In this case, differences in the storage penalty between the modes become meaningful only when the $k\rho$ value is above the intermediate value. Note that the propellant storage penalties are reduced significantly relative to the unshielded stage, especially with low-performance insulation. At the highest $k\rho$ value, the penalty ranges from 8.7% for the partial-recondensation mode to 11.5% for the vent mode and 14.5% for the nonvent mode. Compared to the unshielded case, these penalties are reduced over 30%. Near the lowest $k\rho$ value, the heat transfer is reduced to such an extent that the vent pressure is not reached during the mission, and storage penalties for the vent and the partial-recondensation modes cannot be defined. Note also that the lower limit on the storage penalty, corresponding to the adiabatic tank wall, is more closely approached in the shielded case. This indicates a reduction in the penetration heat transfer in the shielded case.

The relationship between the components of the propellant storage system for the unshielded stage is shown in Figures 4.3-16, 4.3-17, and 4.3-18 for the nonvent, vent, and partial-recondensation modes, respectively. For the nonvent mode (Figure 4.3-16), the tank mass is the largest contributor to the propellant storage system mass over most of the range of insulation performance, with the tank mass fraction ranging from 0.083 to 0.188. The insulation mass fraction is small at low $k\rho$ values, rises rapidly with increasing $k\rho$ value, and finally exceeds the tank mass fraction near the highest $k\rho$ value. Pressurant mass fraction is low, ranging from 0.0034 to 0.068. The meteoroid protection mass fraction shows the least variation with insulation performance, varying from 0.0183 to 0.0204. Note that the general relationship between components is similar to that of the Earth Departure Stage (Figure 4.2-10).

In the vent mode (Figure 4.3-17), the tank is again the dominant component except at the higher $k\rho$ values. The tank mass fraction remains fairly constant at approximately 0.075 over the range of insulation performance. Both the boiloff and the insulation mass fractions are in the vicinity of 0.01 at the lowest $k\rho$ value and increase rapidly to values of 0.170 and 0.118, respectively, at the highest $k\rho$ value, exceeding the tank mass fraction. The meteoroid and the

GENERAL DYNAMICS

Fort Worth Division

pressurant mass fractions remain fairly constant, with values of 0.0183 and 0.0031, respectively. Compared to the Earth Departure Stage (Figure 4.2-11), the general trends are the same with the exception that the boiloff mass fraction now exceeds the insulation mass fraction across the entire range of insulation performance.

The component mass fractions for the partial-recondensation mode (Figure 4.3-18) show trends similar to the vent mode. In fact, the tank, meteoroid protection, and pressurant mass fractions have about the same values as in the vent mode. The boiloff and the insulation mass fractions are reduced at all $k\rho$ values, with the boiloff mass fraction always exceeding the insulation mass fraction. Compared to the Earth Departure Stage (Fig. 4.2-12), the trends are similar with the exception that the boiloff mass fraction exceeds the insulation mass fraction at all $k\rho$ values.

The effect of the solar shield on the propellant storage system component mass fractions can be seen by comparing Figure 4.3-19, the shielded, nonvent case, with Figure 4.3-16, the corresponding unshielded case. System effective mass fraction is significantly reduced, over 30% at the higher $k\rho$ values. The tank and the pressurant mass fractions are reduced in the shielded case, reflecting lower tank pressures at all $k\rho$ values. Insulation mass fraction is much lower and is less than the tank mass fraction over the entire range of $k\rho$ values. The meteoroid protection fraction is only slightly reduced in the shielded case.

In addition to the basic propellant storage modes, it is also possible, for some conditions, to employ a combination vent-nonvent mode or the tanking mode variation of the vent and the partial-recondensation modes. These techniques have been mentioned in Subsection 4.3.1.1 in connection with the possibility of mitigating the effects of Earth orbit staytime or extending the permissible length of the Earth orbit mission phase. The propellant storage system penalty for the combination vent-nonvent mode is shown in Figure 4.3-20 for the unshielded Mars Braking Stage. The range of Earth orbit staytime for this mode is marked by defined maximum and minimum values as explained in Subsection 3.3. At the high $k\rho$ value, the maximum reduction in storage penalty is 23% for a maximum staytime of just over 180 days. The percent reduction at the intermediate $k\rho$ value and the 180-day staytime is down to 5.4%. However, if the maximum

GENERAL DYNAMICS

Fort Worth Division

staytime is increased to 235 days, the percentage savings at that staytime would of course be larger. The combination mode is not defined at the low $k\rho$ value since the vent pressure is not reached during Earth orbit.

The effect of the tanking operation is to increase the permissible length of the Earth orbit staytime without increasing the propellant storage penalty since the propellant boiled off in Earth orbit is replenished from an orbital tanker before engine ignition. The permissible length of Earth orbit staytime is also extended, as compared to the combination mode, since theoretically the entire propellant loading can be boiled off in Earth orbit. The propellant storage penalty to IMIEO is shown in Figure 4.3-21 for the tanking mode for both the vent and the partial-recondensation cases at the high $k\rho$ value. The reductions in penalty at the 180-day staytime are 24% for the vent mode and 20.9% for the partial-recondensation mode. Maximum staytimes corresponding to total propellant boiloff are 885 days and 1441 days for the vent and the partial-recondensation modes, respectively.

Neither the combination mode nor the tanking variation of the vent and the partial-recondensation modes is applicable to the shielded Braking Stage. The solar shield reduces the heat transfer during Mars transfer to such an extent that the expansion volume is minimal for the combination mode. In addition, the reduced heat transfer would result in small optimum insulation thicknesses. Consequently, in both the combination and tanking modes, the propellant loading would be boiled off early in Earth orbit.

4.3.3 Comparison of Shielded and Unshielded Stages

The Mars transfer solar shield accomplishes a large reduction in the severity of the thermal environment encountered by the Mars Braking Stage, as shown in Figure 4.3-22, where the integral of adiabatic wall temperature over time is presented. This reduction is, of course, most important with low-performance insulation. The effect of the solar shield on the propellant storage penalty is presented in Figure 4.3-23, where the penalties for the shielded and unshielded stages are compared for the nonvent mode. With low-performance insulation, the rate of increase in penalty

GENERAL DYNAMICS

Fort Worth Division

with staytime is approximately the same for both the shielded and the unshielded stage. Consequently, the percentage reduction in penalty of the shielded over the unshielded case decreases from 54.7% to 38.5% over the range of staytime. As the insulation performance improves, the effect of the shield is reduced. At the intermediate and low $k\rho$ values, for a 180-day staytime, the percentage reductions in penalty are 33.1% and 17.6%, respectively.

A comparison of the propellant heat transfer in the shielded and unshielded cases is presented in Figure 4.3-24 for the same conditions. Note that the solar shield leads to a reduced total heat transfer. However, the heat transfer during Earth orbit is higher since the optimum insulation thickness is lower in the shielded case.

The effect of the solar shield for the vent and the partial-recondensation modes is shown in Figure 4.3-25. For these modes, comparison of the shielded and unshielded cases can only be made at the highest $k\rho$ value. At the lower values, the vent pressure was not reached in the shielded case and propellant storage penalties could not be evaluated. In both modes, the absolute difference in penalty remains roughly constant with staytime. Note that the shield accomplishes a greater reduction in the vent mode case: at the 180-day staytime, the percentage reductions in penalty are 37.7% and 29.6% for the vent and partial-recondensation modes, respectively.

The reduction in the IMIEO attributable to the shielded Mars Braking Stage is presented in Figure 4.3-26. This represents only the Mars Braking Stage contribution; since the Mars Departure Stage is defined in terms of nominal mass fractions, the reduction in IMIEO due to the shielding of that stage cannot be included. Note that the solar shield system mass, which would act to reduce the mass savings, is not accounted for in the data shown. For all three basic storage modes, the saving in IMIEO increases as the $k\rho$ value increases. The IMIEO difference at the highest value is over five times that at the lowest $k\rho$ value, in all three cases.

GENERAL DYNAMICS
Fort Worth Division

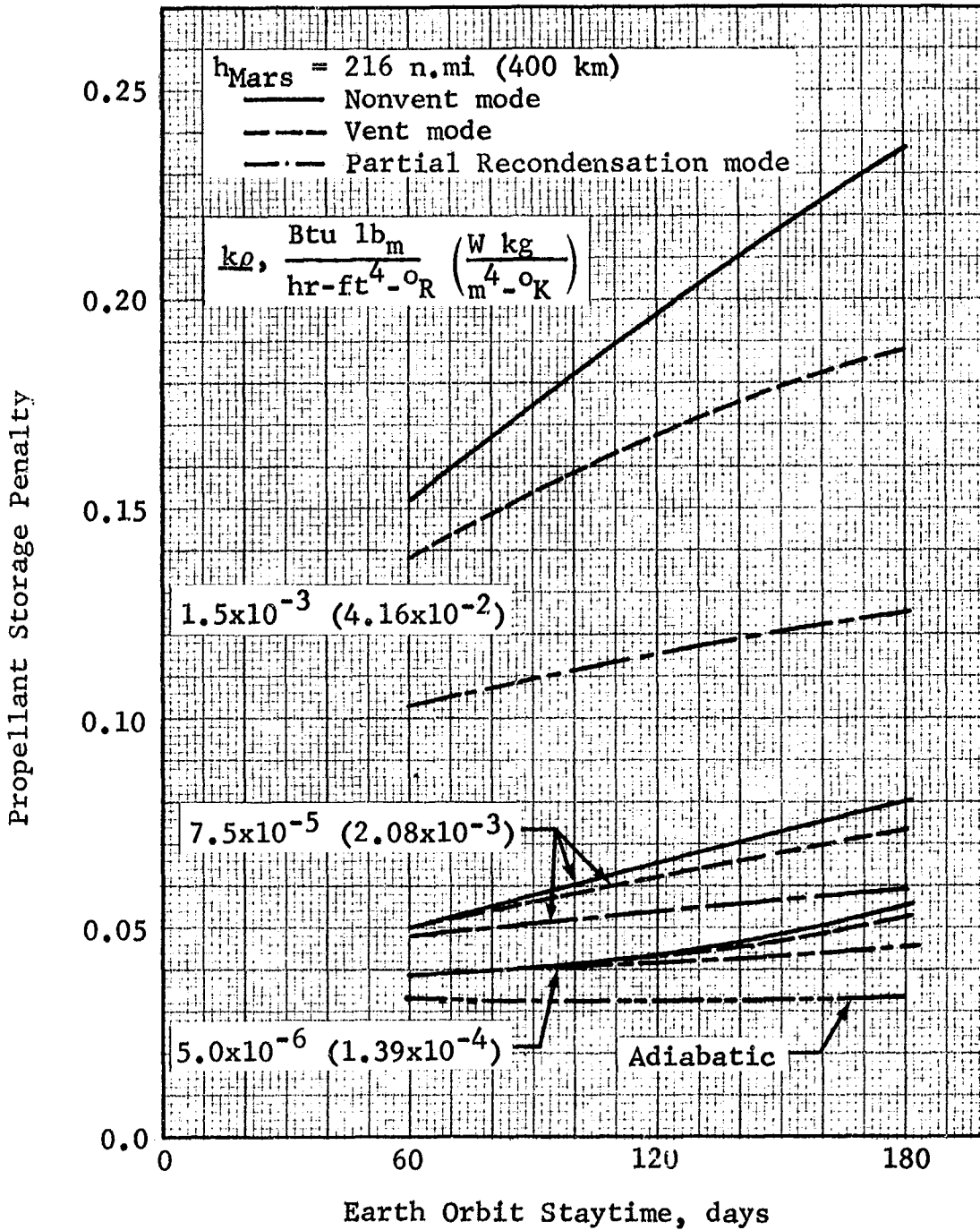


Figure 4.3-1 Propellant Storage Penalty vs Staytime: Unshielded Mars Braking Stage, $h_{Mars} = 216 \text{ n.mi}$

GENERAL DYNAMICS
Fort Worth Division

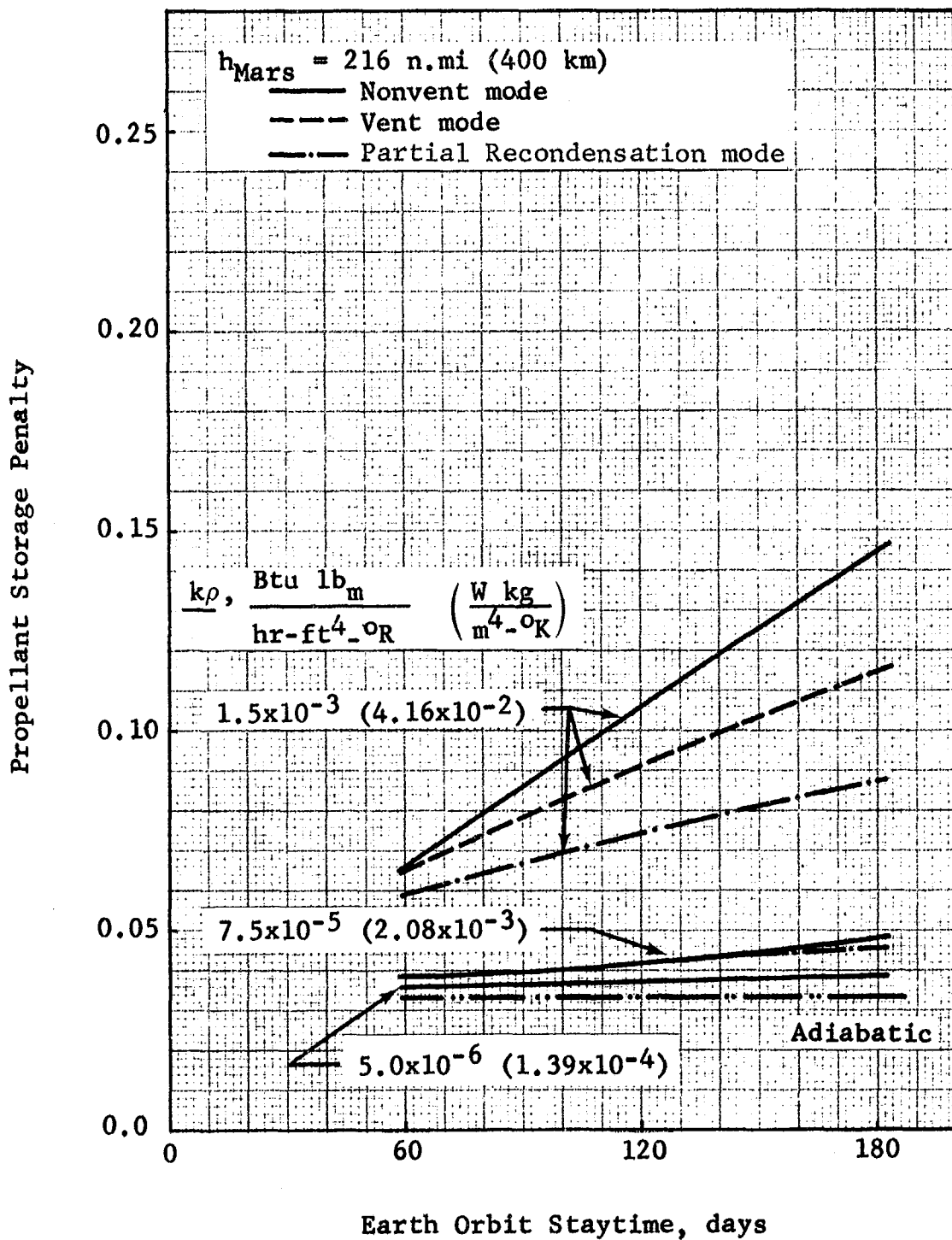


Figure 4.3-2 Propellant Storage Penalty vs Staytime:
 Shielded Mars Braking Stage,
 $h_{Mars} = 216 \text{ n.mi}$

GENERAL DYNAMICS
Fort Worth Division

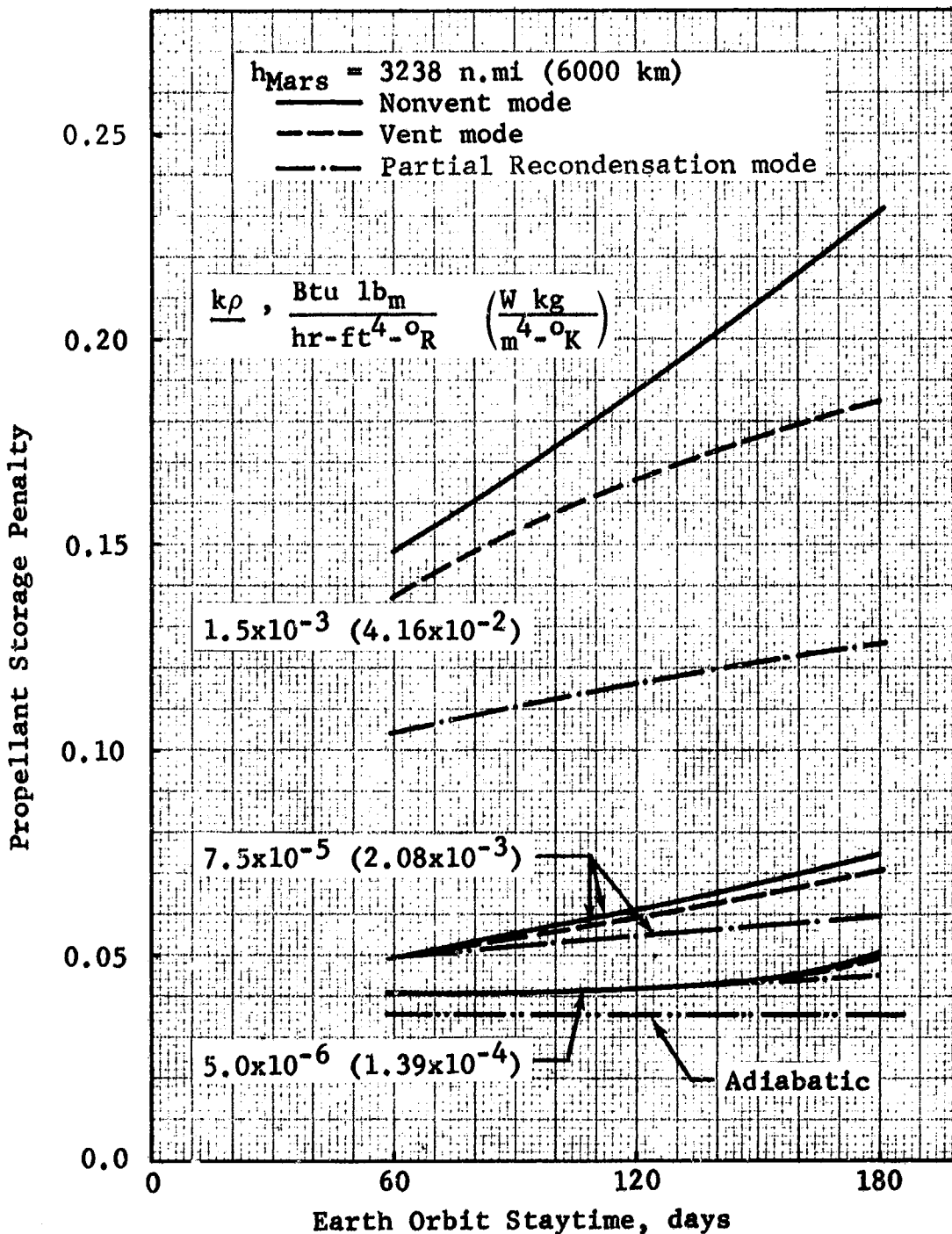


Figure 4.3-3 Propellant Storage Penalty vs Staytime: Unshielded Mars Braking Stage, $h_{Mars} = 3238 \text{ n.mi}$

GENERAL DYNAMICS
Fort Worth Division

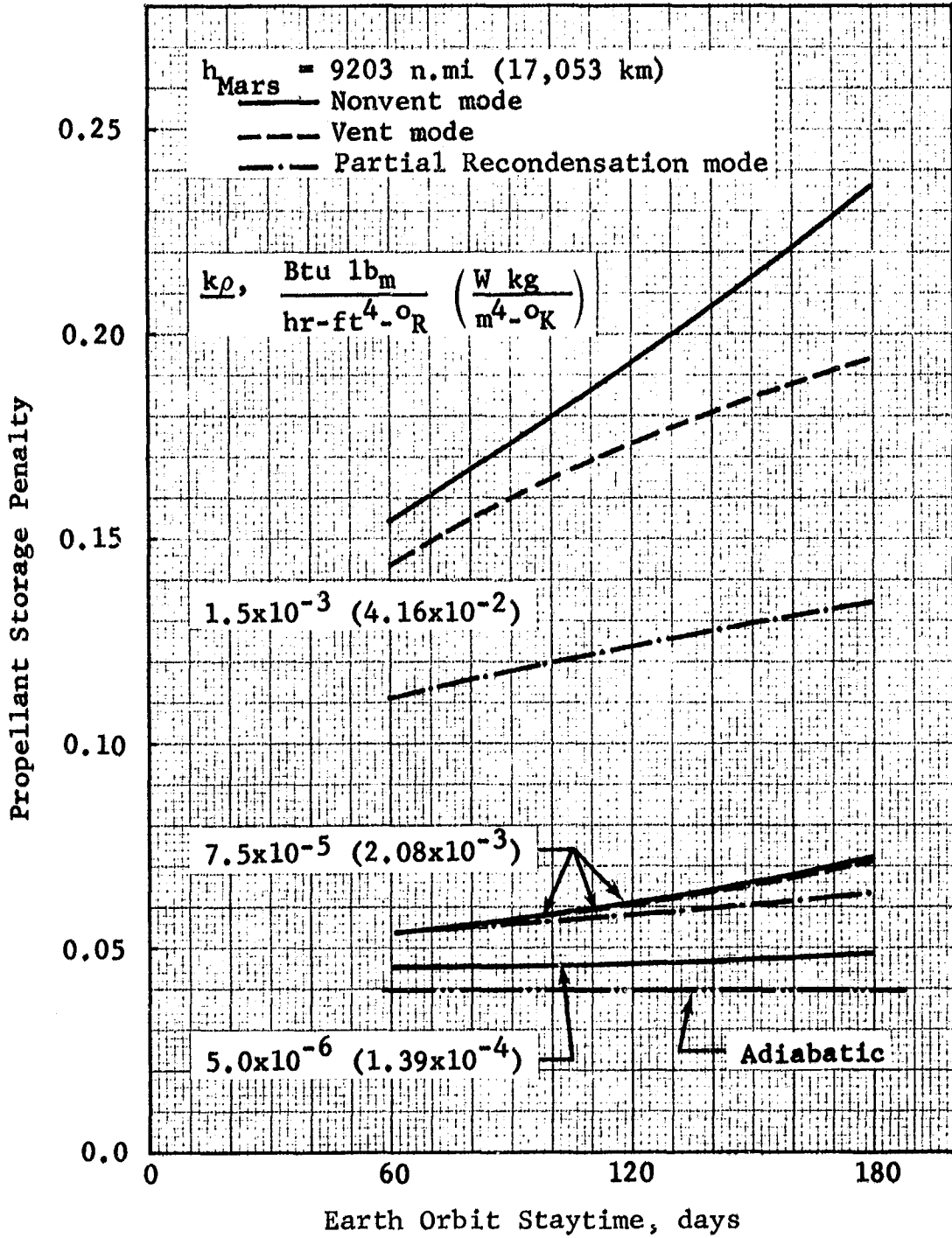


Figure 4.3-4 Propellant Storage Penalty vs Staytime:
Unshielded Mars Braking Stage, $h_{\text{Mars}} = 9203 \text{ n.mi}$

GENERAL DYNAMICS
Fort Worth Division

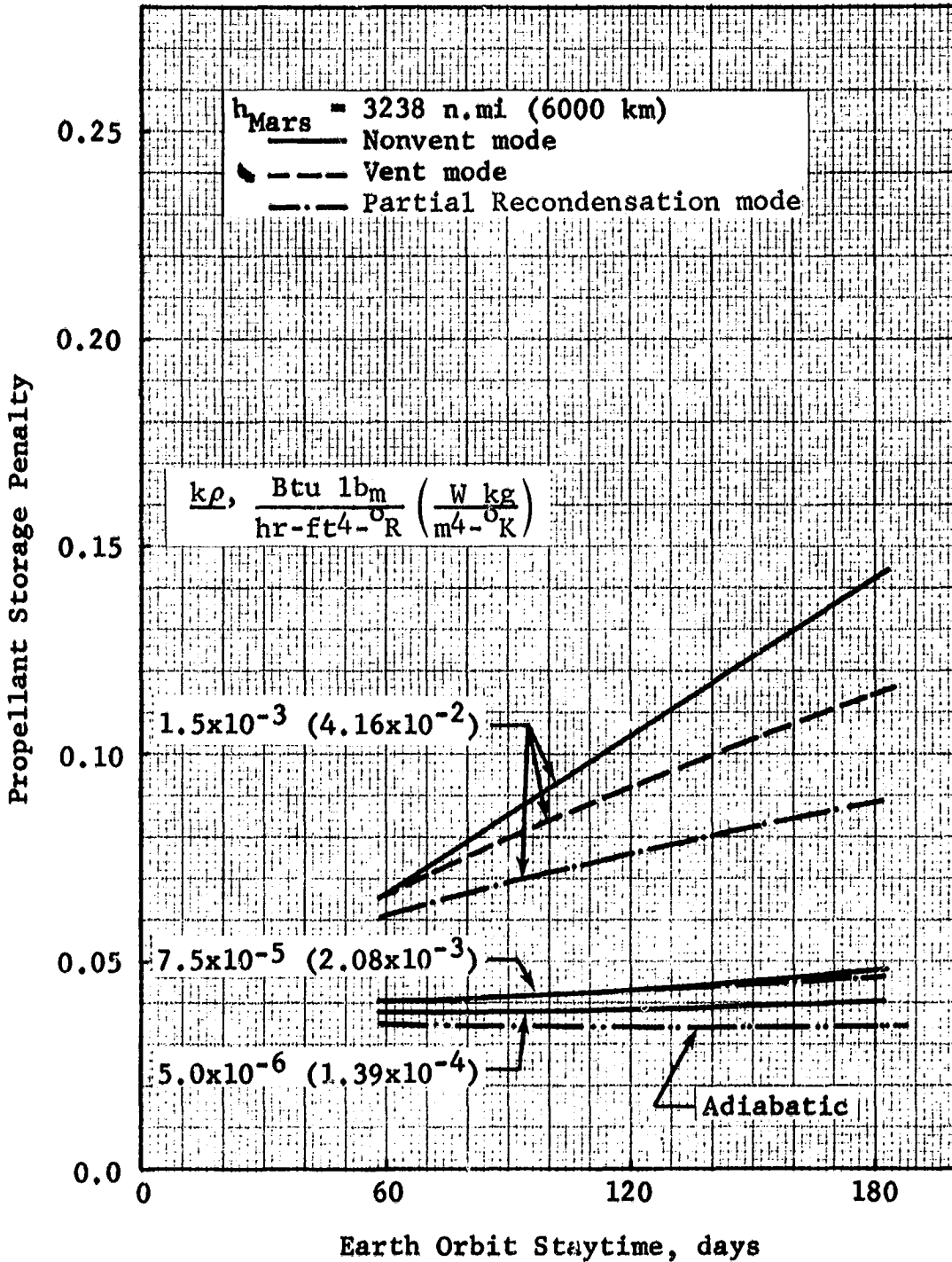


Figure 4.3-5 Propellant Storage Penalty vs Staytime:
Shielded Mars Braking Stage, $h_{Mars} = 3238 \text{ n.mi}$

GENERAL DYNAMICS

Fort Worth Division

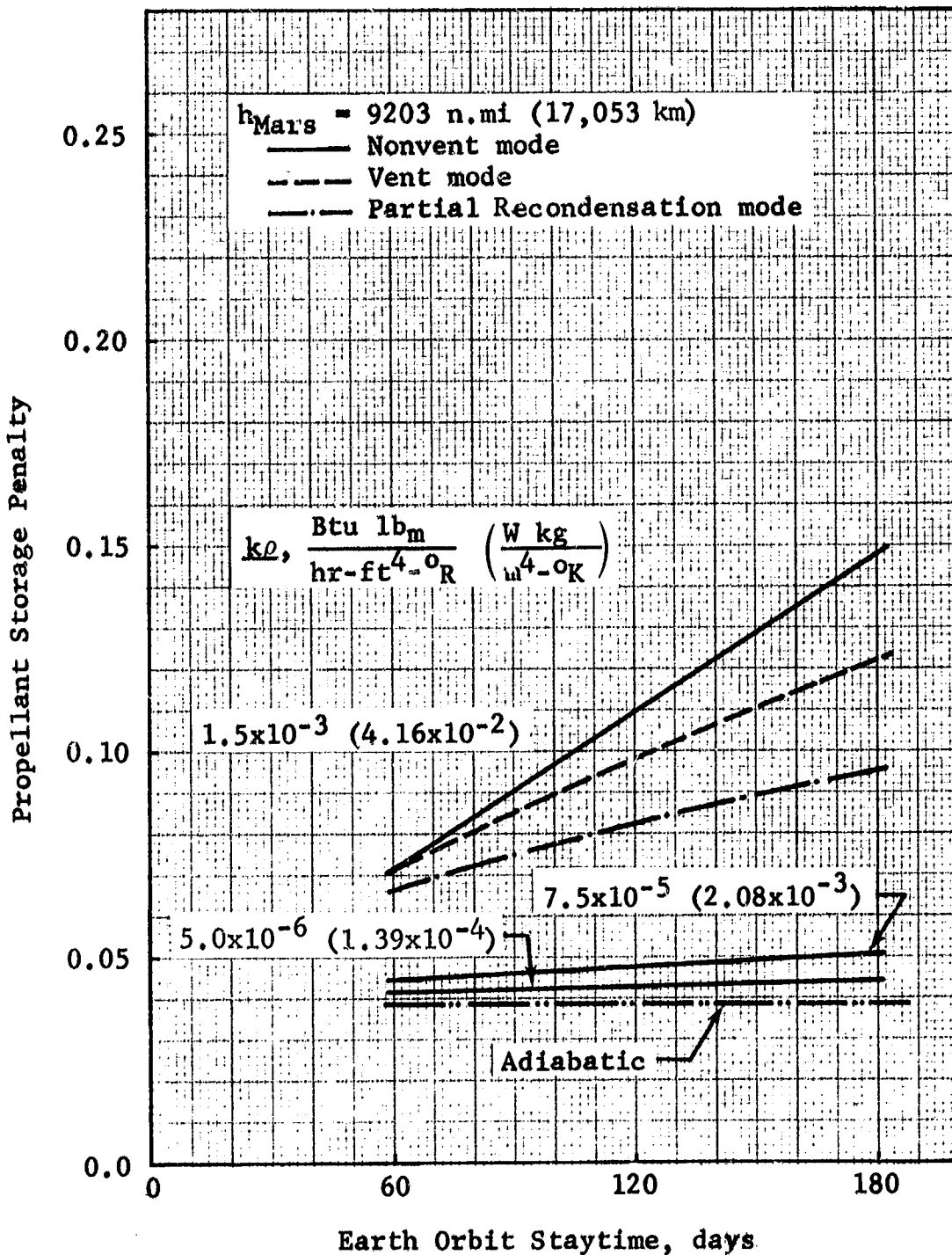


Figure 4.3-6 Propellant Storage Penalty vs Staytime:
Shielded Mars Braking Stage, $h_{Mars} = 9203 \text{ n.mi}$

GENERAL DYNAMICS
Fort Worth Division

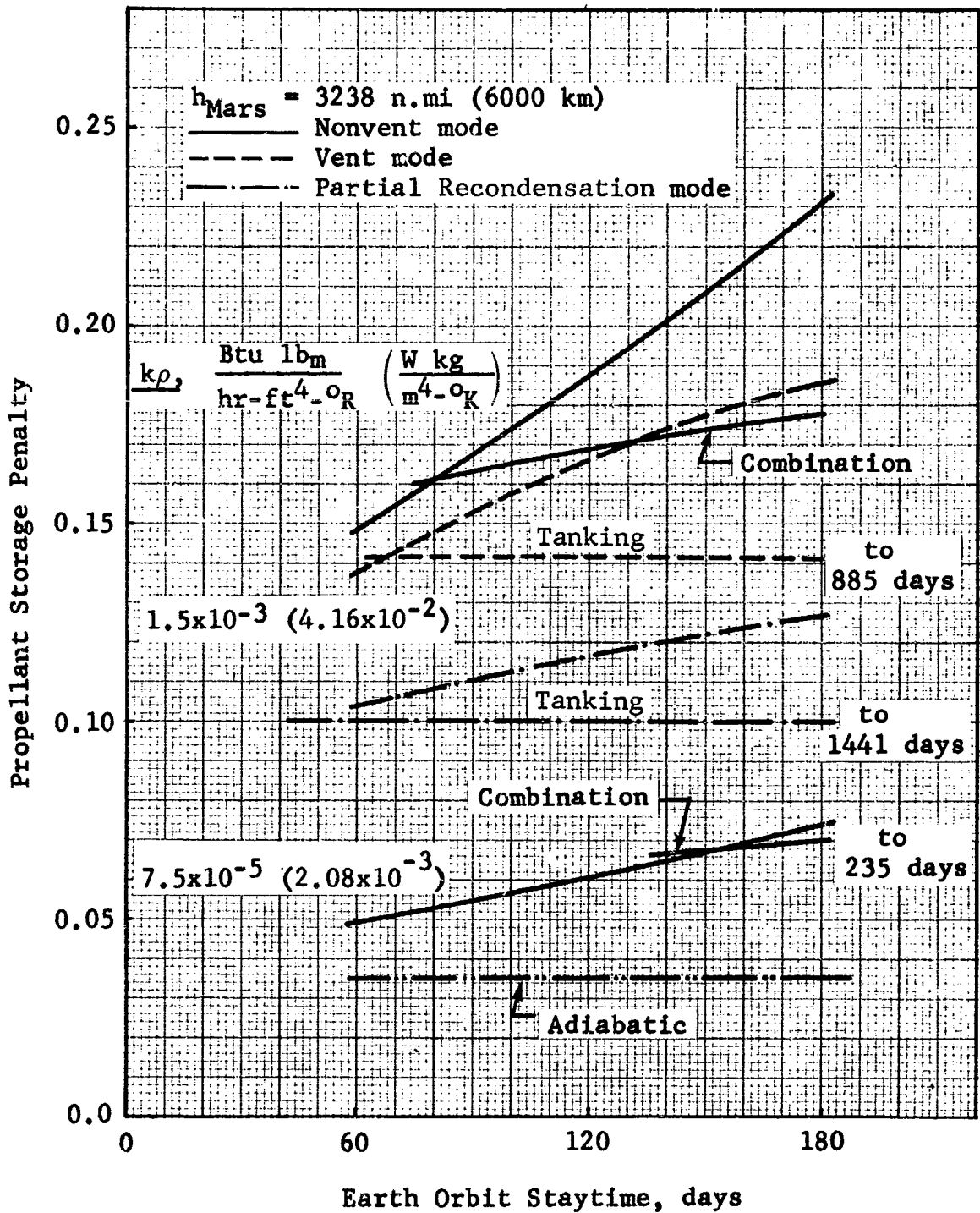


Figure 4.3-7 Comparison of Propellant Storage Penalties for Various Storage Modes: Unshielded Mars Braking Stage

GENERAL DYNAMICS
Fort Worth Division

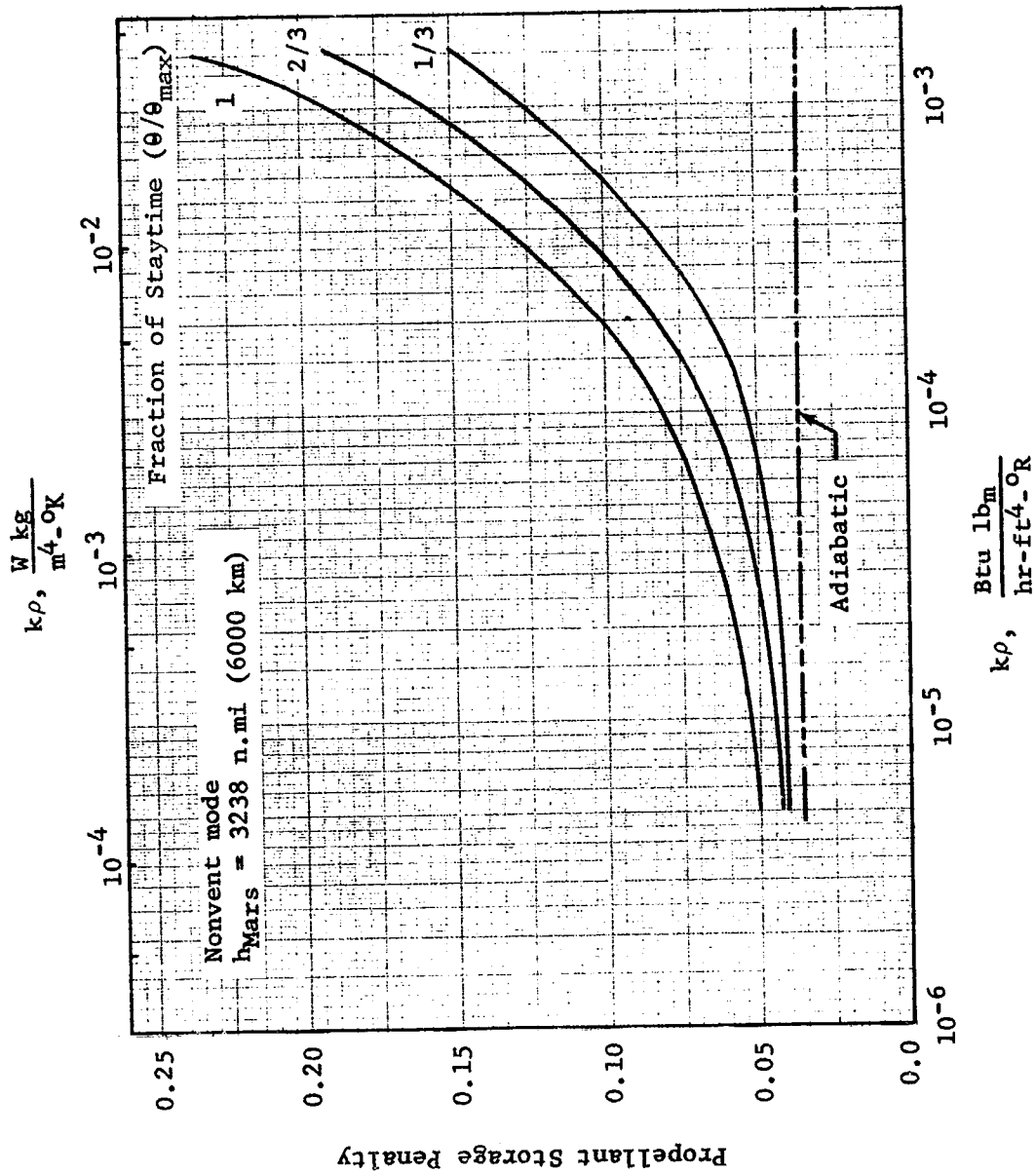


Figure 4.3-8 Effect of Insulation Thermal Performance on Propellant Storage Penalty: Unshielded Mars Braking Stage

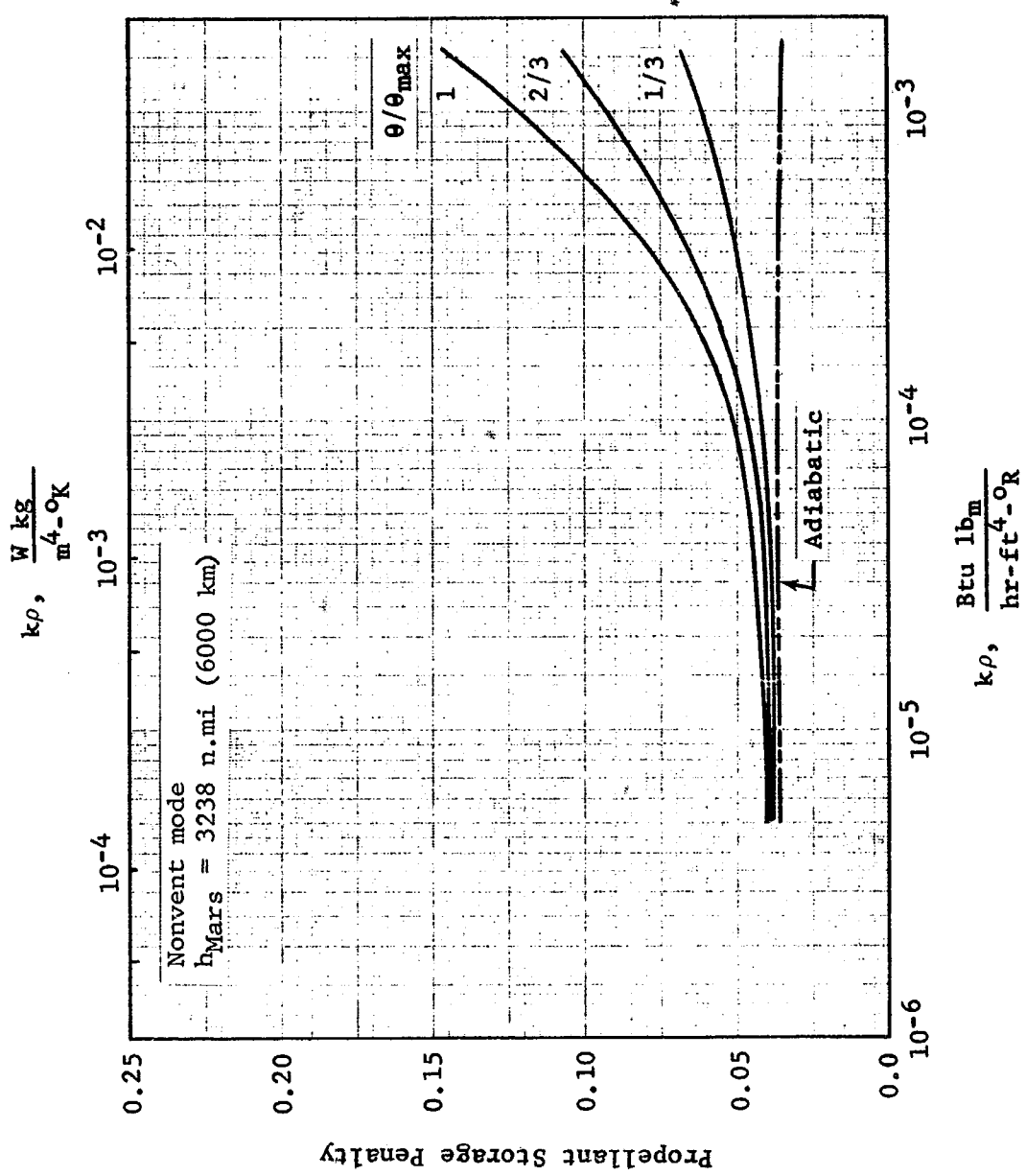


Figure 4.3-9 Effect of Insulation Thermal Performance on Propellant Storage Penalty: Shielded Mars Braking Stage

GENERAL DYNAMICS

Fort Worth Division

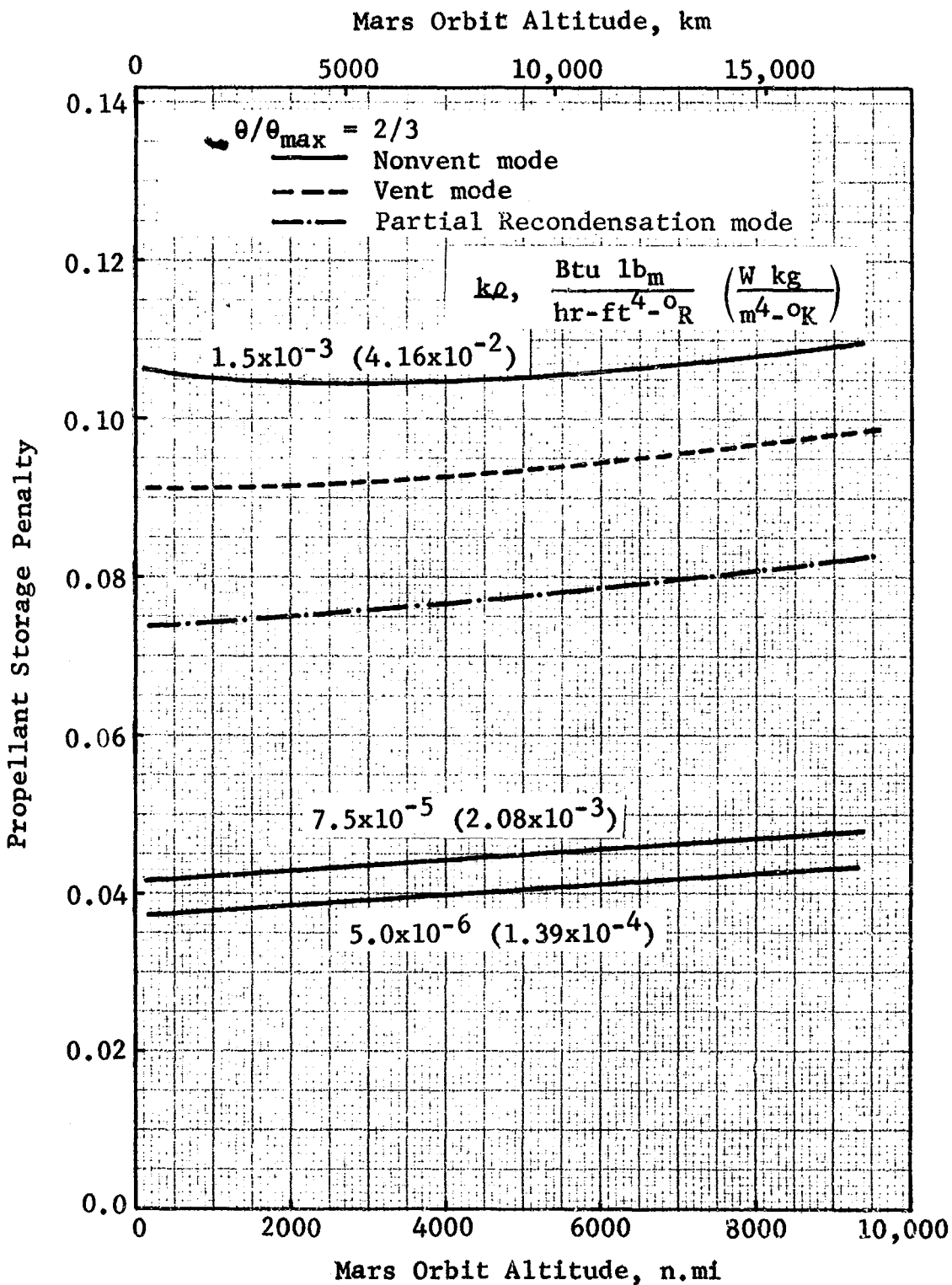


Figure 4.3-10 Propellant Storage Penalty vs Altitude: Shielded Mars Braking Stage

GENERAL DYNAMICS
Fort Worth Division

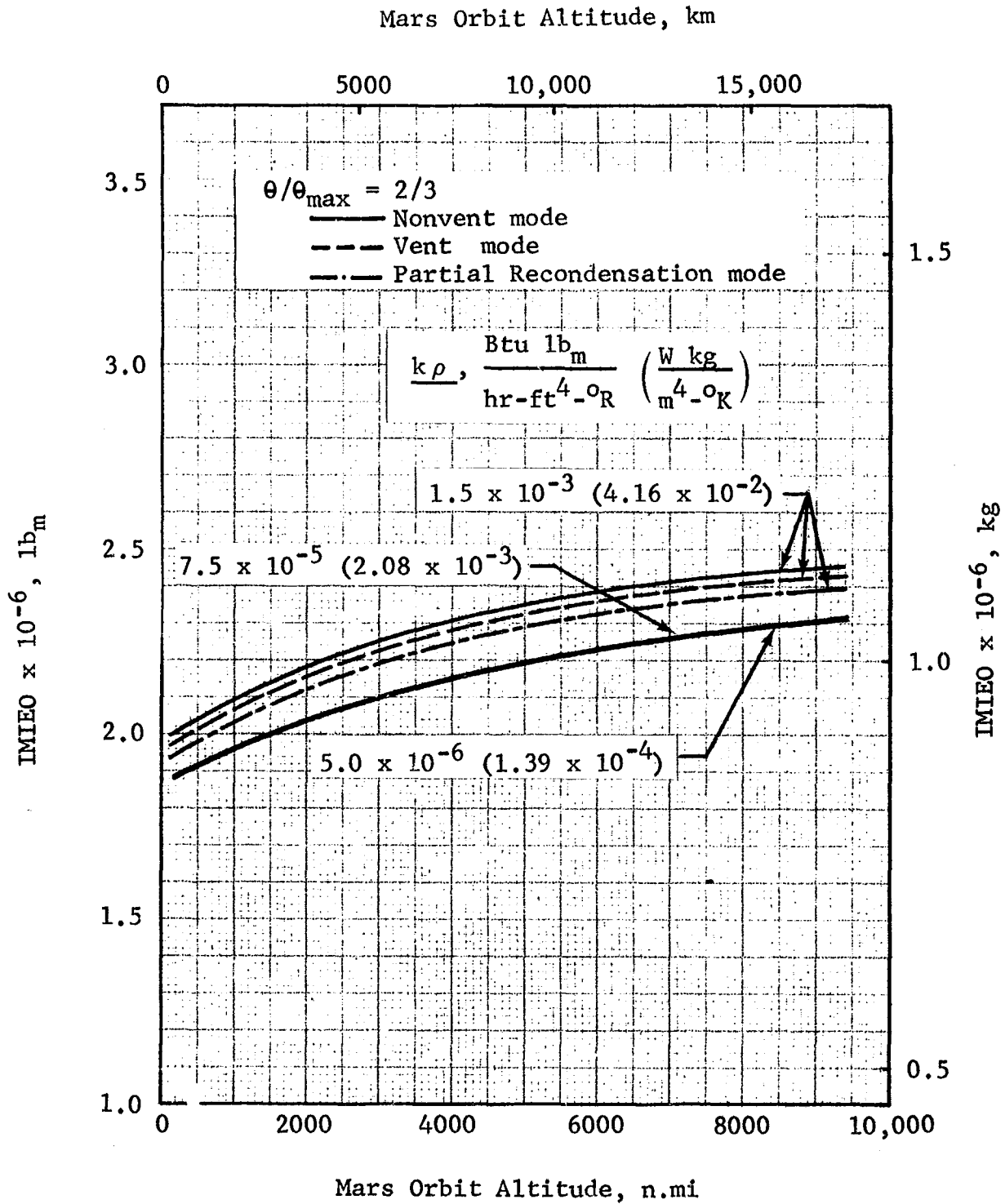


Figure 4.3 .1 Effect of Optimum Propellant Storage System on IMIEO vs Altitude: Shielded Mars Braking Stage

GENERAL DYNAMICS
Fort Worth Division

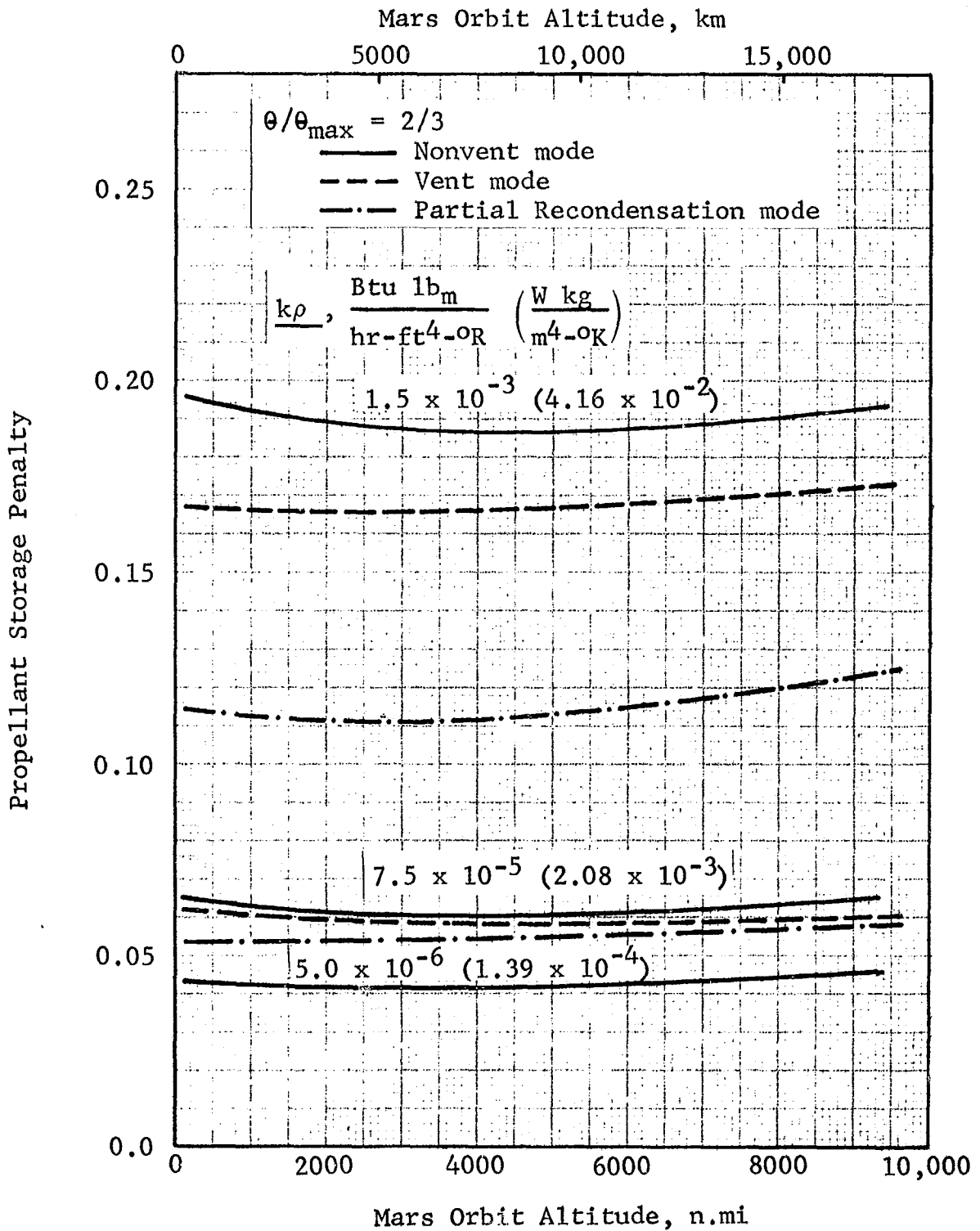


Figure 4.3-12 Propellant Storage Penalty vs
Altitude: Unshielded Mars
Braking Stage

GENERAL DYNAMICS
Fort Worth Division

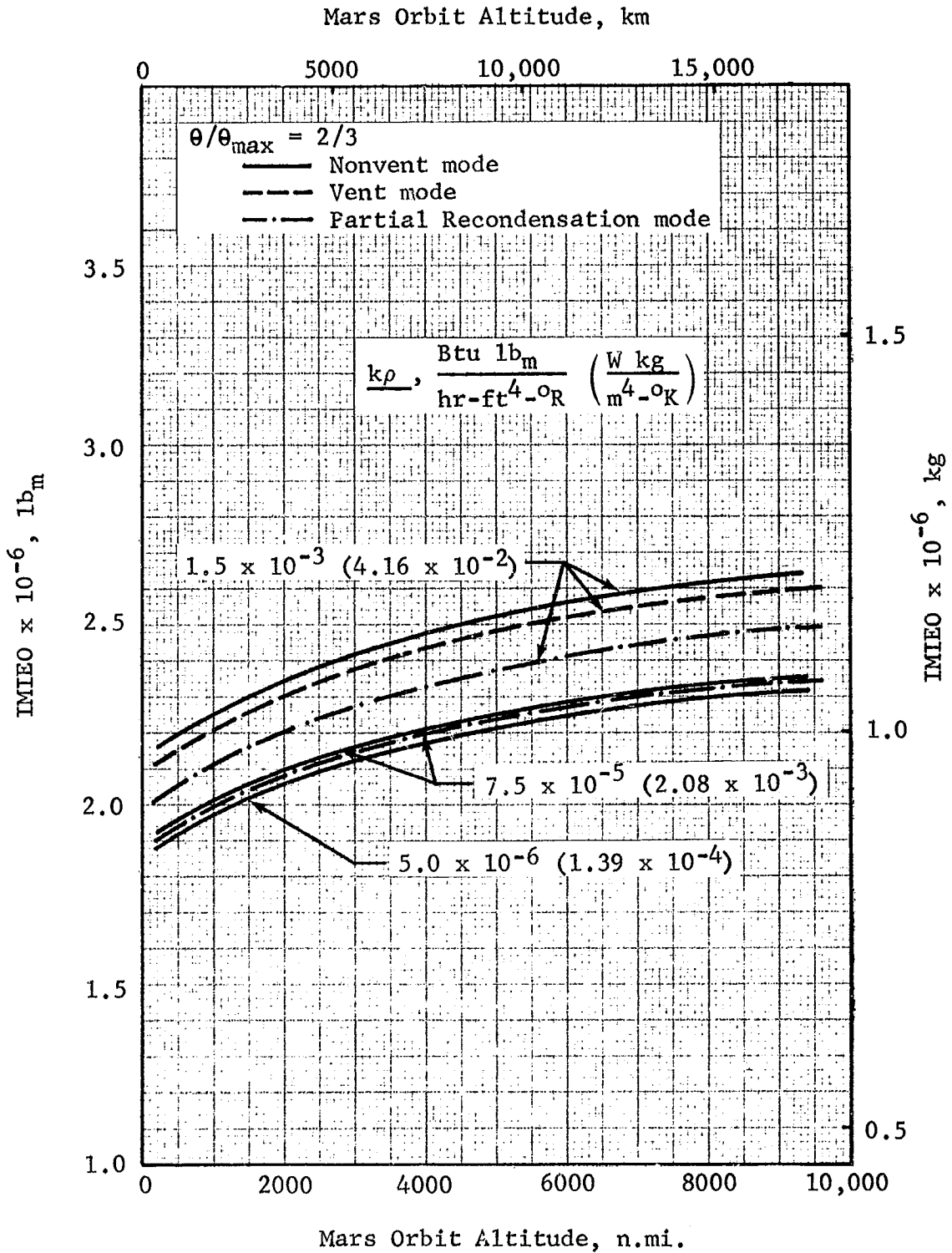


Figure 4.3-13 Effect of Optimum Propellant Storage System on IMIEO vs Altitude: Unshielded Mars Braking Stage

GENERAL DYNAMICS
Fort Worth Division

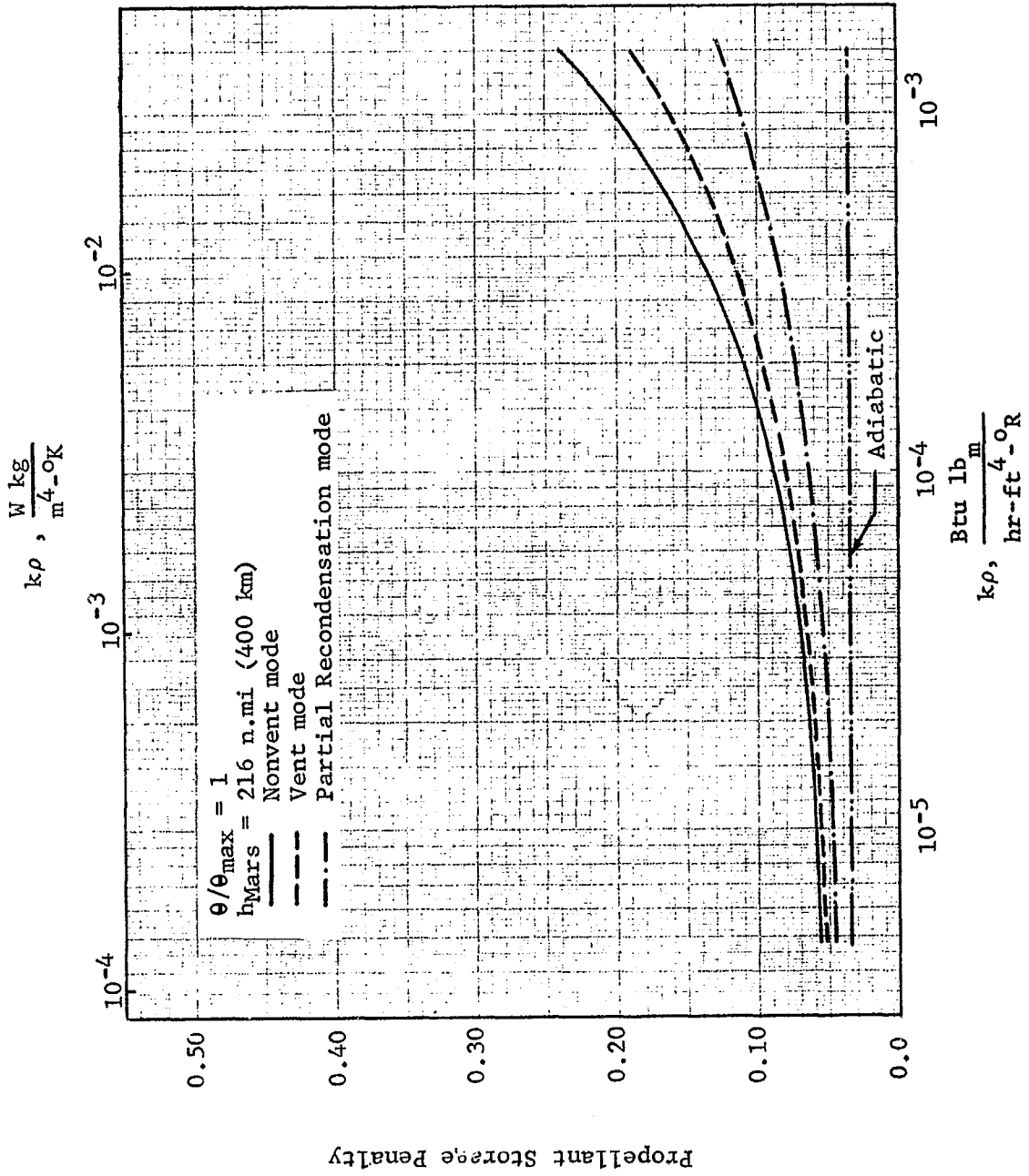


Figure 4.3-14 Effect of Propellant Storage Mode on Propellant Storage Penalty: Unshielded Mars Braking Stage

GENERAL DYNAMICS
Fort Worth Division

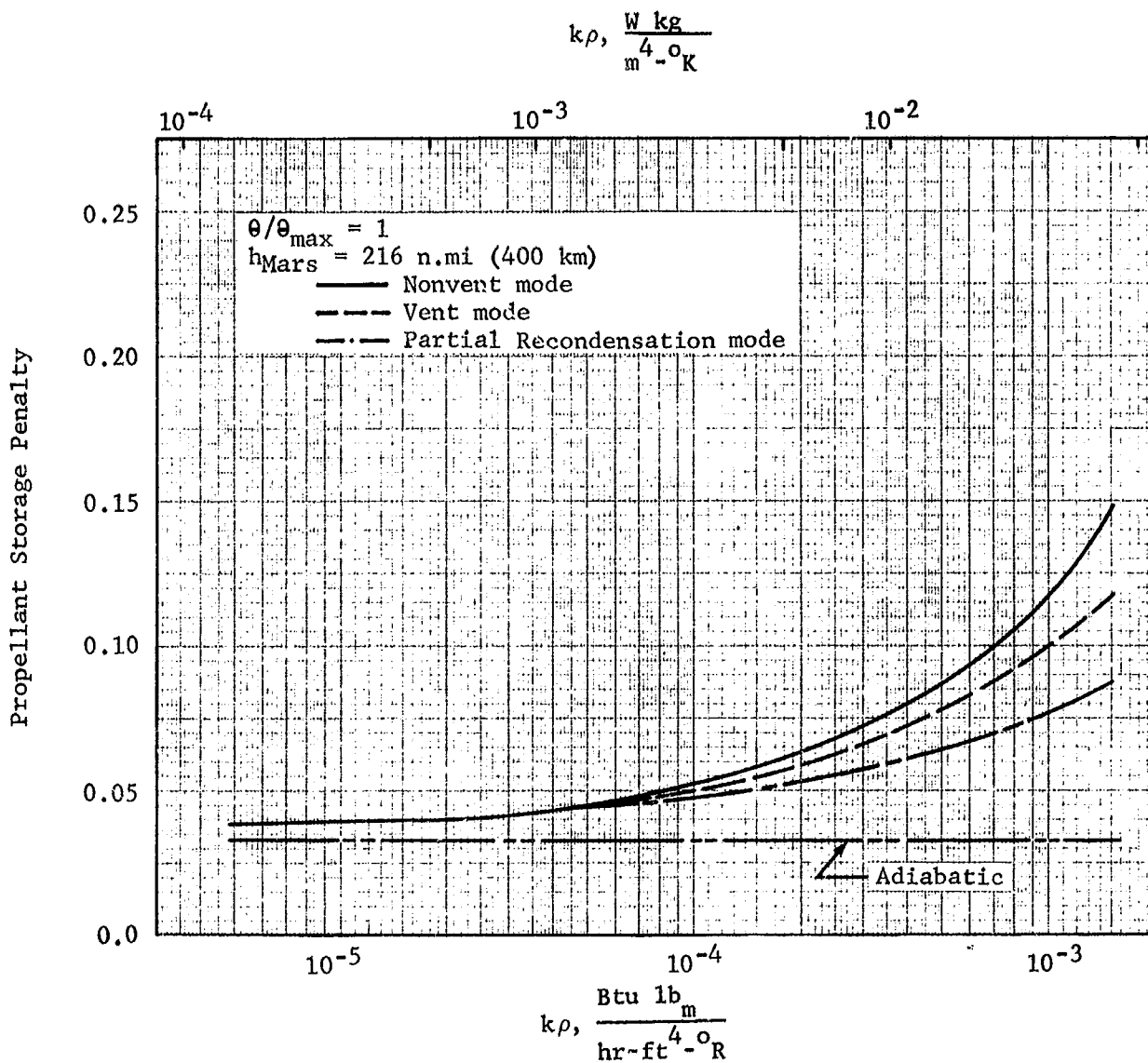


Figure 4.3-15 Effect of Propellant Storage Mode on Propellant Storage Penalty: Shielded Mars Braking Stage

GENERAL DYNAMICS
Fort Worth Division

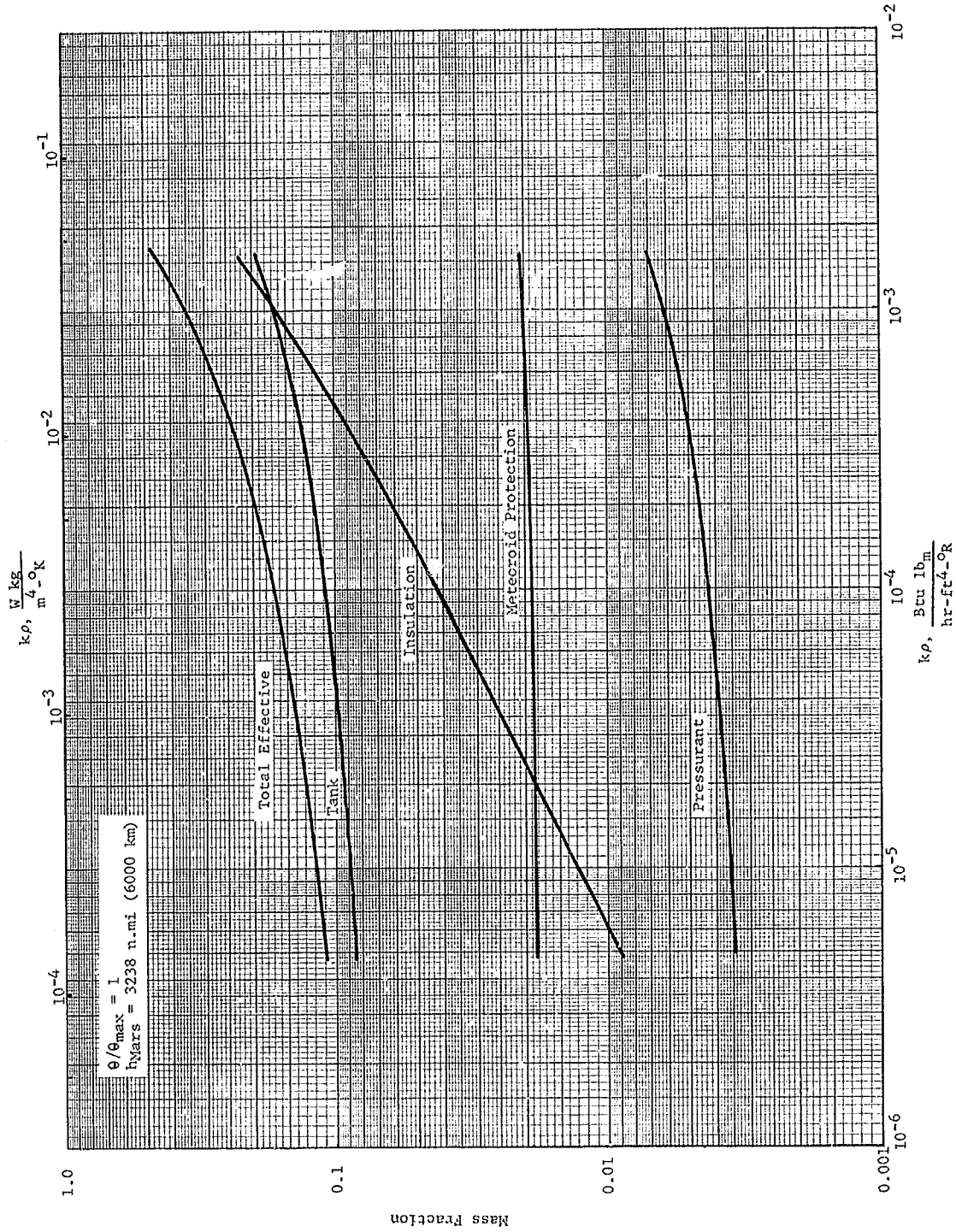


Figure 4.3-16 Optimum Propellant Storage Component Mass Fractions: Unshielded Mars Braking Stage, Nonvent Mode

GENERAL DYNAMICS
Fort Worth Division

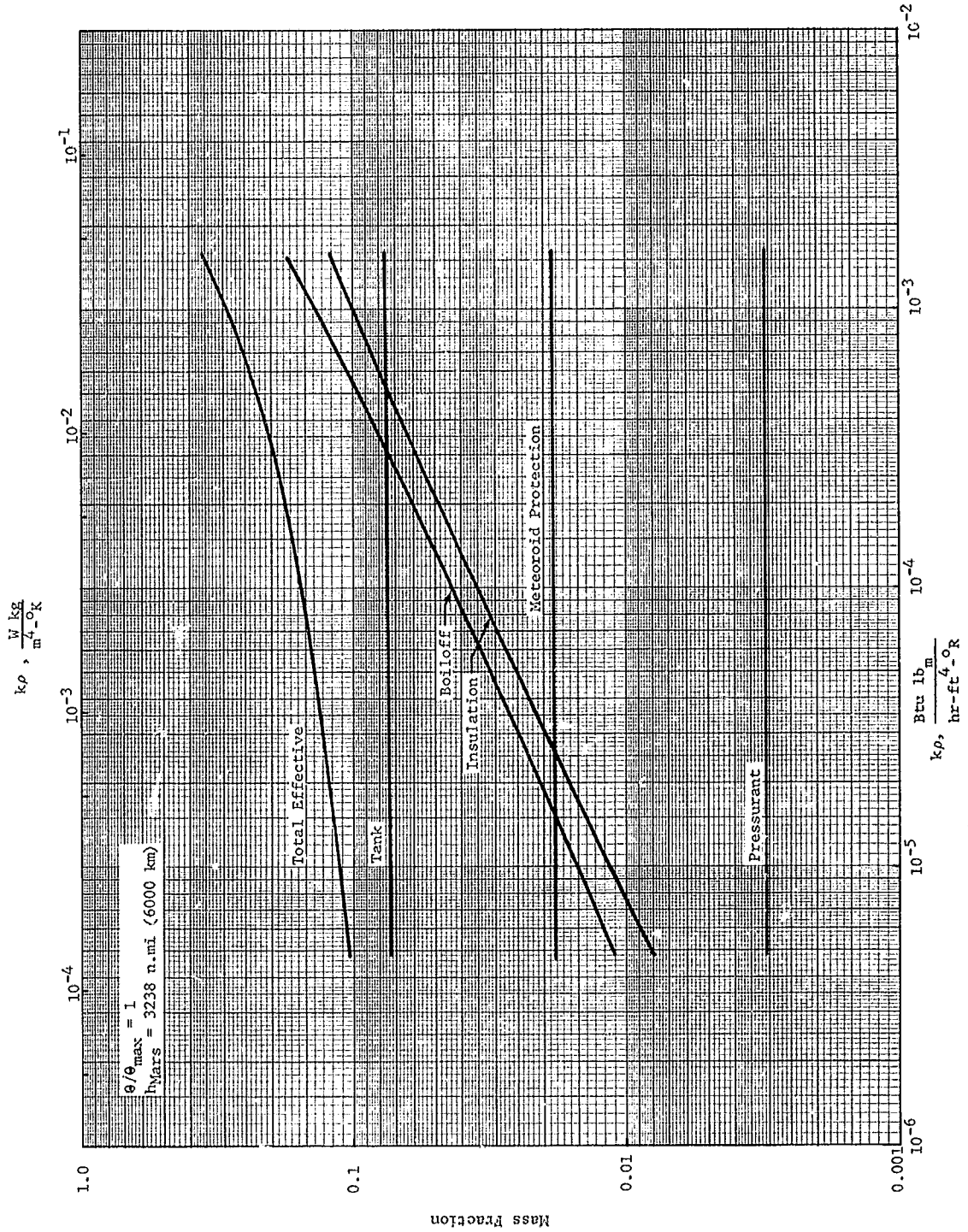


Figure 4.3-17 Optimum Propellant Storage Component Mass Fractions:
Unshielded Mars Braking Stage, Vent Mode

GENERAL DYNAMICS
Fort Worth Division

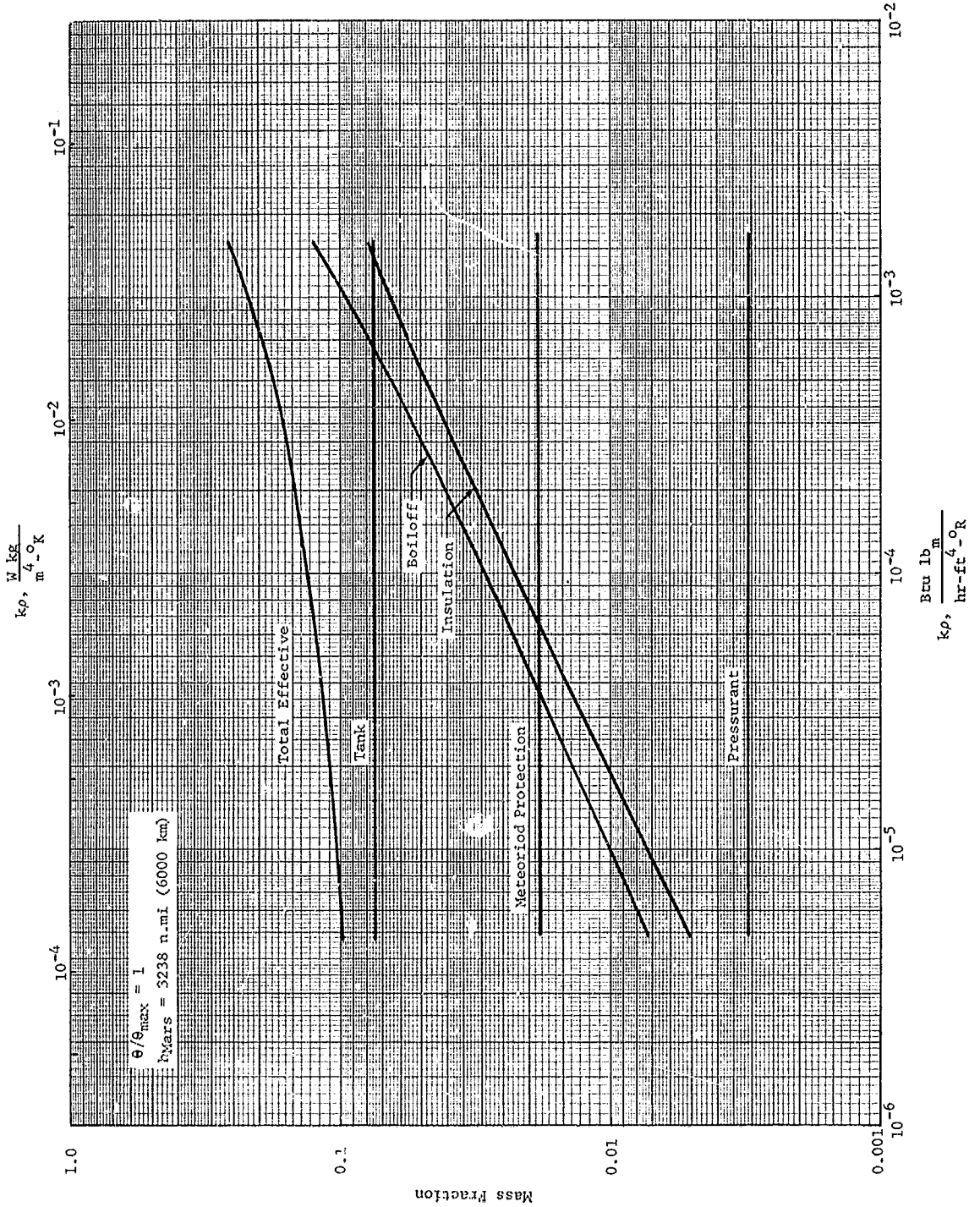


Figure 4.3-18 Optimum Propellant Storage Component Mass Fractions: Unshielded Mars Braking Stage, Partial Recondensation Mode

GENERAL DYNAMICS
Fort Worth Division

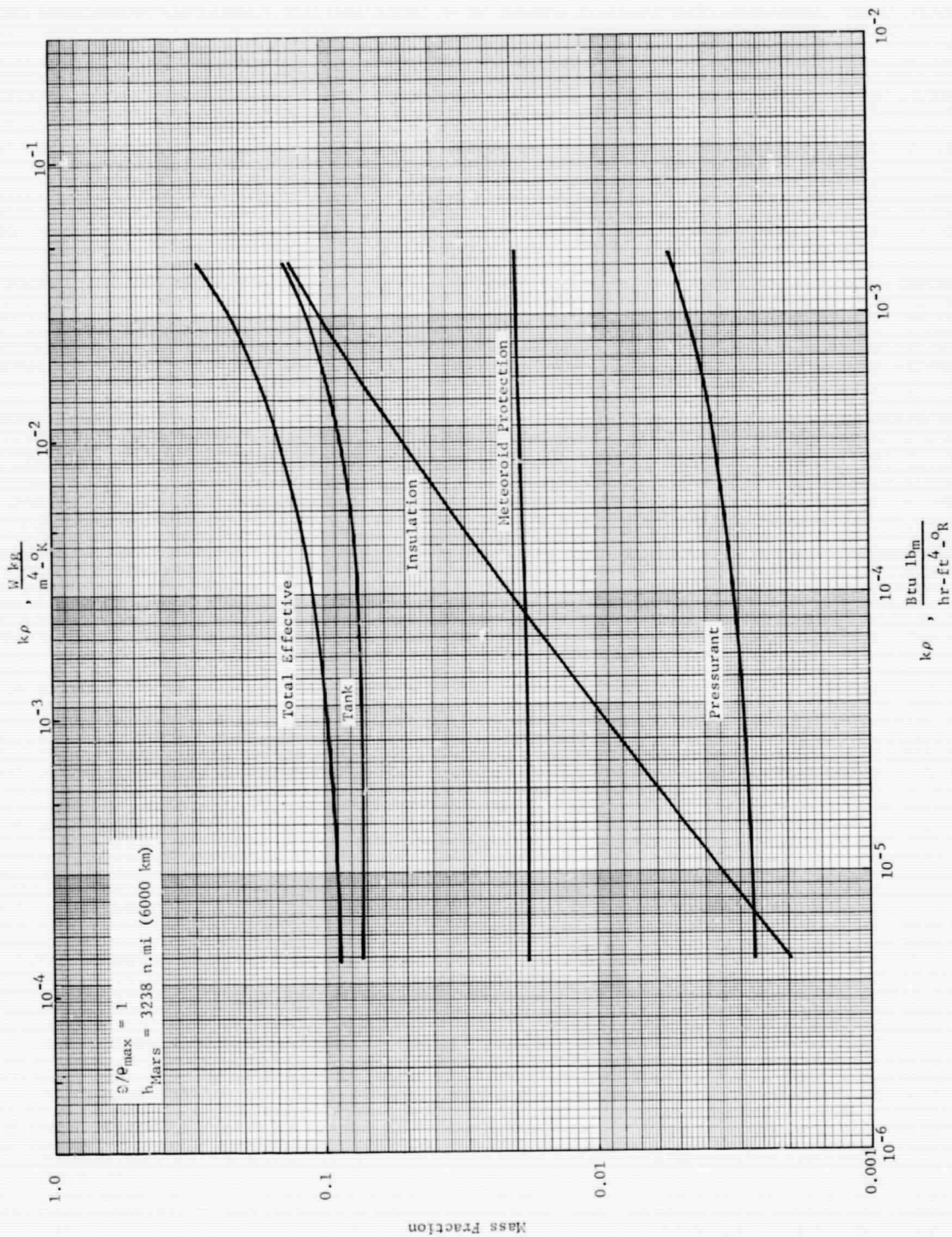


Figure 4.3-19 Optimum Propellant Storage Component Mass Fractions: Shielded Mars Braking Stage, Nonvent Mode

GENERAL DYNAMICS
Fort Worth Division

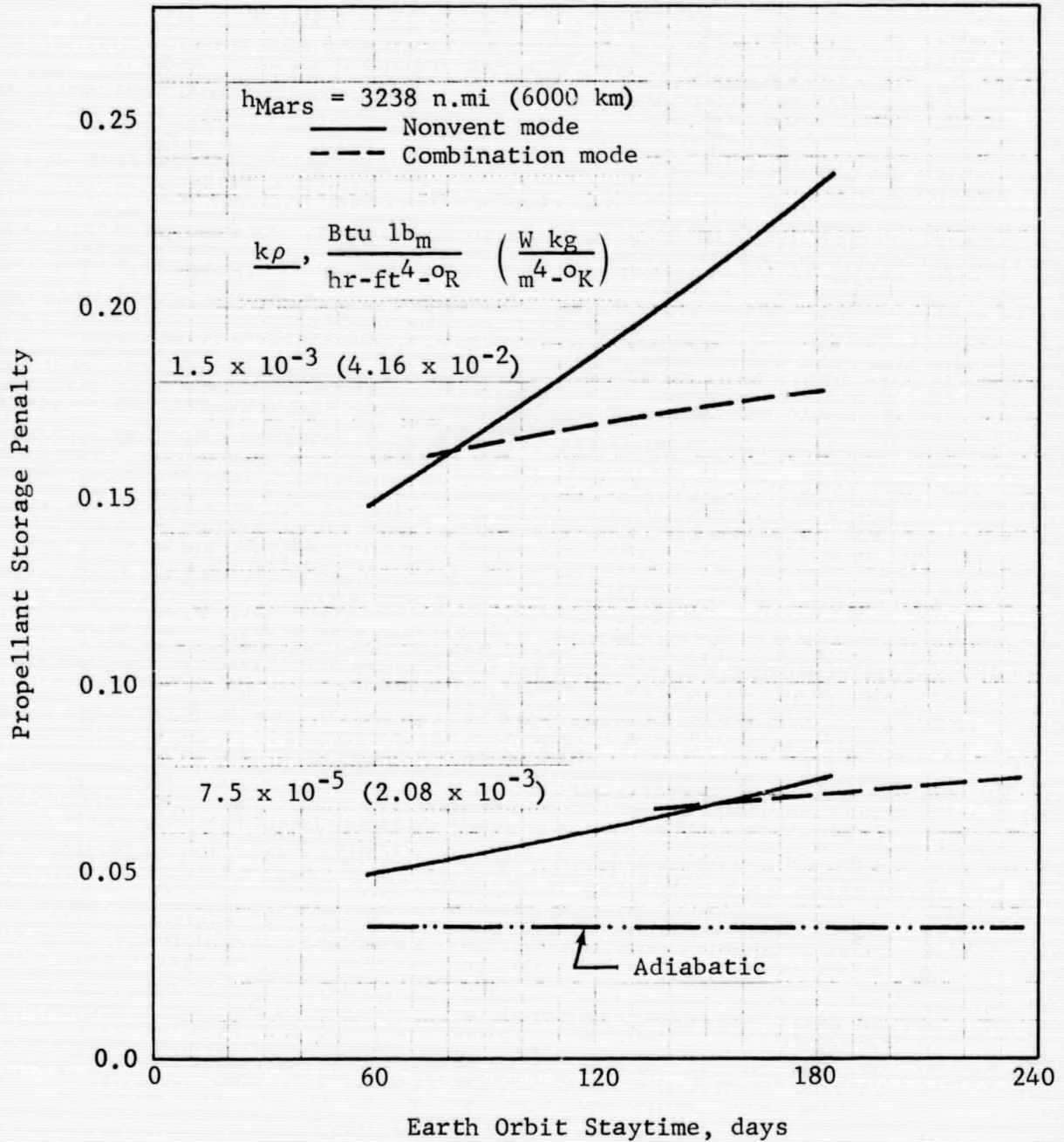


Figure 4.3-20 Comparison of Propellant Storage Penalties for the Combination and Nonvent Storage Modes: Unshielded Mars Braking Stage

GENERAL DYNAMICS
Fort Worth Division

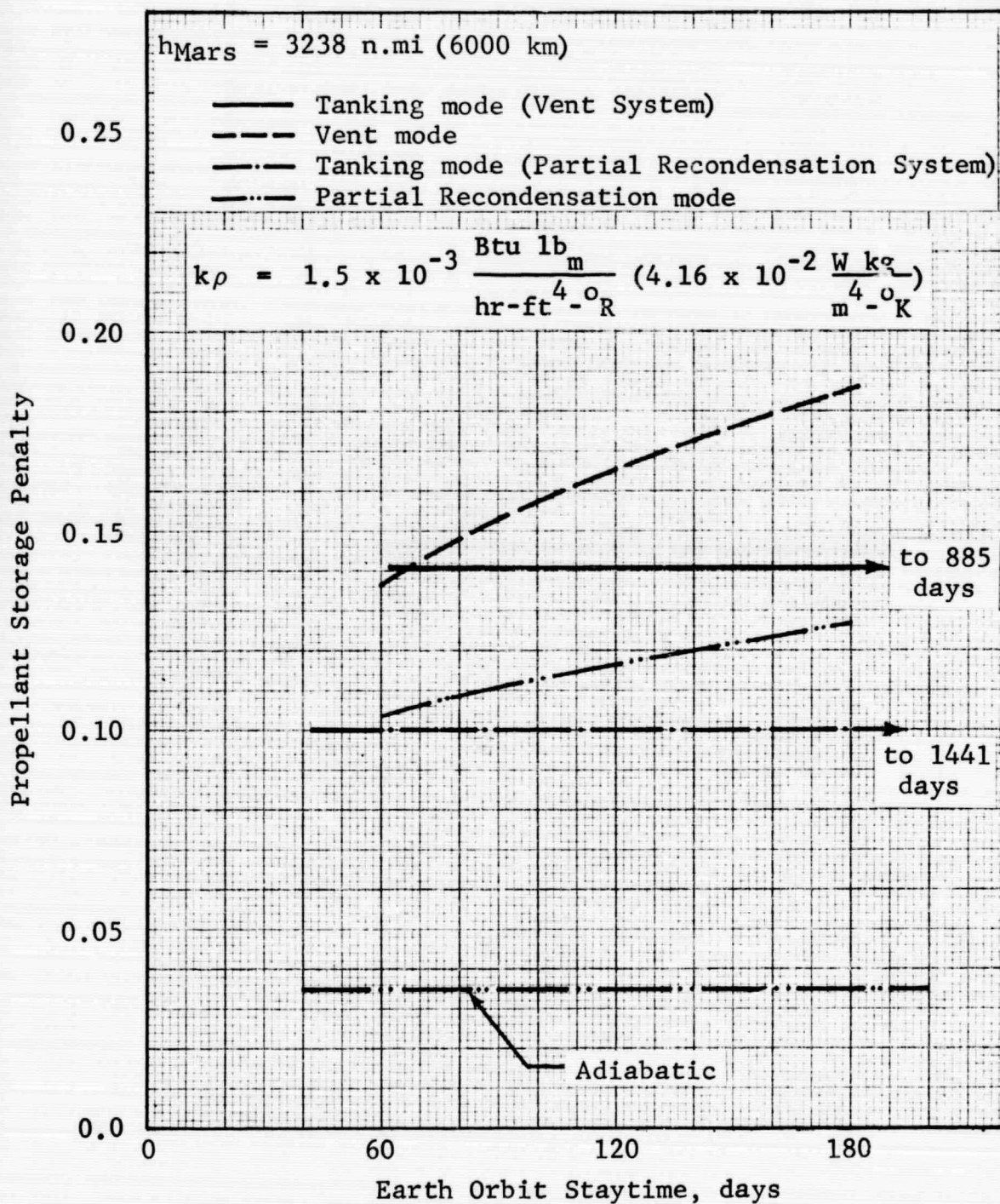


Figure 4.3-21 Effect of Tanking on Propellant Storage Penalty: Unshielded Mars Braking Stage

“REPRODUCIBILITY OF THE ORIGINAL PAGE IS POOR.”

GENERAL DYNAMICS
Fort Worth Division

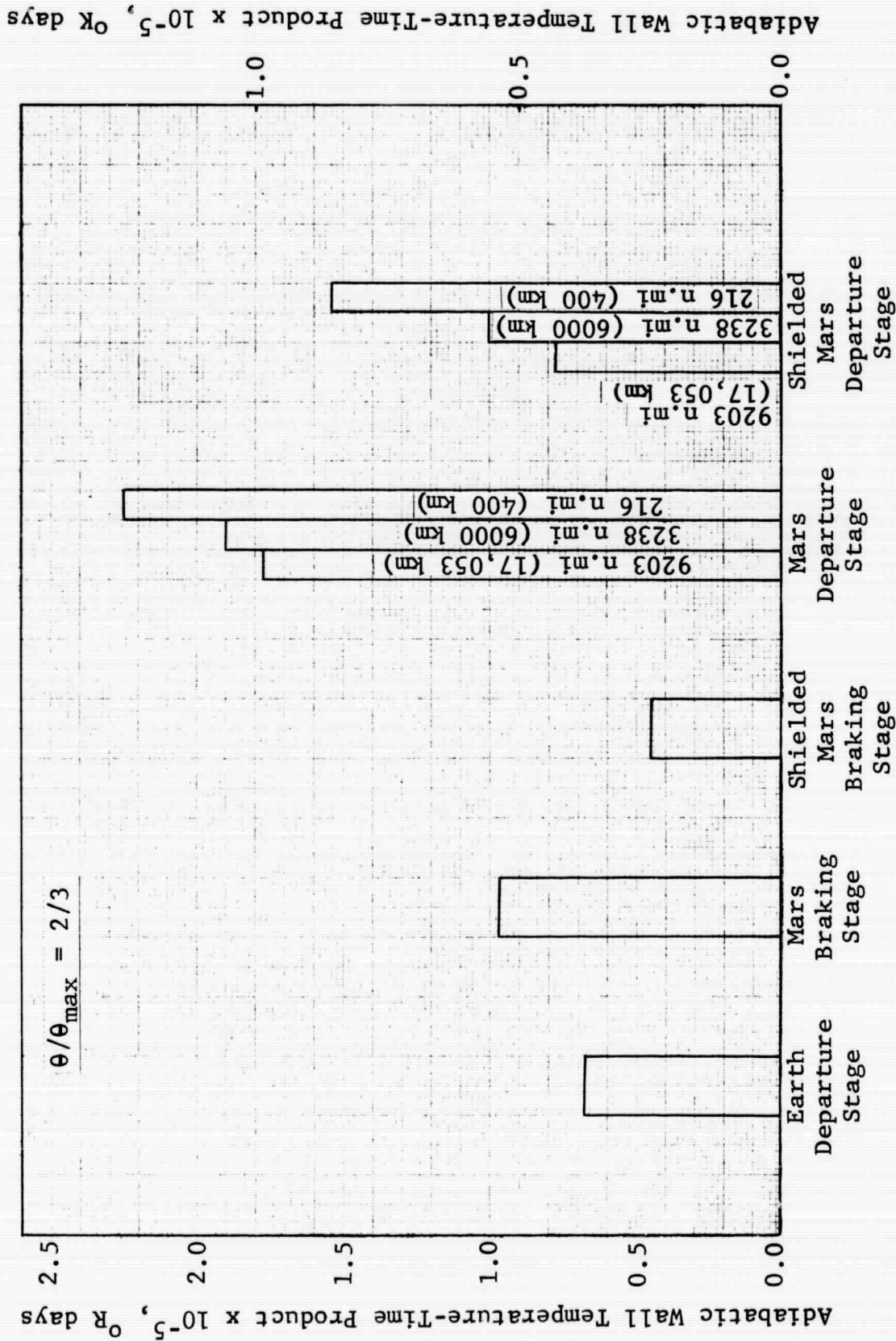


Figure 4.3-22 Thermal Severity of the Mars Mission

GENERAL DYNAMICS

Fort Worth Division

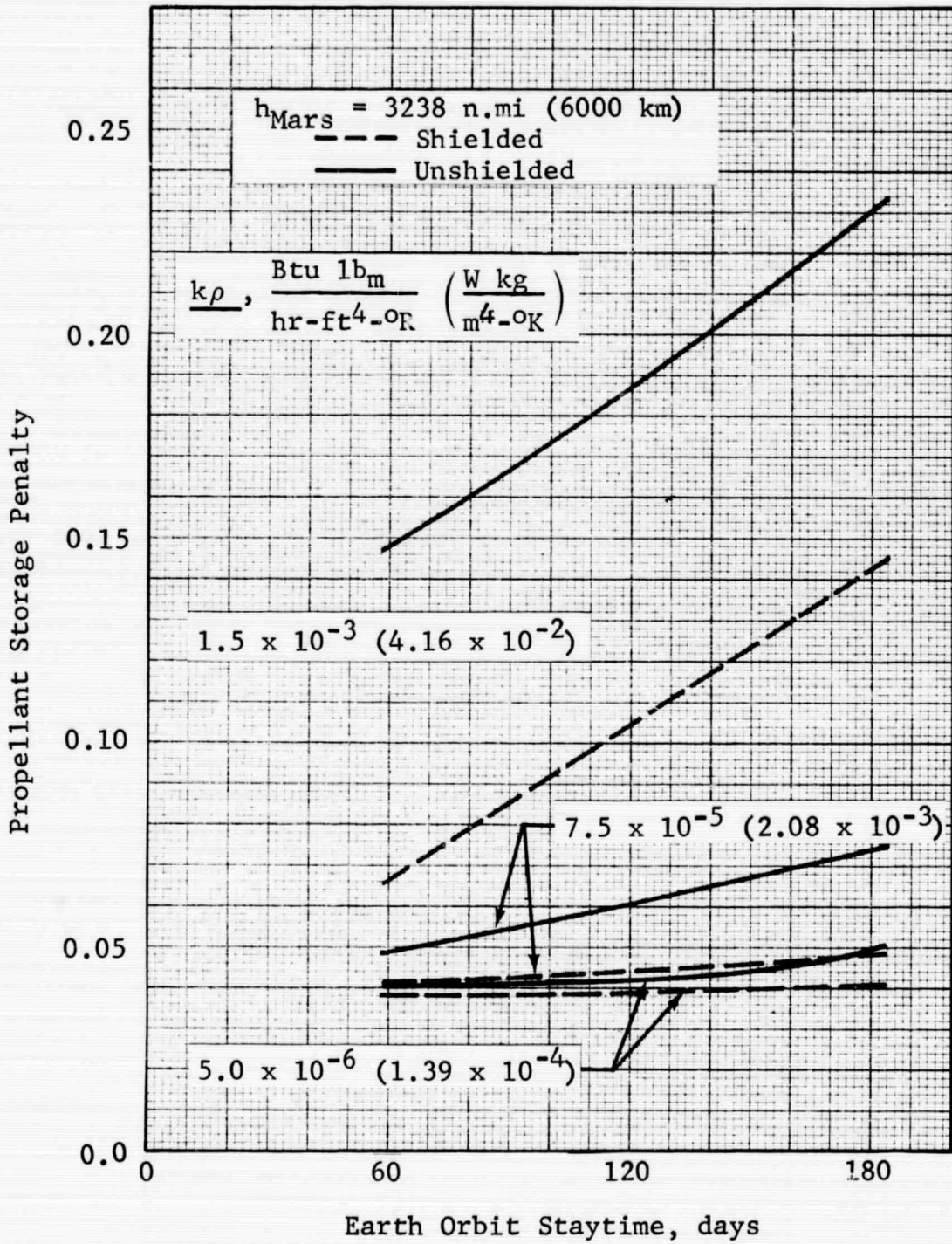


Figure 4.3-23 Effect of Solar Shield on Propellant Storage Penalty: Mars Braking Stage, Nonvent Mode

GENERAL DYNAMICS
Fort Worth Division

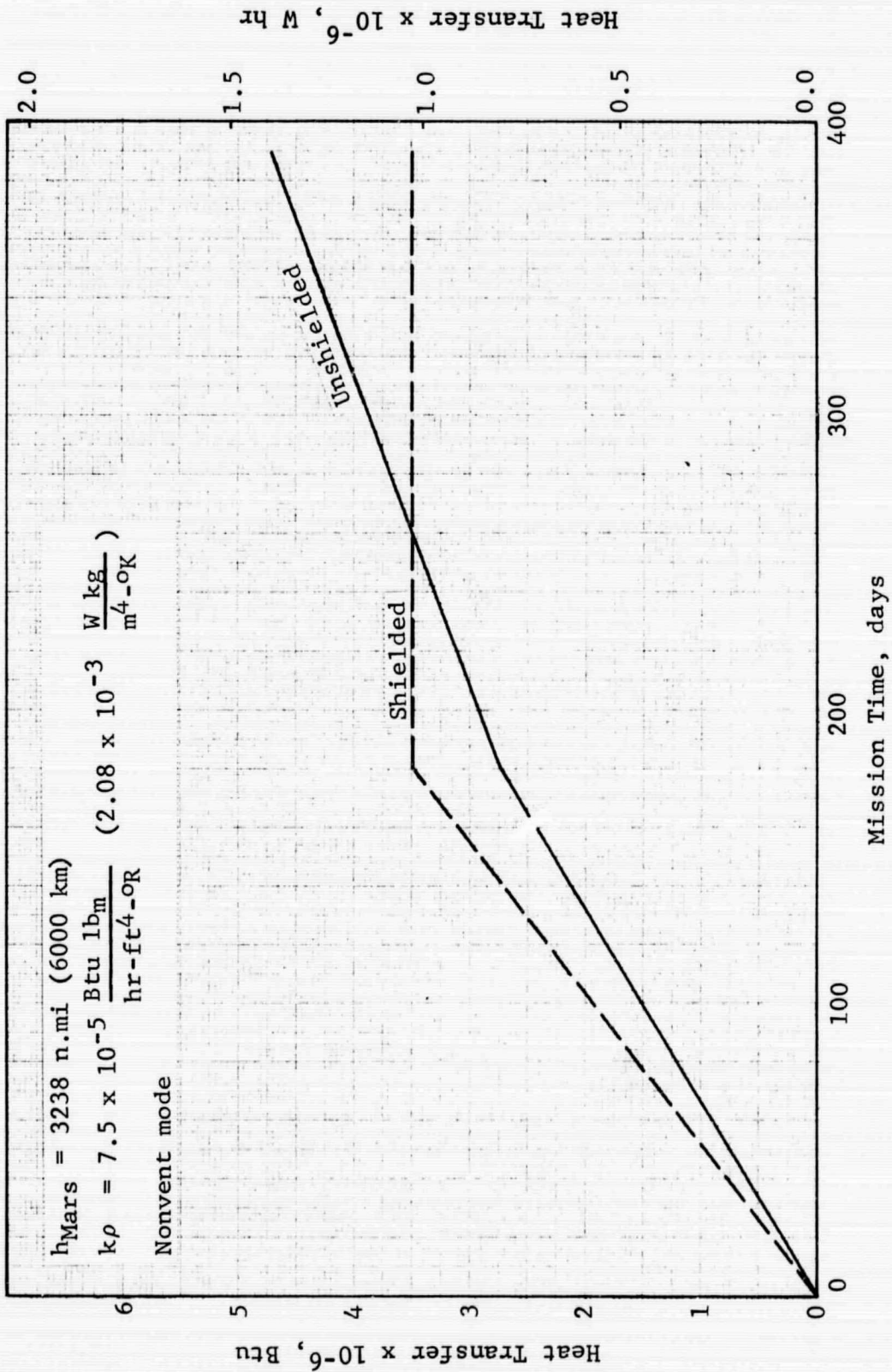


Figure 4.3-24 Effect of Solar Shield on Propellant Heat Transfer: Mars Braking Stage

GENERAL DYNAMICS
Fort Worth Division

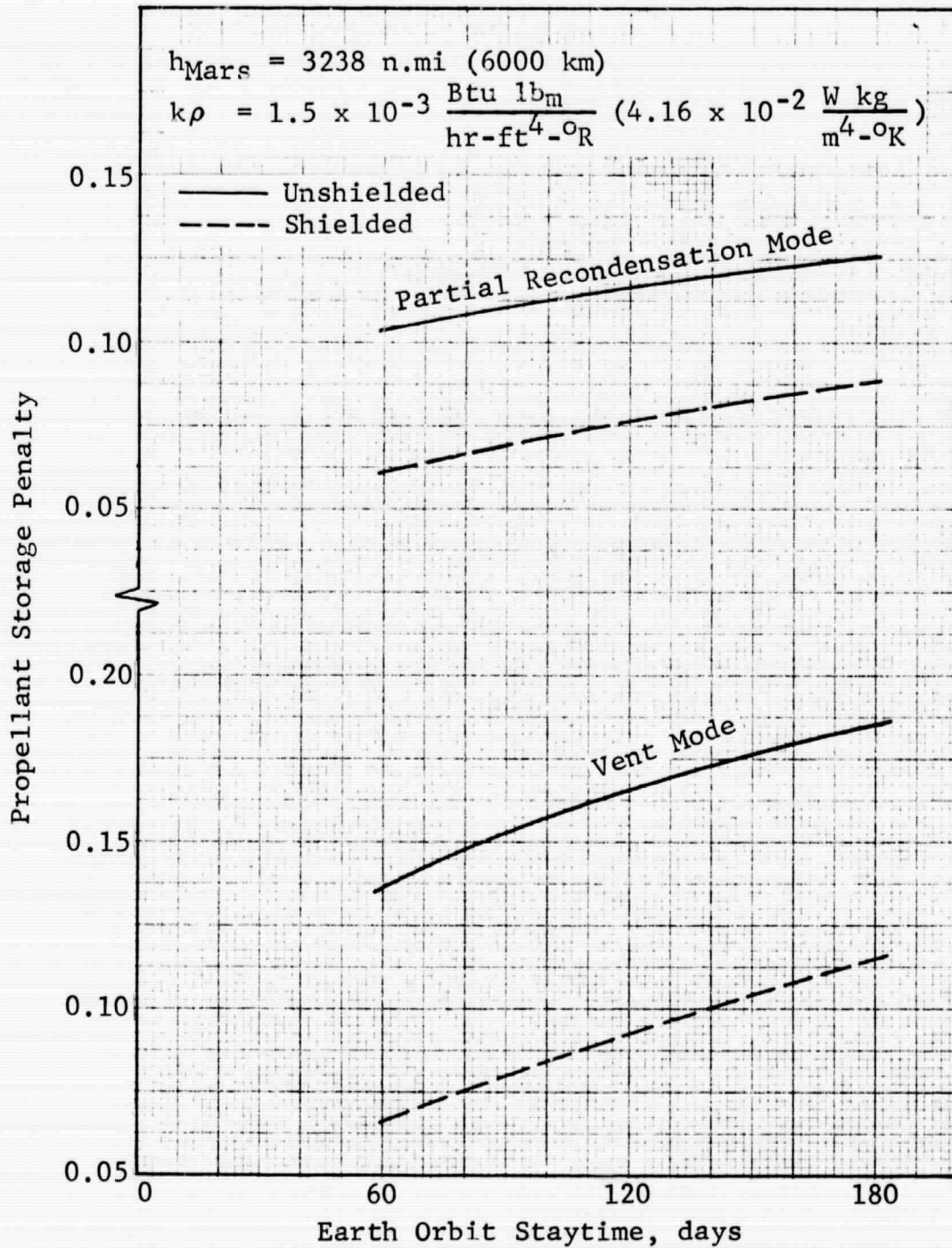


Figure 4.3-25 Effect of Solar Shield on Propellant Storage Penalty: Mars Braking Stage, Vent and Partial Recondensation Modes

GENERAL DYNAMICS
Fort Worth Division

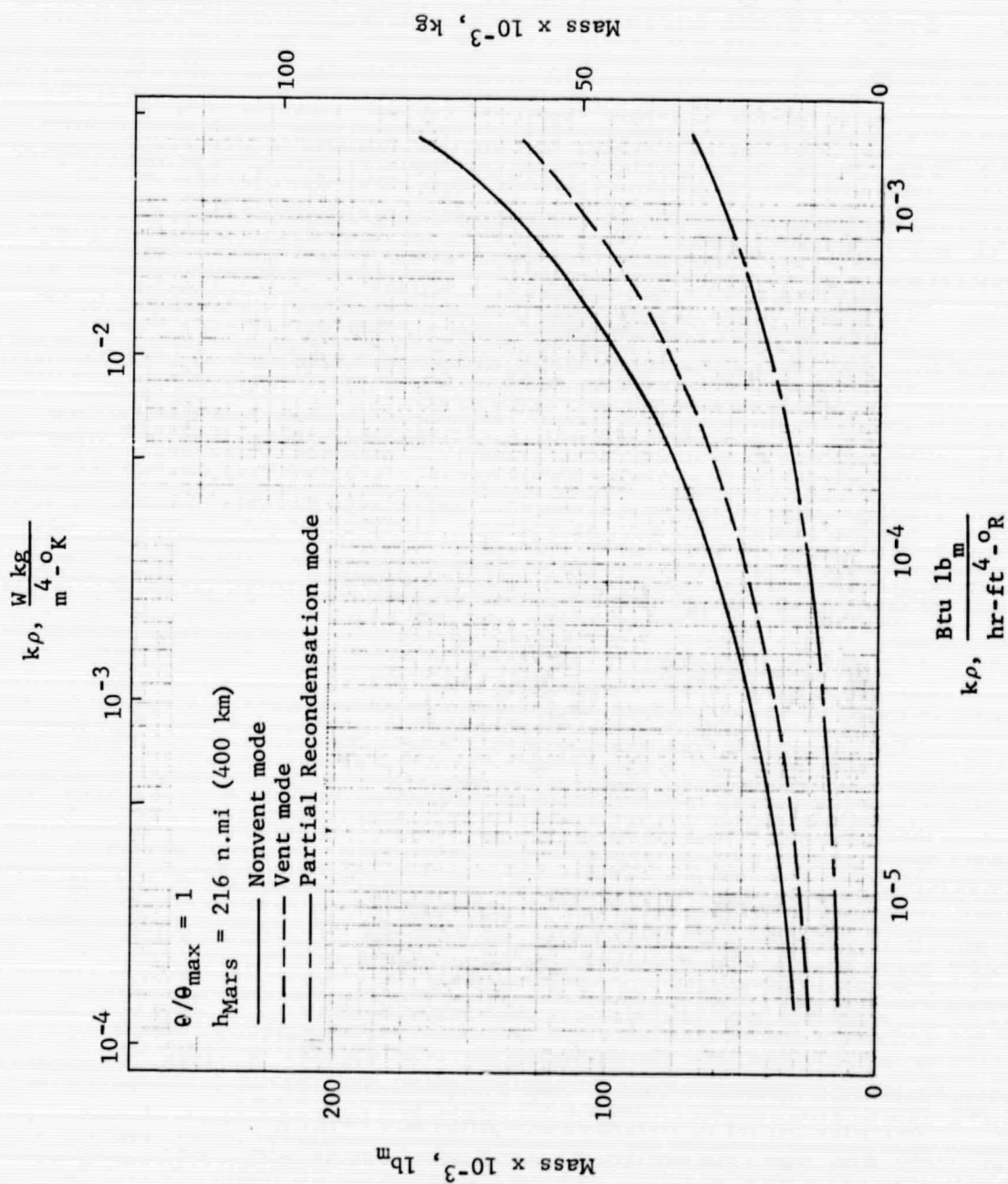


Figure 4.3-26 Difference in IMEO between the Shielded and Unshielded Mars Braking Stages

GENERAL DYNAMICS

Fort Worth Division

4.4 MARS DEPARTURE STAGE PROPELLANT STORAGE PENALTY

Although the Mars Departure Stage is the smallest stage of the vehicle, its effect on the IMIEO is increased relatively by virtue of the three primary propulsive maneuvers it undergoes. Its influence on the IMIEO is also increased by the greater mission time of this stage, which is, at minimum, twice that of the other stages. The longer exposure to the thermal environment results in a higher heat transfer per pound of propellant. In this subsection, the propellant storage penalty to the IMIEO for the Mars Departure Stage is discussed with reference to optimized propellant storage systems. The first two stages of the vehicle are defined in terms of nominal mass fractions, dependent only upon the Mars orbit altitude, in order to determine the vehicle IMIEO.

The bulk of the data presented in this section pertains to the vent and partial-recondensation storage modes. The nonvent mode was investigated only at the 9203-n.mi (17,053 km) altitude for the shielded stage. At the lower altitudes in the shielded case and at all altitudes in the unshielded case, the tank pressure in the nonvent mode was found to be extremely high during the preliminary analysis, well beyond the range considered practical.

4.4.1 Sensitivity to Parameters

4.4.1.1 Earth Orbit Staytime

Because of the long mission time and, in particular the 510 days spent in Mars orbit, the relatively short period (30-90 days) spent in Earth orbit has only a small effect on the propellant storage system of the unshielded Mars Departure Stage. This is demonstrated in Figure 4.4-1, where the total heat transfer is plotted against mission time. Propellant storage penalty to the IMIEO is shown in Figure 4.4-2 for the intermediate altitude. As in the previous two subsections, the storage penalty is referenced to a vehicle with a propellant-storage-system mass fraction of zero for the stage under consideration; the remaining stages are defined in terms of nominal mass fractions. The IMIEO variation for the zero-mass-fraction Mars Departure Stage case is shown in Figure 4.2-1 as the curve labeled MDS. The high $k\rho$ value, vent-mode case yields the largest

GENERAL DYNAMICS

Fort Worth Division

variation in penalty (Fig. 4.4-2). The penalty increases 9.9% over the range of staytime, from 11.9% of the zero-mass-fraction IMIEO value to 13.0%. The minimum percentage increase is 6.6% for the partial-recondensation mode at the high $k\rho$ value. Thus, the influence of staytime is relatively independent of insulation performance or propellant storage mode. Of significance is the large difference between the penalty at the low $k\rho$ value for the partial-recondensation mode and that for the adiabatic tank wall case. This difference is due mainly to penetration heat transfer, which is independent of insulation performance and reflects the long mission time of the Mars Departure Stage (see Figure 4.1-22).

The shielded Mars Departure Stage is more strongly affected by the staytime, as shown in Figure 4.4-3 for the intermediate Mars orbit altitude. The shield reduces the total heat transfer, thereby increasing the influence of the Earth orbit heat transfer (see Figure 4.4-1). Compared to the unshielded case, the percentage increases in penalty are 2 to 3 times greater. Note too the difference between the adiabatic tank wall case and the results of the low- $k\rho$ -value, partial-recondensation mode case which is in large part due to penetration heat transfer. The difference is still large percentagewise, although less than in the unshielded case because the shield is effective in reducing the penetration heat transfer as well as the insulation heat transfer.

Propellant storage penalties for the 216-n.mi (400 km) and 9203-n.mi (17,053 km) altitudes are shown in Figures 4.4-4 through 4.4-7 for both the unshielded and shielded cases. Although the magnitude of the penalty decreases somewhat with increasing altitude, the general trends with staytime remain the same as in the intermediate-altitude case.

Since the effect of Earth orbit staytime on the Mars Departure Stage is small, it is to be expected that tanking or the combination vent-nonvent mode should be of only small value as compared to the basic modes. Figure 4.4-8 illustrates an additional difficulty involved in the use of these techniques. At the intermediate and high insulation performance, the vent pressure is not reached during Earth orbit. For the high $k\rho$ value, where orbital tanking is feasible, a saving of 13.8% of the storage system penalty occurs at the 90-day Earth orbit staytime. This represents

GENERAL DYNAMICS

Fort Worth Division

a saving of 0.74% of the zero-mass-fraction IMIEO or 17,022 lb_m (7721 kg). Note that the maximum staytime for the vent-tanking mode, which corresponds to replenishing the total propellant loading, is 491 days. Although tanking of the total propellant loading may not be feasible, these results indicate that a significant increase in staytime can be obtained through partial tanking.

Propellant storage penalty for the combination mode is compared in Figure 4.4-9 to the nonvent mode. At the high $k\rho$ value, the propellant storage system penalty is reduced 22.3% at the 90-day staytime. This represents an IMIEO reduction of 40,000 lb_m (18,150 kg). For larger staytimes, the savings are, of course, proportionately larger. A staytime of 140 days corresponds to boiling off the maximum permissible excess propellant loading. That is, the tank is initially filled to 95% of capacity. As the insulation performance improves, the savings decreases. At the low $k\rho$ value, the propellant storage penalty is reduced 16.5% at the 90-day staytime, equivalent to 10,350 lb_m (4700 kg) of IMIEO.

4.4.1.2 Insulation Thermal Performance

The figures presented in the previous subsections have demonstrated the strong influence of the insulation thermal performance on the magnitude of the propellant storage penalty of the Mars Departure Stage. Figure 4.4-10 shows the importance of the insulation performance directly for the unshielded stage in the vent mode. At the 216-n.mi (400 km) altitude, the propellant storage penalty increases from 7.4% of the zero-mass-fraction IMIEO value at the low $k\rho$ value to 18.6% at the high $k\rho$ value. This represents a percentage increase of 153%. At the higher altitudes, the magnitude of the penalty drops but the percentage changes are only slightly reduced. Note that most of the increase takes place in the range above the intermediate $k\rho$ value. For the low-altitude case, only the first 22% of the increase occurs below the intermediate value.

Reduction of the incident radiation by solar shields results in a significant decrease in the magnitude of the propellant storage penalty. This is seen by comparing the penalties shown in Figure 4.4-11 for the shielded stage in the vent mode with those of Figure 4.4-10. However the influence of the insulation thermal performance is little

GENERAL DYNAMICS

Fort Worth Division

changed. In fact, in terms of the percentage increase in penalty, the influence is slightly increased. For the 216-n.mi (400 km) altitude, this percentage increase is 160%, slightly above the 153% increase for the unshielded case. At the higher altitudes, the percentage increase is slightly higher, being 175% at the 9203-n.mi (17,053 km) altitude. Again, the bulk of the penalty increase occurs in the range of insulation performance above the intermediate $k\rho$ value.

4.4.1.3 Mars Orbit Altitude

Mars orbit altitude affects the Mars Departure Stage in a different manner than it does the lower stages. The Mars Excursion Module (MEM) mass variation with altitude has no effect, since the MEM does not go through the Mars departure maneuver. Variation of the ΔV requirement with altitude, on the other hand, is more significant for the Mars Departure Stage, as shown in Figure 6.2-1. The effect of the ΔV variation on the propellant storage system penalty to IMIEO for a stage with an adiabatic wall is shown in Figure 4.4-12. This case is chosen in order to isolate the effect of ΔV requirements from heat transfer effects. The variation with altitude follows the trend of the ΔV variation, reaching a minimum in the area of 5000-6000 n.mi. This is expected, since the components of the propellant storage system are limited to the tank, the pressurant, and the meteoroid protection. All of these components increase with the larger propellant loading that results from an increased ΔV requirement. The mass penalties range from 18,000 lb_m (8160 kg) to 19,400 lb_m (8800 kg), a difference of 1400 lb_m (635 kg).

In the comparisons which follow, it must be remembered that since the value of the zero-mass-fraction IMIEO increases with altitude, comparison of propellant storage penalties at two different altitudes must be approached with caution. Figure 4.4-13 shows the effect of Mars orbit altitudes on the propellant storage penalty to IMIEO for the unshielded Mars Departure Stage. The variations here are much larger than that shown in Figure 4.4-12, leading to the conclusion that thermal effects dominate over the ΔV variation. The decrease in propellant storage penalty with increasing altitude is thus due mainly to the less severe thermal environment at the higher altitudes. This affects not only the heat transfer through the insulation but the penetration heat transfer as well (see Figure 4.1-22). Note that the rate of

GENERAL DYNAMICS

Fort Worth Division

decrease is greater at the low altitudes and that all of the curves are relatively flat at the synchronous altitude. This is to be expected since the planetary components of the radiation incident upon the vehicle vary approximately inversely as the square of the sum of the altitude and the planet radius. As the insulation performance improves, the thermal environment has less effect; it also has less effect in the partial recondensation mode than in the vent mode.

The propellant storage penalty for the shielded stage is presented in Figure 4.4-14. Comparison with the unshielded stage data shows that the storage penalties are reduced at all altitudes and at all $k\rho$ values. The variation with altitude is greater in the shielded case, which reflects the increased effectiveness of the solar shield at the higher altitudes. Note also that the adiabatic case is more closely approached at the low $k\rho$ value and high altitude, indicating a smaller penetration heat transfer in the shielded case.

The sum of all effects of Mars orbit altitude on vehicles with optimized propellant storage systems on the Mars Departure Stage is shown in Figures 4.4-15 and 4.4-16 for the unshielded and shielded stage, respectively. Note that the effect of the MEM mass completely dominates the vehicle IMIEO, so that the value of IMIEO increases with increasing altitude, even though the Mars Departure Stage propellant storage penalty decreases with increasing altitude.

4.4.2 Propellant Storage Mode

Since the Mars Departure Stage suffers from the most severe heating history of all the stages, and consequently makes the greatest demands on its thermal protection system, the mode of propellant storage is of great importance. During the preliminary analysis, it was found that the nonvent mode resulted in extreme tank pressures, of the same magnitude as the critical pressure, at all altitudes in the unshielded case. For the shielded case, the nonvent mode was investigated at the 9203-n.mi (17,053 km) altitude only; at the lower altitudes, the tank pressures were also beyond the practical range. The data presented in Subsection 4.4.1 showed that the partial-recondensation mode yielded a reduction in propellant storage penalty over the vent mode of the same order as that due to improving the insulation performance from the high to the intermediate $k\rho$ value. Indeed, the partial-recondensation mode

GENERAL DYNAMICS

Fort Worth Division

offers a greater reduction in penalty at the intermediate value than can be obtained in the vent mode by improving the insulation performance from the intermediate to the lowest $k\rho$ value.

The propellant storage penalties for the vent and the partial-recondensation modes are compared in Figure 4.4-17 for the unshielded stage. At the highest $k\rho$ value, the penalty can be reduced 46.4% by using the partial-recondensation mode. The absolute mass savings decreases as the insulation performance improves, although the percentage reduction remains about the same (45.5% at the lowest $k\rho$ value). For the shielded stage, similar data are presented in Figure 4.4-18, including the storage penalty for the nonvent mode. The percentage change in penalty between the vent and the partial-recondensation modes is reduced, as compared to the unshielded case, and decreases as the insulation performance improves. At the highest $k\rho$ value, the percentage reduction is 37.6%, and this quantity decreases to 28.0% at the lowest $k\rho$ value. The savings between the nonvent and the vent modes is less than that between the vent and the partial-recondensation modes. At the highest $k\rho$ value, the difference is 23.5% between the nonvent and vent modes, decreasing to 15.0% at the lowest $k\rho$ value.

To show the relationship of the various component masses that make up the propellant storage system, component mass fractions are presented for the shielded stage in Figures 4.4-19, 4.4-20 and 4.4-21 for the nonvent, vent, and partial-recondensation modes, respectively. In the nonvent mode (Fig. 4.4-19), the tank mass fraction ranges from 0.18 to 0.33, reflecting the high tank pressure, which increases from 42 to 76 psia as the $k\rho$ value increases. The high pressure level and the large increase in pressure also account for the high pressurant mass fraction and the increase in the mass fraction over the range of insulation performance. The insulation mass fraction exhibits the same rapid increase with increasing $k\rho$ value, as seen in the component-mass-fraction data for the lower stages. In this case, however, the insulation mass fraction is well below the tank mass fraction, even at the highest $k\rho$ values. The variation of the meteoroid protection mass fraction is larger than in the lower stages because of the density decrease and the larger propellant loading at the higher $k\rho$ values.

GENERAL DYNAMICS

Fort Worth Division

For the vent mode (Fig. 4.4-20), the system effective mass fraction is reduced and there is a significant change in the relationship of two of the components. For the Mars Departure Stage, the boiloff mass fraction is the dominant component mass fraction, exceeding the tank mass fraction at all values of insulation performance. Note that the tank mass fraction is approximately the same as for the two lower stages in the vent mode. In this case, the propellant loading is less than one-third that of the Earth Departure Stage, yet the tank mass fractions are roughly equal. This demonstrates that the tank mass is a much stronger function of pressure than of propellant loading. The remaining mass fractions - insulation, meteoroid protection, and pressurant - show the same trends as in the lower stages.

In the partial-recondensation mode (Fig. 4.4-21), the system effective mass fraction drops substantially from that of the vent mode. The boiloff mass fraction is reduced below the tank mass fraction at the lower $k\rho$ values while the tank mass fraction remains relatively unchanged. The difference in mode also produces a reduction in insulation mass, with the meteoroid protection and pressurant mass fractions remaining about the same as in the vent-mode case.

Propellant-storage-component mass fractions for the unshielded Mars Departure Stage are presented in Figure 4.4-22 for the vent mode. Comparison with the corresponding shielded-stage data (Fig. 4.4-20) shows a large increase in the boiloff mass fraction with a smaller increase in the insulation mass fraction. The tank, meteoroid protection, and pressurant mass fractions are only slightly changed for the unshielded case. The total system effective mass fraction ranges from a minimum of 0.41 to 0.87 at the highest $k\rho$ value.

Although the effect of Earth orbit staytime has been shown to be small with respect to the propellant storage penalty of the Mars Departure Stage, some reduction in penalty and extension of allowable staytime is possible using the combination or tanking modes of storage. Figure 4.4-9 shows the effect of the combination vent-nonvent mode of operation. Clearly, the combination mode saves considerable mass at the long staytime, particularly at the high value of the $k\rho$ product. At that condition, the combination mode saves 40,300 lb_m (18,300 kg) or 1.8% of the zero-mass-fraction IMIEO. With the intermediate $k\rho$ value, the saving

GENERAL DYNAMICS

Fort Worth Division

is reduced to 17,260 lb_m (7831 kg) or 0.75%, and with the low value of $k\rho$, the saving is further reduced to 0.54% of the zero-mass-fraction IMIEO. Note that the extension of allowable Earth orbit staytime is minimal in this case; only a few additional days are gained in the best case.

The effect of tanking for the partial-recondensation and vent modes is presented in Figures 4.4-23 and 4.4-24, respectively. It is immediately obvious that the savings achieved by tanking the stage with the partial-recondensation mode are very small, less than 0.5% of the zero mass fraction IMIEO. The availability of extremely long staytimes with no penalty to IMIEO is of some value. However, there is little to be gained, unless the staytime requirements are found to be well beyond the range investigated here. The vent mode offers somewhat greater savings, although the difference in storage penalty is less than 1% of the zero-mass-fraction IMIEO in all of the cases shown. Again, unless significantly longer Earth orbit staytimes are required, tanking saves very little over the basic vent mode of propellant storage for the Mars Departure Stage.

4.4.3 Comparison of Shielded and Unshielded Vehicles

The Mars Departure Stage, because of its long exposure to the thermal environment, is strongly affected by the use of a solar shield (Fig. 4.4-1). The performance of the solar shield in the Mars transfer phase is such that the stage is effectively exposed to direct solar radiation for only two 1-hr periods, one each at the beginning and the end of the transfer phase. In Mars orbit, the orientation of the shielded vehicle is such that it is shielded from solar radiation but receives only minor protection from planetary-emitted or albedo radiation. Since there is little protection from the planetary radiation components, the effectiveness of the Mars orbit solar shield is dependent on the orbit altitude. At the 9203-n.mi (17,053 km) altitude, little planetary radiation will strike the stage, whereas at the 216-n.mi (400 km) altitude, a large percentage of the absorbed radiation is due to planetary radiation. Figure 4.4-25 shows the average penetration heat transfer rate in Mars orbit, for shielded and unshielded vehicles, which reflects the effectiveness of the solar shield. Note that at the 216-n.mi (400 km) Mars orbit altitude the shield

GENERAL DYNAMICS
Fort Worth Division

reduces the penetration heat transfer rate by 30.1 Btu/hr (8.8 W) or 7.1% of the rate for the unshielded stage. At the 9203-n.mi (17,053 km) altitude, the corresponding reduction is 153 Btu/hr (44.8 W) or 56.5% of the unshielded stage penetration heat transfer rate.

Figure 4.4-26 shows a comparison of the propellant storage penalty to IMIEO for the shielded and unshielded stages in the vent mode. The reduced effectiveness of the shield at the low altitude is less pronounced than that shown in Figure 4.4-25 because of the varying insulation thickness. The use of the shield at the high $k\rho$ value reduces the propellant storage penalty by 76,930 lb_m (34,990 kg) or 4.2% of the zero-mass-fraction IMIEO at the 216-n.mi (400 km) altitude, and by 134,700 lb_m (61,080 kg) or 5.9% at the 9203-n.mi (17,053 km) altitude. As the insulation thermal performance improves, the value of the shield diminishes, so that at the low value of $k\rho$ the saving is only 26,640 lb_m (12,080 kg) or 0.66% of the zero-mass-fraction IMIEO at the 216-n.mi (400 km) altitude and 59,460 lb_m (26,970 kg) or 2.6% at the 9203-n.mi (17,053 km) altitude. Since the partial-recondensation mode is a more efficient thermal management technique, it should show less effect of the solar shield. Figure 4.4-27 shows a comparison of the penalties for the unshielded and shielded stages in the partial-recondensation mode and, as expected, the savings in propellant storage penalty is less than in the vent-mode case. In this case, the greatest saving, at the high altitude and high $k\rho$ value, is 62,230 lb_m (28,230 kg) or 2.7% of the zero-mass-fraction IMIEO.

The shielded stage data shown in Figures 4.4-26 and 4.4-27 is based on deployment of solar shields during both the Mars transfer and Mars orbit mission phases. A question arises as to the distribution of the mass savings between the Mars transfer and the Mars orbit solar shields. The distribution can be seen from Figure 4.4-28 where the propellant storage penalty for the case where the stage is shielded only during Mars orbit is compared with the unshielded and shielded cases (vent mode). It is seen that at low altitude the major part of the storage penalty reduction is attributable to the Mars transfer shield. As the altitude increases, the Mars orbit shield becomes a more important factor. Finally, at the highest altitude, more than one-half of the reduction is attributable to the Mars orbit shield.

GENERAL DYNAMICS
Fort Worth Division

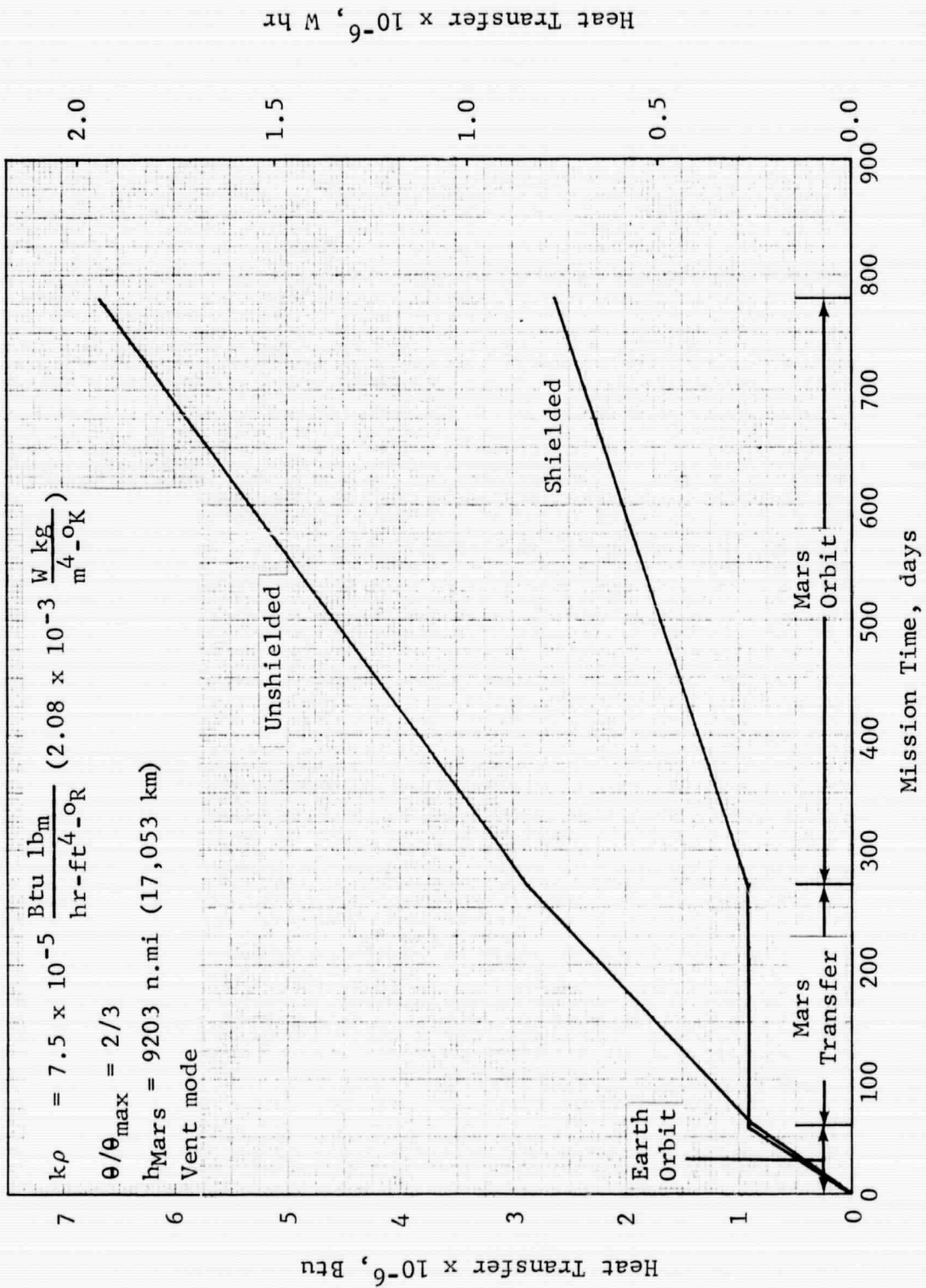


Figure 4.4-1 Effect of Solar Shield on Propellant Heat Transfer:
Mars Departure Stage

GENERAL DYNAMICS
Fort Worth Division

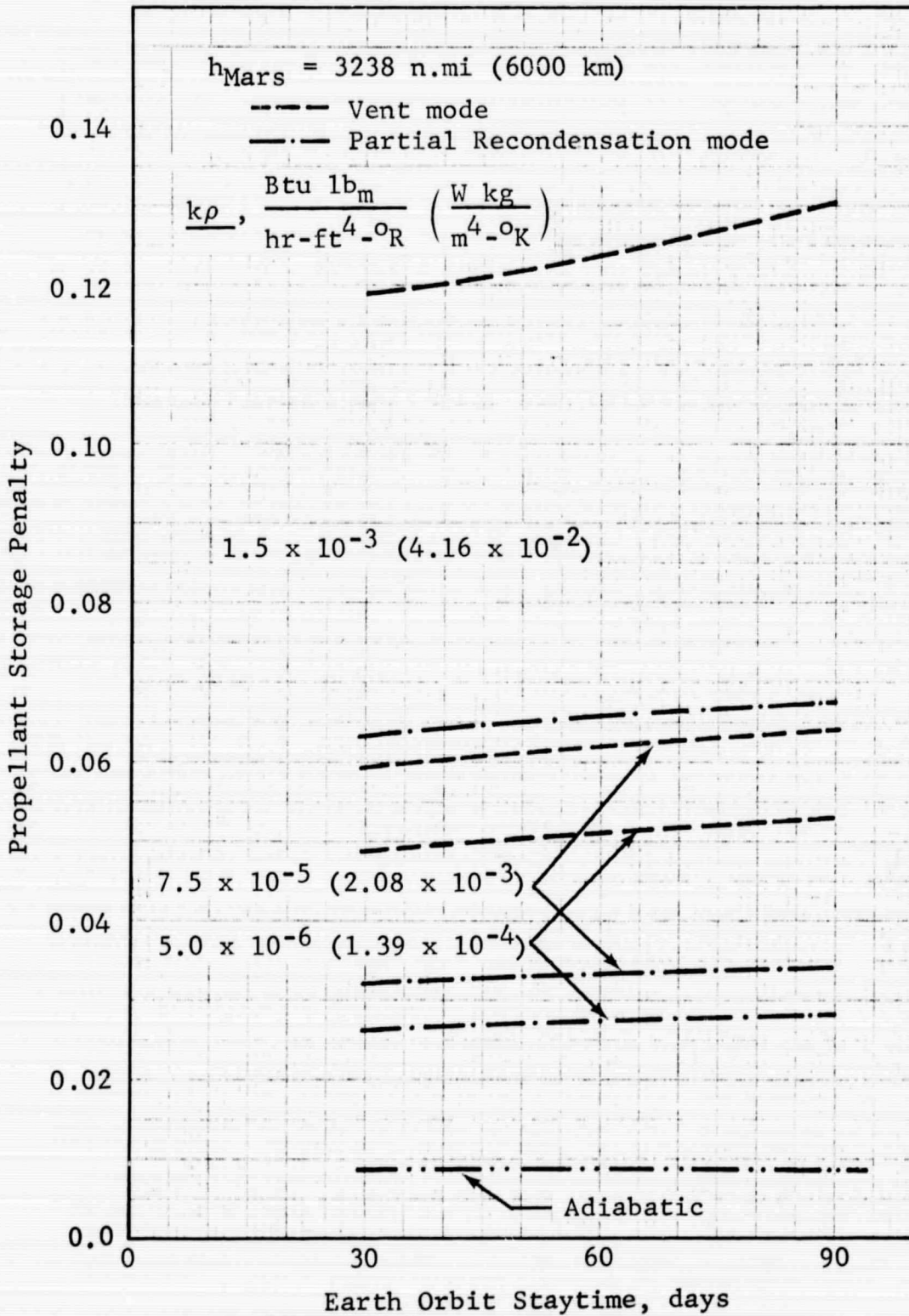


Figure 4.4-2 Propellant Storage Penalty vs Staytime: Unshielded Mars
Departure Stage, $h_{\text{Mars}} = 3238 \text{ n.mi}$

GENERAL DYNAMICS

Fort Worth Division

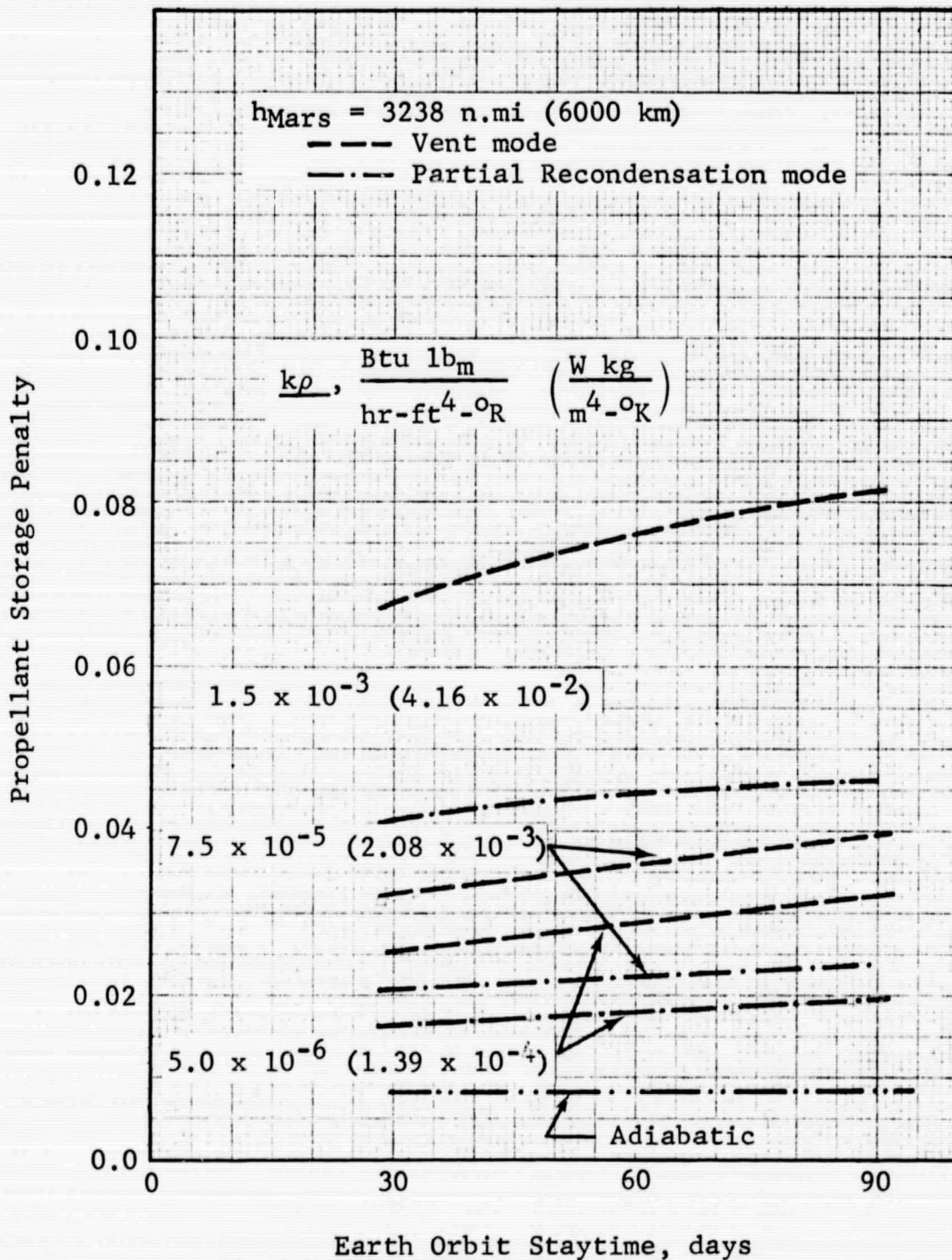


Figure 4.4-3 Propellant Storage Penalty vs Staytime: Shielded Mars Departure Stage, $h_{Mars} = 3238 \text{ n.mi}$

GENERAL DYNAMICS
Fort Worth Division

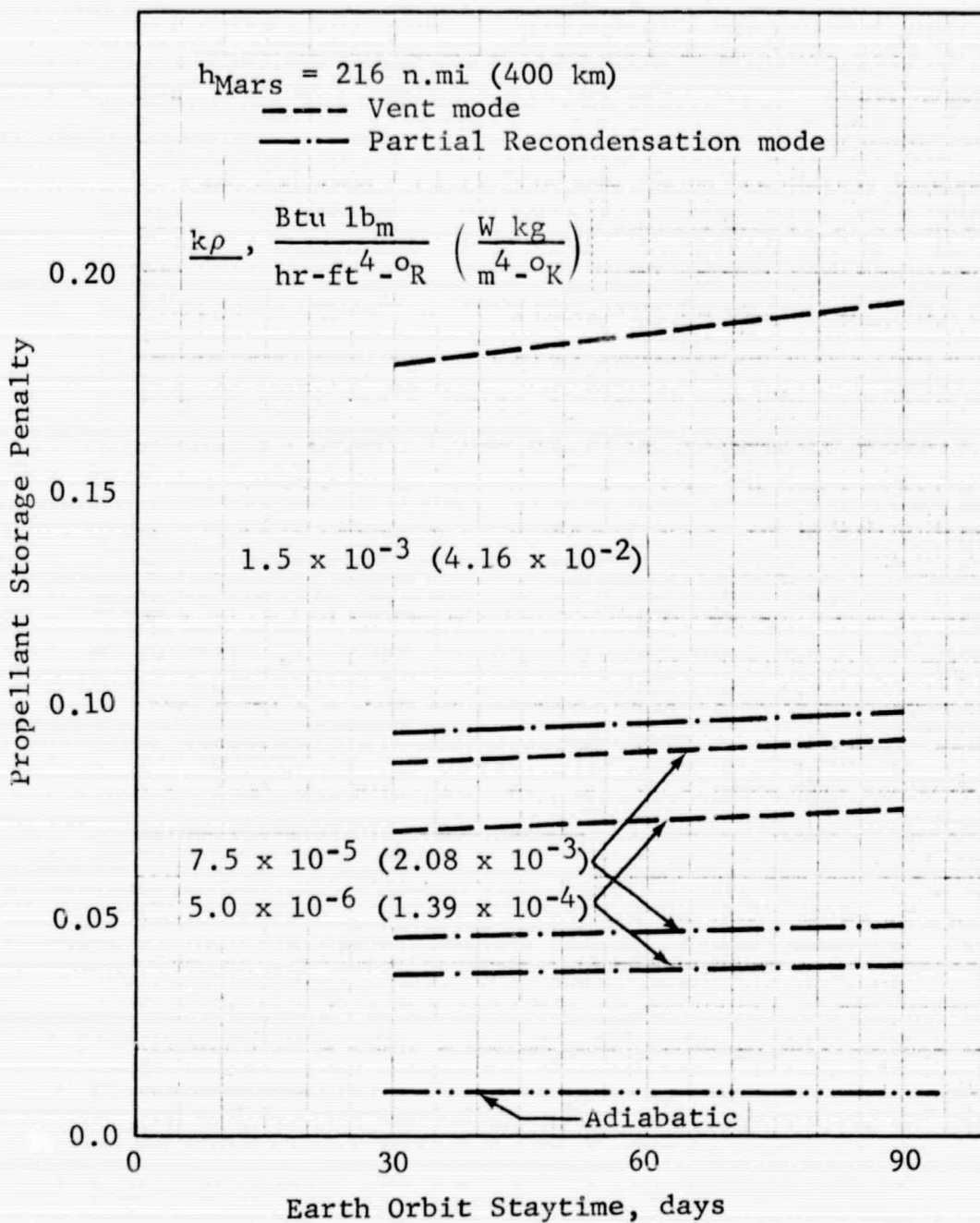


Figure 4.4-4 Propellant Storage Penalty vs Staytime: Unshielded Mars
Departure Stage, $h_{\text{Mars}} = 216 \text{ n.mi}$

GENERAL DYNAMICS
Fort Worth Division

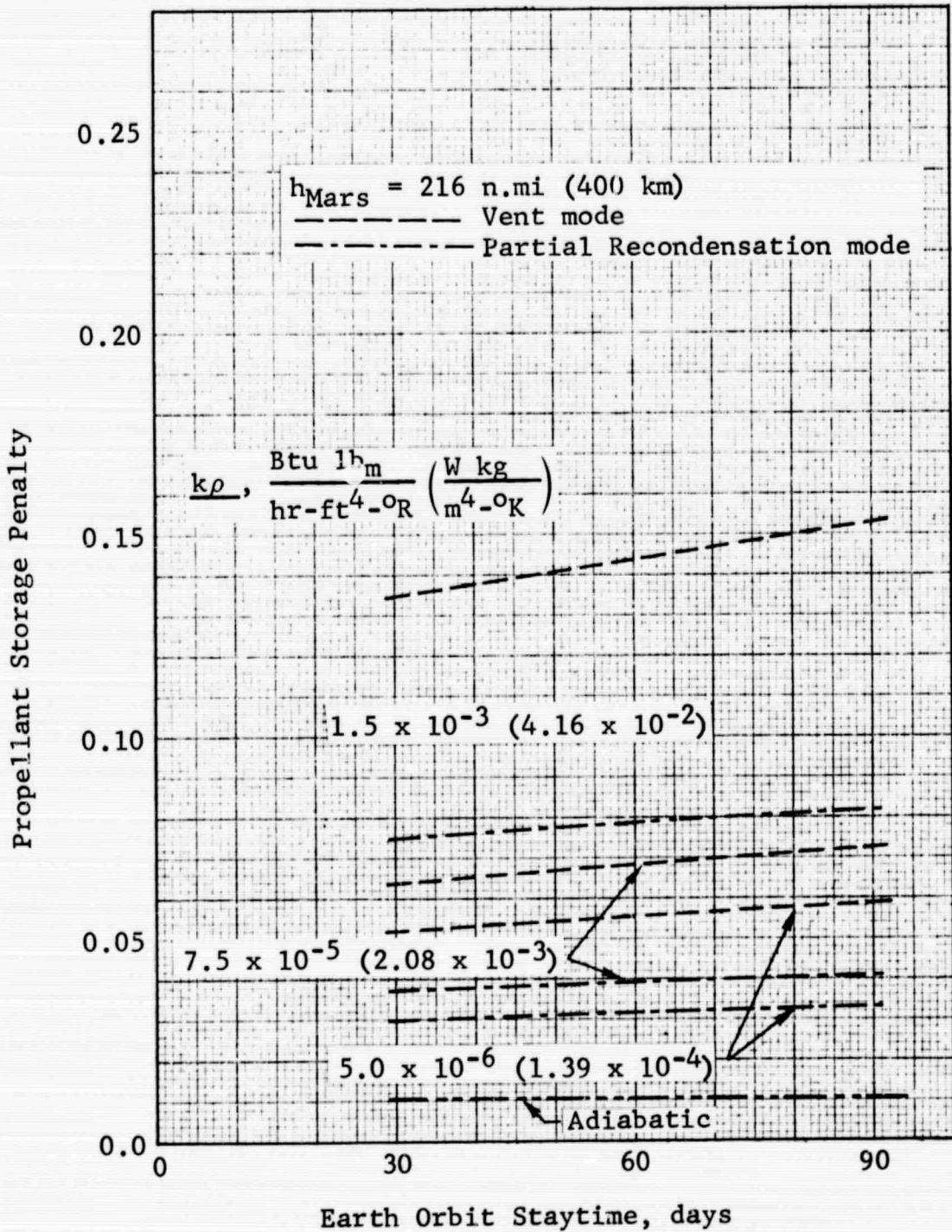


Figure 4.4-5 Propellant Storage Penalty vs. Staytime: Shielded Mars Departure Stage, $h_{Mars} = 216 \text{ n.mi}$

GENERAL DYNAMICS
Fort Worth Division

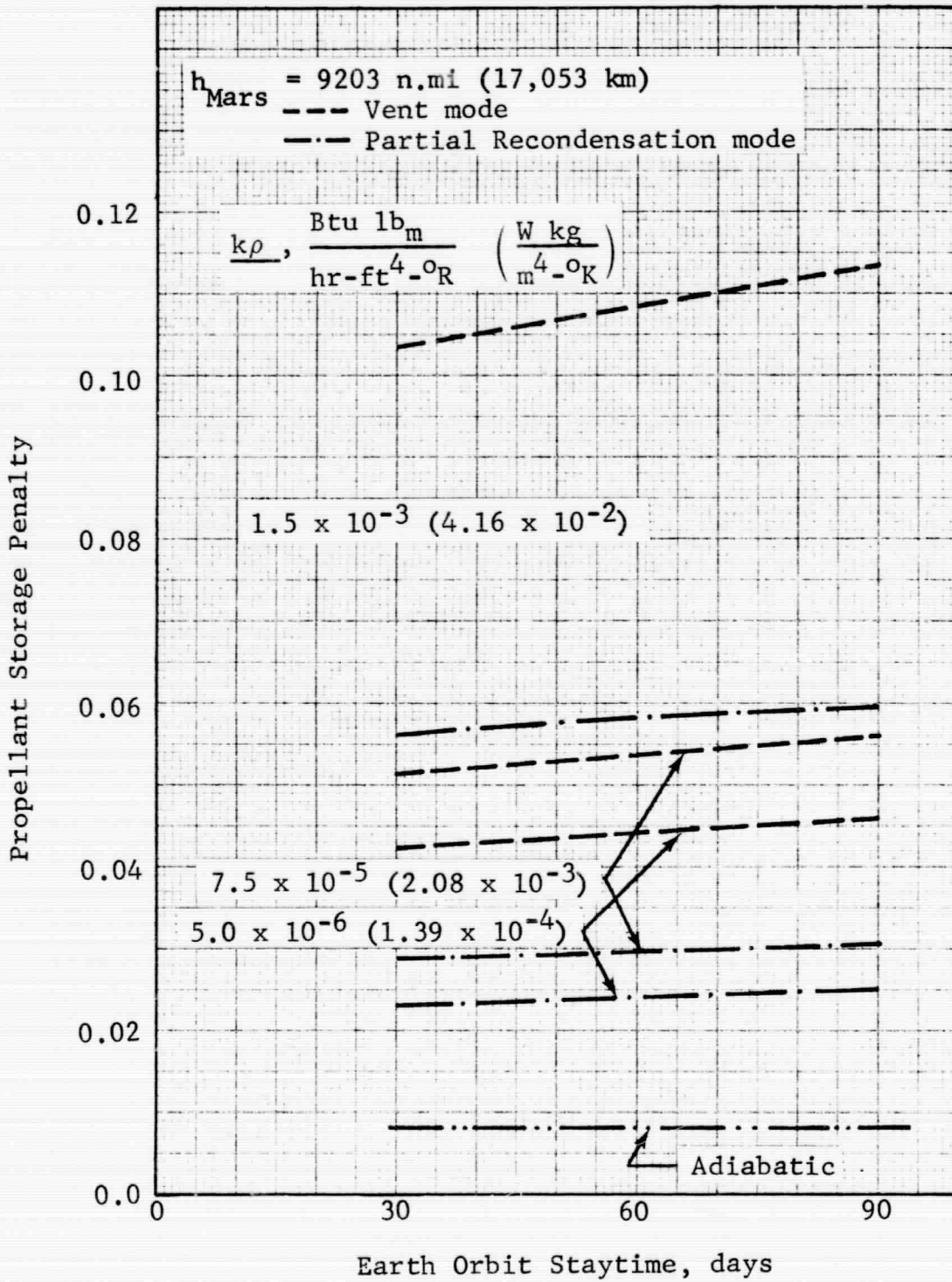


Figure 4.4-6 Propellant Storage Penalty vs Staytime: Unshielded Mars Departure Stage, $h_{Mars} = 9203 \text{ n.mi}$

GENERAL DYNAMICS

Fort Worth Division

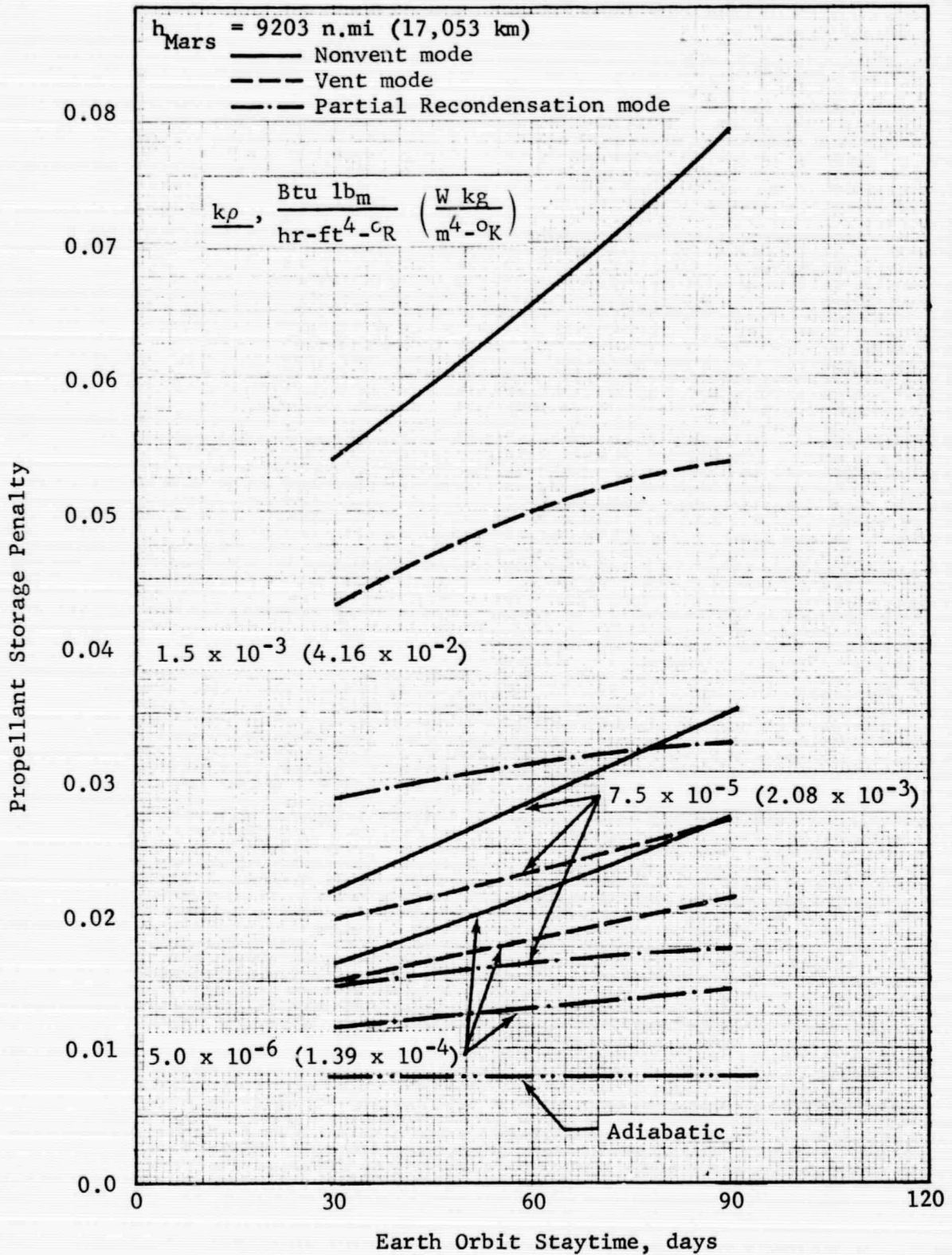


Figure 4.4-7 Propellant Storage Penalty vs Staytime: Shielded Mars Departure Stage, $h_{\text{Mars}} = 9203 \text{ n.mi}$

GENERAL DYNAMICS
Fort Worth Division

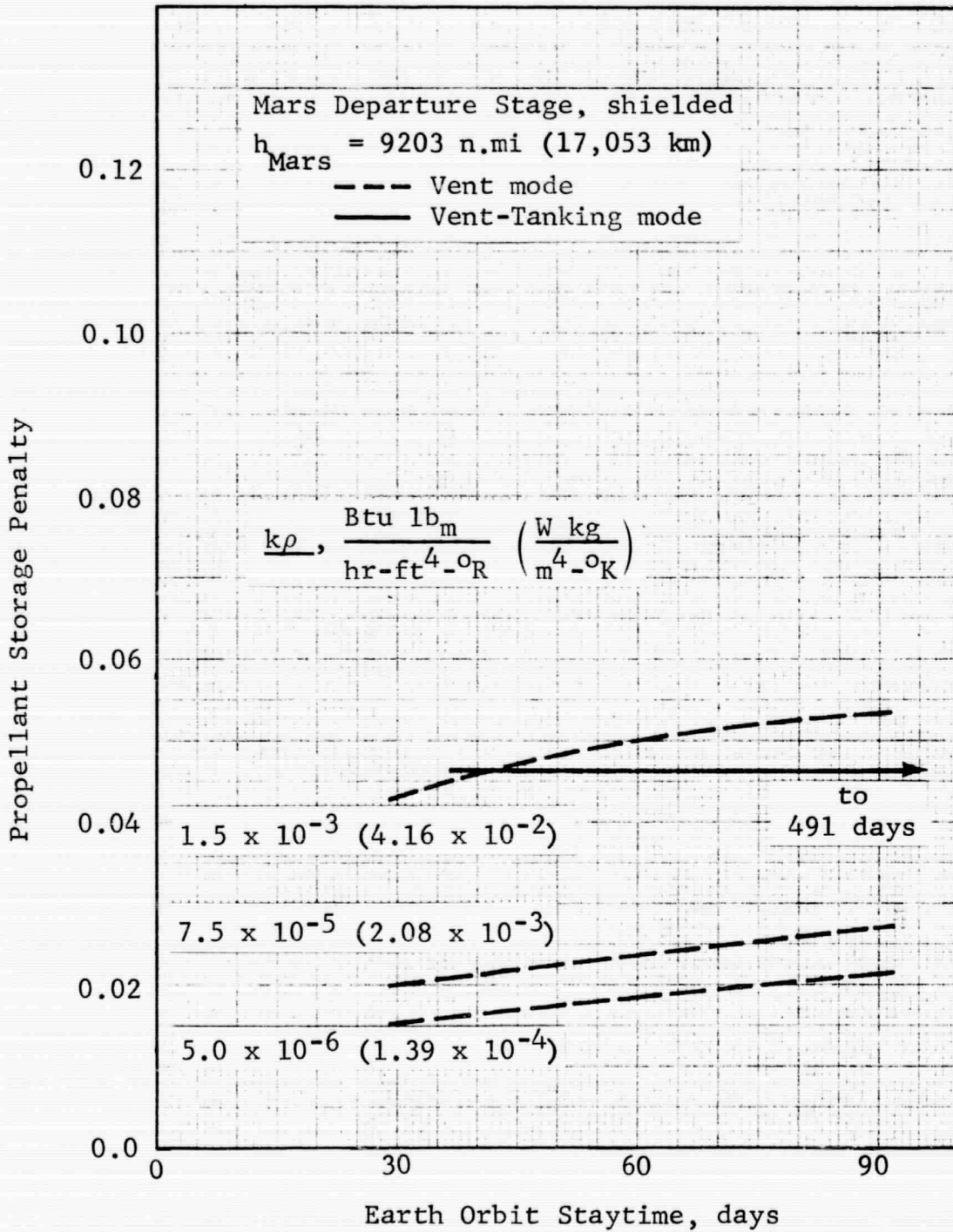


Figure 4.4-8 Comparison of Propellant Storage Penalties for the Vent and Vent-Tanking Modes

GENERAL DYNAMICS

Fort Worth Division

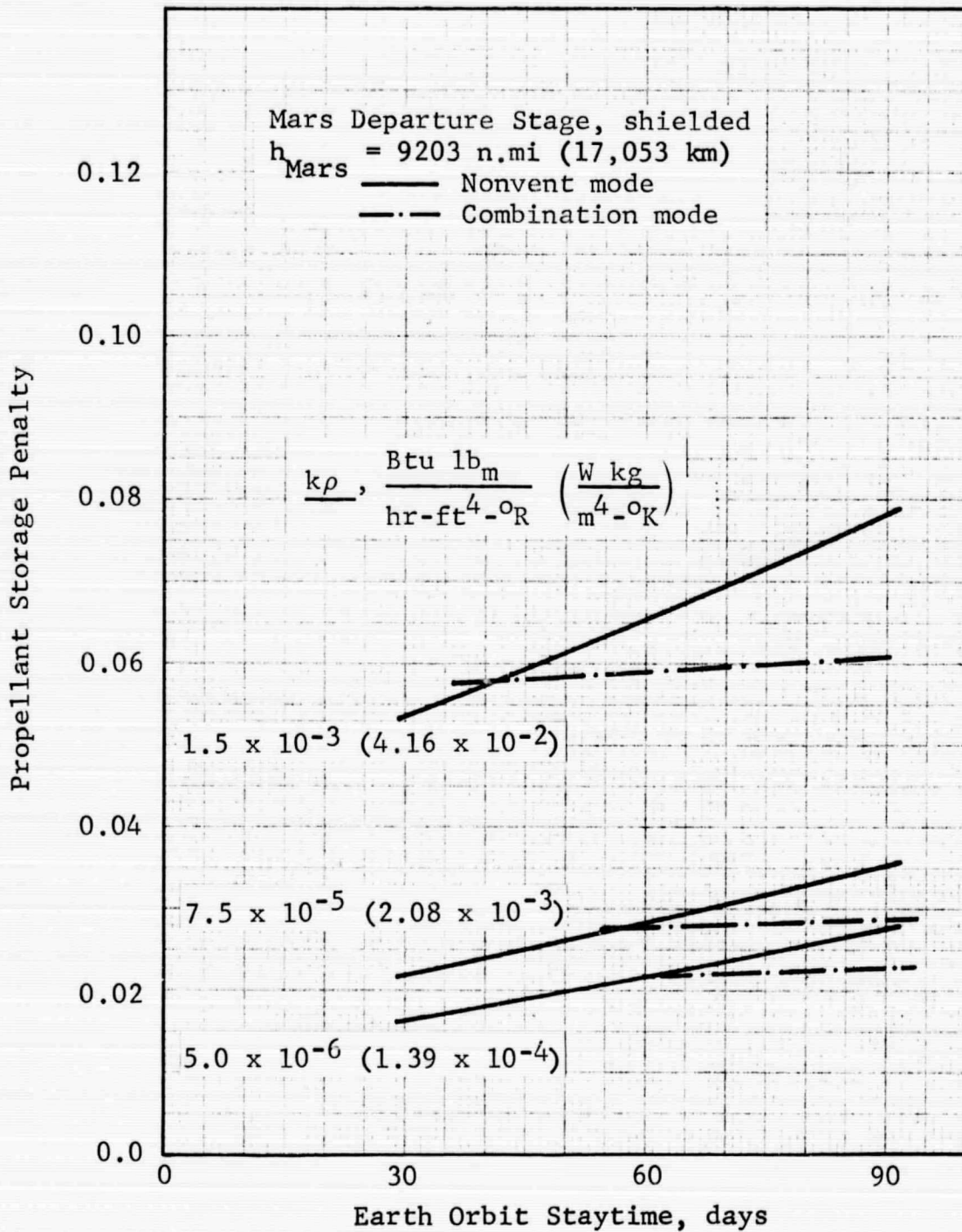


Figure 4.4-9 Comparison of Propellant Storage Penalties for the Combination and Nonvent Modes

GENERAL DYNAMICS
Fort Worth Division

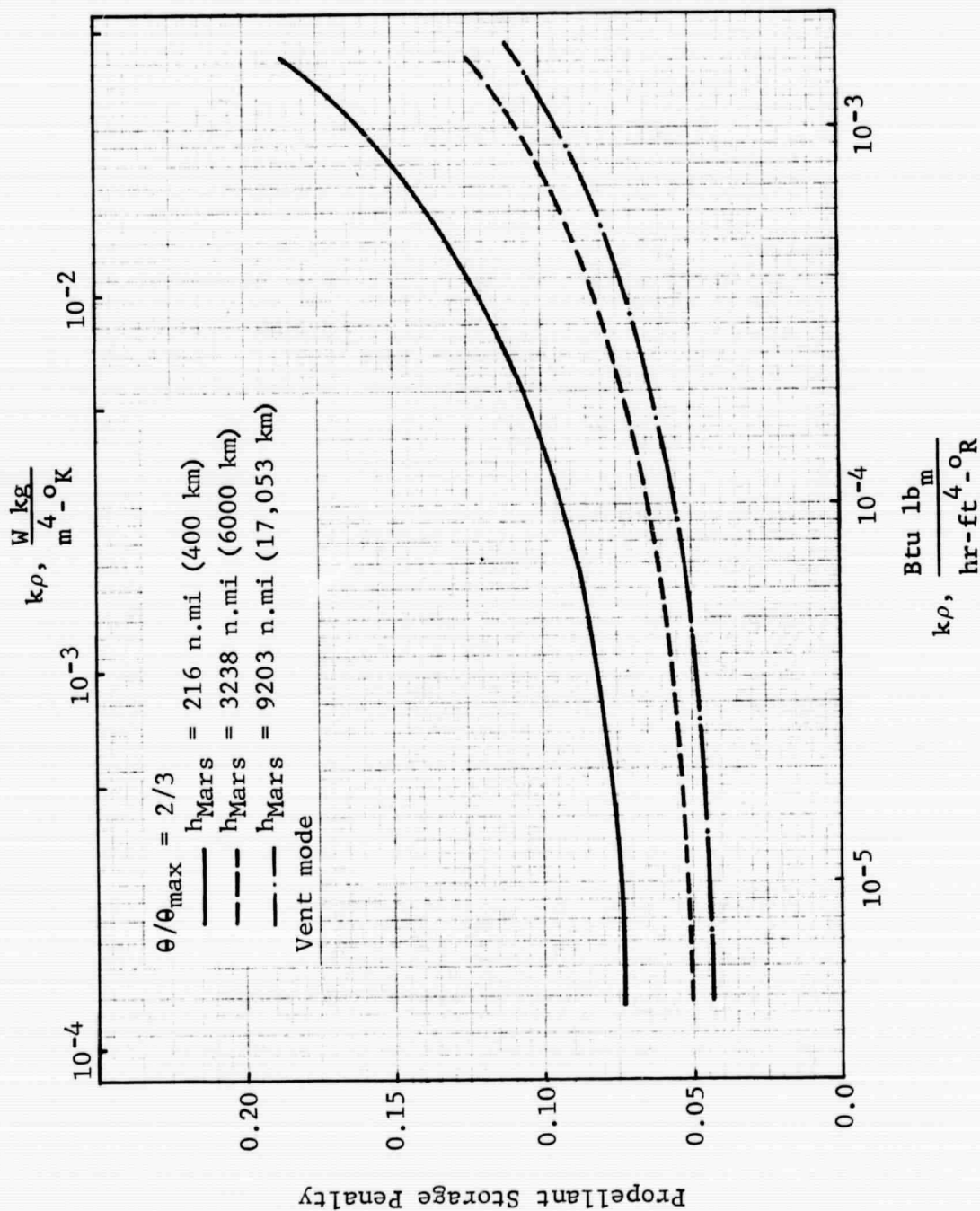


Figure 4.4-10 Effect of Insulation Thermal Performance on Propellant Storage Penalty: Unshielded Mars Departure Stage

GENERAL DYNAMICS
Fort Worth Division

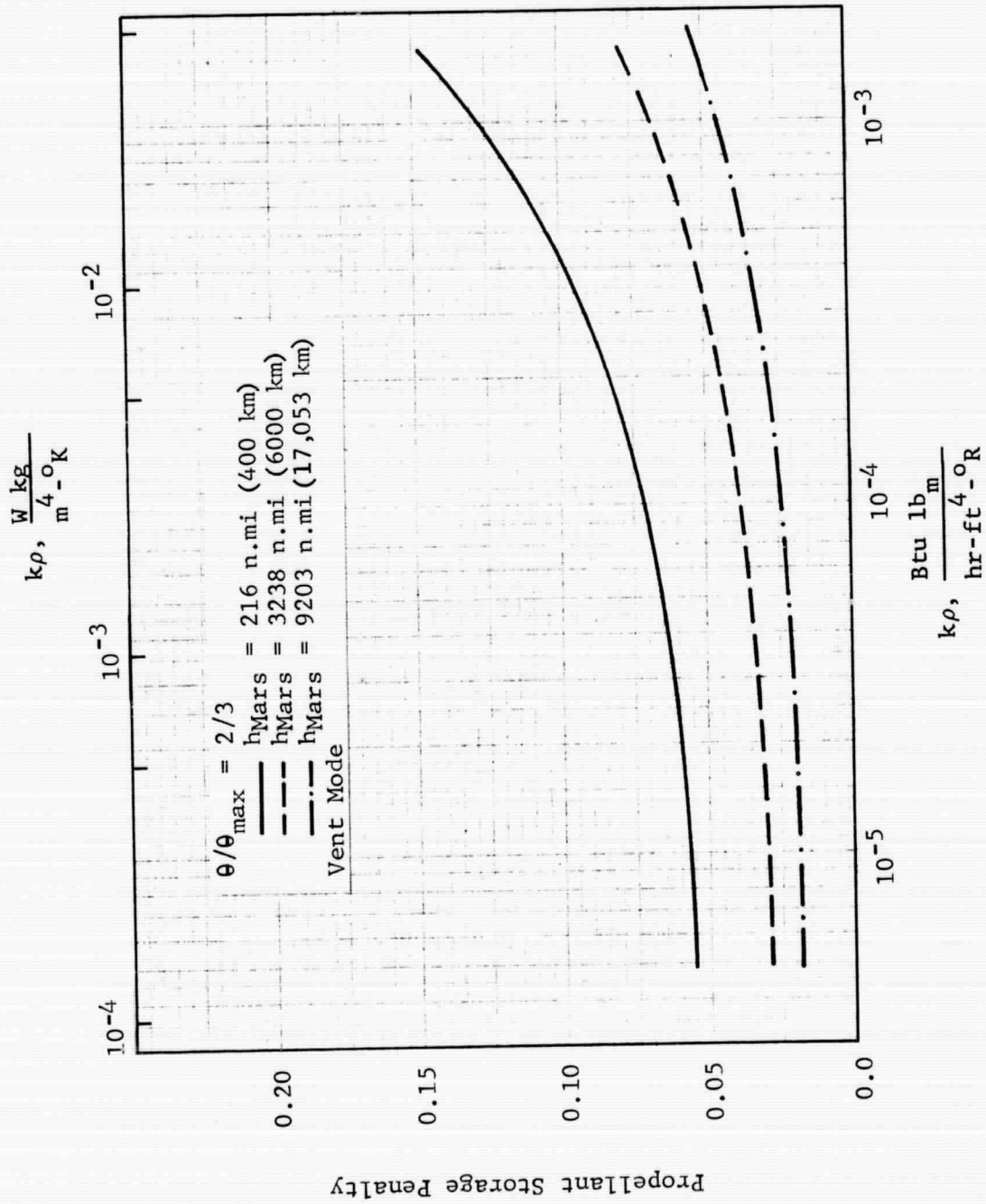


Figure 4.4-11 Effect of Insulation Thermal Performance on Propellant Storage Penalty: Shielded Mars Departure Stage

GENERAL DYNAMICS
Fort Worth Division

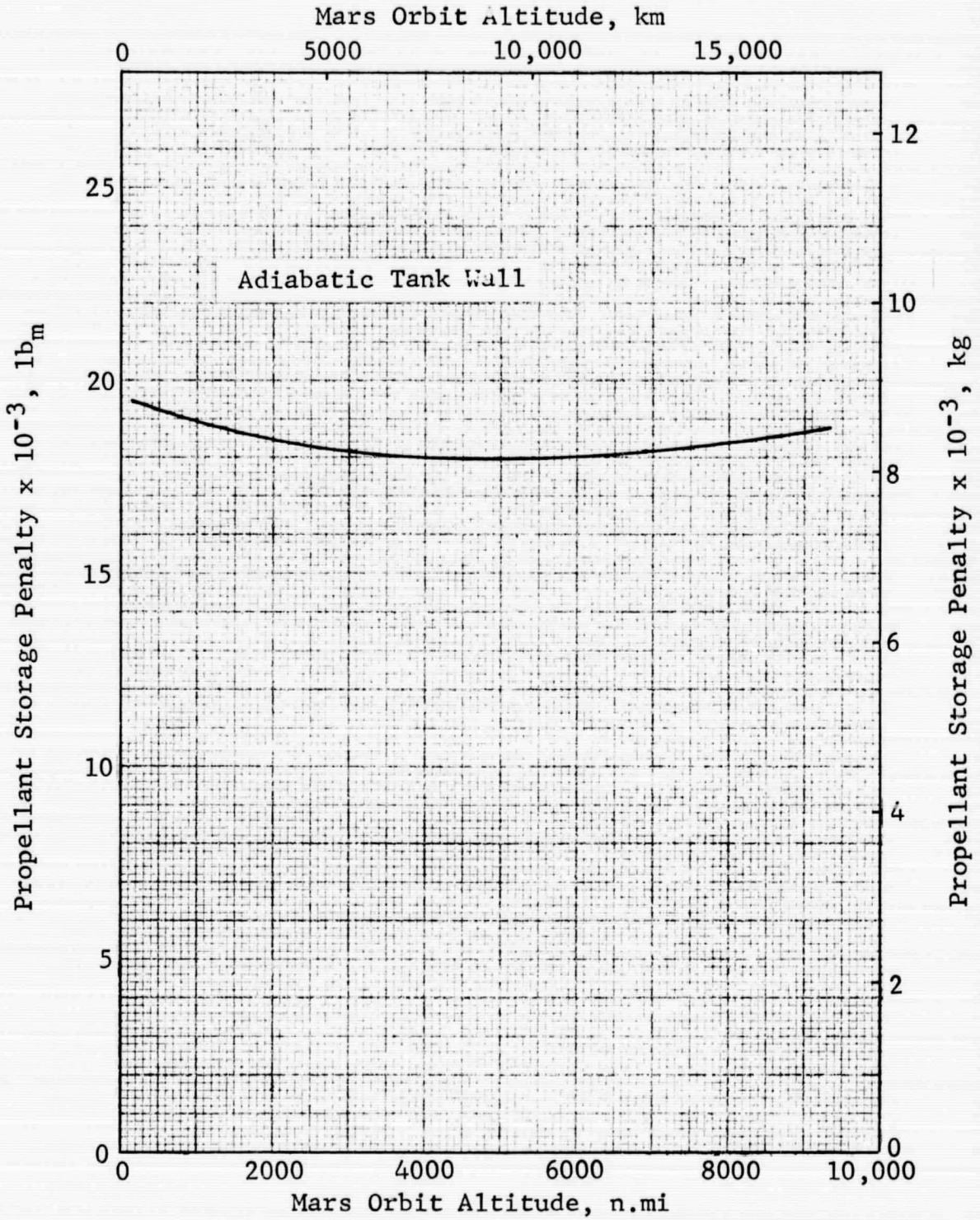


Figure 4.4-12 Effect of ΔV Variation with Altitude on Mars Departure Stage Propellant Storage Penalty

GENERAL DYNAMICS
Fort Worth Division

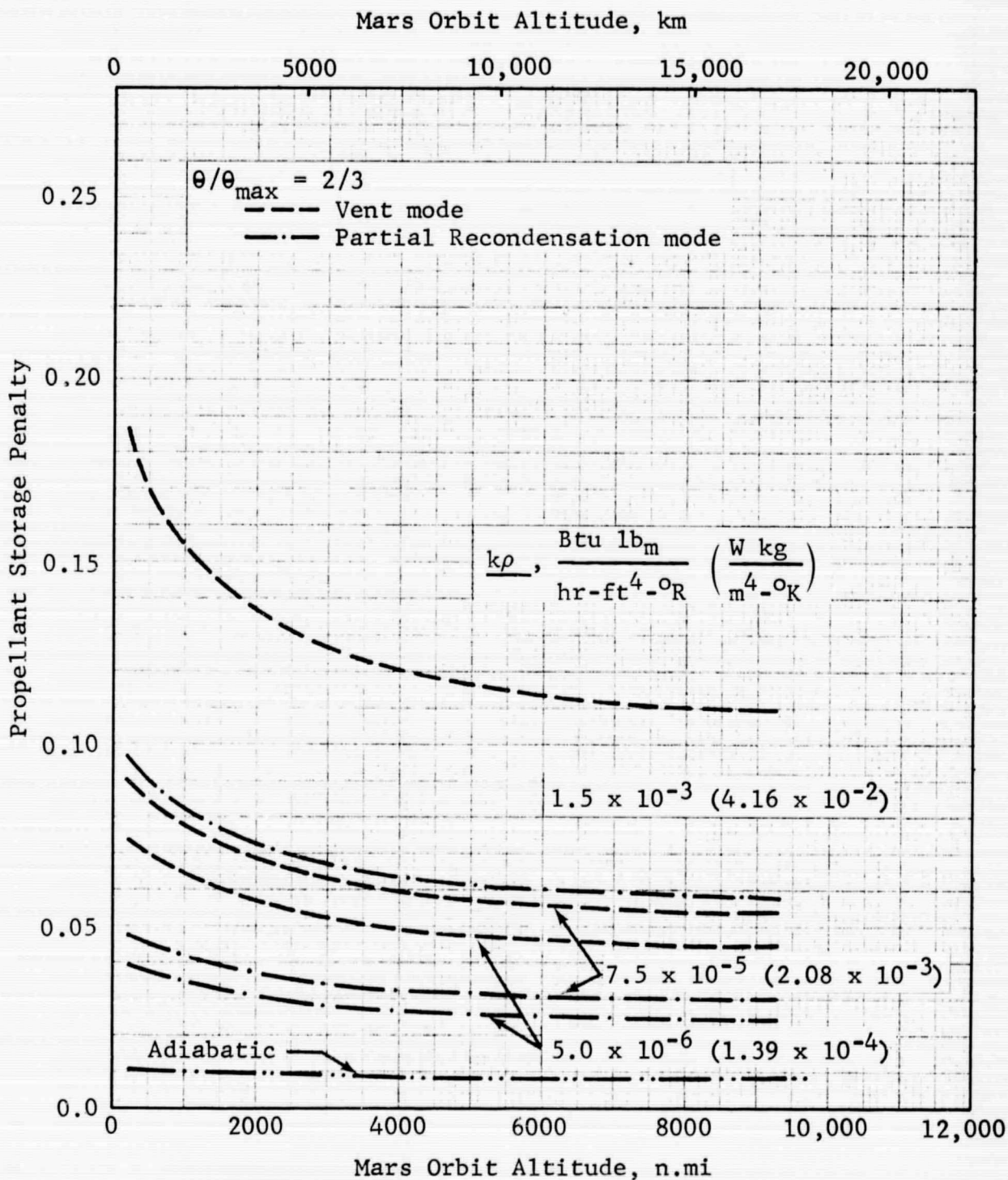


Figure 4.4-13 Propellant Storage Penalty vs Altitude: Unshielded Mars Departure Stage

GENERAL DYNAMICS
Fort Worth Division

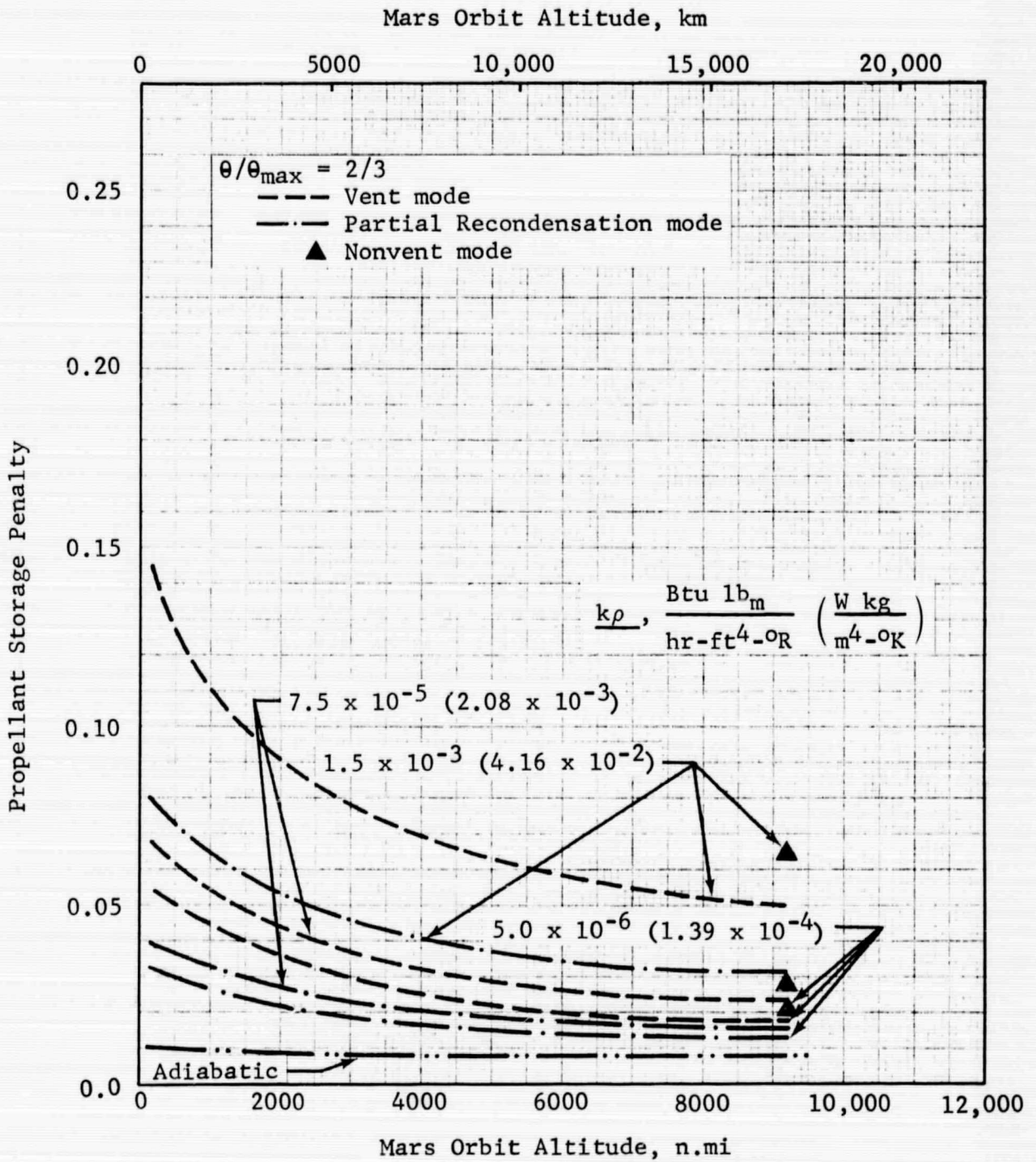


Figure 4.4-14 Propellant Storage Penalty vs Altitude: Shielded Mars Departure Stage

GENERAL DYNAMICS

Fort Worth Division

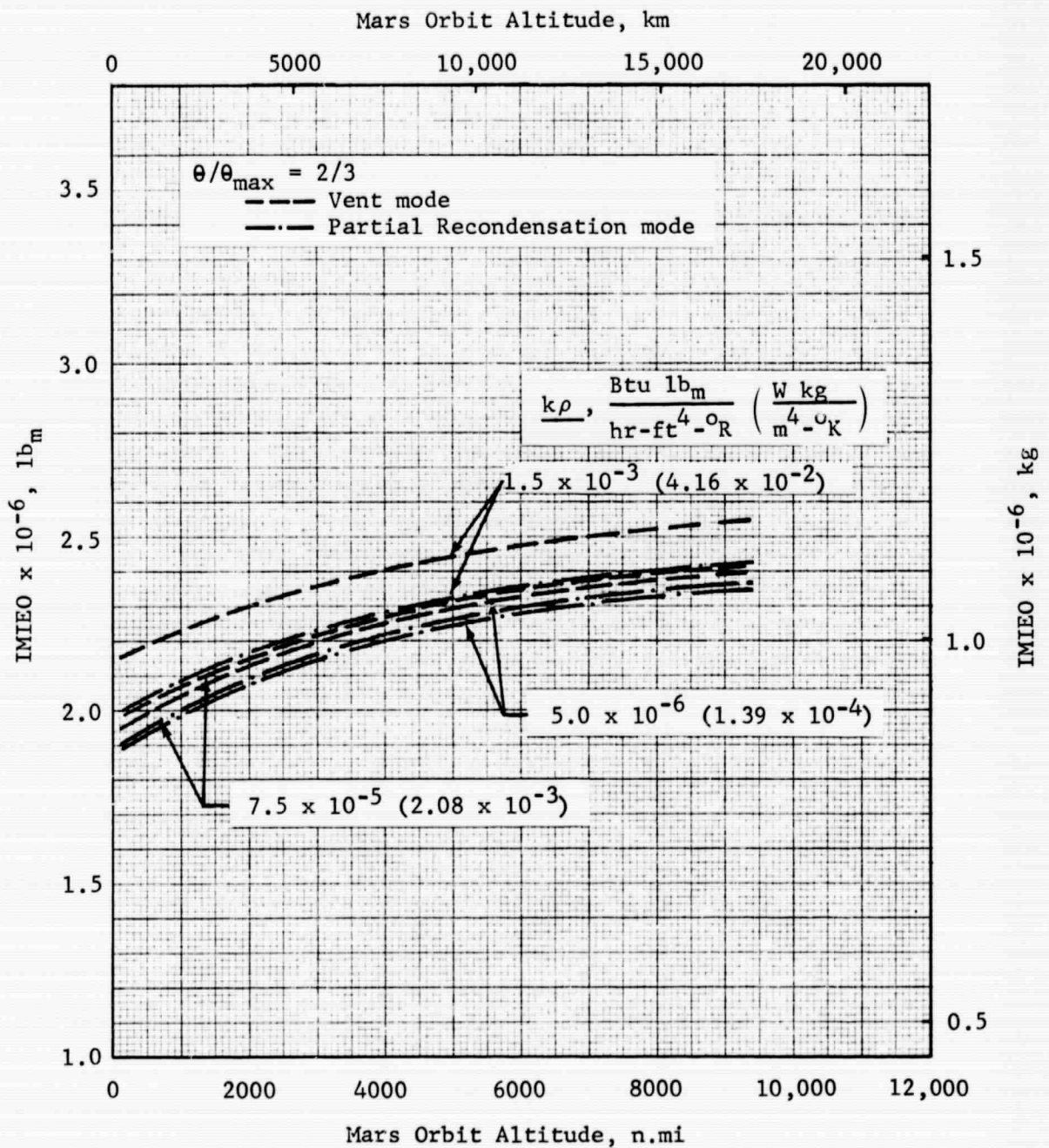


Figure 4.4-15 Effect of Optimum Propellant Storage System on IMIEO vs Altitude: Unshielded Mars Departure Stage

GENERAL DYNAMICS
Fort Worth Division

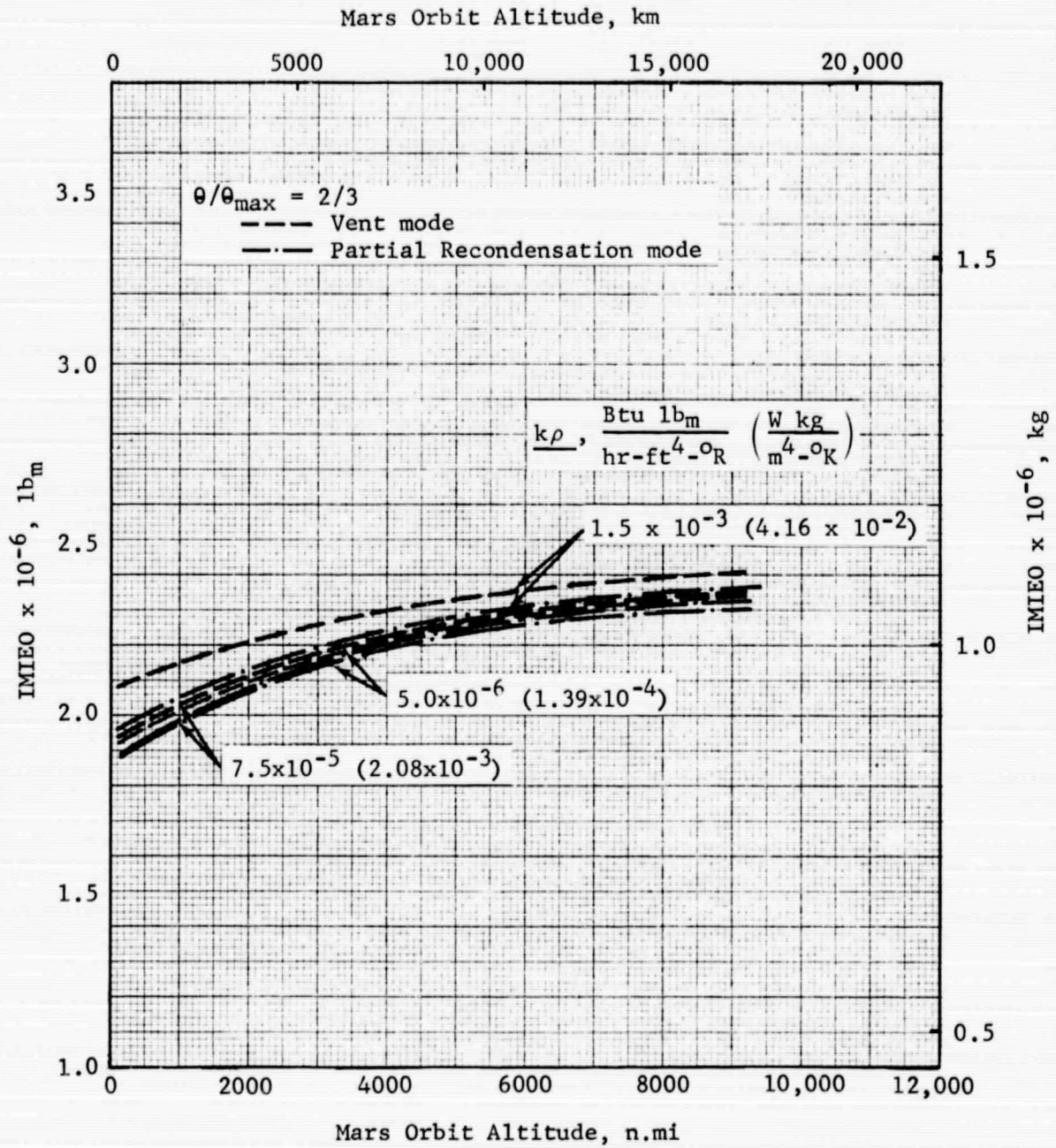


Figure 4.4-16 Effect of Optimum Propellant Storage System on IMIEO vs Altitude: Shielded Mars Departure Stage

GENERAL DYNAMICS
Fort Worth Division

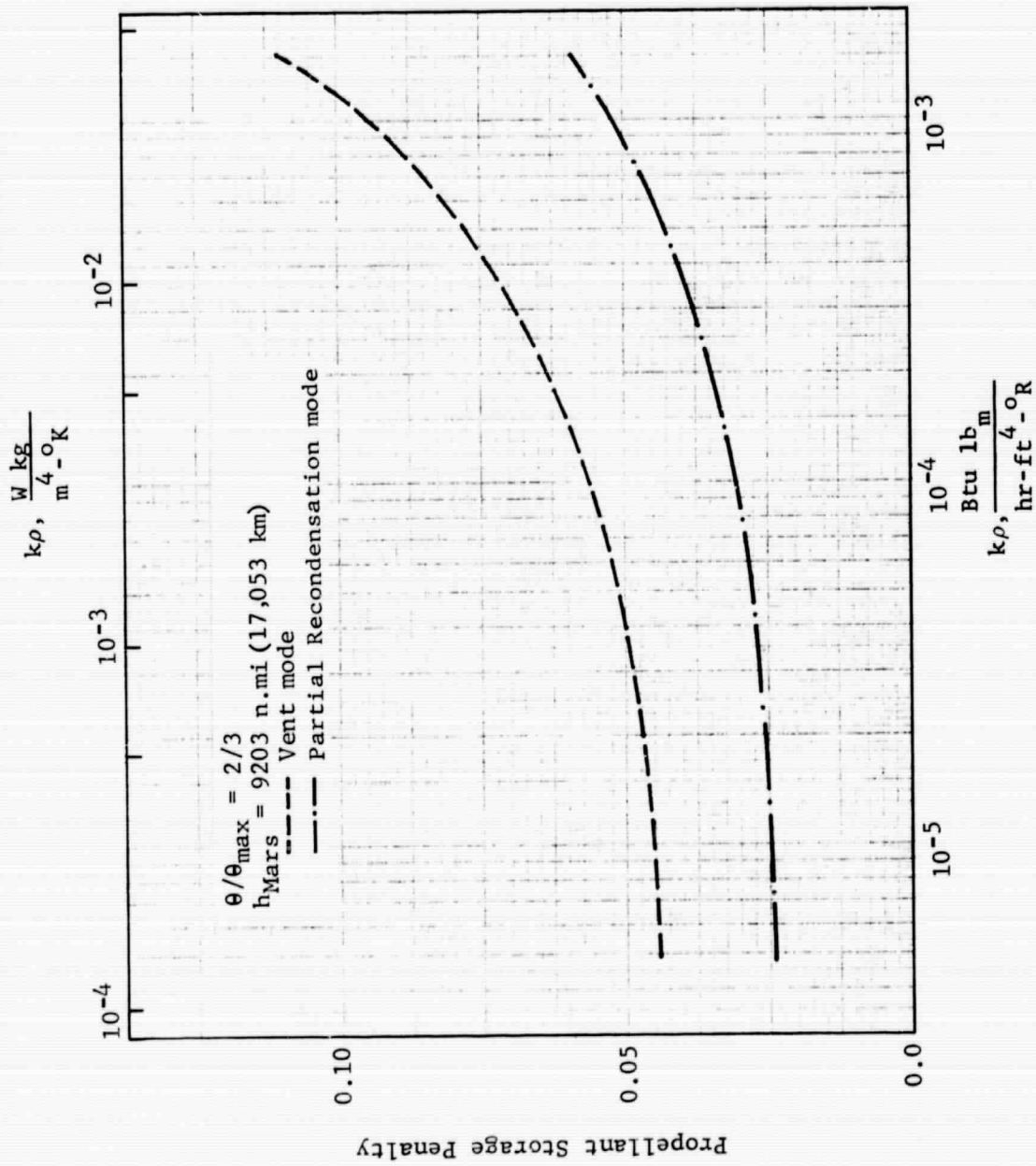


Figure 4.4-17 Effect of Propellant Storage Mode on Propellant Storage Penalty: Unshielded Mars Departure Stage

GENERAL DYNAMICS
Fort Worth Division

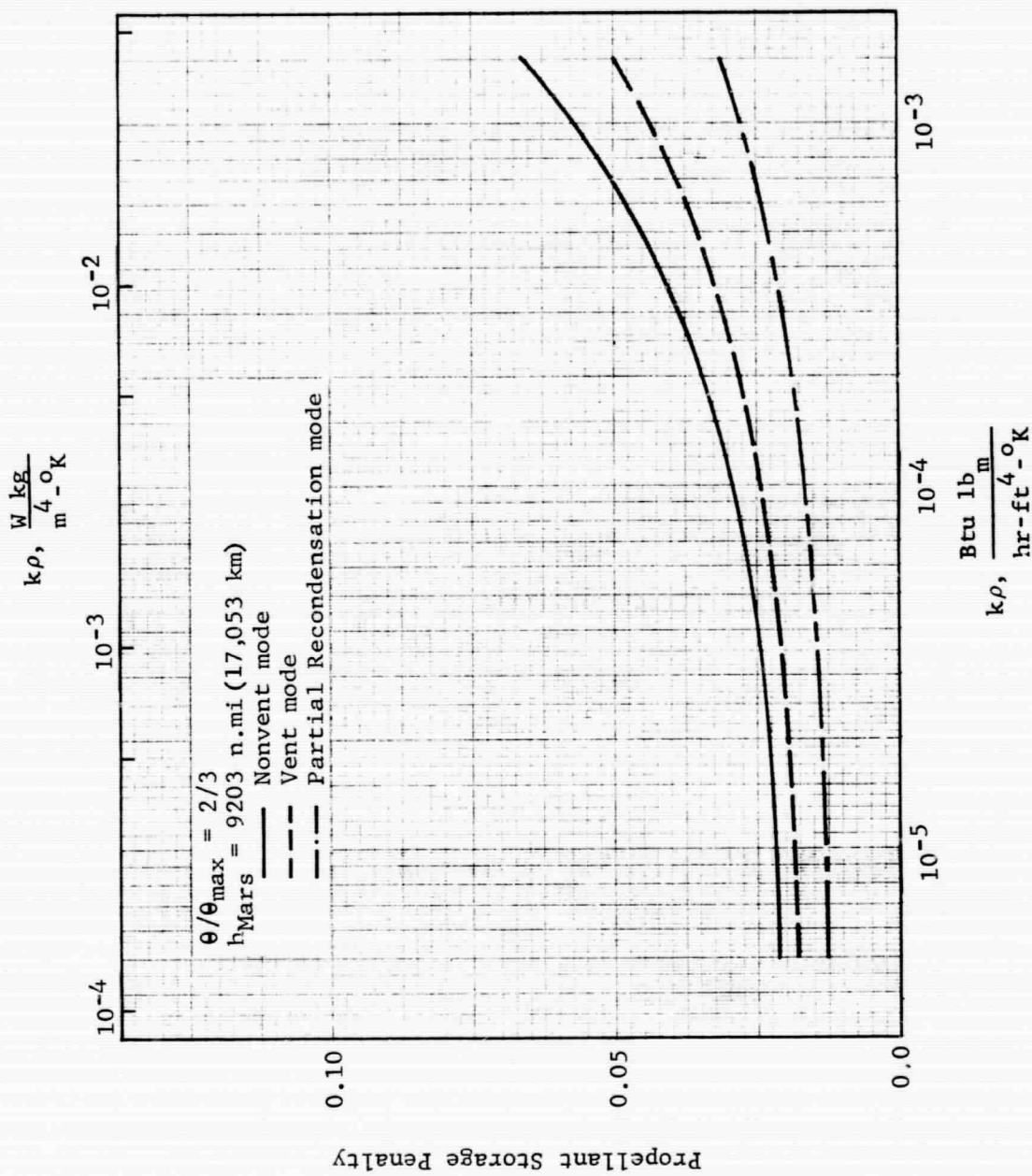


Figure 4.4-18 Effect of Propellant Storage Mode on Propellant Storage Penalty: Shielded Mars Departure Stage

GENERAL DYNAMICS
Fort Worth Division

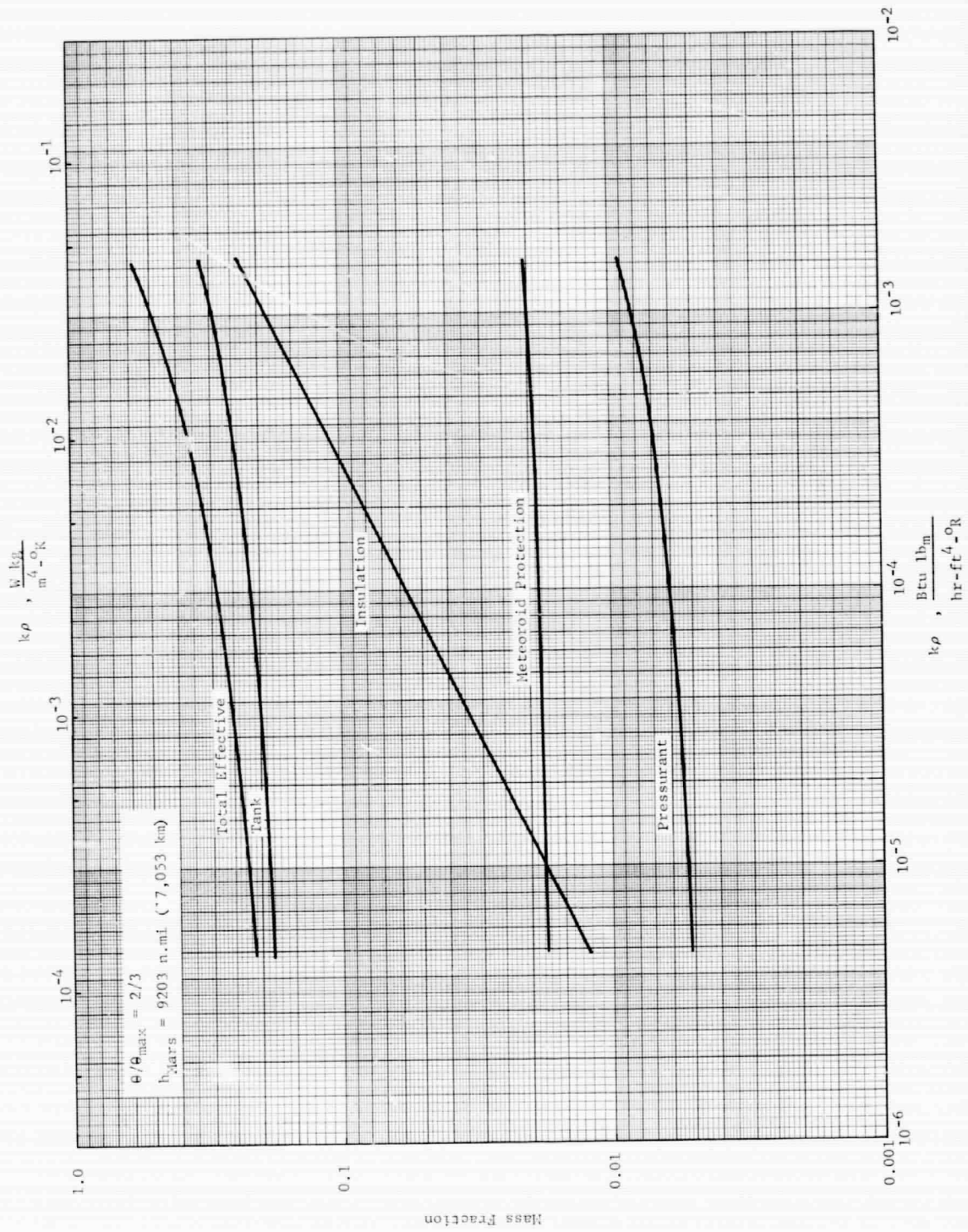


Figure 4.4-19 Optimum Propellant Storage Component Mass Fractions:
Shielded Mars Departure Stage, Nonvent Mode

GENERAL DYNAMICS
Fort Worth Division

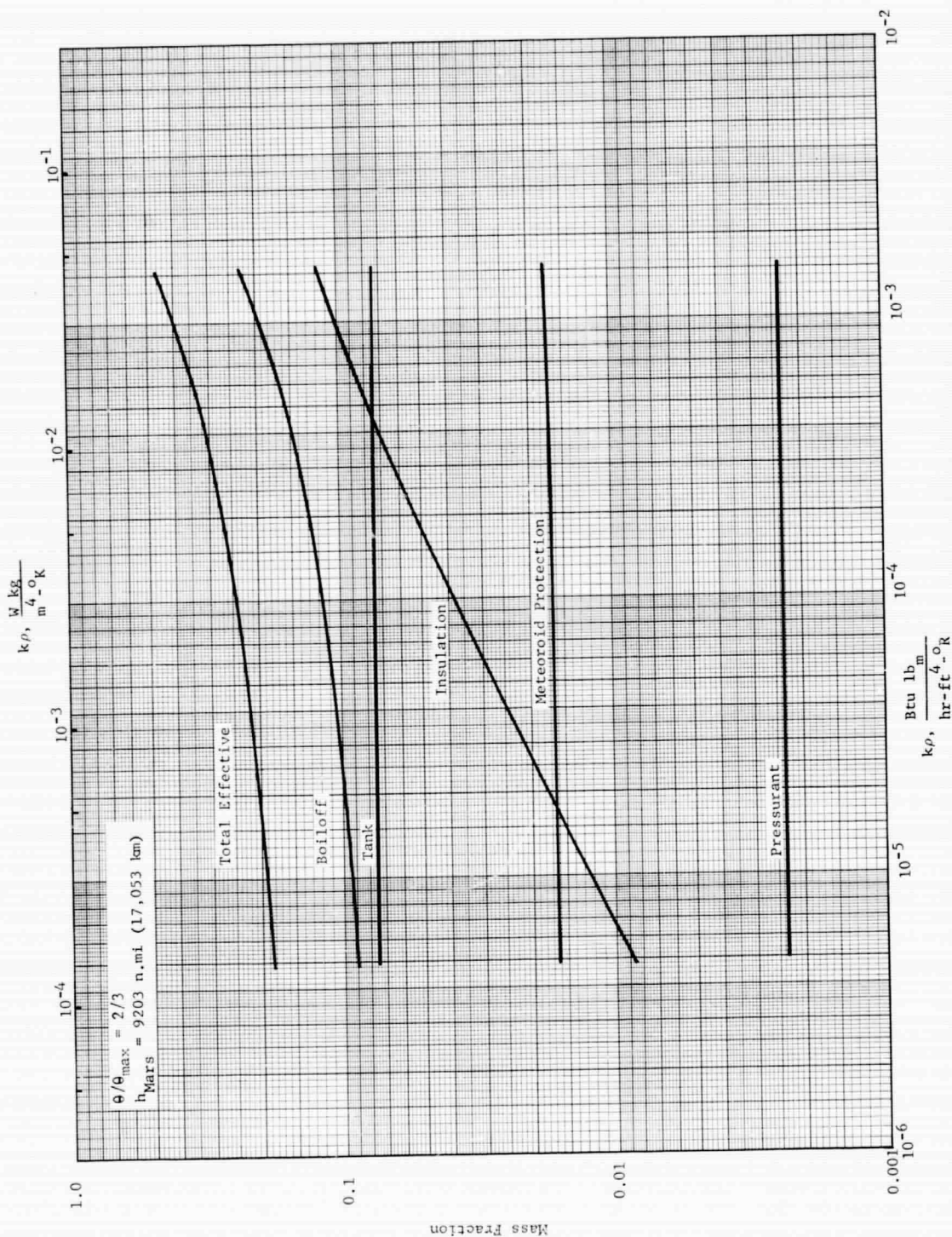


Figure 4.4-20 Optimum Propellant Storage Component Mass Fractions: Shielded Mars Departure Stage, Vent Mode

GENERAL DYNAMICS
Fort Worth Division

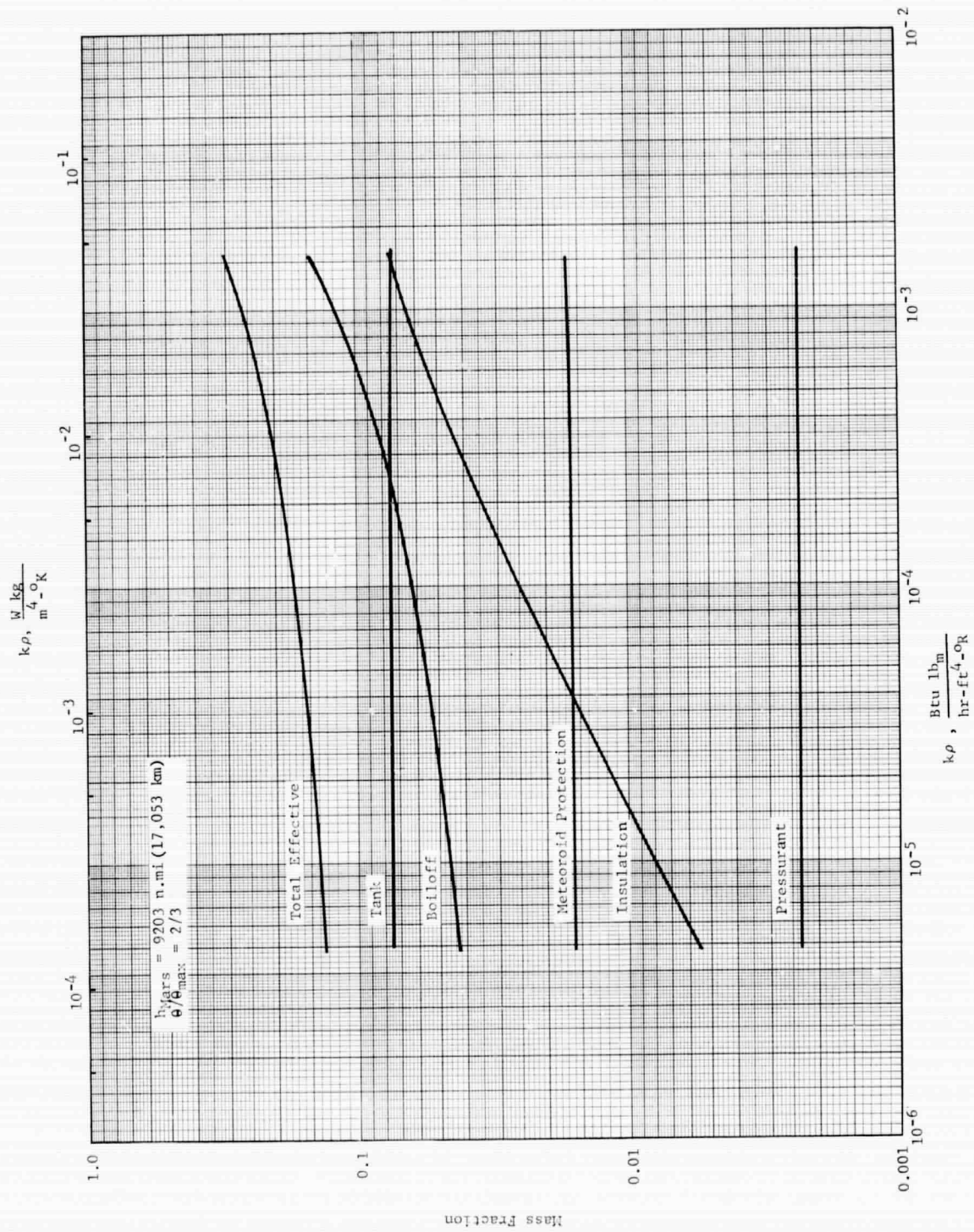


Figure 4.4-21 Optimum Propellant Storage Component Mass Fractions: Shielded Mars Departure Stage, Partial Recondensation Mode

GENERAL DYNAMICS
Fort Worth Division

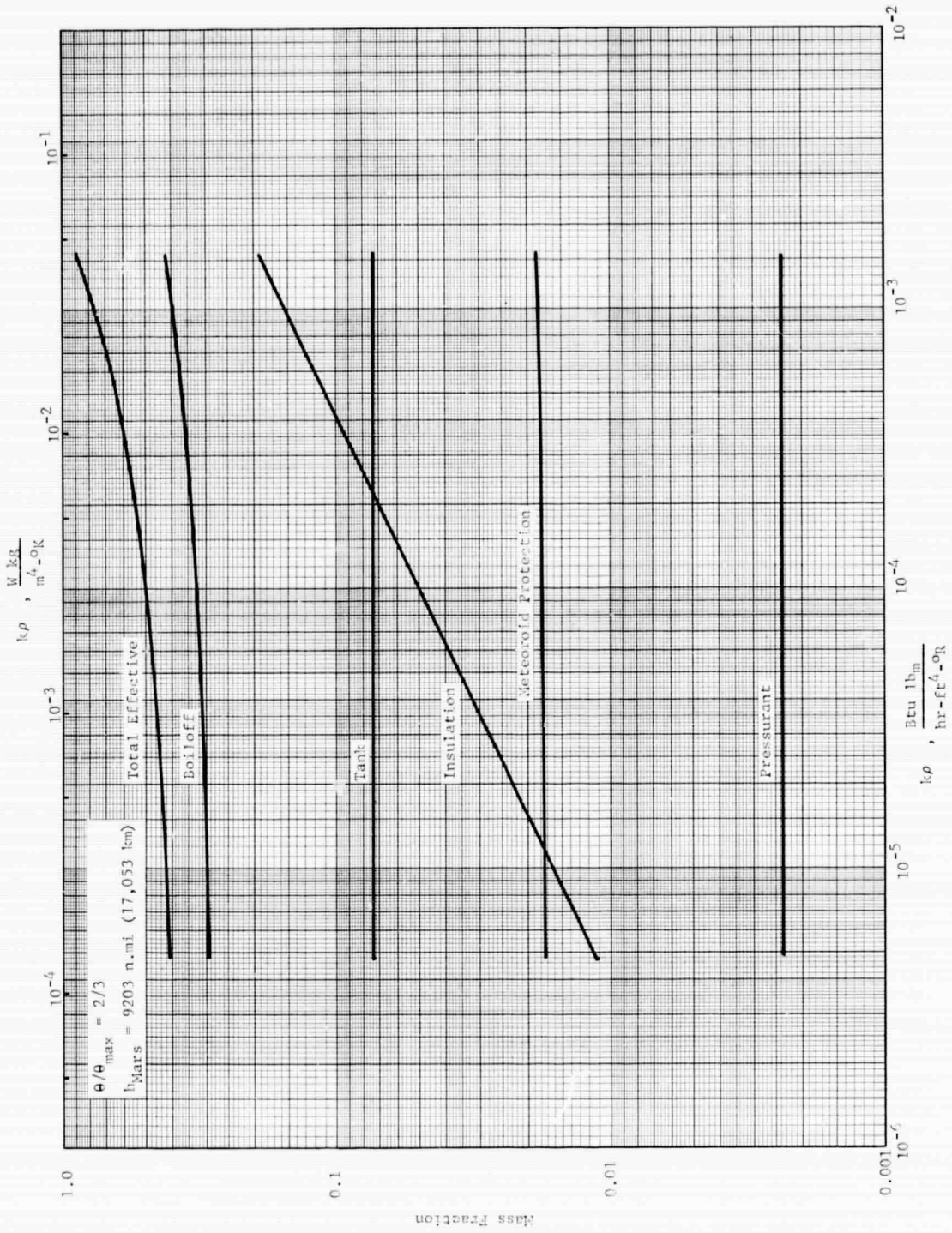


Figure 4.4-22 Optimum Propellant Storage Component Mass Fractions:
Unshielded Mars Departure Stage, Vent Mode

GENERAL DYNAMICS
Fort Worth Division

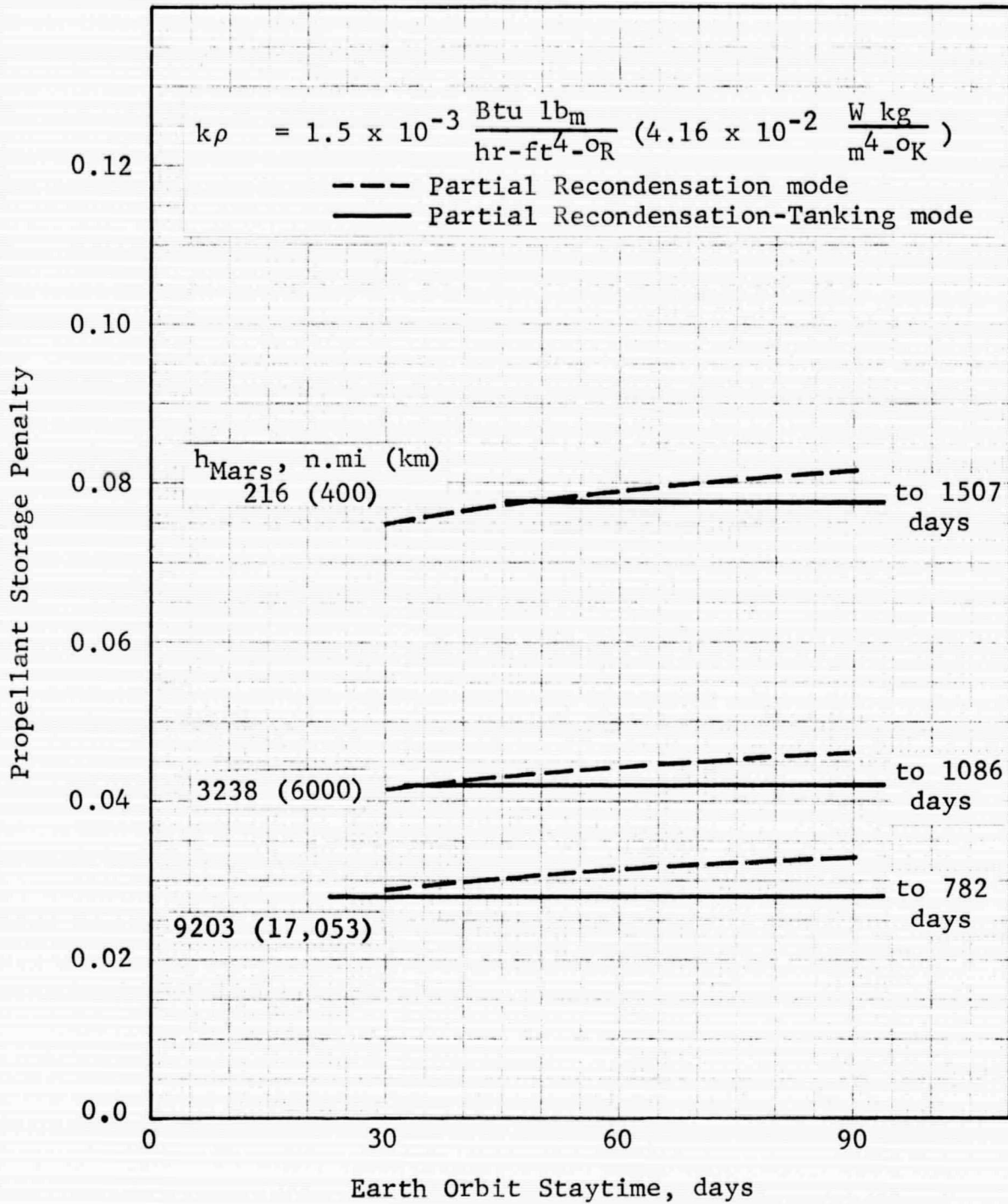


Figure 4.4-23 Effect of Tanking on Propellant Storage Penalty: Shielded Mars, Departure Stage, Partial Recondensation Mode

GENERAL DYNAMICS
Fort Worth Division

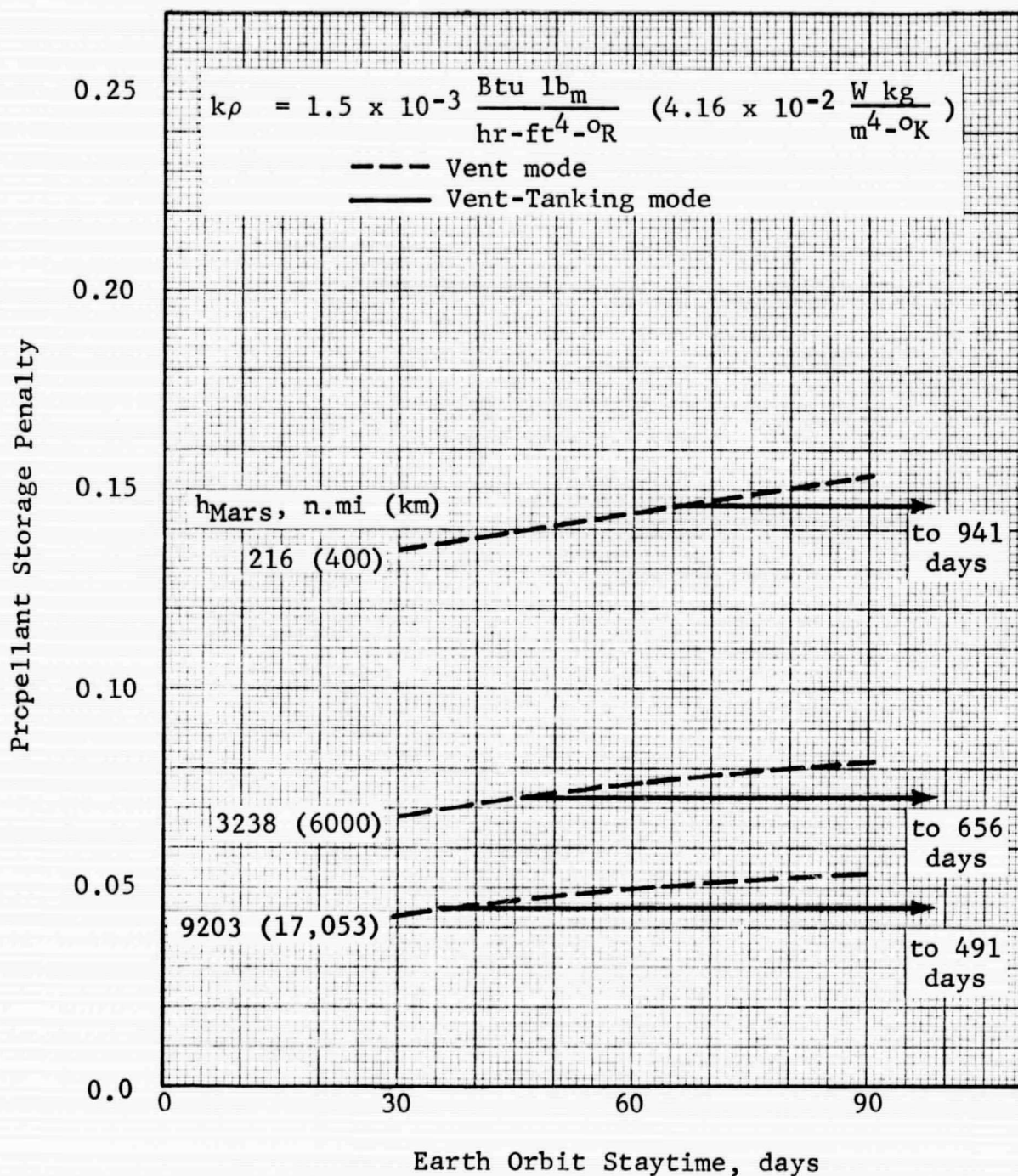


Figure 4.4-24 Effect of Tanking on Propellant Storage Penalty: Shielded Mars Departure Stage, Vent Mode

GENERAL DYNAMICS
Fort Worth Division

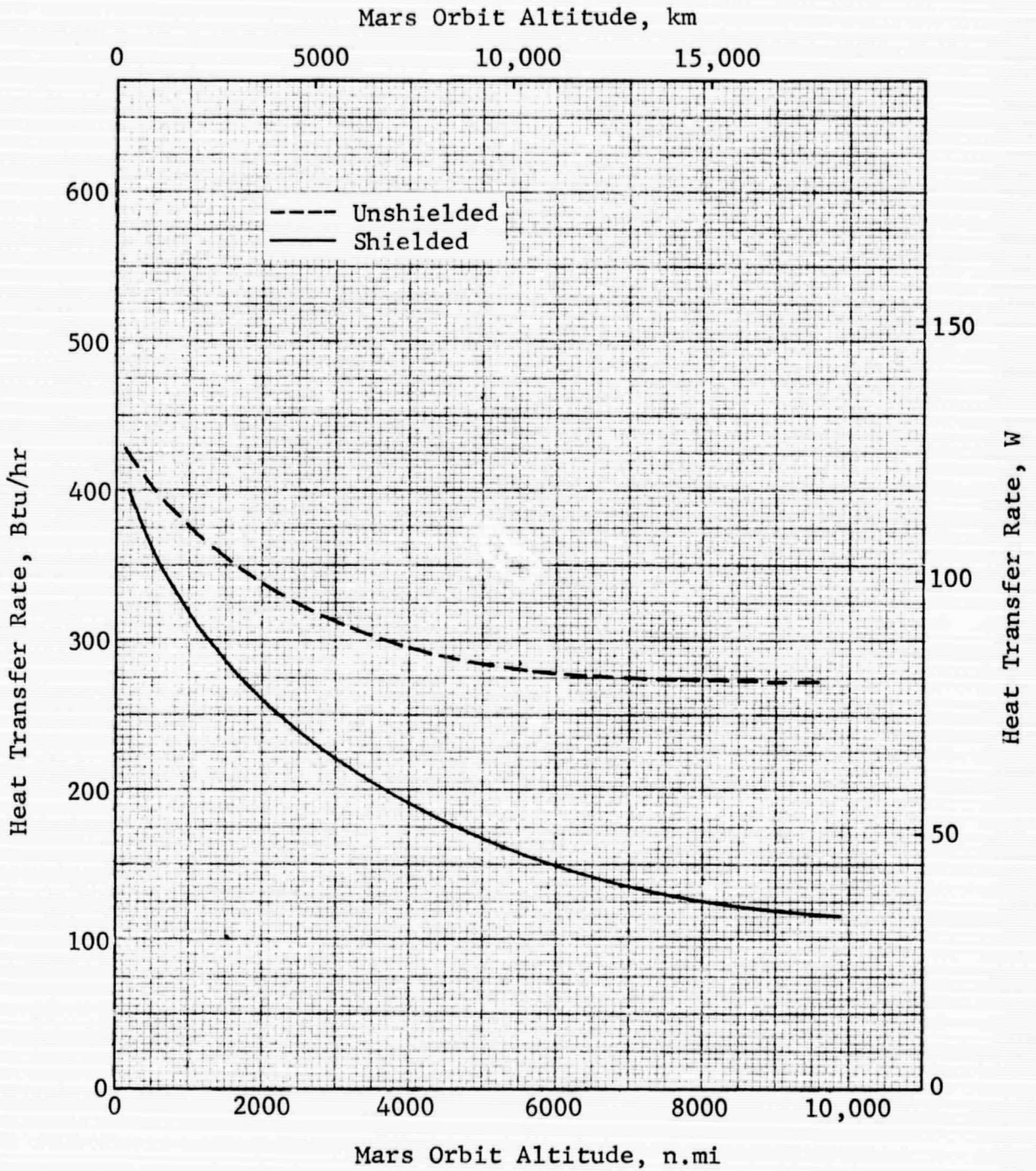


Figure 4.4-25 Effect of Solar Shield on Penetration Heat Transfer Rate during Mars Orbit

GENERAL DYNAMICS
Fort Worth Division

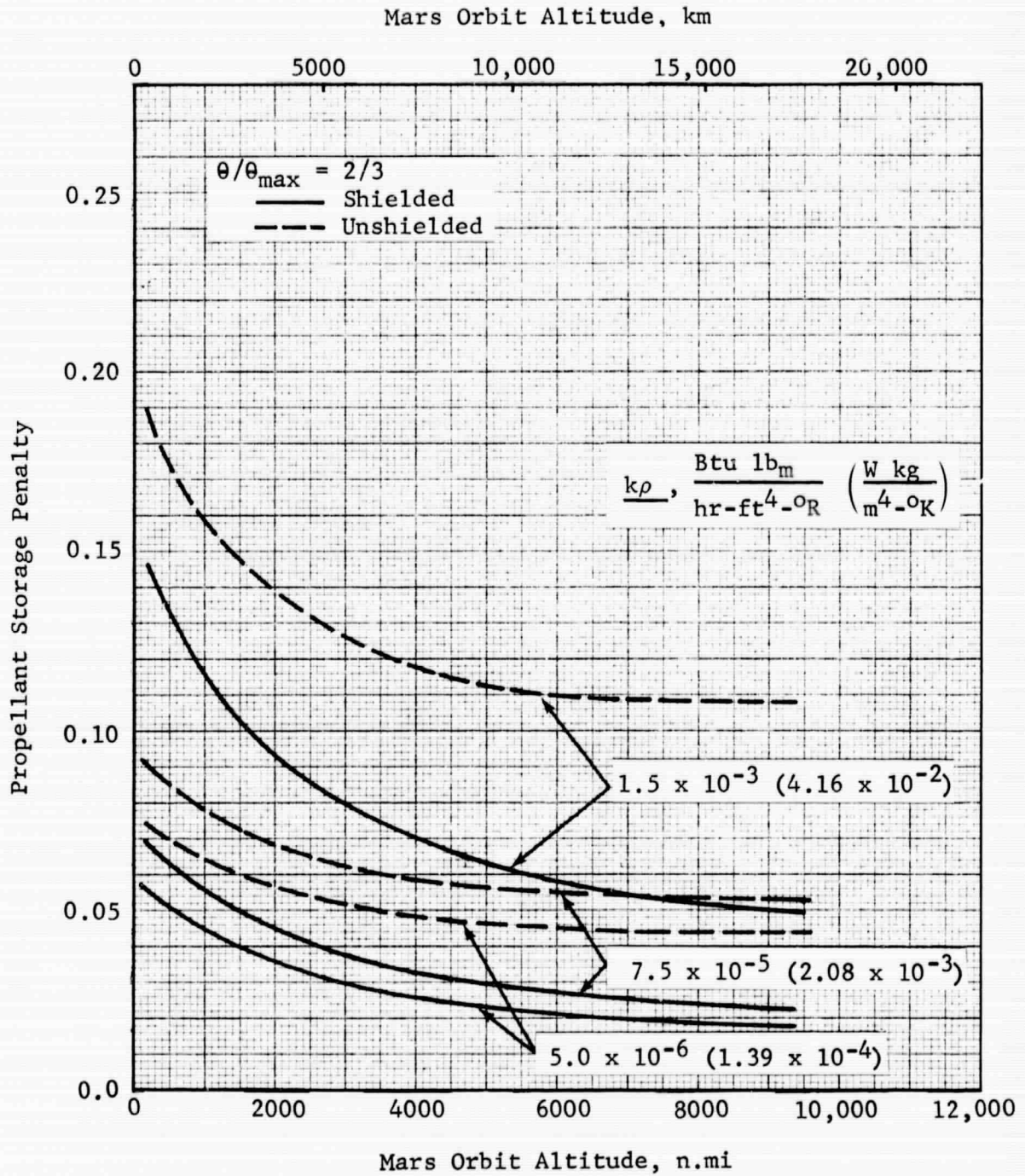


Figure 4.4-26 Effect of Solar Shield on Propellant Storage Penalty: Mars Departure Stage, Vent Mode

GENERAL DYNAMICS
Fort Worth Division

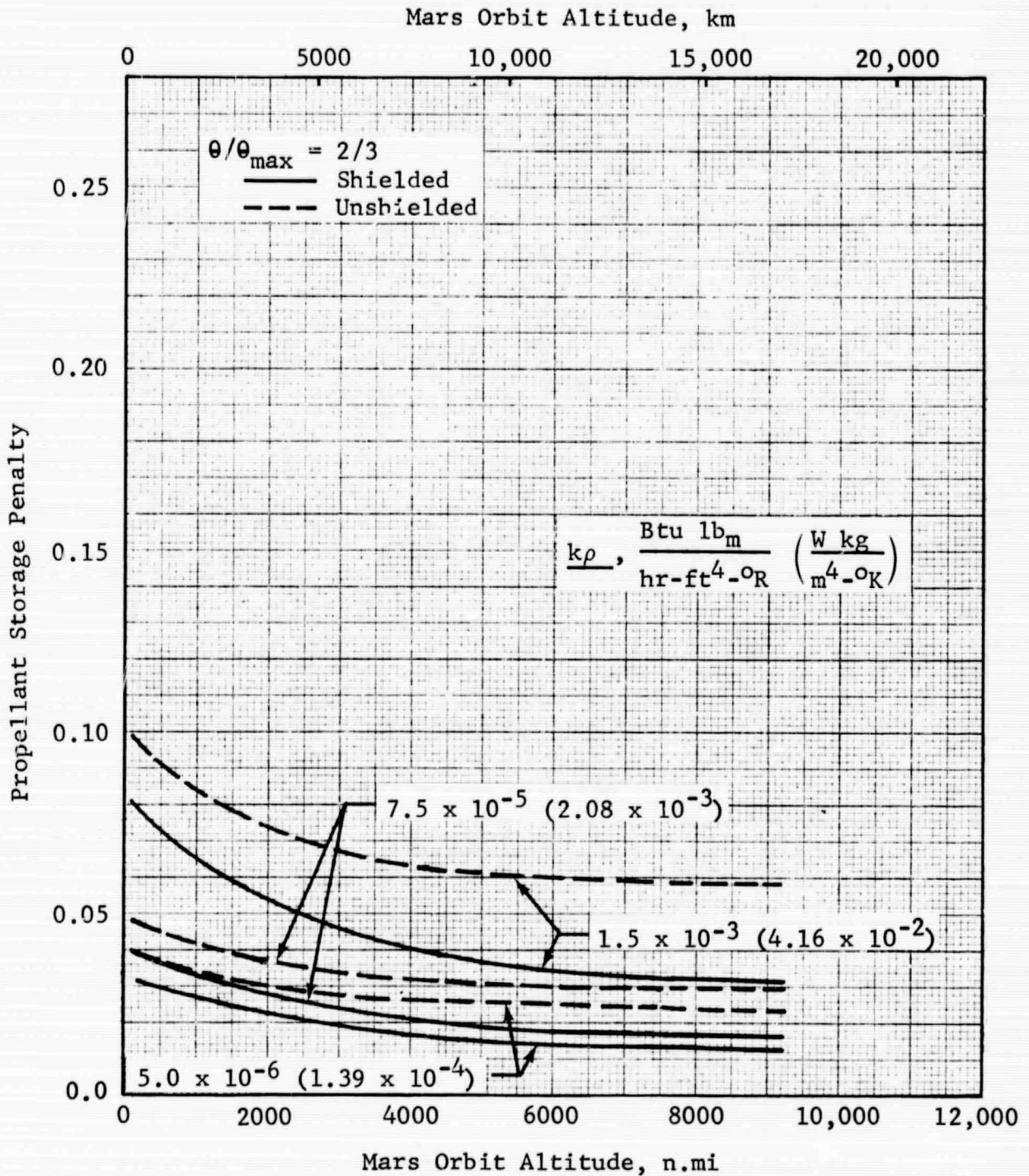


Figure 4.4-27 Effect of Solar Shield on Propellant Storage Penalty: Mars Departure Stage, Partial Recondensation Mode

GENERAL DYNAMICS
Fort Worth Division

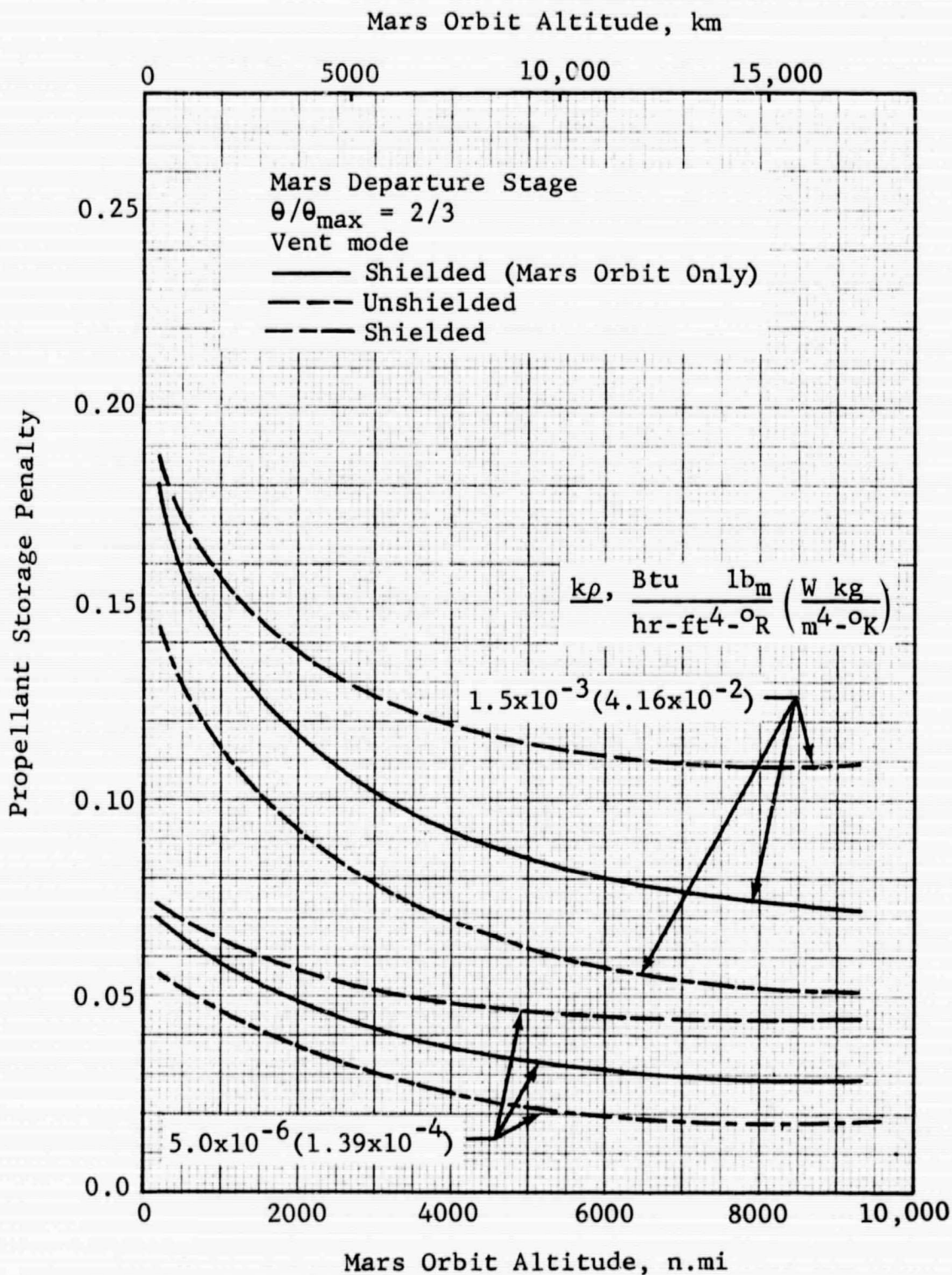


Figure 4.4-28 Relative Effect of Mars Transfer and Mars Orbit Solar Shields on Propellant Storage Penalty

GENERAL DYNAMICS

Fort Worth Division

4.5 OFF-OPTIMUM DATA

Most of the data presented in this report are the result of a computerized optimization analysis. Although the optimum case is of the most interest and utility to the objectives of this study, it is of interest to examine the off-optimum data as well. This examination serves two purposes. First, it points out the penalties associated with a system design that varies from the optimum. Second, it is useful in explaining the trends in the optimum case results.

A typical set of off-optimum data for the nonvent mode where the minimum tank design pressure of 19.7 psia (13.6 N/cm²) is not exceeded is presented in Figure 4.5-1 for the Earth Departure Stage. At insulation thicknesses exceeding 1.4 in. (3.56 cm), the tank mass is fairly constant, reflecting the effect of the minimum tank design pressure: actual tank pressure is decreasing below the minimum design value with increasing insulation thickness; however, the tank wall thickness is based on the 19.7-psia (13.6 N/cm²) value. As the insulation thickness decreases below 1.4 in. (3.56 cm), the pressure increases and the tank mass rises rapidly. Insulation mass increases with thickness, but the relation is nonlinear since the tank surface area also changes with insulation thickness. Note also that for this case the insulation mass is less than one-half of the tank mass. Pressurant mass remains fairly constant over the entire range, decreasing slightly with increasing insulation thickness as the pressure falls. Note that the optimum insulation thickness is determined by the tank mass variation with insulation thickness. This is true in general when the propellant heat transfer is such that the minimum tank design pressure is not exceeded over a wide range of insulation thickness near the optimum.

The well-defined minimum system effective mass shown in Figure 4.5-1 implies that the penalty for off-optimum design may be large. In the case discussed here, this is especially true at thicknesses below the optimum value. For example, a design thickness of 1.0 in. (2.54 cm) rather than the optimum 1.37 in. (3.48 cm) results in a 17.8% increase in the propellant storage system effective mass and an increase in IMIEO of approximately 19,900 lb_m (9030 kg). If a greater thickness such as 2.0 inches (5.08 cm) is chosen, the system effective mass increases 4% and the IMIEO penalty is approximately 4400 lb_m (2000 kg).

GENERAL DYNAMICS

Fort Worth Division

As the propellant heat transfer increases, the insulation mass becomes a factor in determining the optimum insulation thickness and the optimum insulation thickness becomes less well defined. These effects are shown in Figure 4.5-2 for the unshielded Mars Braking Stage in the nonvent mode with low-performance insulation. Note that the tank and insulation masses are roughly equal near the optimum insulation thickness (the minimum value on the system-effective-mass curve). The meteoroid protection mass and the pressurant mass fall well below the tank and insulation masses; both show small variation with insulation thickness.

A comparison of the off-optimum mass data between the vent and the nonvent modes is presented in Figure 4.5-3 for the shielded Mars Departure Stage. For the given conditions, the tank pressure is well above the minimum design value; this can be seen from the shape of the tank mass curve for the nonvent mode. Also, note that tank mass for the vent mode is much lower than for the nonvent mode since the pressure is lower. The variation with insulation thickness is also reduced because the vent pressure is independent of insulation thickness. The difference in insulation mass between the vent and nonvent mode is due to the lower propellant density in the nonvent mode. Even though the propellant loading is larger for the vent mode, the lower propellant density results in larger tanks for the nonvent mode. Note also that for the nonvent mode, the tank and the insulation masses are the dominant factors in the optimization. For the vent mode, the effective boiloff mass and the insulation mass are dominant.

The minimum in the system effective mass curve for the vent mode shown in Figure 4.5-3 does not define the optimum insulation thickness. This optimum is defined by the minimum system effective mass fraction (system effective mass divided by propellant loading) which yields a different optimum insulation thickness, as shown in Figure 4.5-4. For the nonvent mode, the minimum mass fraction and the minimum mass occur at the same point. The reason for the difference between modes is that the propellant mass varies in the vent mode with insulation thickness: the required impulse propellant is held constant, but the boiloff mass varies with insulation thickness. In the nonvent mode, the total propellant mass is independent of insulation thickness.

GENERAL DYNAMICS
Fort Worth Division

In many of the vent-mode and partial-recondensation-mode cases, the conditions are such that the pressure does not reach the vent level and the results are identical to those of the nonvent mode. Off-optimum data for a typical case of this type is presented in Figure 4.5-5, where the vent and nonvent modes are compared for the Earth Departure Stage. The nonvent mode data are the same as that of Figure 4.5-1 and, as pointed out earlier, the tank mass curve exhibits a sharp change in slope at the insulation thickness where the pressure first exceeds 19.7 psia (13.6 N/cm²). Since this corresponds to a vent pressure of 14.7 psia (10.1 N/cm²), boiloff occurs at and below this particular insulation thickness. However, the optimum insulation thickness is determined solely by the tank mass variation with the result that the pressure in the optimum case is 19.7 psia with zero boiloff mass.

One other situation that occurs frequently at the lowest $k\rho$ value is where the pressure in the nonvent mode is well below 19.7 psia, in the 3-6 psia (2.07-4.14 N/cm²) range. Off-optimum data for such a case are presented in Figure 4.5-6 for the shielded Mars Braking Stage with high-performance insulation. Here again the optimum insulation thickness is determined by the tank mass variation. However, in this case, the reason for the change in slope of the tank mass curve is a propellant density change, not the minimum-tank-design-pressure effect. The insulation thicknesses are so low that small changes in insulation thickness yield proportionately larger changes in tank surface area. At the larger thicknesses, the tank is essentially adiabatic and the density is approximately constant.

GENERAL DYNAMICS
Fort Worth Division

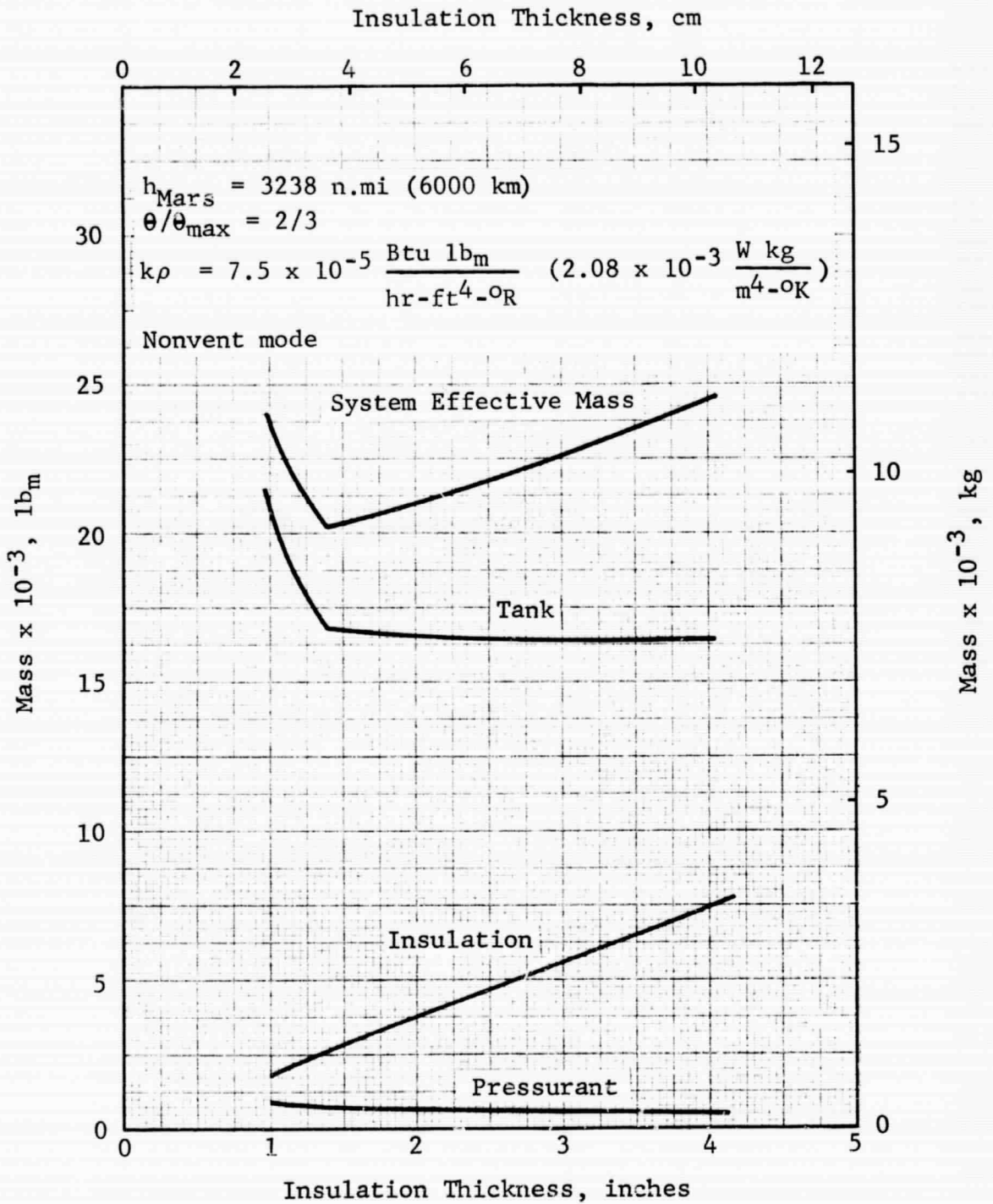


Figure 4.5-1 Off-Optimum Propellant Storage System Mass Data: Earth Departure Stage

GENERAL DYNAMICS
Fort Worth Division

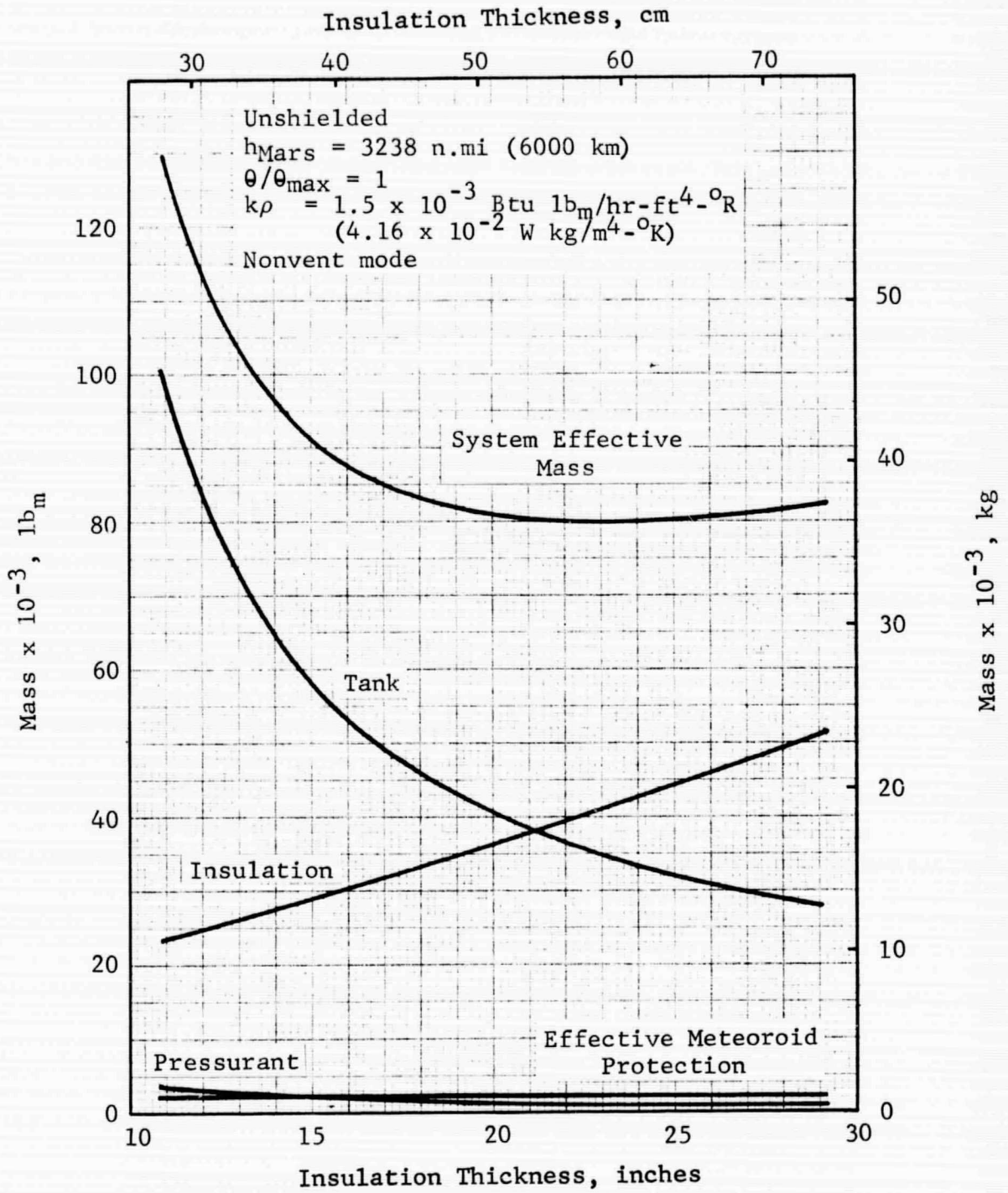


Figure 4.5-2 Off-Optimum Propellant Storage System Mass Data: Mars Braking Stage

GENERAL DYNAMICS
Fort Worth Division

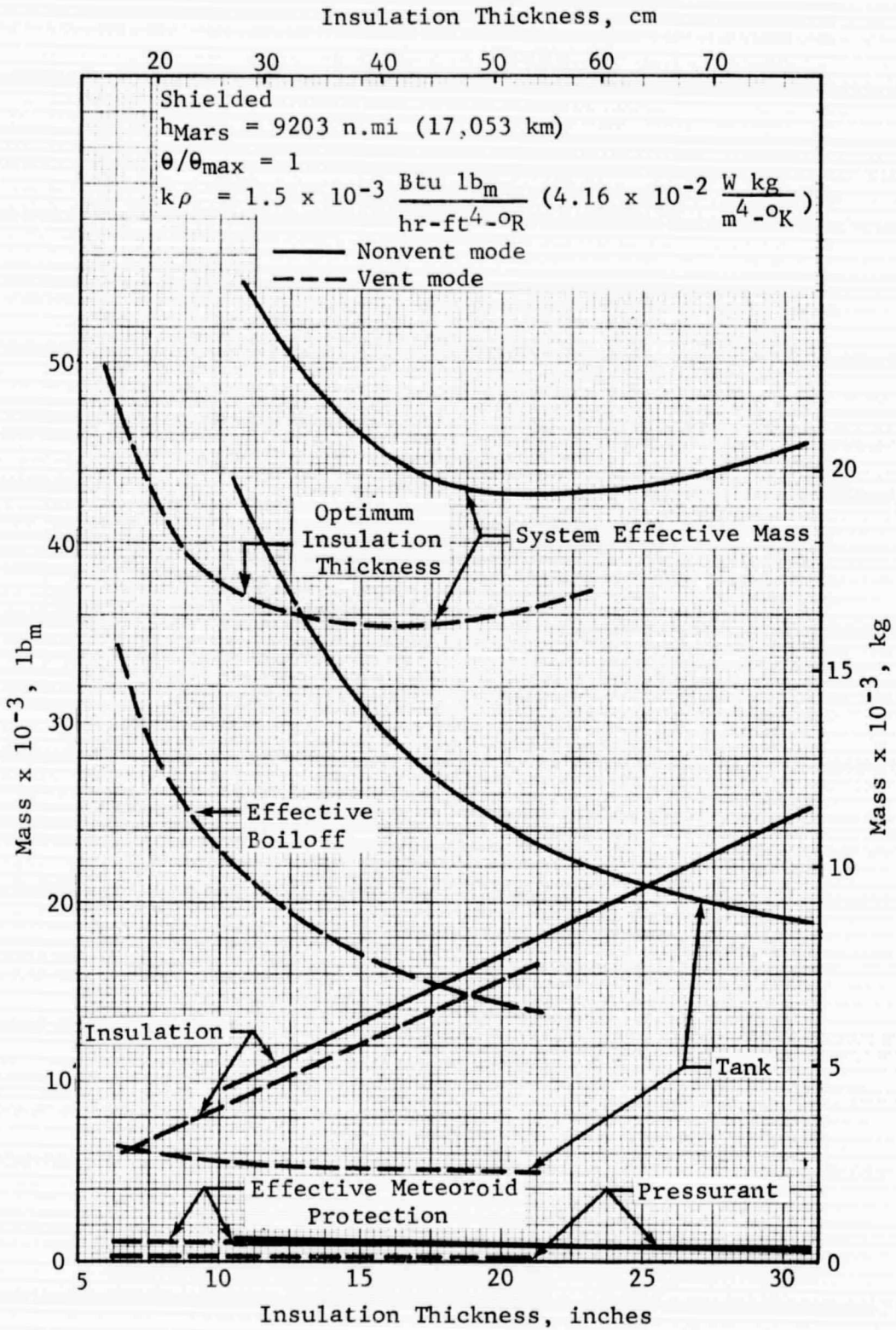


Figure 4.5-3 Comparison of Off-Optimum Mass Data for the Nonvent and Vent Modes: Mars Departure Stage

GENERAL DYNAMICS
Fort Worth Division

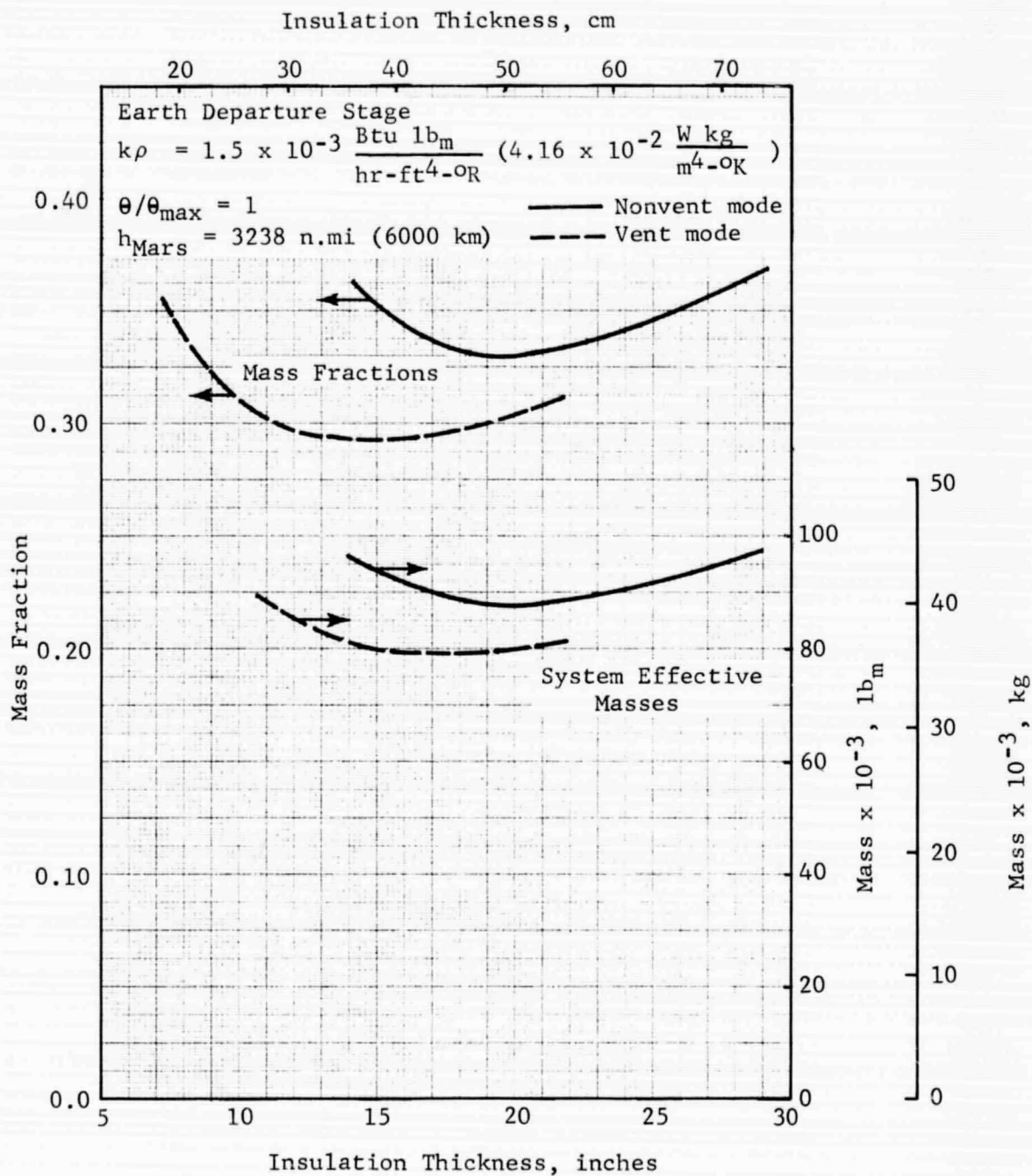


Figure 4.5-4 Location of the Optimum Insulation Thickness

GENERAL DYNAMICS
Fort Worth Division

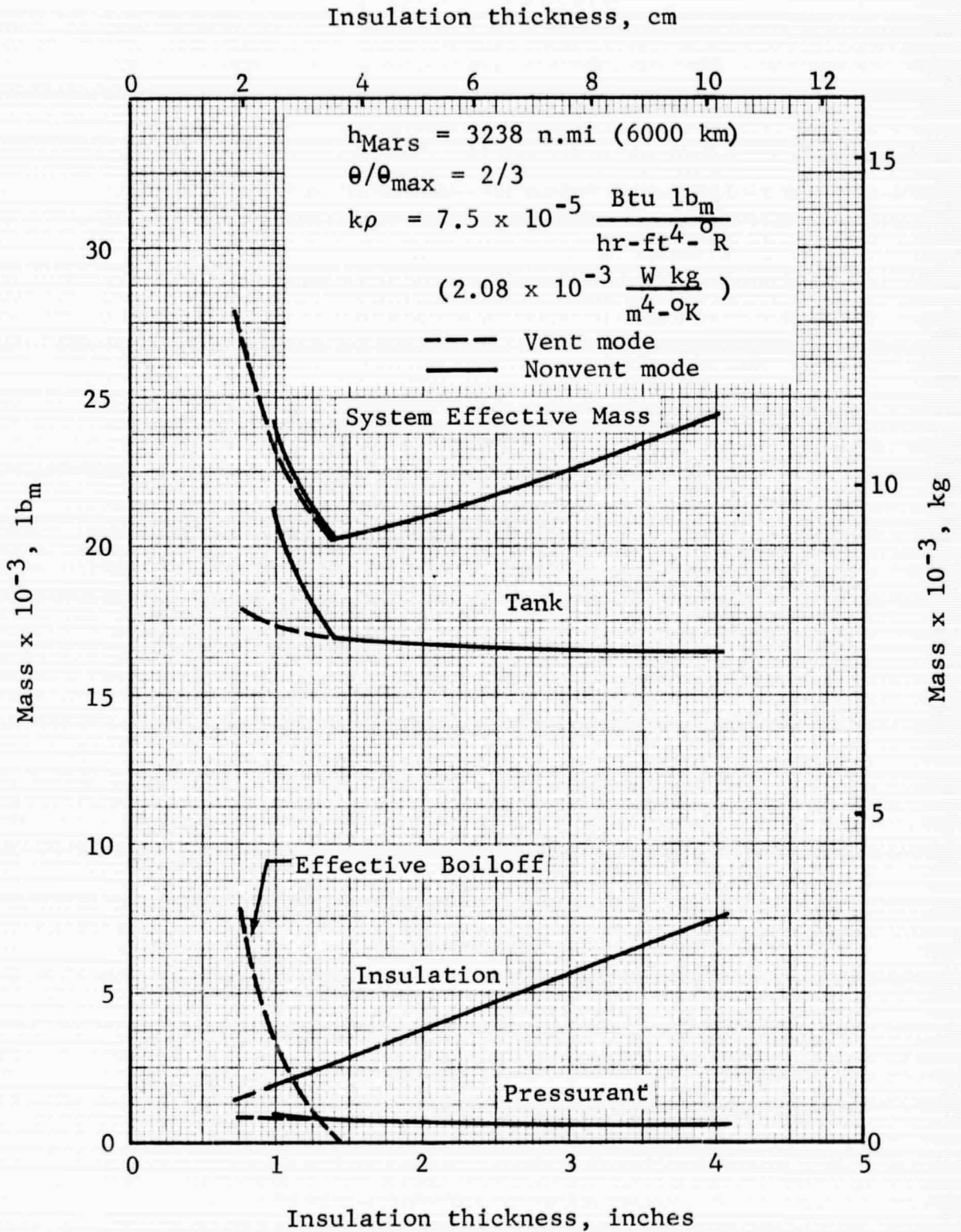


Figure 4.5-5 Comparison of Off-Optimum Mass Data for the Nonvent and Vent Modes: Earth Departure Stage

GENERAL DYNAMICS
Fort Worth Division

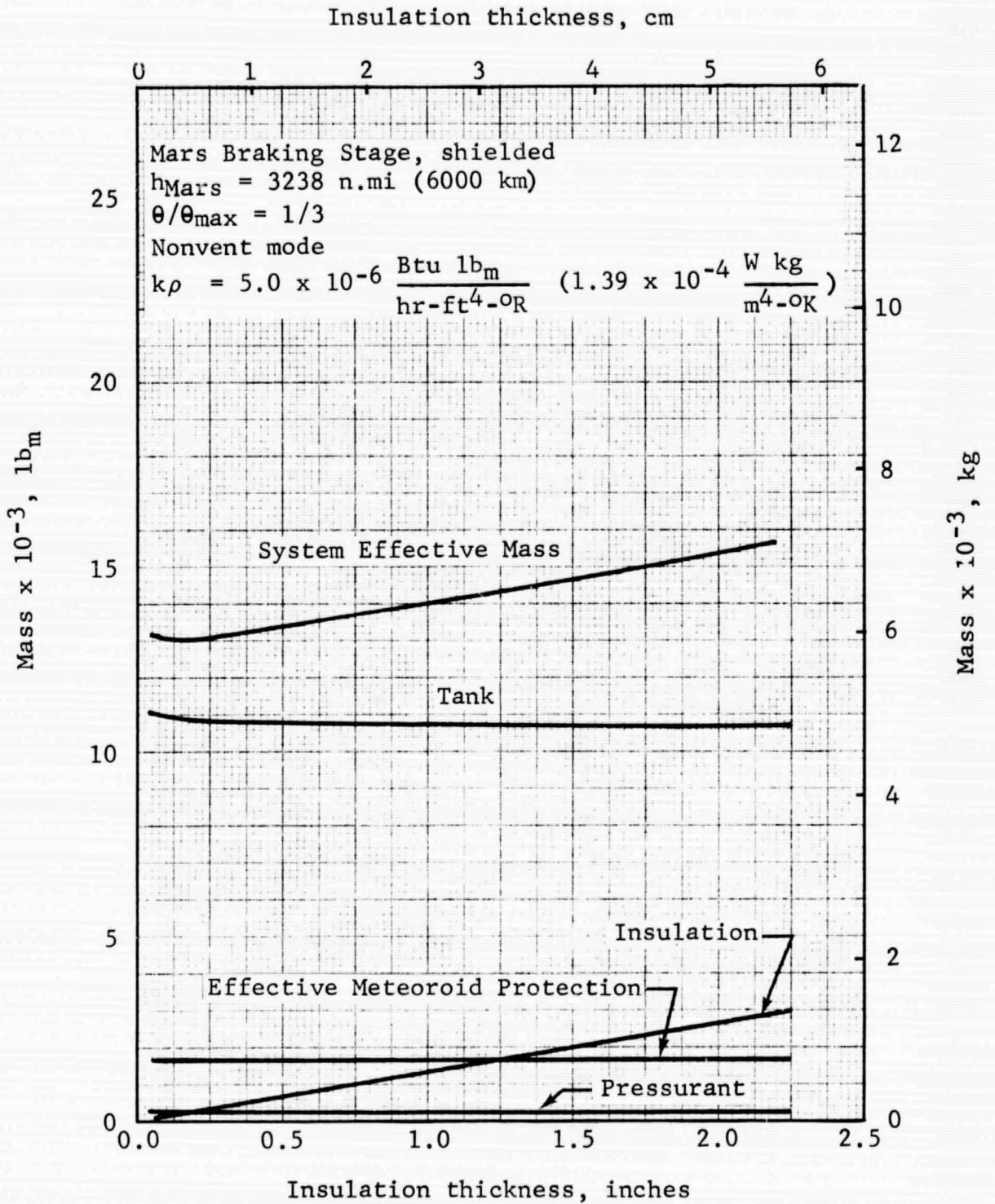


Figure 4.5-6 Off-Optimum Mass Data for a Low-Pressure Condition

GENERAL DYNAMICS
Fort Worth Division

PRECEDING PAGE BLANK NOT FILMED
SECTION 5

SYSTEM PERFORMANCE
CRITERIA

Investigations of propellant storage mode effects and solar shield effectiveness were conducted without considering the masses of these various systems. That is, their functional effects were included in the analyses while assuming that the necessary system hardware had zero mass. Following this approach, the results can be used to generate relative performance criteria for these systems.

Performance criteria for the thermal management systems are evaluated relative to the nonvent system. It would appear that the necessary subsystems for the nonvent mode (stratification reduction device, pressure relief subsystems, etc) would be duplicated in the other storage modes so that the nonvent mode can readily serve as the data baseline. The performance criteria generated in this study are a function of the difference in the vehicle IMIEO for nonvent storage mode and that for the particular mode being considered. The IMIEO values were obtained by using the optimization computer program described in Subsection 6.2 of Volume 2, which operates on a stage basis. Thus, the IMIEO differences reflect the effects of differing propellant storage modes on a single stage, with the remaining stages defined in terms of nominal mass fractions. Since the thermal management system mass for each mode is not included in the IMIEO value, the actual IMIEO difference will differ from the calculated IMIEO difference by an amount proportional to the system mass. Thus, the calculated IMIEO difference can be interpreted as an upper limit on the IMIEO penalty for the particular thermal management system on the stage being considered. It is an upper limit in the sense that no reduction in the IMIEO relative to the nonvent mode will be realized if the system IMIEO penalty equals or exceeds the calculated IMIEO difference.

These performance criteria can be reduced to system mass units by applying an appropriate factor to the IMIEO difference. This factor accounts for the additional propellant, tankage, etc. required on the particular stage and all lower stages by virtue of the additional mass of the thermal management system and for the number of propellant tanks in the stage. In this latter form, the performance criteria can be

GENERAL DYNAMICS

Fort Worth Division

termed an "allowable mass;" it is the maximum system mass that can be allowed without the vehicle IMIEO exceeding the IMIEO for the nonvent mode.

For the solar shield systems, the performance criteria are referenced to the unshielded stage and are a function of the IMIEO difference between the vehicle with the stage shielded and the vehicle with the same stage unshielded. Since the shield system mass has not been considering in evaluating the IMIEO for the shielded case, the calculated IMIEO difference can again be considered an upper limit on the IMIEO penalty for the system. As in the thermal management system case, the calculated IMIEO difference can be reduced to system mass units by applying an appropriate factor accounting for the additional propellant, tankage, etc. However, the factor in the solar shield case is different from that for a thermal management system. The difference arises because the solar shields are jettisoned from the vehicle prior to primary propulsion maneuvers while the thermal management systems remain with the stages and are carried through the velocity changes.

GENERAL DYNAMICS

Fort Worth Division

5.1 VENT SYSTEM

The vent thermal management system provides a means of jettisoning energy absorbed by the propellant from the vehicle in the form of propellant boiloff. This reduces the specific internal energy and the vapor pressure of the remaining propellant and increases the propellant density as compared to the nonvent mode. Both the lower pressure and the higher density act to reduce the tank mass, while the boiloff acts to increase the tank mass by virtue of the larger propellant loading. In Subsection 4.5, typical examples of the variation with insulation thickness of the propellant storage component masses and the total effective mass are presented for the vent mode. The relationship between these component masses for a given storage mode is a function of the insulation performance, the thermal environment, the stage, and the nature of the component (jettisoned or nonjettisoned).

Performance criteria for the vent system are presented in this section in terms of the system allowable mass. Data are presented for each of the three stages on a per-tank basis. Where tanking is advantageous, the effect of tanking on the allowable mass is described.

5.1.1 Earth Departure Stage

Vent system allowable mass for the Earth Departure Stage is presented as a function of Earth orbit staytime in Figure 5.1-1. The solid curve represents the low-performance insulation condition (highest $k\rho$ value); one point at the intermediate $k\rho$ value was definable and is shown at the maximum staytime. With low-performance insulation, the allowable mass increases by a factor of 20 over the 90- to 270-day staytime interval, reaching 8800 lb_m (3990 kg) at the maximum staytime. The data are extrapolated^m to determine the staytime at which the allowable mass is zero; a staytime of approximately 80 days results in equal IMIEO values for the vent and nonvent modes (neglecting vent system mass). At the intermediate $k\rho$ value and the maximum staytime, the allowable mass is only 390 lb_m (177 kg). Thus, the higher insulation performance results in a reduction of allowable mass by a factor of 22. Similar results were obtained at the 216-n.mi (400 km) and 9203-n.mi (17,053 km) Mars orbit altitudes and are not presented here.

PRECEDING PAGE BLANK NOT FILMED.

GENERAL DYNAMICS

Fort Worth Division

(1640 kg) to 12,400 lb_m (5620 kg) over the range of staytime. Even at zero staytime, the vent mode yields some savings. As the insulation performance improves, the allowable mass drops sharply to values below 2000 lb_m (910 kg). Extrapolation to staytimes corresponding to zero allowable mass are also possible and are indicated in the figure.

For the Braking Stage, the boiloff rates show a greater variation than in the Earth Departure Stage case, as shown in Figure 5.1-2. The lower limit of zero for the Earth orbit phase pertains to cases where the vent pressure is not reached until the Mars transfer phase. Because of the differing thermal environments between Earth orbit and Mars transfer, the boiloff rates may vary considerably between mission phase for a given insulation performance and staytime. As an example, the boiloff rate during Earth orbit for the high- $k\rho$ value, maximum-staytime case is 12.5 lb_m/hr (5.7 kg/hr) and decreases to 4.9 lb_m/hr (2.2 kg/hr) during Mars transfer.

As in the Earth Departure Stage case, the mass savings that lead to the allowable mass are due to reductions in tank and insulation mass. To estimate the actual savings in IMIEO for a given vent system mass, a ratio of IMIEO to allowable mass of 3.3 can be used, on a per-tank basis, for the unshielded stage.

When the solar shield is used on the Mars Braking Stage, the heat transfer during the Mars transfer phase is negligible compared to that occurring during Earth orbit. Thus, from a thermal standpoint, a shielded Braking Stage is similar to an Earth Departure Stage. It is not surprising then that the vent system allowable mass for the shielded Mars Braking Stage (Figure 5.1-4) follows the same trends as in the Earth Departure Stage case. The allowable mass at the high $k\rho$ value ranges from 370 lb_m (168 kg) at the 60 day staytime to 8000 lb_m (3630 kg) at the 180-day staytime. Note that this maximum value is over 35% below that for the unshielded case. The staytime at which the allowable mass reaches zero is approximately 54 days. At the intermediate $k\rho$ value, the allowable mass is a mere 130 lb_m (59 kg).

Boiloff rates for the shielded case during Earth orbit range from 9.0 to 12.7 lb_m/hr (4.1 to 5.8 kg/hr) at the high $k\rho$ value. The boiloff during Mars transfer is negligible. At the intermediate $k\rho$ value, the boiloff rate is reduced to 3.8 lb_m/hr (1.7 kg/hr) during Earth orbit. Since the boiloff

GENERAL DYNAMICS

Fort Worth Division

during Mars transfer is so low, the design problems associated with a wide variation in boiloff rates over the mission are alleviated. To estimate actual savings in the IMIEO associated with a given vent system mass, a factor of 3.2 can be used to relate allowable mass to the IMIEO.

Tanking is advantageous for the vent propellant storage mode only for the unshielded Mars Braking Stage and only with low-performance insulation (highest $k\rho$ value). For the shielded stage, the optimum insulation thickness would be near zero because the propellant heat transfer during Mars transfer is small. As a result, the entire propellant loading would be boiled off early in Earth orbit, leaving dry tanks. With higher performance insulation, the vent pressure is not reached during Earth orbit in most cases; where the vent pressure is reached the boiloff is minimal.

The system allowable mass for the vent-tanking case is compared with the normal vent mode results in Figure 5.1-5. At a staytime of approximately 64 days, tanking begins to yield savings in mass as the allowable mass begins to exceed that for the vent mode. At the maximum staytime of 180 days, the allowable mass for the vent-tanking mode is 28,100 lb_m (12,750 kg) which is 125% greater than the vent-mode value. Use of a tanking operation generally extends the permissible Earth orbit staytime well beyond the range defined in this study, as shown in Figure 5.1-6. For the unshielded Braking Stage, the indicated maximum staytime approaches 900 days. This maximum staytime corresponds to boiloff of the total propellant loading which may not be compatible with the pressure-stabilized-tank concept. However, it is seen that even partial tanking allows a significant extension of the staytime.

5.1.3 Mars Departure Stage

The Mars Departure Stage presents a problem with regard to evaluating the vent-system allowable mass. Because of the length of the mission, especially the 510 days spent in Mars orbit, the heat load is such that the nonvent mode of operation results in very high pressures and associated low liquid-hydrogen densities. The high pressure and low density combine to produce systems which are outside the bounds of reasonable tank design. This fact precludes the possibility of using the nonvent mode, and of calculating allowable masses for the vent

GENERAL DYNAMICS

Fort Worth Division

mode, except for those cases which employ a solar shield and operate at the high orbit altitude. These conditions give a lower heat transfer rate in the Mars orbit phase of the mission, reducing the effect of the long mission time. However, the tank pressures are still high, exceeding 80 psia (55.2 N/cm²) at the high- $k\rho$ -value, maximum-staytime condition.

Vent-system allowable masses for the shielded, high-altitude case are presented in Figure 5.1-7 as a function of insulation performance. The allowable masses range from 740 lb_m (336 kg) for the combination of short Earth orbit staytime and low $k\rho$ value to 11,710 lb_m (5310 kg) for the maximum staytime and high $k\rho$ value. Note that the variation with insulation performance is similar at all staytimes and that the curves are fairly flat at the low $k\rho$ value. Thus, the vent system yields some reduction in the IMIEO even with the highest insulation performance. This is due to the penetration heat transfer which is independent of insulation performance.

The range of boiloff rates for the Mars Departure Stage is shown in Figure 5.1-2 for each of the mission phases. The envelopes shown include unshielded stages as well as the shielded, high-altitude case shown in Figure 5.1-7. For this high-altitude case, boiloff occurs only during Mars orbit at the intermediate and low $k\rho$ values. The boiloff rate is thus relatively constant, with values ranging from 0.64 to 0.75 lb_m/hr (0.3 kg/hr), depending upon the insulation performance. At the high $k\rho$ value, boiloff occurs during Earth orbit and Mars transfer as well as Mars orbit. This results in a large variation in boiloff rate, ranging from 5.9 lb_m/hr (2.7 kg/hr) in Earth orbit to 1.3 lb_m/hr (0.6 kg/hr) in Mars orbit. The amount of boiloff occurring during the transfer period is negligible.

The factor relating IMIEO to allowable mass for the shielded Mars Departure Stage is approximately 4.6. This value can be used to obtain estimates of the actual savings in IMIEO to be gained by using a vent system of given mass.

Tanking is advantageous for the vent storage mode of the shielded stage only. For the unshielded stage, the vent pressure is not reached during Earth orbit. As in the case of the Braking Stage, tanking yields significant savings only at the high $k\rho$ value. Allowable mass for the vent-tanking mode is compared to that of the vent mode in Figure 5.1-8. Tanking begins to yield mass savings at a staytime of approximately

GENERAL DYNAMICS

Fort Worth Division

35 days. The allowable mass increases with staytime, reaching 16,200 lb_m (7350 kg) at the 90-day staytime. This represents an increase of 38.5% relative to the vent-mode allowable mass. The tanking operation yields a significant increase in permissible staytime, as seen in Figure 5.1-6, where the maximum staytime for the shielded stage at the 9203-n.mi (17,053 km) altitude is almost 500 days. Again, the maximum value corresponds to complete propellant boiloff during Earth orbit.

GENERAL DYNAMICS
Fort Worth Division

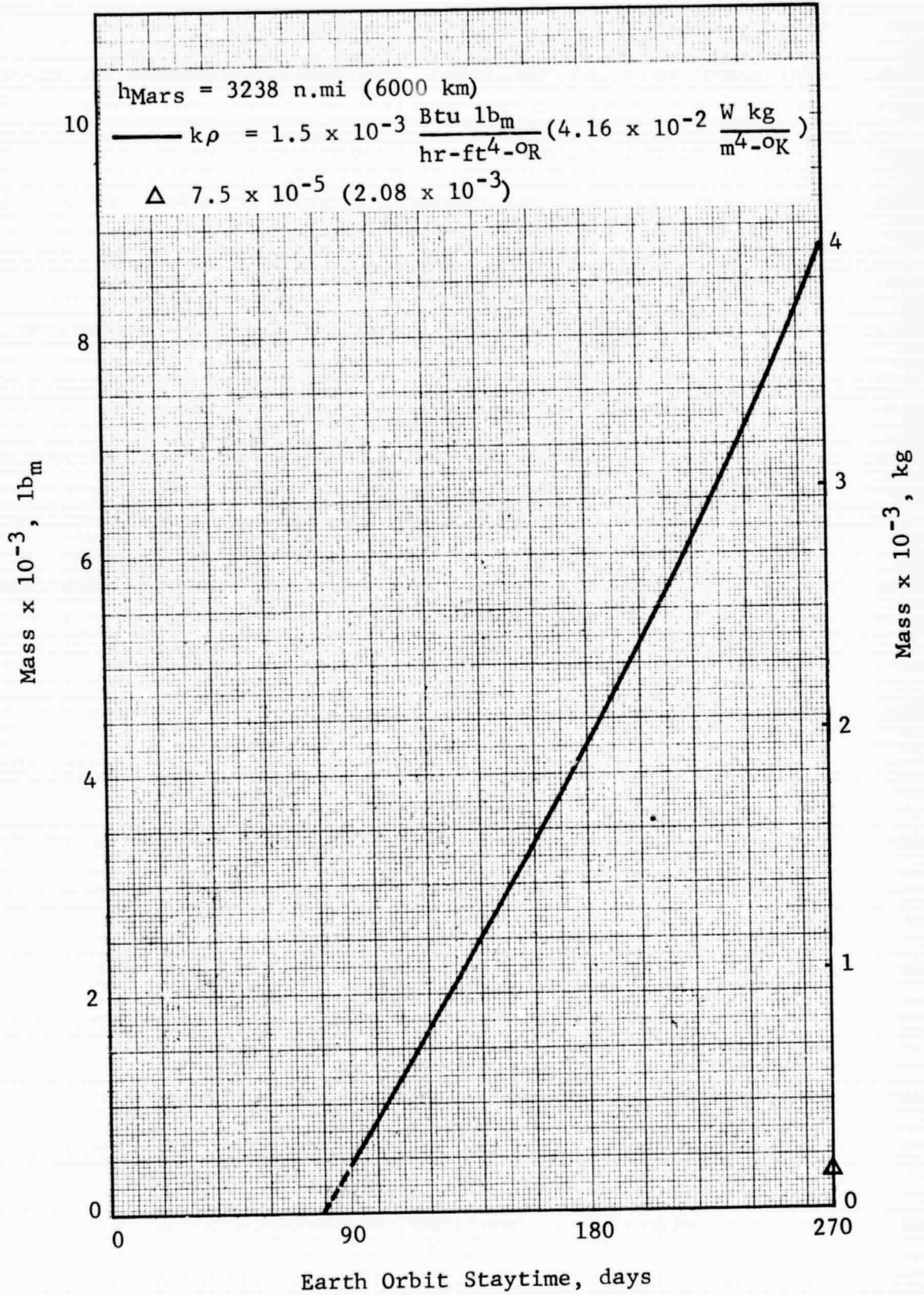


Figure 5.1-1 Vent System Allowable Mass:
Earth Departure Stage

GENERAL DYNAMICS
Fort Worth Division

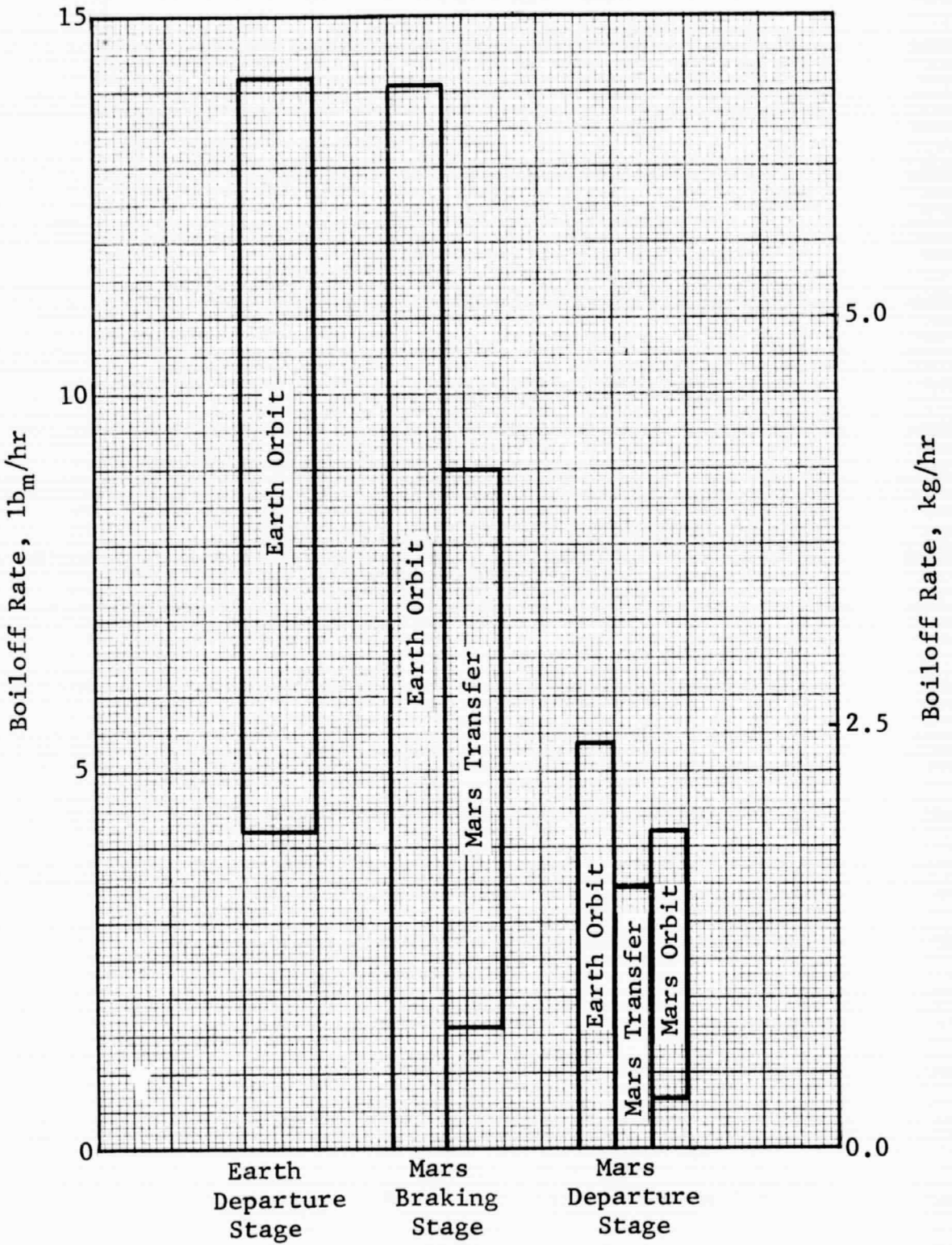


Figure 5.1-2 Vent System Boiloff Rates

GENERAL DYNAMICS
Fort Worth Division

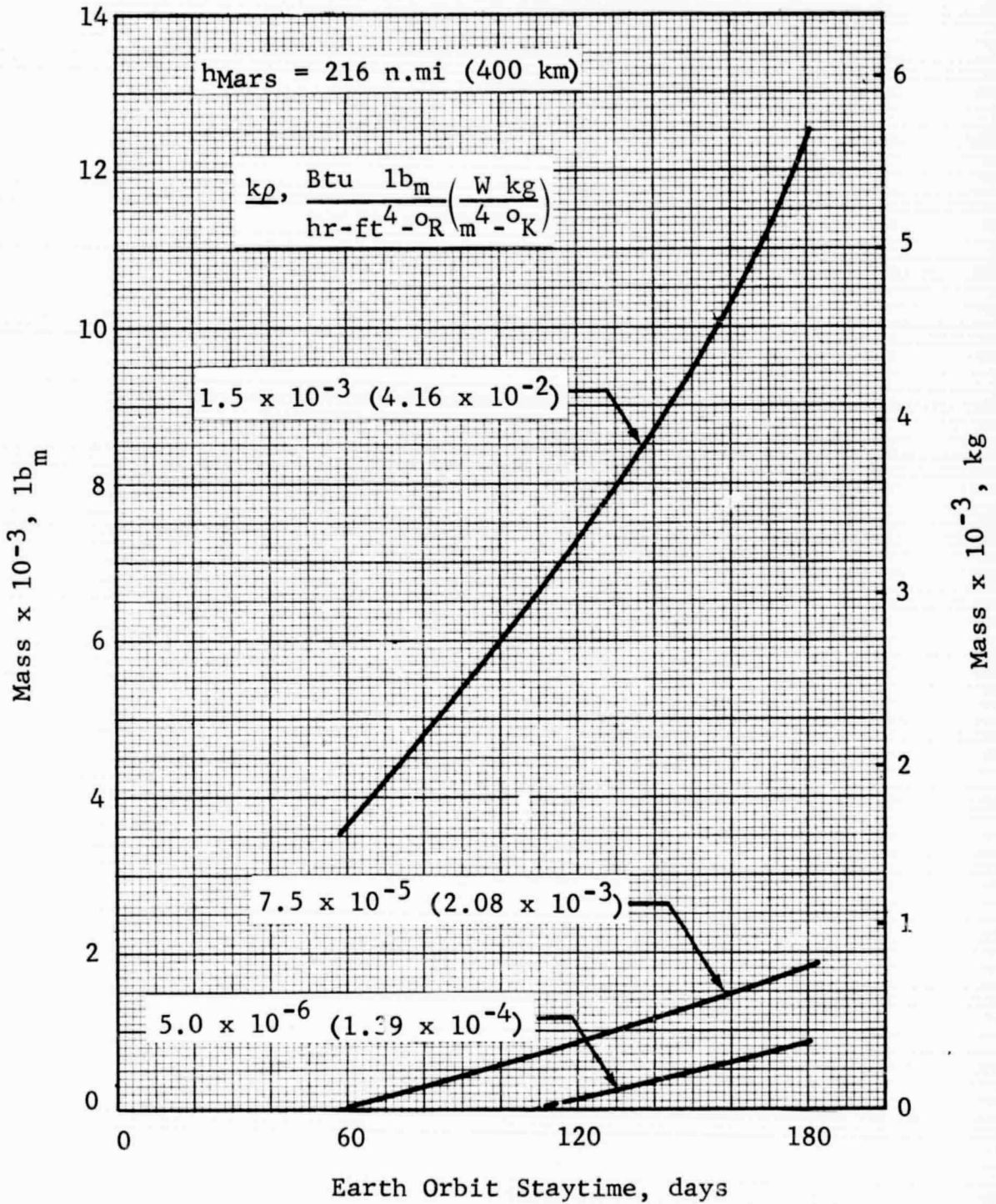


Figure 5.1-3 Vent System Allowable Mass:
Unshielded Mars Braking Stage

GENERAL DYNAMICS
Fort Worth Division

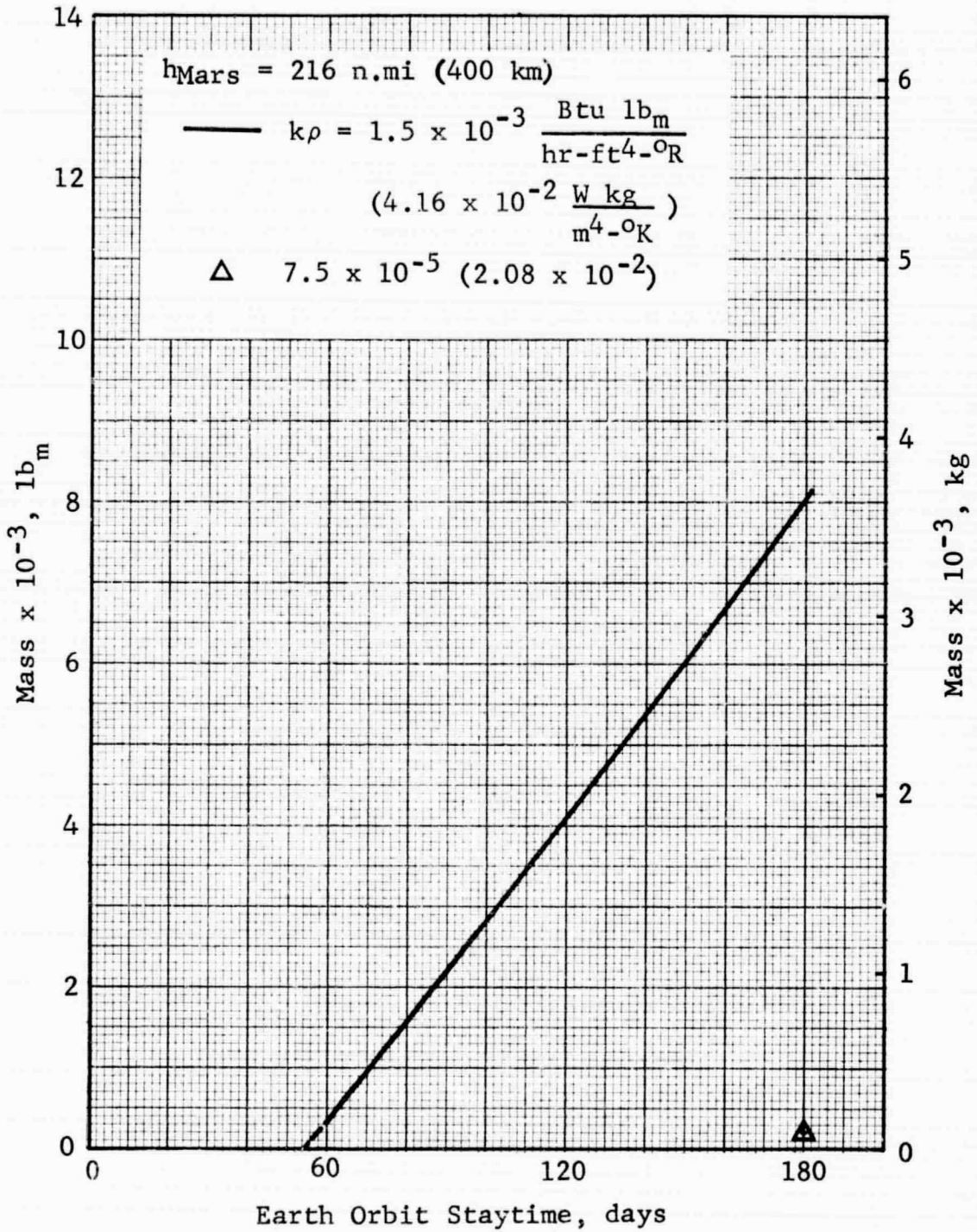


Figure 5.1-4 Vent System Allowable Mass:
Shielded Mars Braking Stage

GENERAL DYNAMICS
Fort Worth Division

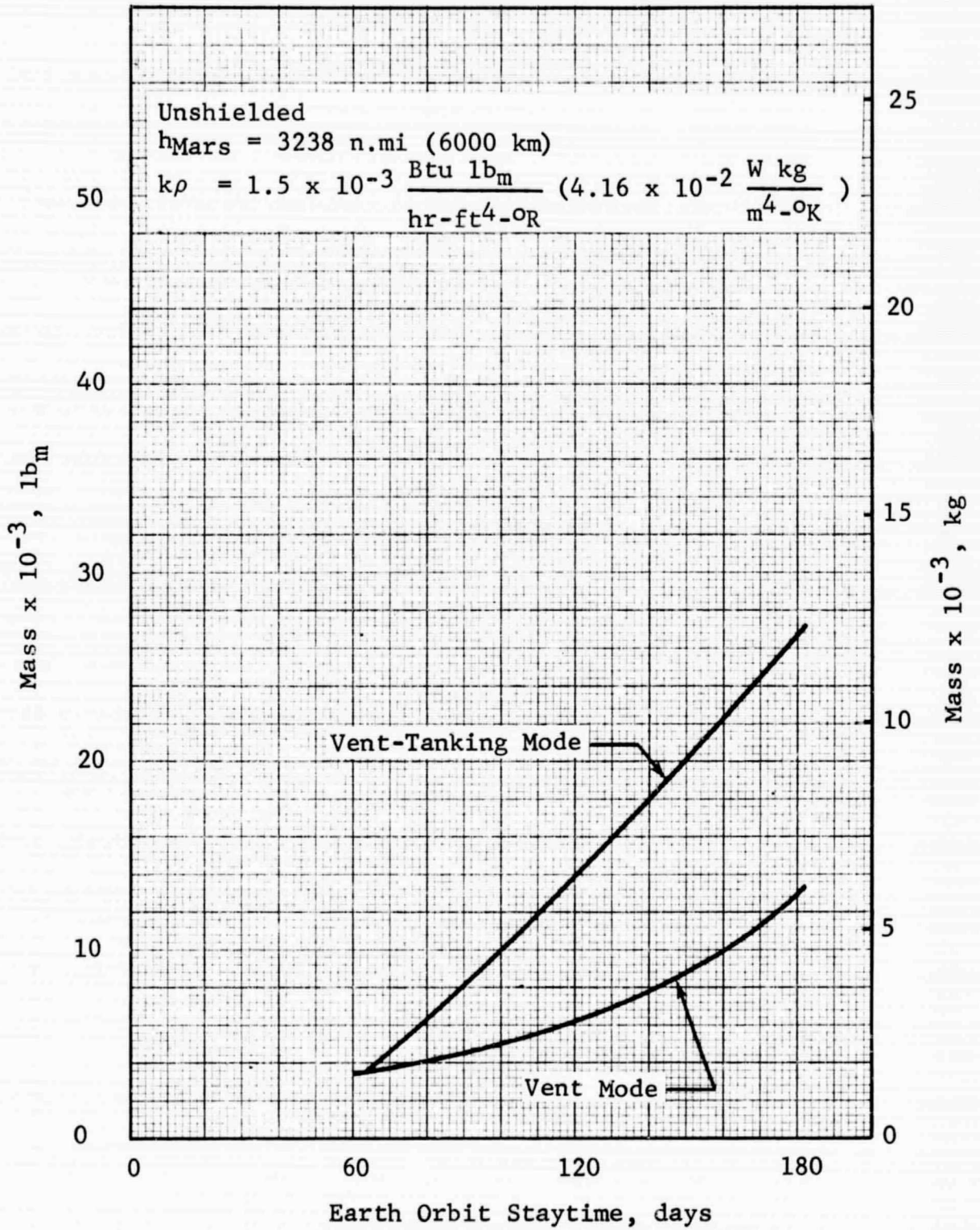


Figure 5.1-5 Vent System Allowable Mass With and Without Tanking: Mars Braking Stage

GENERAL DYNAMICS
Fort Worth Division

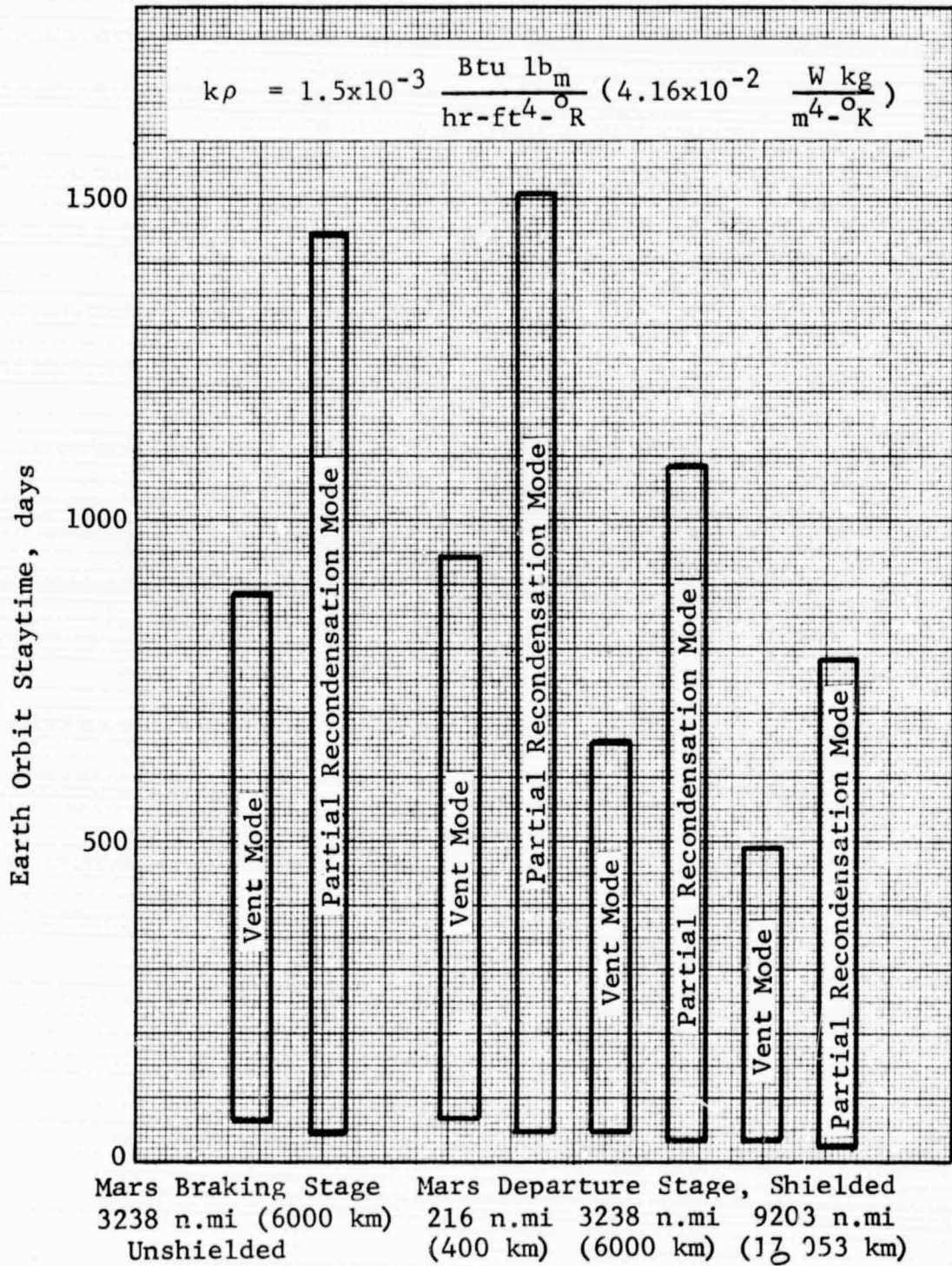


Figure 5.1-6 Effect of Tanking on Earth Orbit Staytime

GENERAL DYNAMICS
Fort Worth Division

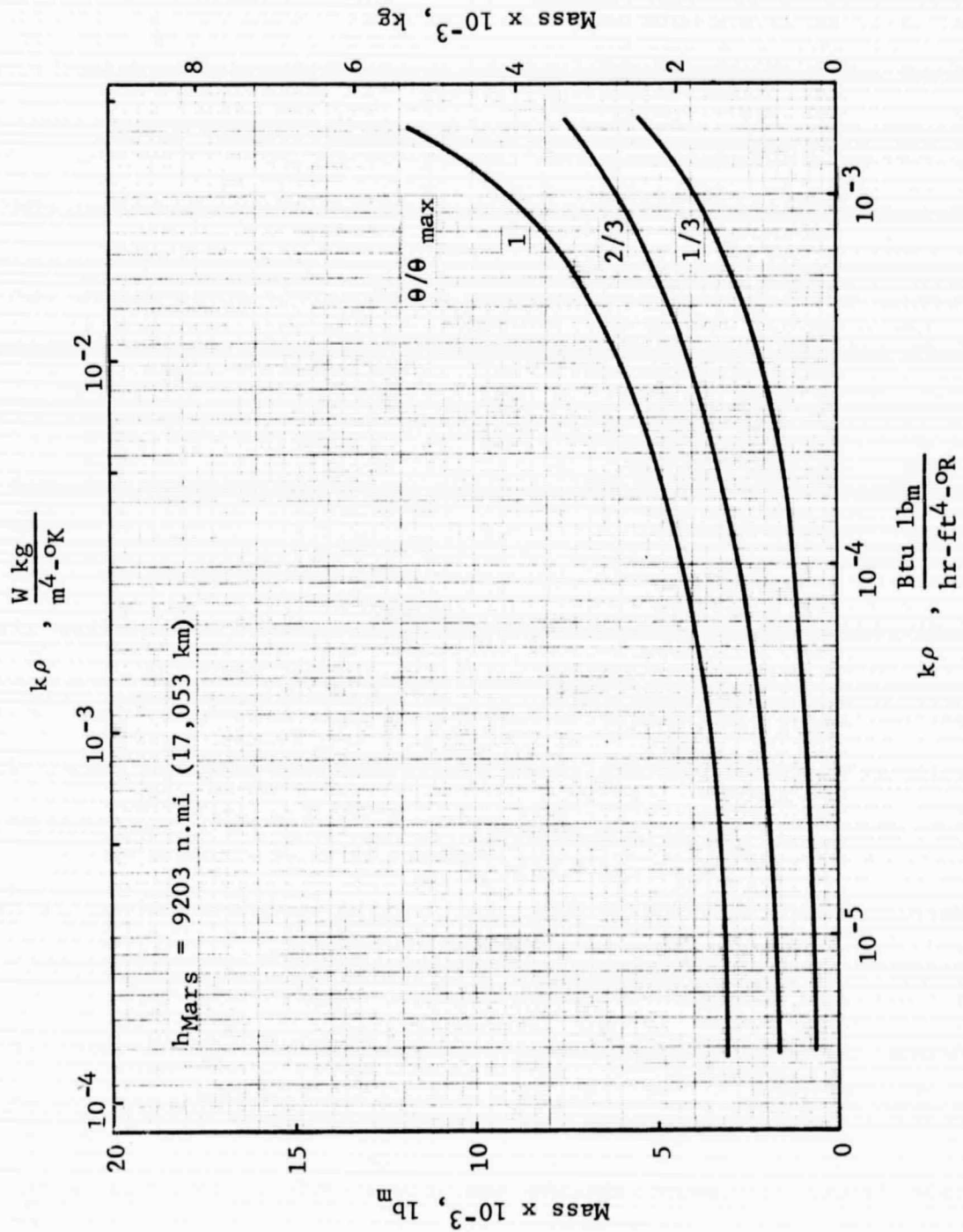


Figure 5.1-7 Vent System Allowable Mass: Shielded Mars
Departure Stage

GENERAL DYNAMICS
Fort Worth Division

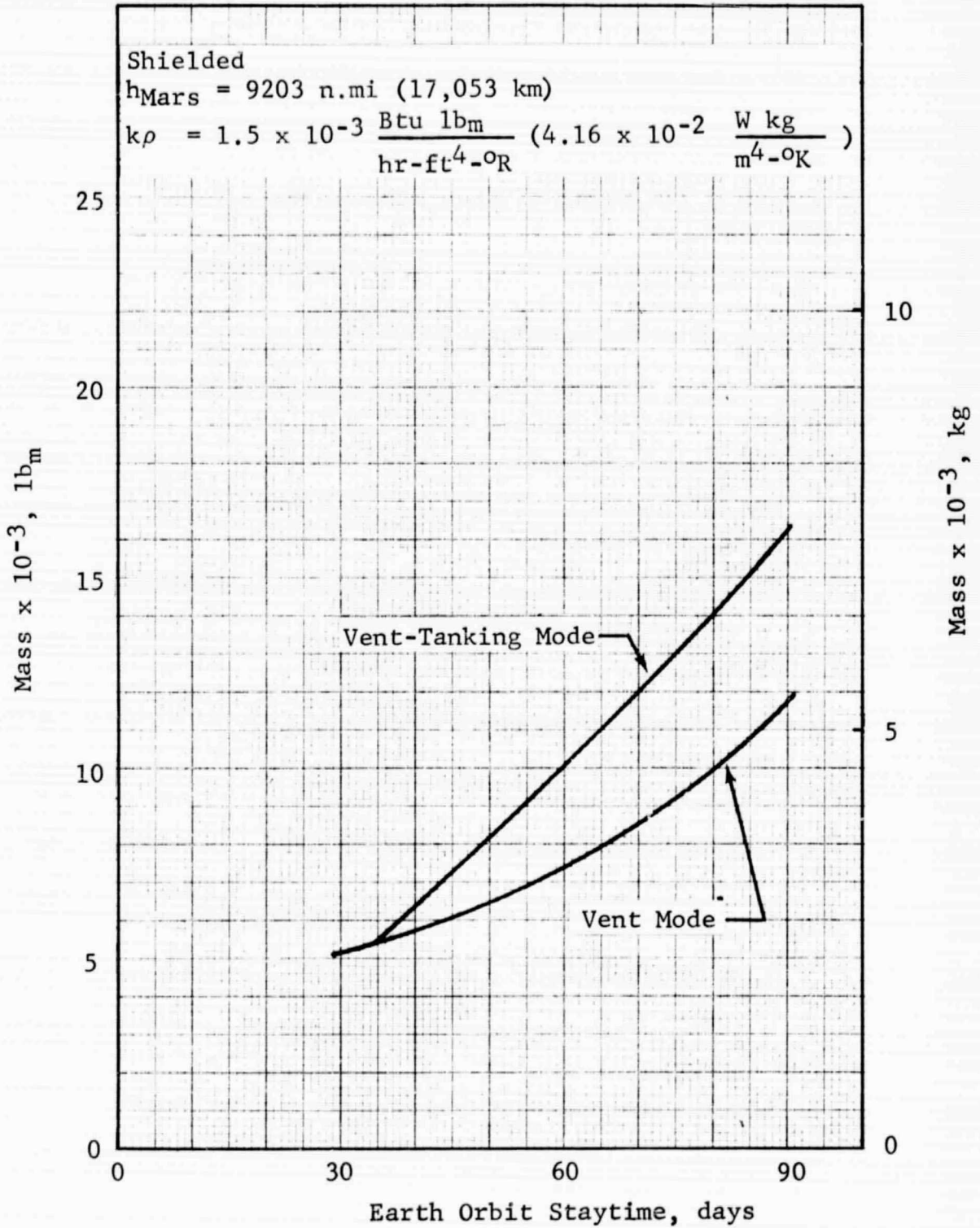


Figure 5.1-8 Vent System Allowable Mass With and Without Tanking: Mars Departure Stage

GENERAL DYNAMICS

Fort Worth Division

5.2 PARTIAL-RECONDENSATION SYSTEM

Performance criteria for the partial-recondensation thermal management system are presented in this subsection in terms of the system allowable mass, on a per-tank basis. A second measure of the system performance, the allowable mass per unit heat load or allowable specific mass, is also presented. The heat load used in the computations is the average value, averaged over the mission phases. Since the allowable masses of both the vent system and the partial-recondensation system are referenced to the nonvent system, it is natural to inquire as to the magnitude of the difference between these systems, and a limited comparison is included. For other conditions, the data on partial-recondensation systems in this section can be compared directly to the vent system data of the previous subsection.

5.2.1 Earth Departure Stage

Allowable mass of a partial-recondensation system for the Earth Departure Stage is shown in Figure 5.2-1 for the 3238-n.mi Mars orbit altitude. The solid line represents the low-performance-insulation condition, with the allowable mass ranging from 3600 lb_m (1630 kg) to 27,900 lb_m (12,650 kg) as the staytime increases from 90 to 270 days. The allowable mass is a result mainly of savings in insulation mass and in tank mass at the longer staytimes. Only a single point could be plotted for the intermediate $k\rho$ value, at the maximum Earth orbit staytime. The allowable mass at that condition is 2030 lb_m (920 kg), which differs from the low-performance insulation value at the same staytime by a factor of 18. Again the allowable mass is mainly from savings in insulation mass. For the shorter staytimes at the intermediate $k\rho$ value and all staytimes at the low $k\rho$ value, the vent pressure is not reached during the mission and the system remains in the non-vent mode. Allowable mass data at the other altitudes are similar to that of Figure 5.2-1 and are not presented here.

The allowable specific mass or allowable mass per unit heat load is presented in Figure 5.2-2 for the same conditions as in Figure 5.2-1. The value increases strongly as the staytime increases, from less than 1 lb_m/Btu/hr to 10.7 lb_m/Btu/hr (1.5 to 16.6 kg/W). For the single data point at the intermediate $k\rho$ value, the allowable specific mass is 2.1 lb_m/Btu/hr

GENERAL DYNAMICS
Fort Worth Division

(3.3 kg/W). The heat loads upon which the allowable specific masses are based are presented in Table 5.2-1. Note that the heating rate decreases as the staytime increases due to the larger insulation thickness. This implies a smaller system, although the total power requirement will increase with staytime. Because the heating history of the stage is limited to Earth orbit, the heat load will be fairly constant. This restricts the operating range of the system and eases the problem of establishing the system design point.

Actual savings in the IMIEO attributable to the partial recondensation system can be estimated by multiplying the allowable mass less the system mass by 1.90. For example at the high- $k\rho$ -value, maximum-staytime condition, the allowable mass is 27,900 lb_m (12,650 kg). Assuming a partial recondensation system mass of 100 lb_m (45 kg), the estimated savings in the IMIEO is 52,820 lb_m (23,950 kg), on a per tank basis, for a total IMIEO reduction of 211,300 lb_m (95,800 kg).

5.2.2 Mars Braking Stage

Partial-recondensation-system allowable-mass data for the unshielded Mars Braking Stage are shown in Figure 5.2-3 for the 216-n.mi (400 km) Mars orbit altitude. Values vary widely, ranging from 600 to 29,900 lb_m (270 to 13,570 kg) and increasing as the $k\rho$ value and the Earth orbit staytime increase. A value for the minimum staytime at the low $k\rho$ value could not be defined because the vent pressure is not reached for that condition. Note that staytime has more influence on allowable mass with higher performance insulation. At the higher $k\rho$ values, the curves are tending to merge. The allowable mass results from savings in both insulation and tank mass in the partial-recondensation mode as compared to the nonvent mode.

An estimate of the savings in the IMIEO for a given partial recondensation system mass can be computed using a factor of 3.22 to relate the IMIEO to system mass. For example, at the intermediate $k\rho$ value and maximum staytime, the allowable mass is 5940 lb_m (2690 kg). Assuming a partial-recondensation-system mass of 100 lb_m (45 kg), the total reduction in the IMIEO is 37,610 lb_m (17,060 kg).

Corresponding allowable-specific-mass data are shown in Figure 5.2-4, based on the average heat load during Earth orbit

GENERAL DYNAMICS
Fort Worth Division

Table 5.2-1 HEAT LOADS: PARTIAL RECONDENSATION MODE

Stage	$\frac{\text{Btu lb}_m}{\text{hr-ft}^2-\text{o}_R}$ $k\rho, \left(\frac{\text{W kg}}{\text{m}^2-\text{o}_K} \right)$	Heat Load at Indicated $\theta/\theta_{\text{Max}}$		
		Btu/hr (W)		
		1/3	2/3	1
Earth Departure (3238 n.mi)	1.5×10^{-3} (4.16×10^{-2})	3780 (1108)	2940 (862)	2600 (762)
	7.5×10^{-5} (2.08×10^{-3})	--	--	975 (286)
Mars Braking (Unshielded, 216 n.mi)	1.5×10^{-3} (4.16×10^{-2})	1180 (346)	1330 (390)	1380 (404)
	7.5×10^{-5} (2.08×10^{-3})	446 (131)	441 (129)	479 (140)
	5.0×10^{-6} (1.39×10^{-4})	--	312 (91)	316 (93)
Mars Braking (Shielded, 216 n.mi)	1.5×10^{-3} (4.16×10^{-2})	3650 (1070)	2790 (818)	2430 (712)
	7.5×10^{-5} (2.08×10^{-3})	--	--	882 (259)
Mars Departure (Shielded, 9203 n.mi)	1.5×10^{-3} (4.16×10^{-2})	298 (87)	352 (103)	397 (116)
	7.5×10^{-5} (2.08×10^{-3})	156 (46)	153 (45)	172 (50)
	5.0×10^{-6} (1.39×10^{-4})	128 (38)	127 (37)	126 (37)

GENERAL DYNAMICS
Fort Worth Division

and Mars transfer. The average heat loads are tabulated in Table 5.2-1. Note that the average heat load in this case generally increases with increased Earth orbit staytime at the high $k\rho$ value and is relatively constant at the other $k\rho$ values. The rise is due to increased Earth orbit boiloff at the longer staytimes. At the other $k\rho$ values, there is little, if any, boiloff during Earth orbit and the insulation thickness variation with staytime is small. The design problems associated with a varying heat load exist for only a small number of conditions. In the majority of cases, the vent pressure is not reached during Earth orbit, which is the most severe thermal environment. Venting of propellant begins during the Mars transfer mission phase, where the heat load variation is much less than the difference between the Earth orbit heat load and the average during the Mars transfer phase. This not only reduces the design problem but results in a smaller system.

The effect of Mars orbit altitude on the partial-recondensation-system allowable mass for the unshielded Braking Stage is shown in Figure 5.2-5 for the intermediate $k\rho$ value only. The general downtrend in allowable mass with increasing altitude is the result of larger propellant loadings. In the partial-recondensation mode, the larger propellant loading leads to a longer nonvent period and reduced boiloff. In the nonvent mode, the larger propellant mass yields a lower final pressure so that the tank mass does not increase proportionately to propellant loading. Both effects tend to reduce the allowable mass of the partial-recondensation system. At the high $k\rho$ value, the variation of allowable mass with altitude is minimal.

Partial-recondensation-system allowable mass for the shielded Braking Stage is presented in Figure 5.2-6. The solar shield reduces the propellant heat transfer during the Mars transfer mission phase to a negligible value as compared to that during Earth orbit. As a result, the allowable-mass data in Figure 5.2-6 is similar to that of the Earth Departure Stage (Figure 5.2-1). At the high $k\rho$ value, the partial-recondensation mode yields mass savings at all values of staytime, with the allowable mass ranging from 2000 lb_m (907 kg) to 16,040 lb_m (7,270 kg). At the intermediate $k\rho$ value, only the maximum staytime produces a pressure in excess of the vent pressure, and the allowable mass at that condition is 590 lb_m (270 kg).

GENERAL DYNAMICS
Fort Worth Division

To relate the IMIEO to system mass, a factor of 3.19 can be used for the range of conditions shown in Figure 5.2-6. The corresponding allowable specific mass is shown in Figure 5.2-7 based on the heat loads tabulated in Table 5.2-1. Note again the similarity to the Earth Departure Stage, with the heating rate decreasing as the staytime increases because of a larger optimum insulation thickness at the longer staytimes. Since the boiloff occurs for the most part during Earth orbit, the rate is constant with time.

As in the vent mode, tanking of the propellant boiled off from the Mars Braking Stage during Earth orbit is considered only for the unshielded stage. For the shielded stage, the optimum insulation thickness would be near zero because of the low propellant heat transfer during the transfer phase. The result would be dry tanks since the initial propellant loading would be boiled off early in Earth orbit. The system allowable mass for the partial-recondensation-tanking mode is compared to that for the normal partial-recondensation mode in Figure 5.2-8. Note that tanking is beneficial at all staytimes and that the difference in allowable mass increases as the staytime increases. At the minimum, 60-day staytime, the allowable mass for the tanking variation is 14,800 lb_m (6710 kg), 8% greater than the value for the normal partial-recondensation mode. The allowable mass at the 180-day staytime is 40,400 lb_m (18,320 kg), an increase of 28% over the normal mode value.

Note that tanking generally yields less mass savings in the partial-recondensation mode than in the vent mode. However, it does increase the permissible staytime relative to the vent-tanking mode, as shown in Figure 5.1-6. For the unshielded Mars Braking Stage, the maximum staytime is increased to over 1400 days, which is well beyond the range considered in this study.

5.2.3 Mars Departure Stage

Partial-recondensation-system allowable mass for the shielded Mars Departure Stage is presented in Figure 5.2-9 for the 9203-n.mi Mars orbit altitude. When compared to the allowable-mass data presented earlier for the other stages, it will be noted that the variation with insulation performance is much less. This is the result of the long mission

GENERAL DYNAMICS
Fort Worth Division

time of the Mars Departure Stage and the solar shield's effectiveness in reducing the incident radiation. Both factors tend to increase the percentage of the total heat transfer attributable to penetrations, which is independent of insulation performance. Values of the allowable mass range from 2480 lb_m (1125 kg) to 21,730 lb_m (9850 kg) and increase with increasing $k\rho$ value and staytime. As noted earlier, the Earth orbit staytime has more influence on the allowable mass at the higher insulation performance. Allowable-mass data for the lower altitudes and for the unshielded stage could not be defined because the corresponding nonvent mode results were not obtained.

To evaluate the reduction in the IMIEO for a particular system mass, the IMIEO is related to system mass by a factor of 4.50. As an illustration, assume a 100-lb_m (45 kg) partial recondensation system at the maximum staytime and intermediate $k\rho$ value. The system allowable mass for that condition is 9052 lb_m (4100 kg) and the corresponding reduction in the IMIEO amounts to 40,280 lb_m (18,270 kg).

Allowable-specific-mass data for the same conditions as in Figure 5.2-9 are presented in Figure 5.2-10. It will be noted that the specific-mass values are much higher than for the lower stages of the vehicle. In addition, there is less variation with insulation performance, especially at the longer staytimes. The heat loads are presented separately in Table 5.2-1. The heat load increases with staytime at the high $k\rho$ value, reflecting an increasing percentage of boiloff in Earth orbit. This same trend also occurs between θ/θ_{\max} values of 2/3 and 1 at the intermediate $k\rho$ value.

Since the nonvent mode was analyzed only at the 9203-n.mi (17,053 km) altitude, system allowable masses as defined in this study could be computed only at that altitude. However, it is of interest to examine the differences between the vent and the partial-recondensation modes at all altitudes. This can be accomplished on the same basis as system allowable mass by computing the difference in the IMIEO between the two modes and applying an appropriate factor to reduce the IMIEO value to system mass units. This factor varies to some extent with all of the basic parameters and between the storage modes. However, for purposes of comparison, the variation can be neglected and the values for the partial-recondensation mode will be applied. The resultant mass value is an

GENERAL DYNAMICS

Fort Worth Division

estimate of the difference in allowable masses between the vent and the partial-recondensation modes. If a certain fraction of the hardware components for the two modes are identical, this allowable mass difference applies to the remaining nonsimilar items. Otherwise, it can be compared to total system mass differences between vent and partial-recondensation systems.

The difference in allowable masses for the shielded and unshielded Mars Departure Stages is presented in Figures 5.2-11 and 5.2-12, respectively. In both cases, the difference decreases as the altitude increases, but the rate of decrease is higher in the shielded case. The smaller allowable mass difference at higher altitudes is indicative of a less-severe thermal environment (especially in the shielded case), thereby reducing the necessity for the higher-effectiveness partial-recondensation system. With low-performance insulation, the difference in allowable mass decreases from 24,200 lb_m (10,980 kg) to 9400 lb_m (4260 kg) in the shielded case. As the insulation performance improves, the mass difference drops; at the lowest $k\rho$ value, the range is 9800 lb_m (4440 kg) to 2630 lb_m (1190 kg). For the unshielded stage, the allowable mass differences are generally higher (Fig. 5.2-12) because of the larger total heat transfer. At the highest altitude, the curves are fairly flat at all $k\rho$ values, indicating that the planetary-emitted and albedo radiation have been reduced to the point where they have a negligible influence on the total heat transfer.

Tanking for the Mars Departure Stage in the partial-recondensation mode is advantageous only for the shielded stage. In the unshielded case, the vent pressure is not reached during Earth orbit for any set of parameters. Also, tanking was found to be advantageous only at the highest $k\rho$ value. Allowable system mass for the partial-recondensation-tanking mode is compared in Figure 5.2-13 to that for the normal partial-recondensation mode. It is seen that tanking offers only a small savings in mass, which is to be expected since the staytime is small and the Earth orbit heat transfer is a small part of the total. At the 30-day staytime, the difference in allowable mass is only 163 lb_m (74 kg). At the maximum 90-day staytime, the difference is 3580 lb_m (1620 kg).

GENERAL DYNAMICS
Fort Worth Division

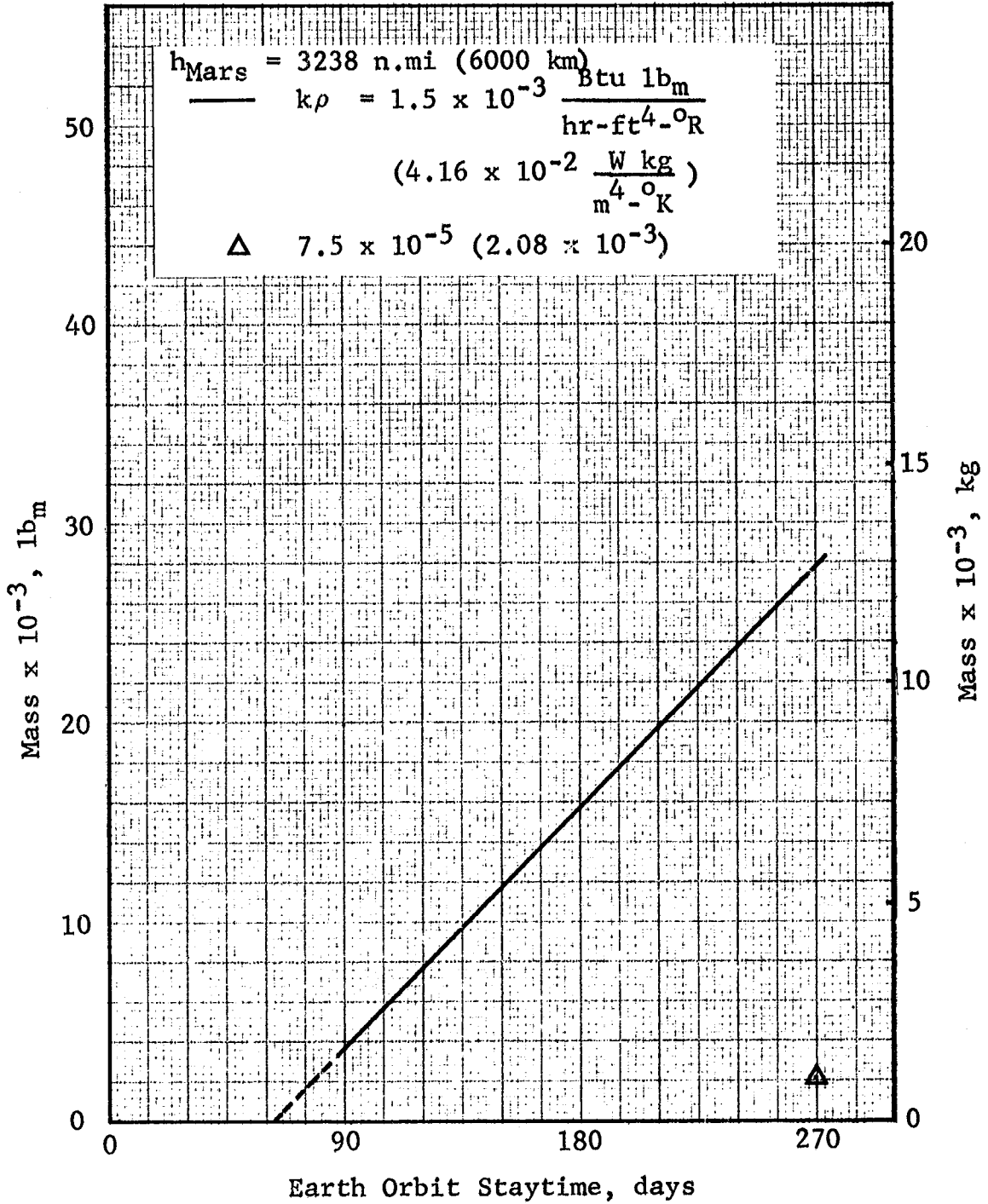


Figure 5.2-1 Partial Recondensation System
Allowable Mass; Earth Departure
Stage

GENERAL DYNAMICS
Fort Worth Division

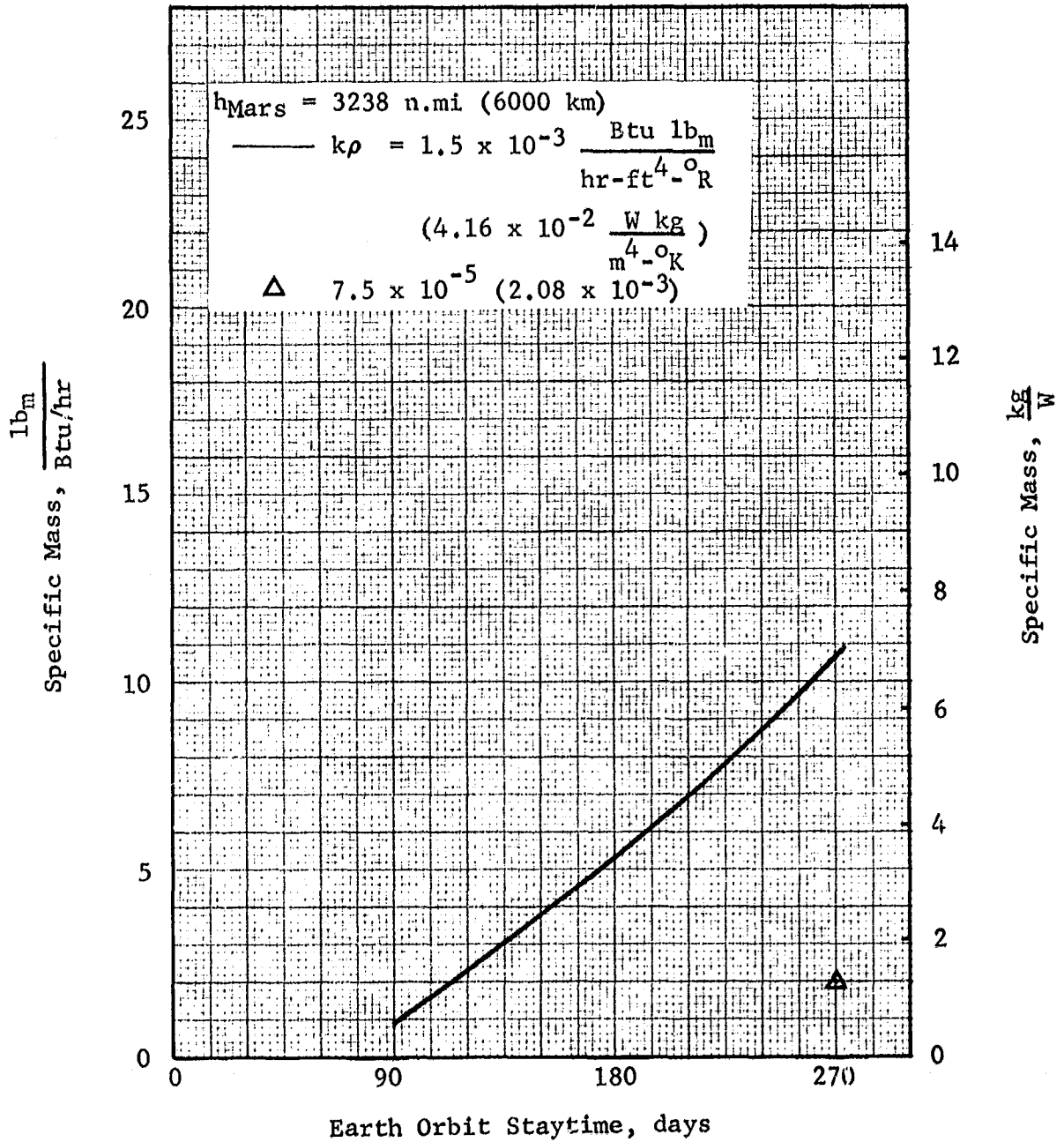


Figure 5.2-2 Partial Recondensation System Allowable Specific Mass: Earth Departure Stage

GENERAL DYNAMICS
Fort Worth Division

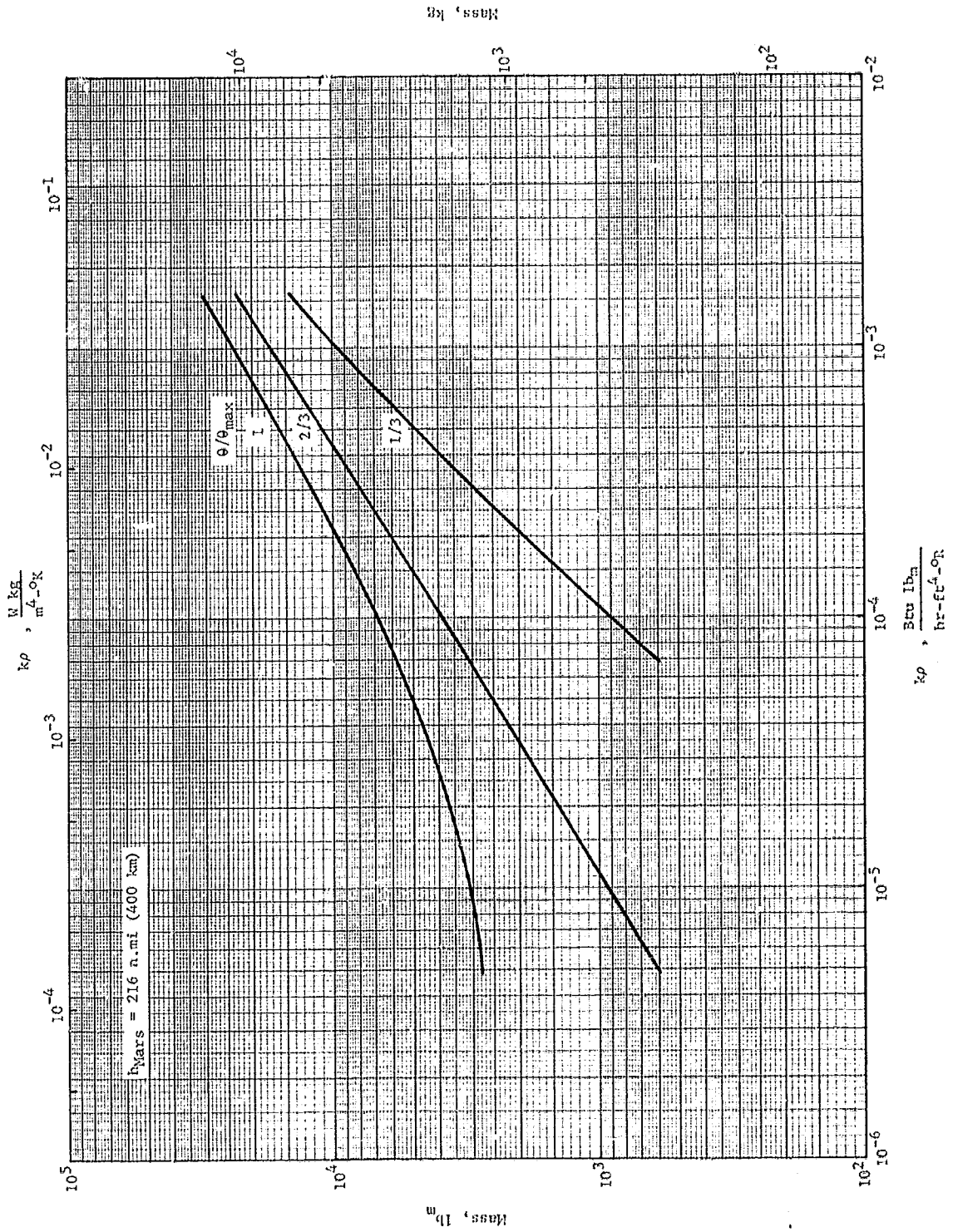


Figure 5.2-3 Partial Recondensation System Allowable Mass: Unshielded Mars Braking Stage

GENERAL DYNAMICS
Fort Worth Division

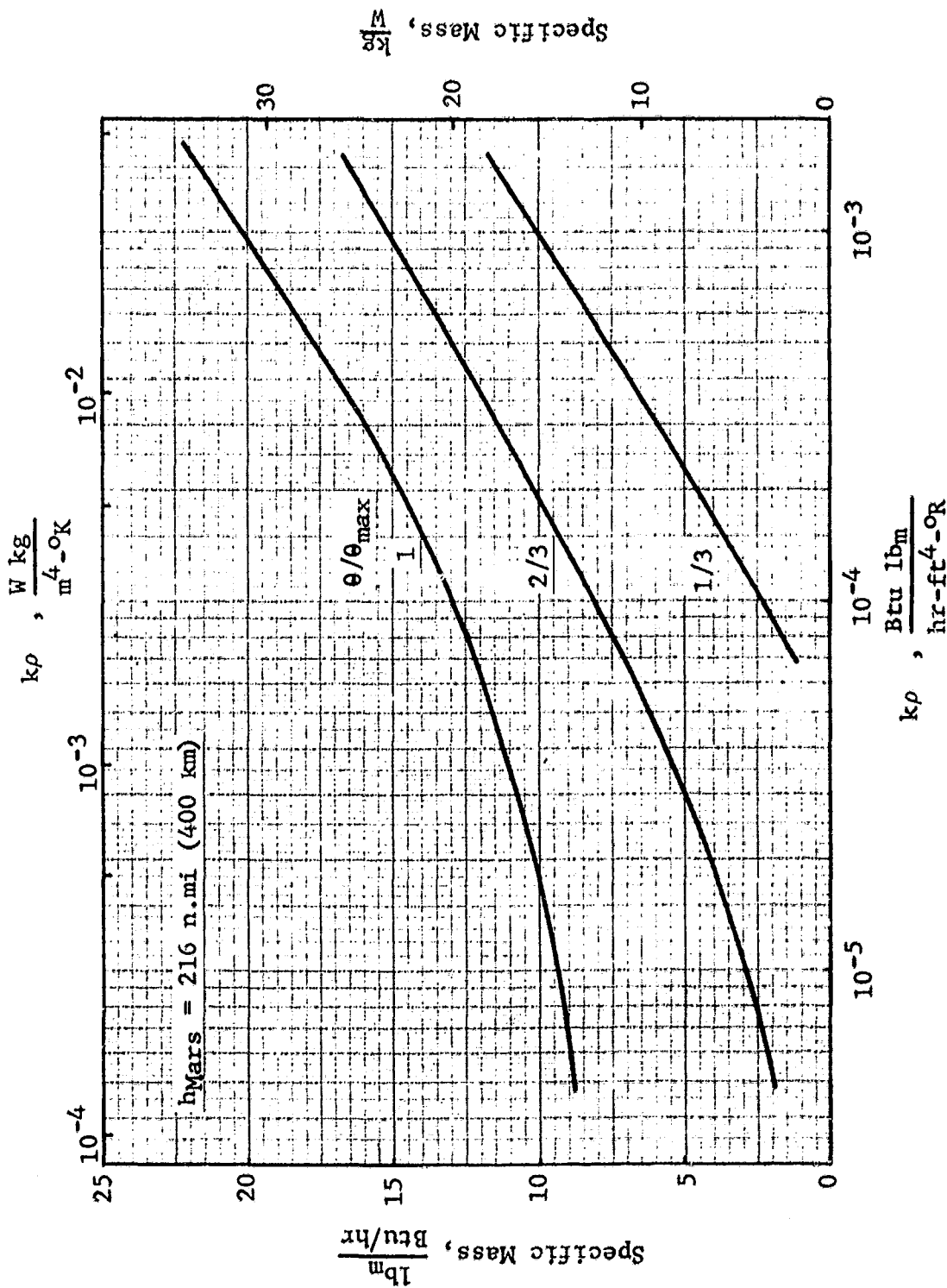


Figure 5.2-4 Partial Recondensation System Allowable Specific Mass:
Unshielded Mars Braking Stage

GENERAL DYNAMICS
Fort Worth Division

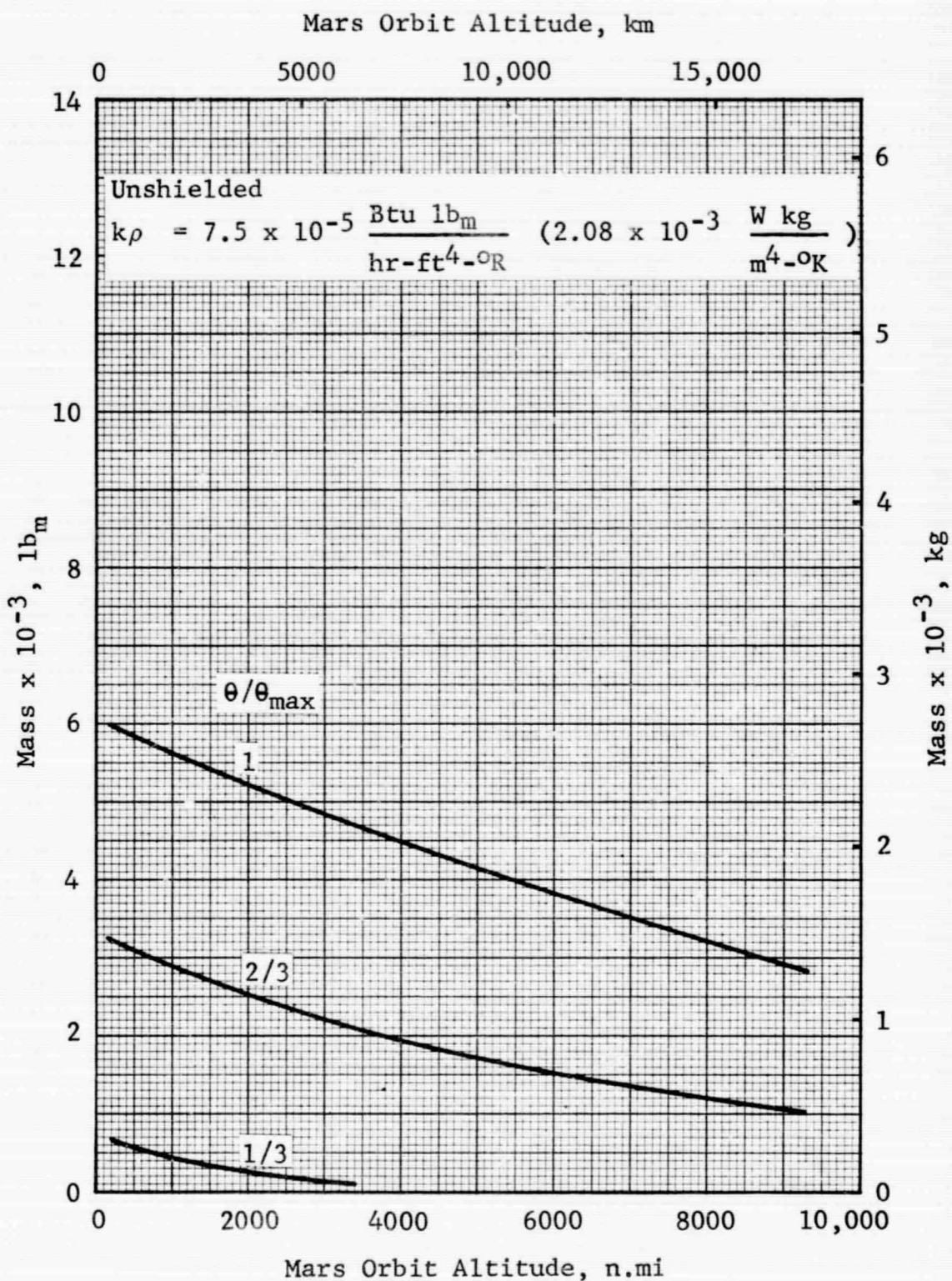


Figure 5.2-5 Effect of Mars Orbit Altitude on Partial Recondensation System Allowable Mass: Mars Braking Stage

GENERAL DYNAMICS
Fort Worth Division

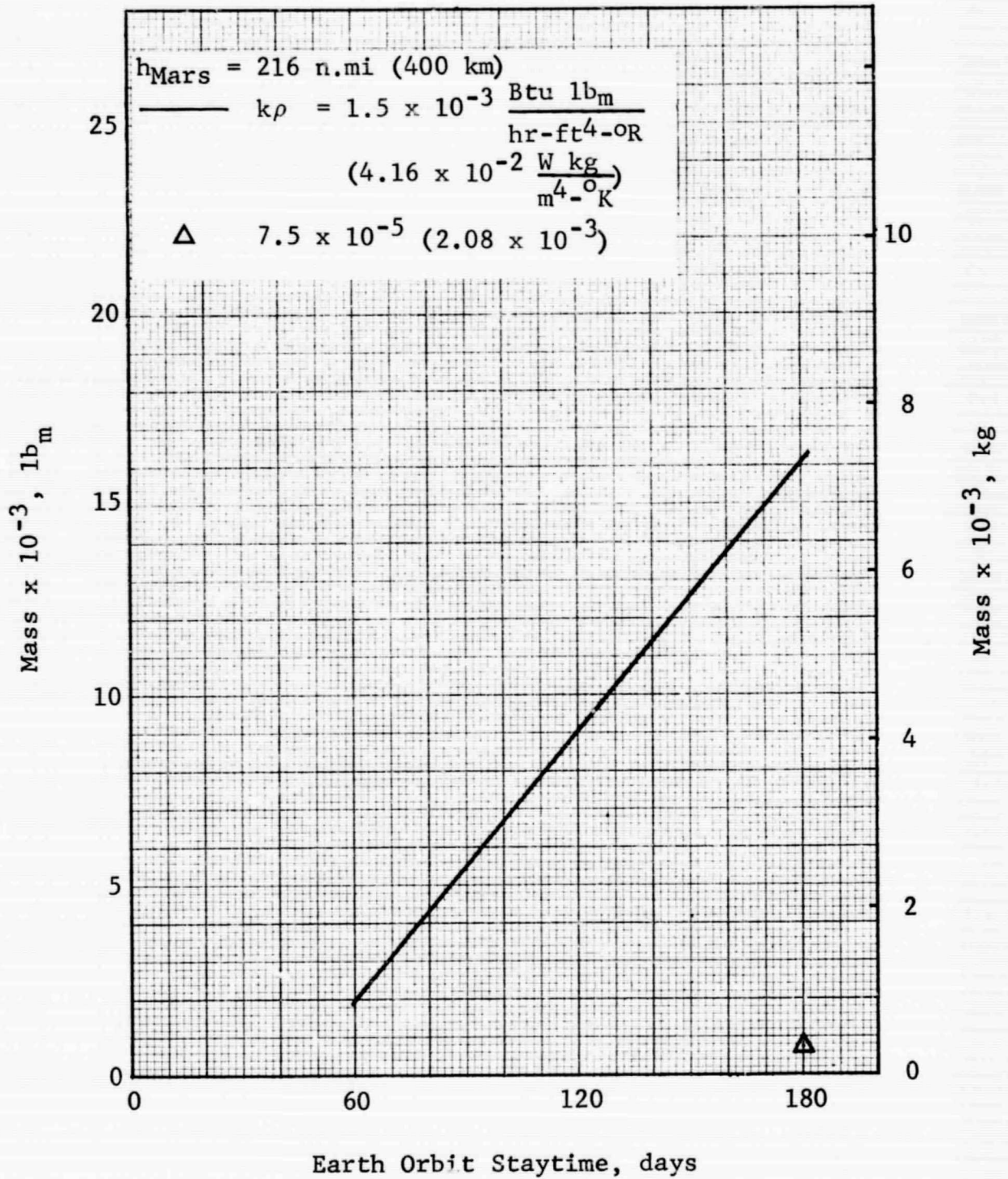


Figure 5.2-6 Partial Recondensation System
Allowable Mass: Shielded Mars
Braking Stage

GENERAL DYNAMICS
Fort Worth Division

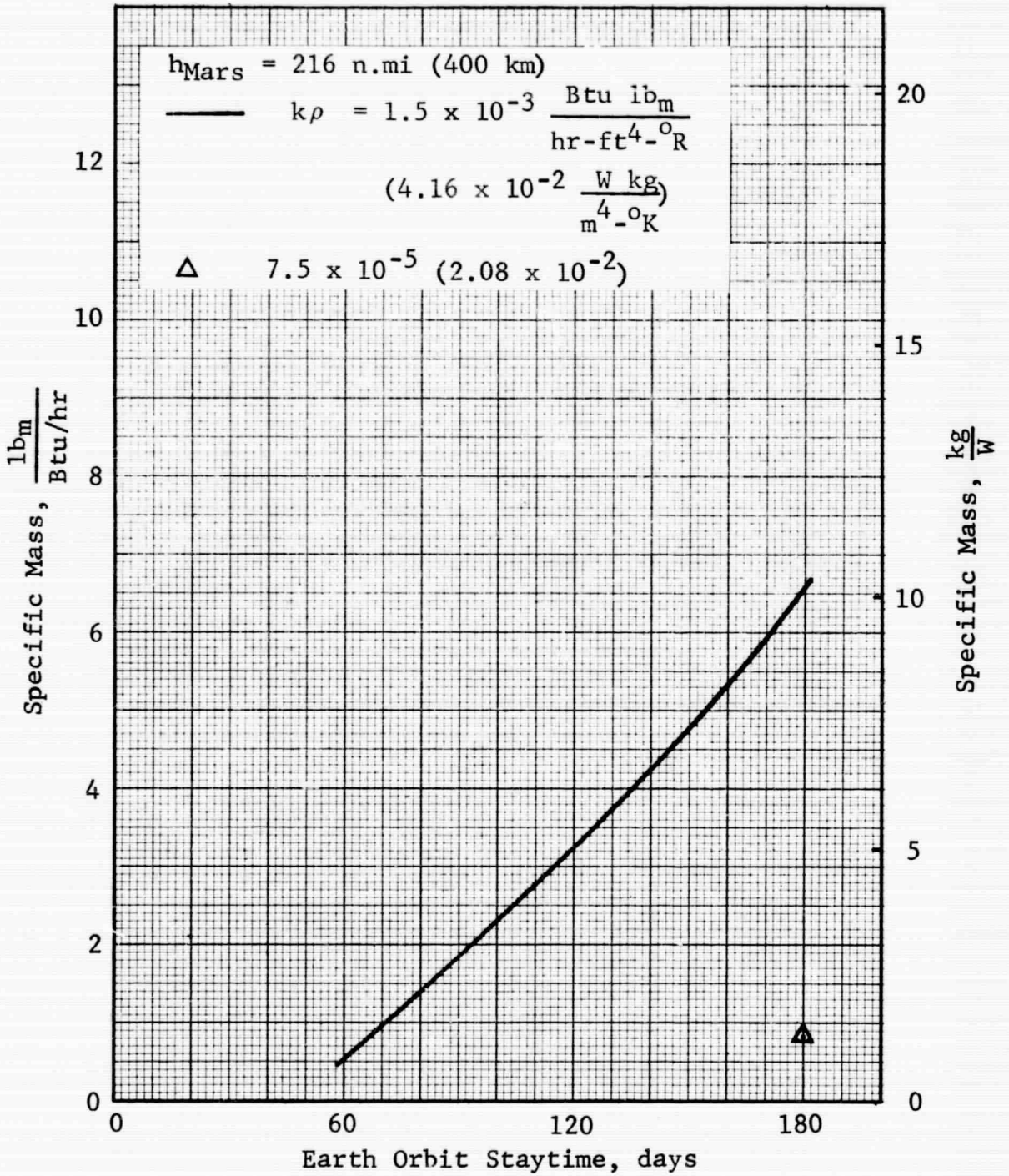


Figure 5.2-7 Partial Recondensation System
Allowable Specific Mass:
Shielded Mars Braking Stage

GENERAL DYNAMICS
Fort Worth Division

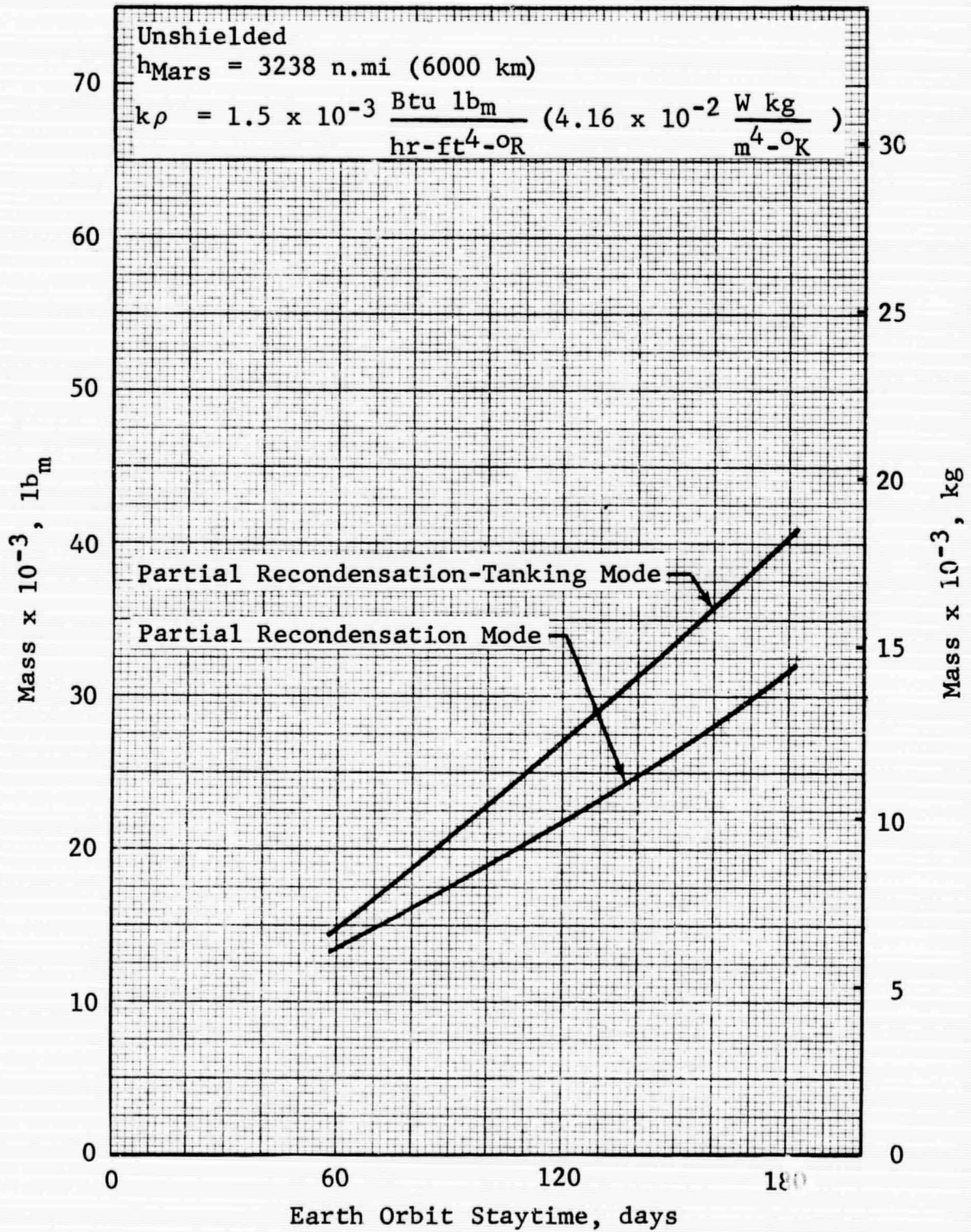


Figure 5.2-8 Effect of Tanking on Allowable Mass of the Partial Recondensation System: Mars Braking Stage

GENERAL DYNAMICS
Fort Worth Division

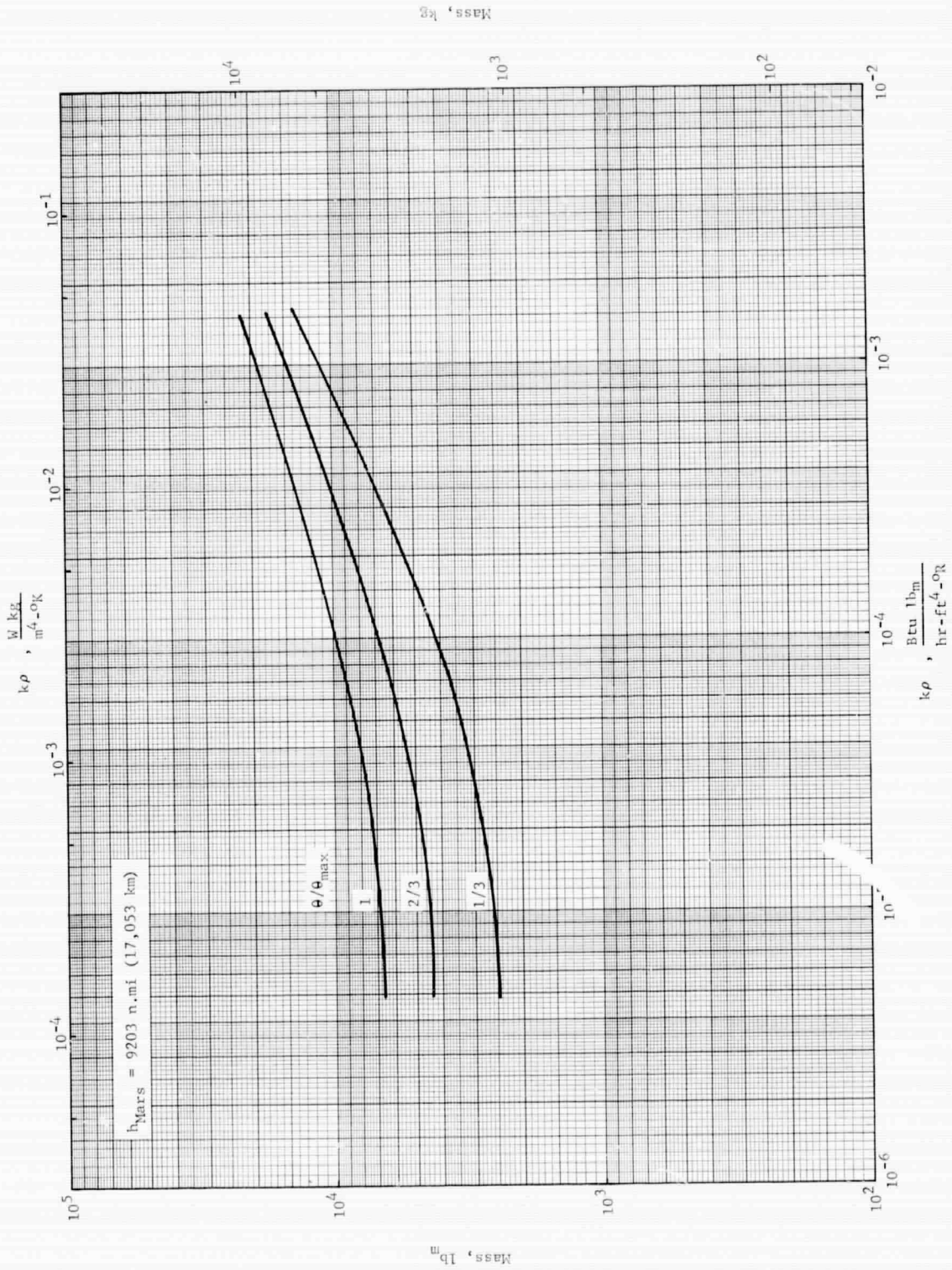


Figure 5.2-9 Partial Reconnaissance System Allowable Mass: Shielded Mars Departure Stage

GENERAL DYNAMICS
Fort Worth Division

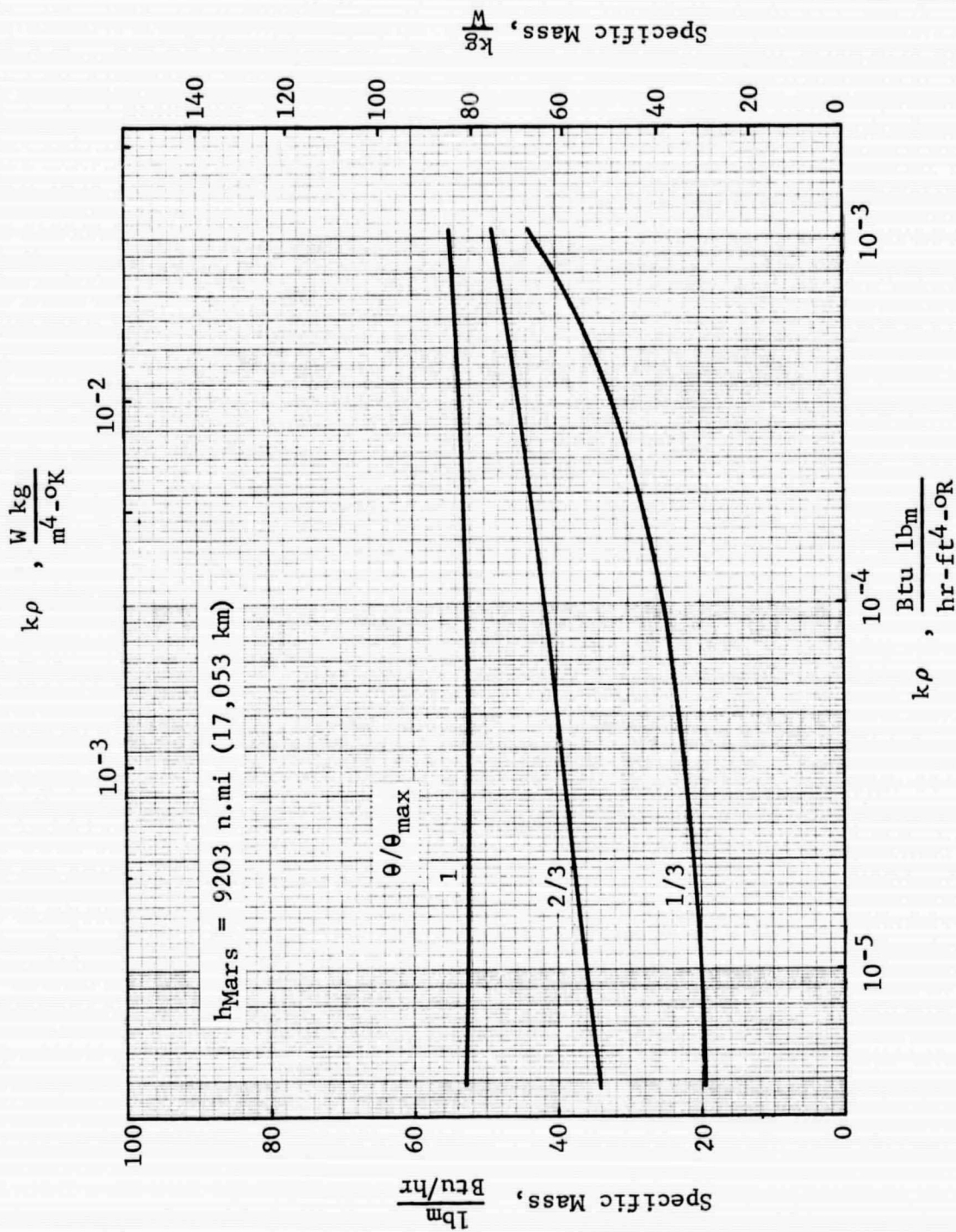


Figure 5.2-10 Partial Recondensation System Allowable Specific Mass: Shielded Mars Departure Stage

GENERAL DYNAMICS
Fort Worth Division

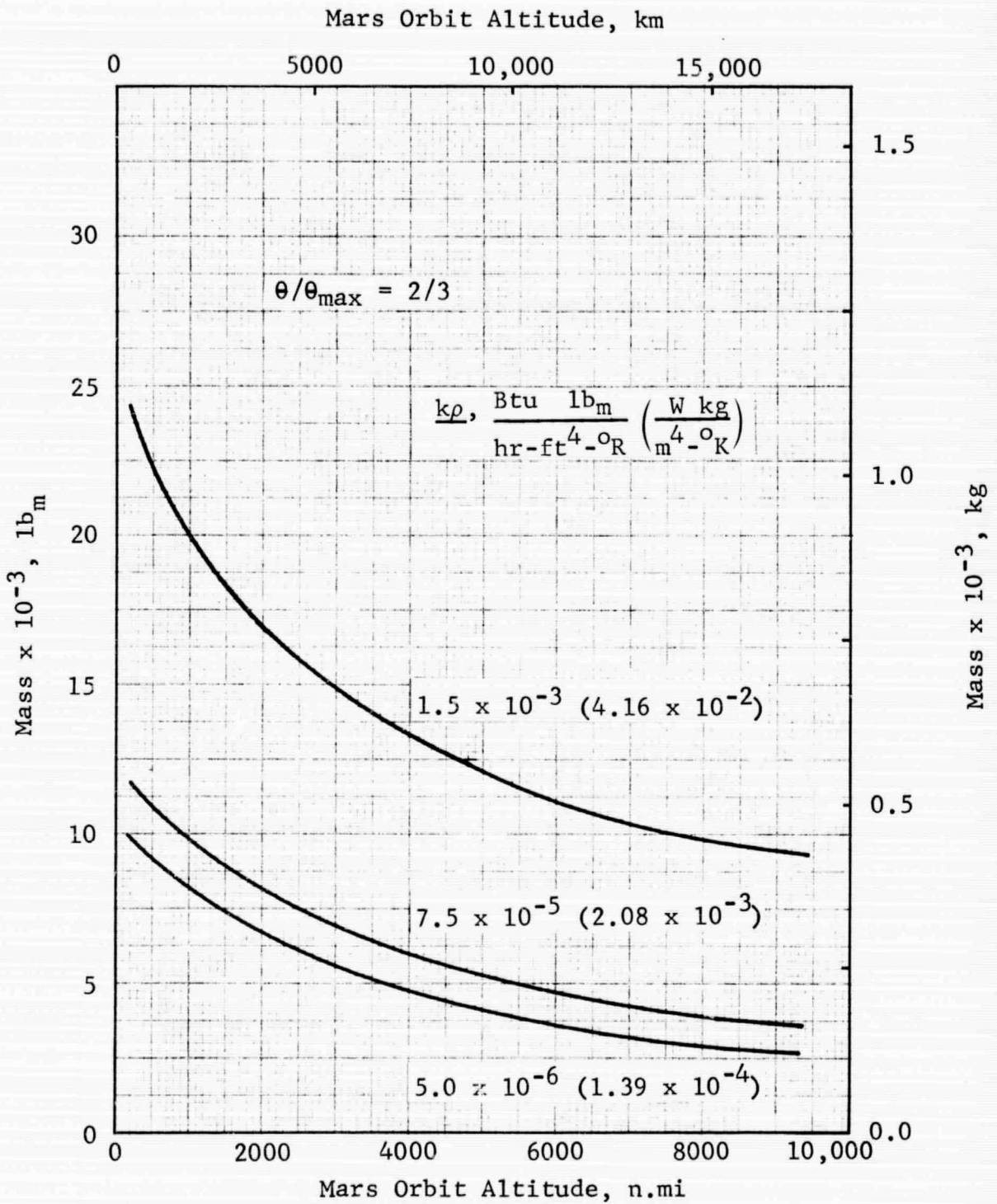


Figure 5.2-11 Partial Recondensation System Allowable Mass Relative to the Vent System: Shielded Mars Departure Stage

GENERAL DYNAMICS
Fort Worth Division

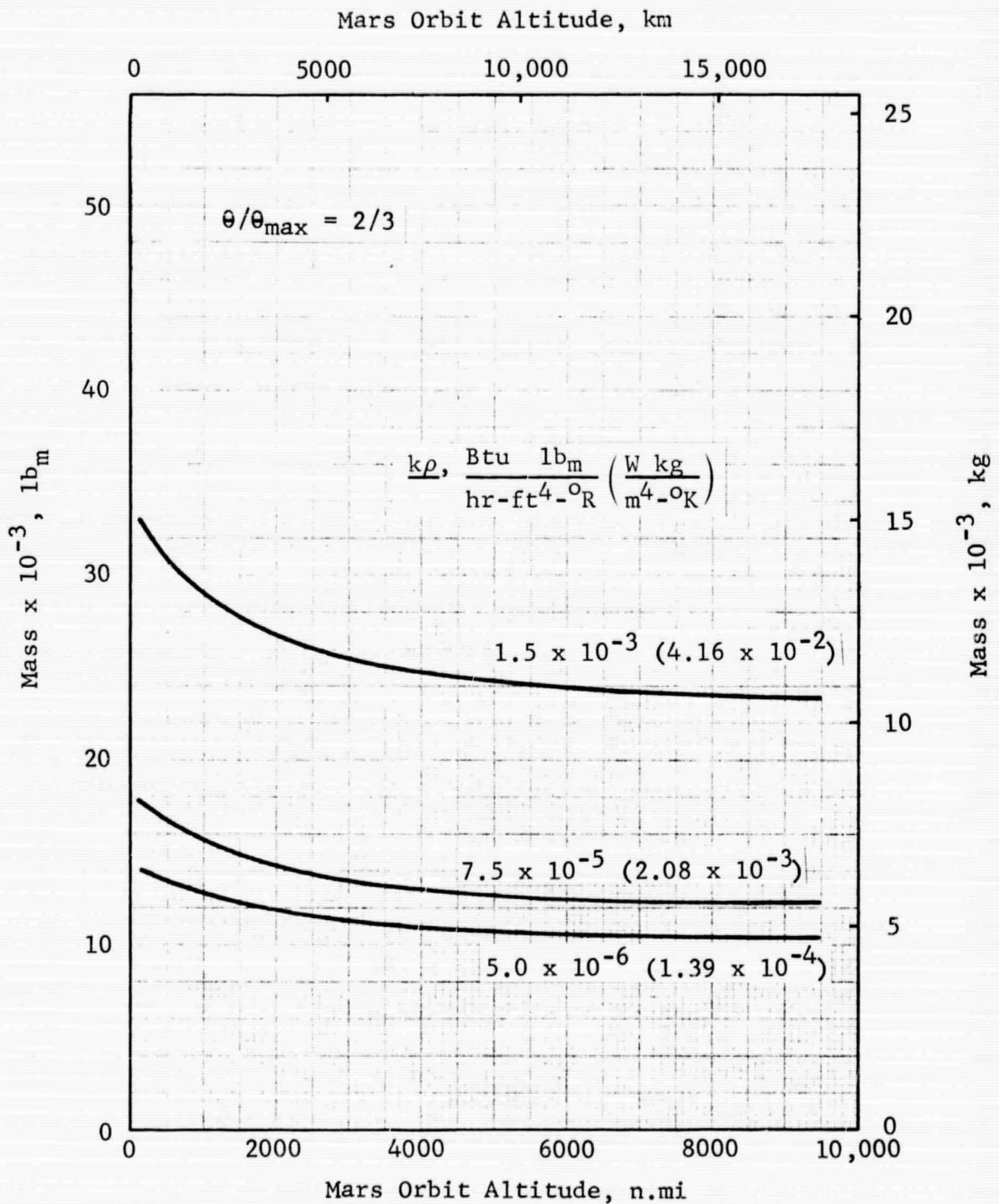


Figure 5.2-12 Partial Recondensation System Allowable Mass Relative to the Vent System: Unshielded Mars Departure Stage

GENERAL DYNAMICS
Fort Worth Division

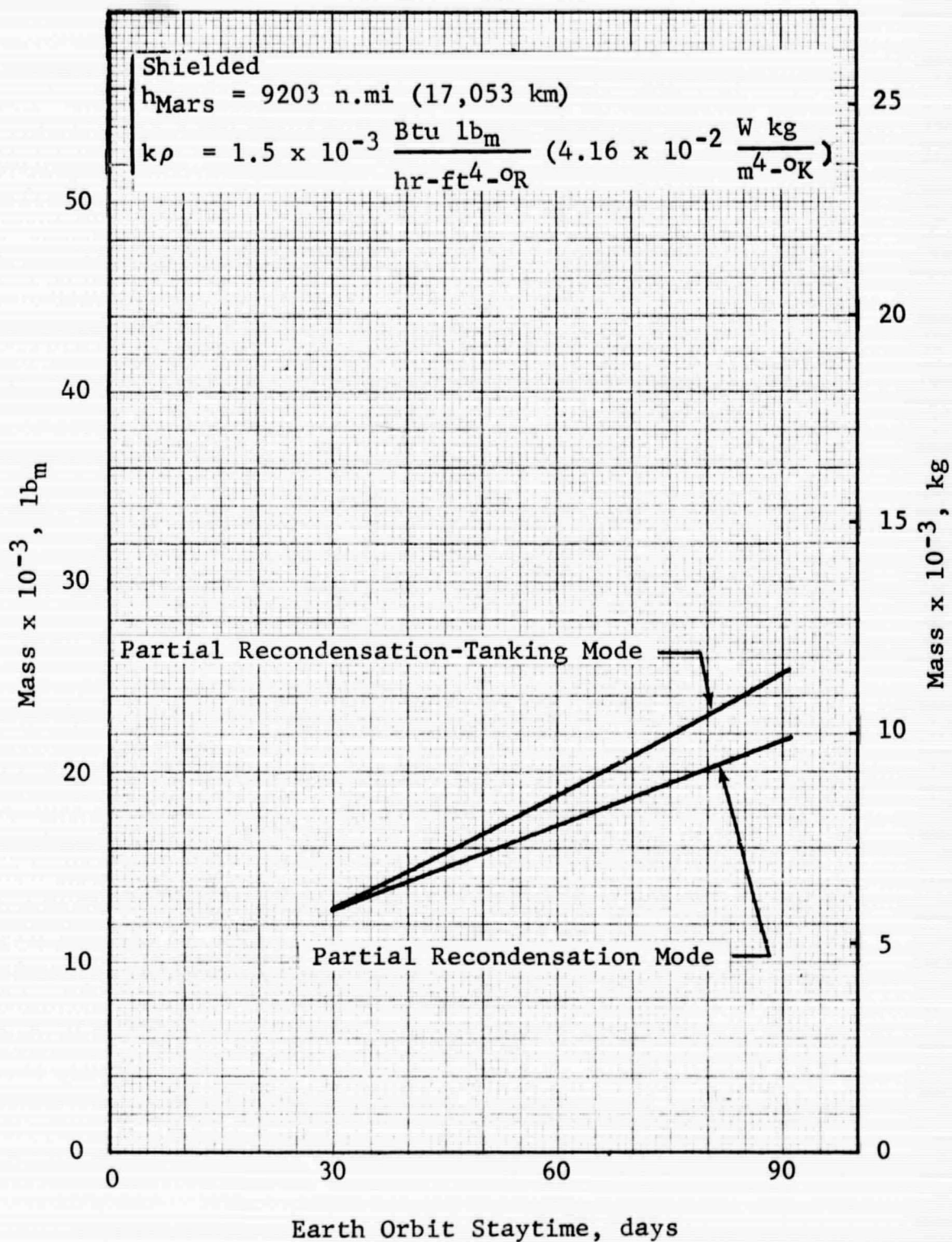


Figure 5.2-13 Effect of Tanking on Allowable Mass of the Partial Recondensation System: Mars Departure Stage

GENERAL DYNAMICS
Fort Worth Division

5.3 COMBINATION SYSTEM

The basic idea behind the combination system is to utilize the tank volume required for propellant expansion during nonvented operation to store excess propellant to be boiled off during the Earth orbit mission phase. The thermal management system required to accomplish the boiloff may be either a vent system or a partial-recondensation system. An advantage with the partial-recondensation system is a longer Earth orbit staytime per pound of excess propellant. Required system components for the combination mode are identical to those for the corresponding basic mode (vent or partial recondensation). However, since the system operating time will generally be much lower than for the basic mode, total power requirements should be reduced. Note that the combination system is not applicable to the Earth Departure Stage since functionally it is similar to the normal vent or partial-recondensation mode. From an optimization standpoint, an optimum insulation thickness is not definable since there is no nonvent-mode period beyond Earth orbit upon which to perform the optimization.

5.3.1 Mars Braking Stage

Figure 5.3-1 presents the system allowable mass for the combination vent-nonvent mode for the unshielded Mars Braking Stage with low-performance insulation. Also shown is a comparison of the IMIEO for the combination and nonvent modes. The latter is included in order to show the range of staytime and the variation of the IMIEO with staytime. Note that the combination mode becomes definable at a staytime of approximately 74 days and that the maximum staytime for the indicated condition is 181 days. This maximum staytime is only one day beyond the range defined in this study, and it corresponds to filling the tank to 95% (by volume) of the total tank volume. In other words, the maximum amount of excess propellant is loaded into the ullage volume. The allowable mass rises rapidly with staytime, reaching a value of 15,600 lb_m (7075 kg) at 180 days. IMIEO for the combination mode rises slightly with staytime, reflecting the excess propellant loading, which is directly additive to the IMIEO. At the staytime of 180 days, the difference in the IMIEO is 110,300 lb_m (50,000 kg) or 4.4% of the IMIEO.

GENERAL DYNAMICS
Fort Worth Division

Similar data for the intermediate $k\rho$ value is presented in Figure 5.3-2. The system allowable mass is an order-of-magnitude lower than in the highest- $k\rho$ -value case, and the combination mode becomes definable at a much later staytime, 136 days. Beyond 180 days, the allowable mass can not be computed since the corresponding nonvent mode results were not obtained. However, the IMIEO can be evaluated since the value at any staytime less than the maximum is the value at 136 days plus the excess propellant mass. Note that while the combination mode does not offer large mass savings at this condition, a significant extension of the staytime can be realized relative to the nonvent mode without incurring a penalty to the IMIEO.

With the highest-performance insulation, the combination mode becomes definable at a staytime of 180 days, which is the maximum considered in this study. The maximum combination-mode staytime for this condition is 276 days, as shown in Figure 5.3-3. Allowable mass data are not presented since the IMIEO for the combination mode will exceed that for the nonvent mode except at the 180-day staytime, where the IMIEO's are equal (neglecting the system mass for the combination mode).

It is possible to further increase the permissible staytime by substituting a partial-recondensation system for the vent system in the combination mode. For the same excess propellant loading, the staytime after boiloff begins is increased 2-1/2 times. The effect on the range of staytimes is presented in Figure 5.3-4. At the lower $k\rho$ values, the staytimes are probably beyond the range of interest, even for the vent-nonvent combination mode.

Results for the combination mode could not be obtained for the shielded Mars Braking Stage. The low propellant heat transfer during Mars transfer results in only a small ullage volume at the beginning of the transfer phase. Therefore, the excess propellant loading would be minimal. In addition, the low heat transfer would result in a small optimum insulation thickness and the excess propellant would be boiled off early in Earth orbit. Thus, the combination mode is not compatible with the shielded Mars Braking Stage.

GENERAL DYNAMICS

Fort Worth Division

5.3.2 Mars Departure Stage

Allowable mass data for the combination vent-nonvent mode is shown for the shielded Mars Departure Stage in Figures 5.3-5, 5.3-6, and 5.3-7 for the high, intermediate, and low $k\rho$ values, respectively. The mass savings in IMIEO are small over the 30- to 90-day staytime interval regardless of insulation performance, but significant extensions of the staytime can be realized with little or no penalty to the IMIEO. With low-performance insulation, the system allowable mass increases with staytime to the maximum definable value of 8163 lb_m (3700 kg) at 90 days. For longer staytimes, the allowable mass would continue to rise; extrapolation of the data of Figure 5.3-5 indicates an allowable mass of the order of 25,500 lb_m (11,600 kg) at the maximum combination-mode staytime of 140 days.

As the insulation performance improves, the mass savings decrease, but the maximum staytime increases, as shown in Figures 5.3-6 and 5.3-7. The staytime range can be extended even further by substituting a partial recondensation system for the vent system. The effect on staytime is shown in Figure 5.3-4. However, as in the Braking Stage case, these staytimes are probably beyond the range of interest.

Combination-mode data for the unshielded Mars Departure Stage are not presented since, as in the nonvent mode, the final pressures are extremely high. The Earth orbit propellant heating is only a small fraction of the total and the combination mode does not offset the large amount of heat transfer during the interplanetary mission phases.

GENERAL DYNAMICS
Fort Worth Division

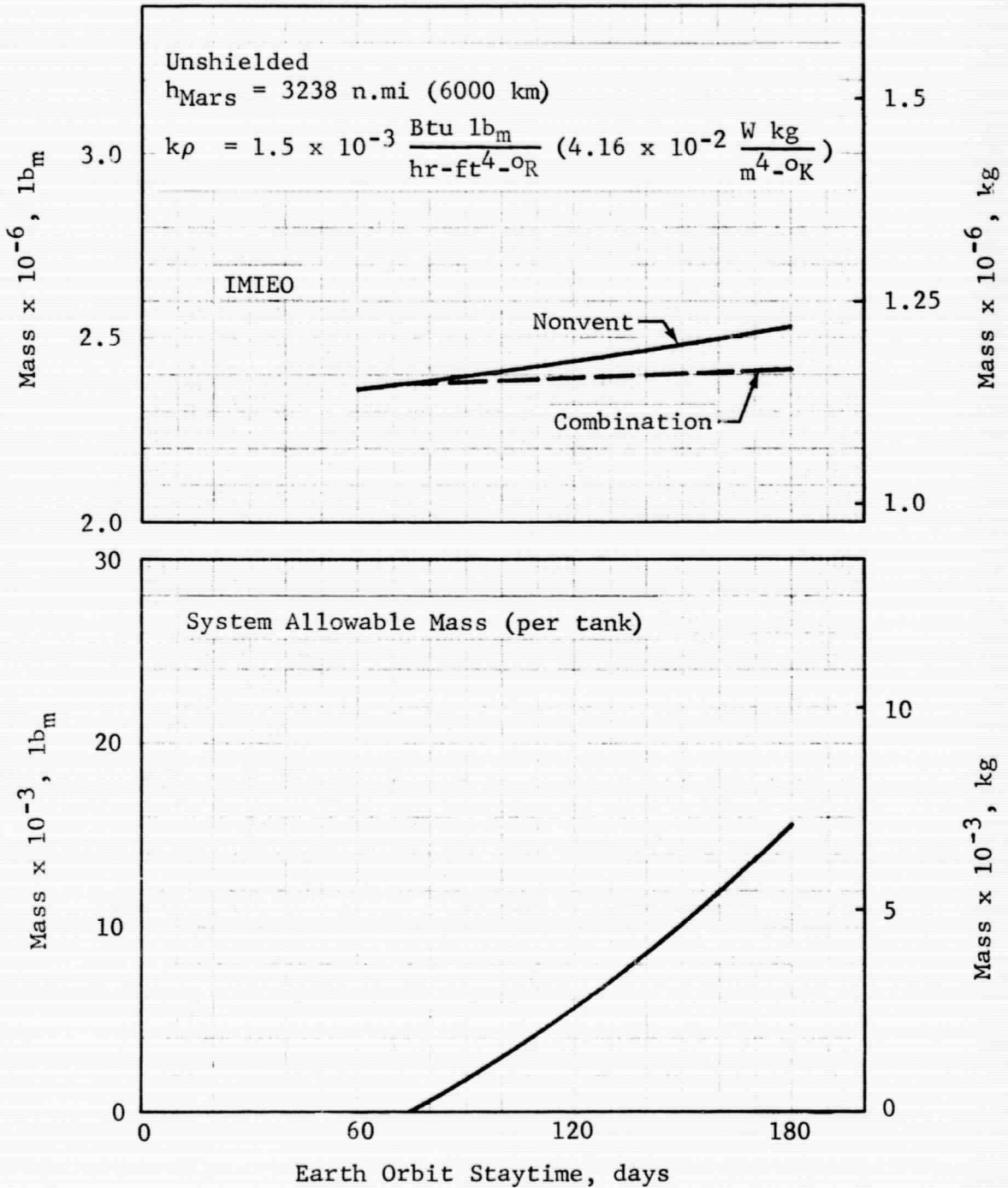


Figure 5.3-1 IMIEO and System Allowable Mass for the Combination Mode: Mars Braking Stage,
 $k\rho = 1.5 \times 10^{-3} \frac{\text{Btu lb}_m}{\text{hr-ft}^4\text{-OR}}$

GENERAL DYNAMICS
Fort Worth Division

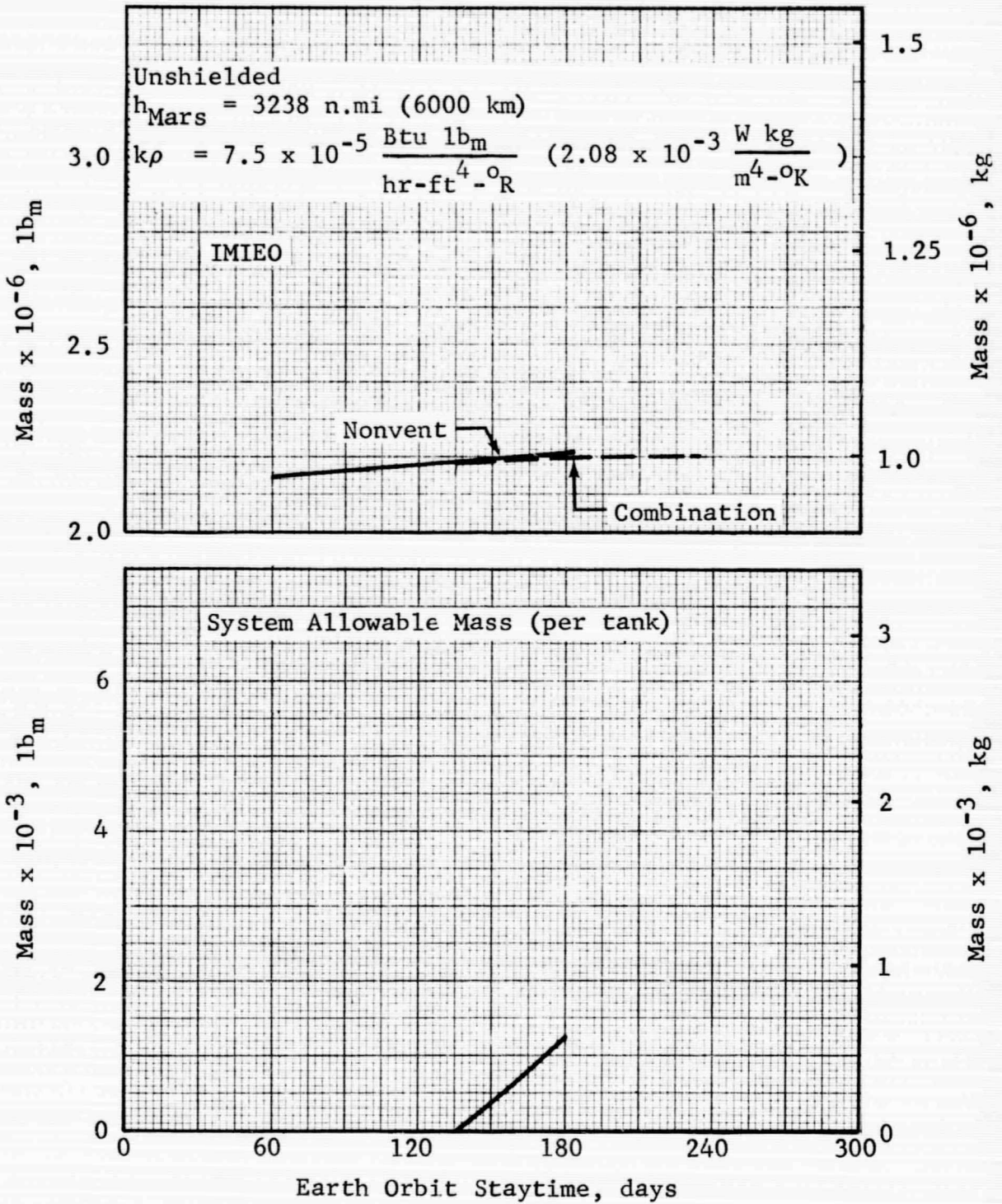


Figure 5.3-2 IMIEO and System Allowable Mass for the Combination Mode: Mars Braking Stage,
 $k\rho = 7.5 \times 10^{-5} \frac{\text{Btu lb}_m}{\text{hr-ft}^4-\text{OR}}$

GENERAL DYNAMICS
Fort Worth Division

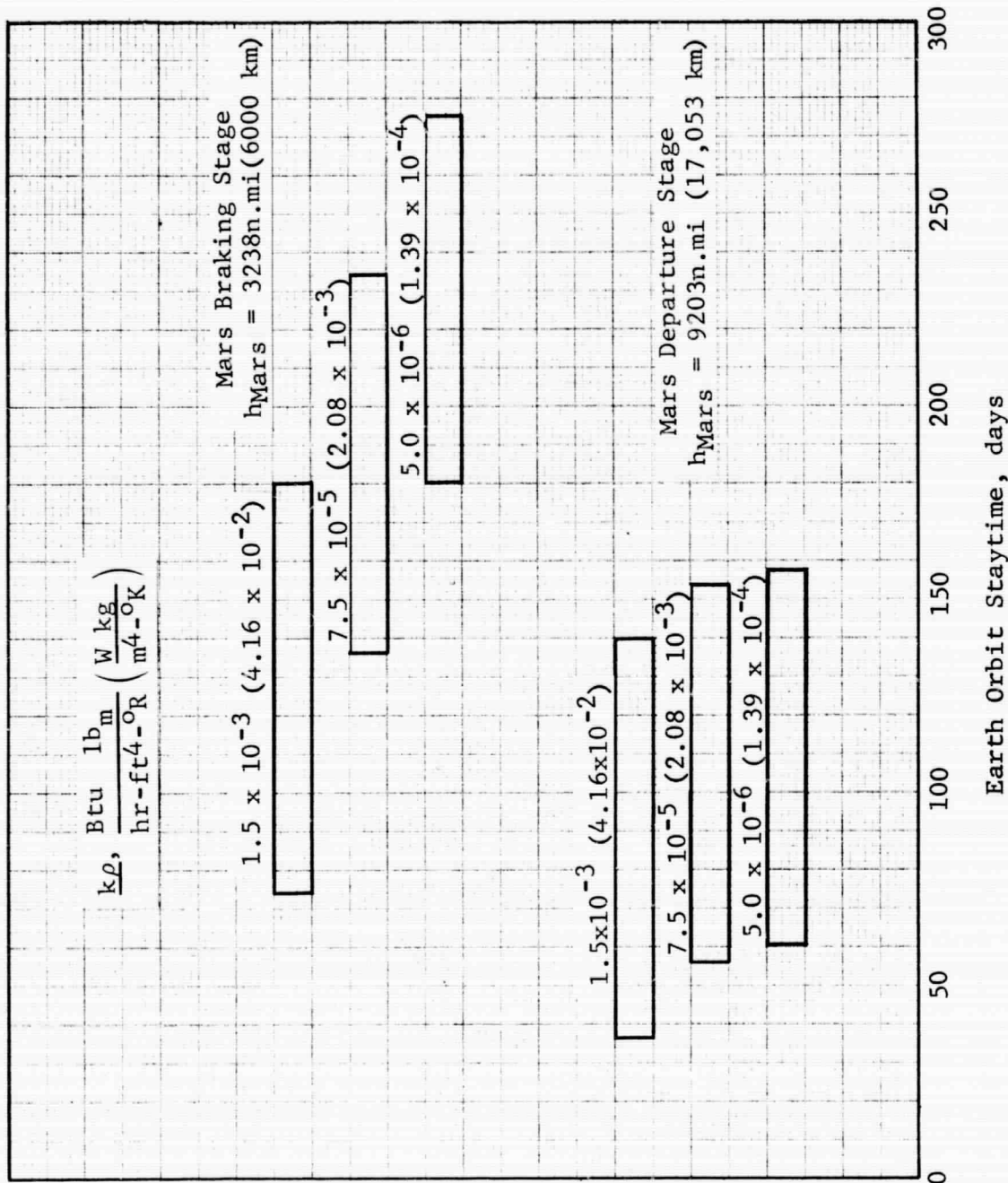


Figure 5.3-3 Range of Earth Orbit Staytime for the Combination Mode

GENERAL DYNAMICS
Fort Worth Division

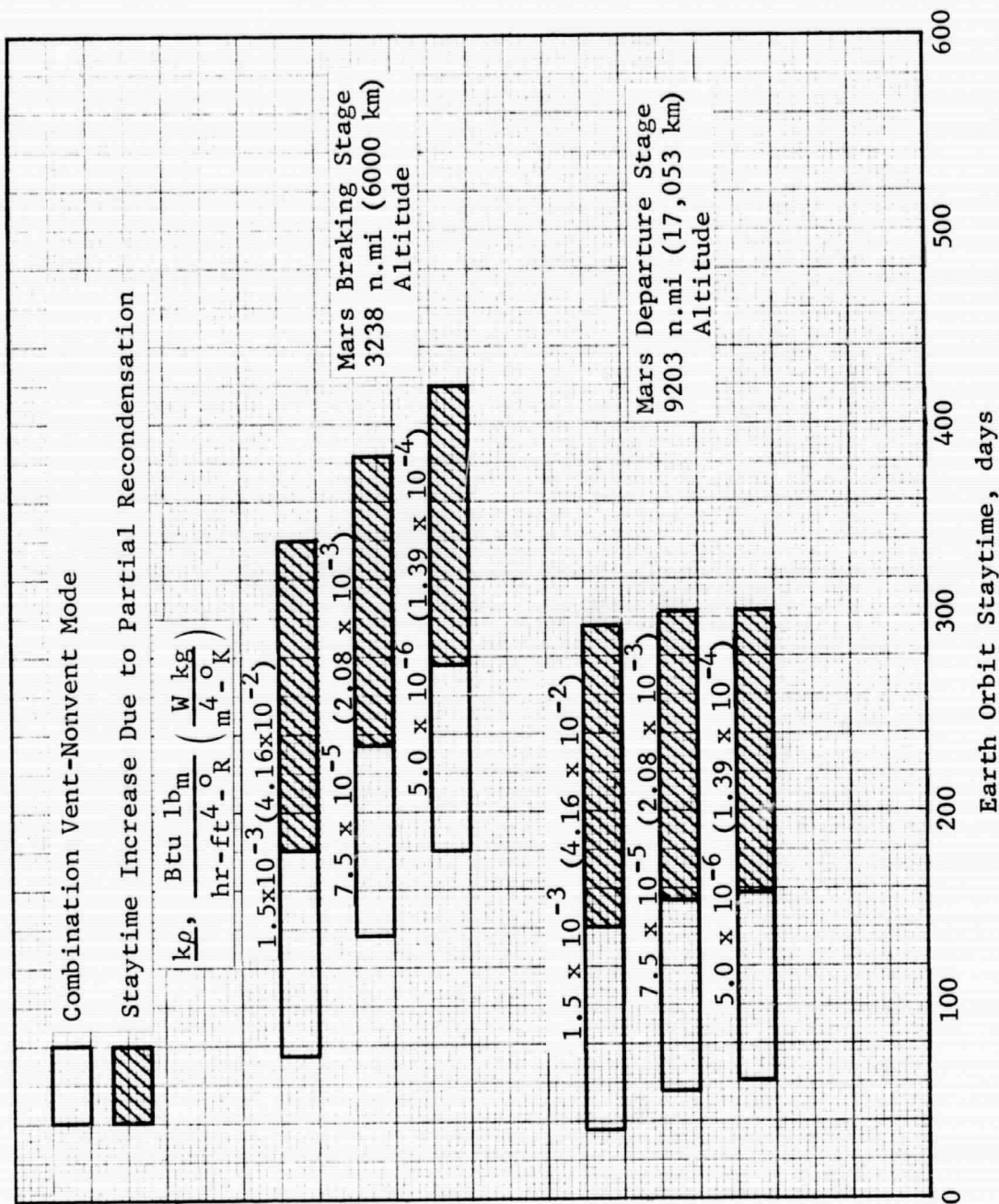


Figure 5.3-4 Effect of Partial Recondensation on the Range of Earth Orbit Staytimes for the Combination Mode

GENERAL DYNAMICS
Fort Worth Division

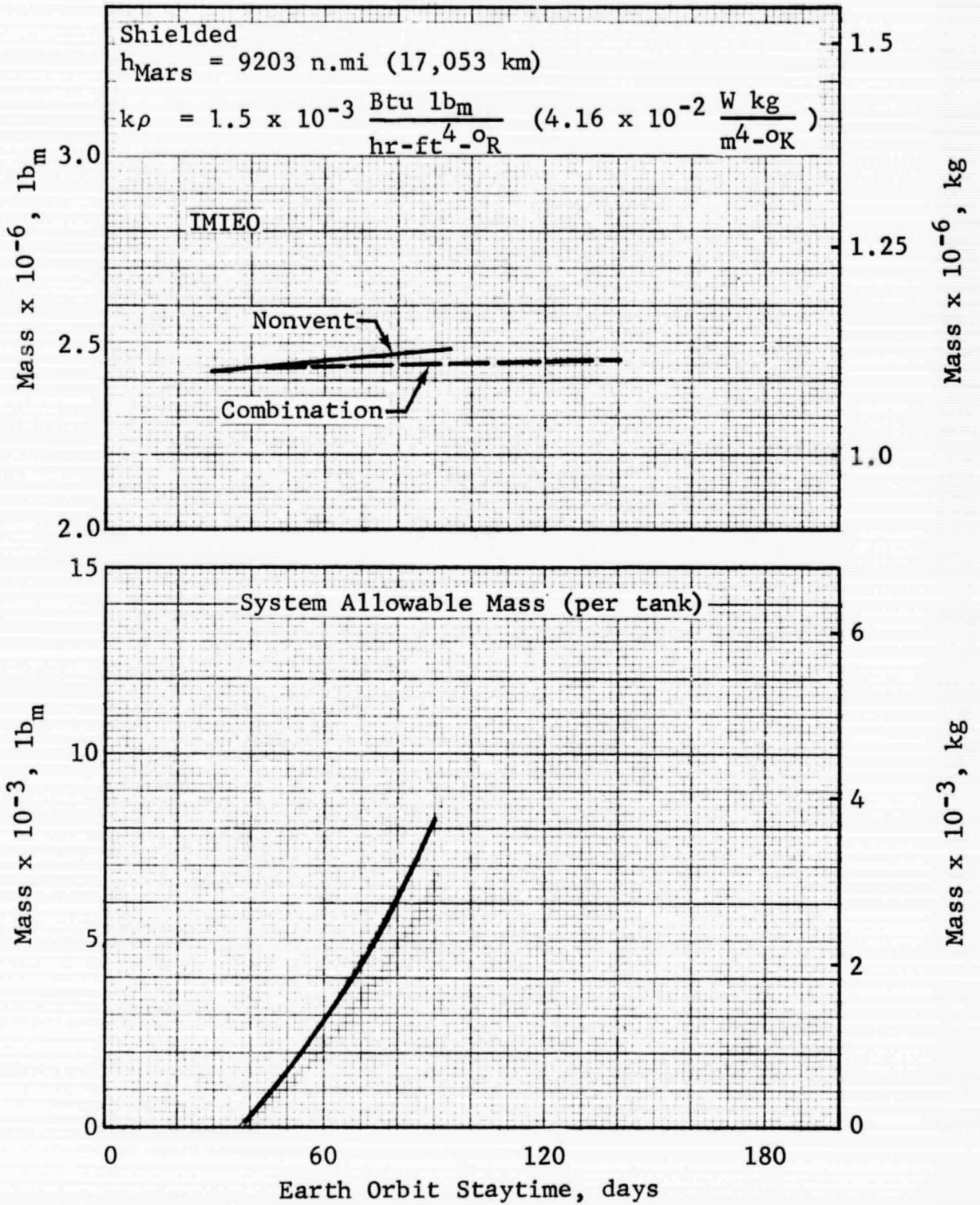


Figure 5.3-5 IMIEO and System Allowable Mass for the Combination Mode: Mars Departure Stage, $k\rho = 1.5 \times 10^{-3} \frac{\text{Btu lb}_m}{\text{hr-ft}^4\text{-}^\circ\text{R}}$

GENERAL DYNAMICS
Fort Worth Division

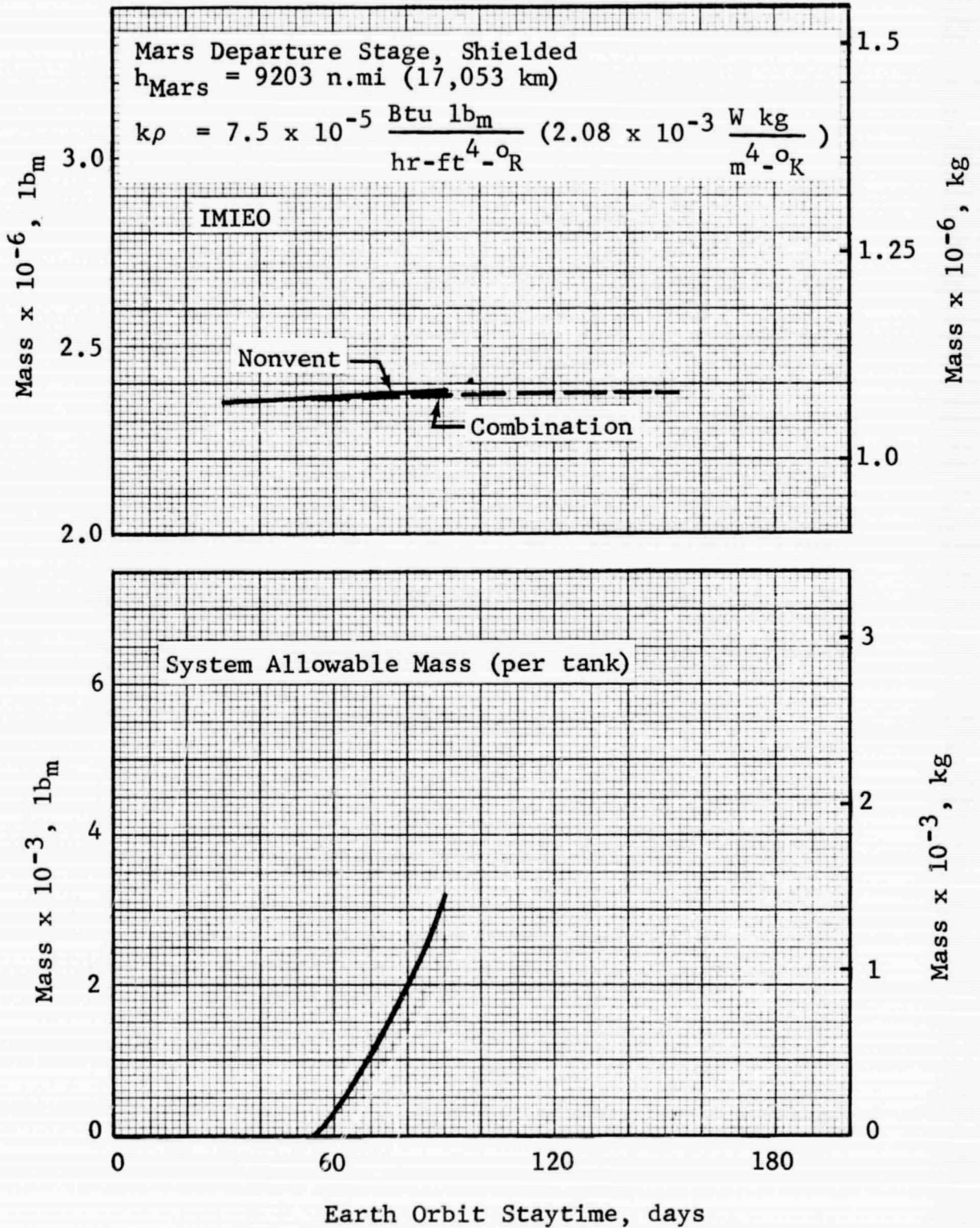


Figure 5.3-6 IMIEO and System Allowable Mass for the Combination Mode: Mars Departure Stage, $k\rho = 7.5 \times 10^{-5} \frac{\text{Btu lb}_m}{\text{hr-ft}^4\text{-}^\circ\text{R}}$

GENERAL DYNAMICS
Fort Worth Division

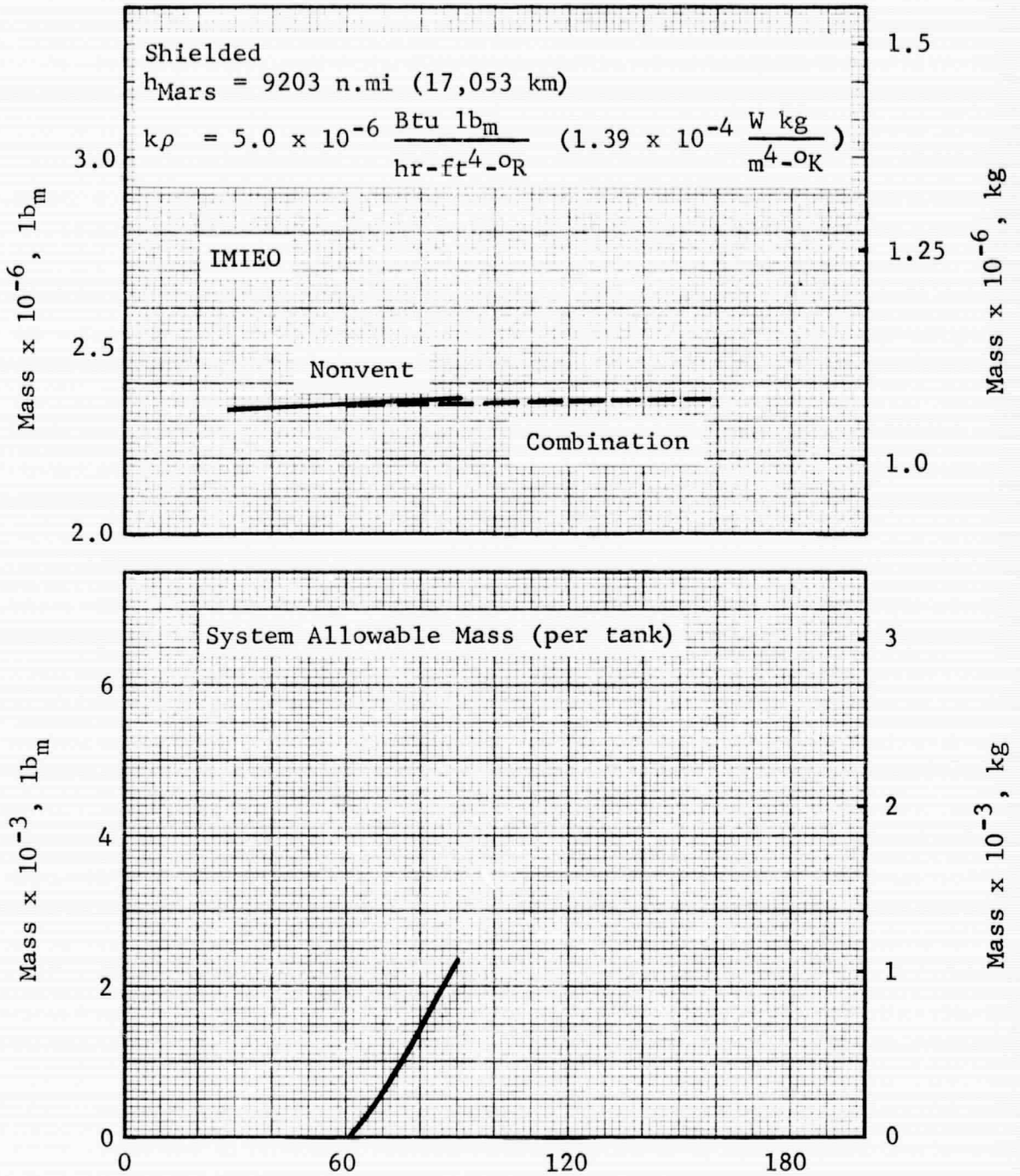


Figure 5.3-7 IMIEO and System Allowable Mass for the Combination Mode: Mars Departure Stage, $k\rho = 5.0 \times 10^{-6} \frac{\text{Btu lb}_m}{\text{hr-ft}^4\text{-}^\circ\text{R}}$

GENERAL DYNAMICS
Fort Worth Division

5.4 SOLAR SHIELD SYSTEMS

It has been shown in Section 4 that deployment of solar shields during Mars transfer and Mars orbit can lead to an appreciable reduction in the vehicle IMIEO. However, the results presented in that section did not take into account the mass of the solar shield system. If the shield is to be effective, the mass penalty to the IMIEO attributable to the solar shield system must be only a small fraction of the mass savings achieved by use of the shield.

In this subsection, solar-shield-system allowable-mass data are presented separately for the Mars transfer solar shield and the Mars orbit solar shield since individual systems are required. As noted previously, the allowable mass is the upper limit to system mass, being that mass which yields no difference in IMIEO between the shielded and unshielded cases. Estimates of the solar-shield-system mass for particular cases are also presented, based on data obtained from Reference 5-1. These system mass estimates are compared with the corresponding allowable mass to obtain the actual savings in IMIEO gained by utilization of solar shields.

5.4.1 Mars Transfer Solar Shield

During the Mars transfer mission phase, the spherical solar shield is deployed from the aft end of the Mars Braking Stage with the vehicle longitudinal axis parallel to the solar vector (see Figure 3.2-3). With this orientation, both the Mars Braking Stage and the Mars Departure Stage are shielded from direct solar radiation, and the mass savings on both stages contribute to the allowable mass for the Mars transfer solar shield. The contribution of the Mars Braking Stage is straightforward; it is proportional to the IMIEO difference between the shielded and the unshielded cases. For the Mars Departure Stage, however, two approaches can be taken. The first approach is to compare the unshielded case with the case where the stage is shielded only during Mars transfer. The second approach is to compare the shielded case (shielded during both Mars transfer and Mars orbit) with the case where the stage is shielded only during Mars orbit. Allowable masses resulting from the two approaches are not equal. The first approach generally yields the largest allowable mass; the long period in Mars orbit penalizes

GENERAL DYNAMICS

Fort Worth Division

the unshielded case more strongly than the shielded case. The allowable mass data presented herein are based on the second approach, which results in conservative (low) estimates of shield allowable mass.

Allowable mass for the Mars transfer solar shield is presented for the vent mode in Figure 5.4-1 as a function of Mars orbit altitude. With low-performance insulation, the allowable mass is constant at a value of approximately 100,000 lb_m (45,360 kg) up to an altitude of 5000 n.mi (9265 km). Above that altitude, the allowable mass increases slightly to 109,000 lb_m (49,440 kg) at the 9203-n.mi (17,053 km) altitude. The increase at higher altitudes is due to a larger Mars Braking Stage and a less-severe thermal environment for the Mars Departure Stage, which results in reduced insulation requirements for the shielded stages. At the intermediate $k\rho$ value, the allowable mass decreases from 34,190 lb_m (15,510 kg) to 27,190 lb_m (12,330 kg) as the altitude increases. The decrease is due to reduced savings in boiloff mass for both stages. With the highest-performance insulation, the allowable mass decreases rather sharply from 18,660 lb_m (8460 kg) to 14,560 lb_m (6600 kg) at low altitudes and remains constant at the higher altitudes. The decrease is due to reduced savings in boiloff and insulation masses on the Mars Braking Stage and in boiloff mass on the Mars Departure Stage.

Allowable shield mass for the partial-recondensation mode is shown in Figure 5.4-2. The general trends are comparable to those of the vent mode although the magnitudes are roughly one-half those for the vent mode. At the high $k\rho$ value, the allowable mass ranges from 49,420 lb_m (22,420 kg) to 58,350 lb_m (26,470 kg) as the altitude increases. The rise is due to larger savings in insulation and boiloff masses on the Mars Braking Stage. With the intermediate-performance insulation, the allowable mass falls in the interval of 16,500 to 17,200 lb_m (7480 to 7800 kg) over the entire altitude range. The allowable mass decreases in the lower-altitude range with the highest-performance insulation, decreasing from 9140 lb_m (4150 kg) to 7710 lb_m (3500 kg) because of lesser savings in boiloff mass on both stages.

The influence of Earth orbit staytime on the Mars-transfer solar-shield allowable mass is dependent upon the insulation performance, as shown in Figure 5.4-3 for the vent mode. With low-performance insulation, the influence

GENERAL DYNAMICS

Fort Worth Division

of staytime is negligible; the allowable mass is approximately constant at 108,000 lb_m (48,990 kg). At the intermediate $k\rho$ value, the allowable mass increases from 23,000 lb_m (10,430 kg) to 33,270 lb_m (15,090 kg) with increased staytime because of larger savings in insulation mass and boiloff mass on the Mars Braking Stage. With the highest-performance insulation, there is a slight decrease at short staytimes from 18,660 lb_m (8460 kg) to an essentially constant value of 14,600 lb_m (6620 kg). Similar data for the partial-recondensation mode are shown in Figure 5.4-4. Again, the influence of staytime is dependent upon the insulation performance. Note that the allowable masses are almost 50% less than in the vent mode.

Allowable mass data for the nonvent mode were obtained only at the synchronous altitude and are presented in Figure 5.4-5 as a function of Earth orbit staytime. Data are not shown for the highest $k\rho$ value because the tank pressures in the Mars Departure Stage are beyond the range of interest at that condition. At both the intermediate and the low $k\rho$ values, the allowable mass increases with staytime. The rate of increase is higher at the intermediate value, with the allowable mass ranging from 43,500 to 63,100 lb_m (19,700 to 28,600 kg) over the range of staytime. The corresponding range of values at the lowest $k\rho$ value is 32,200 lb_m to 39,000 lb_m (14,600 to 17,700 kg).

The actual savings in the IMIEO accomplished by the shield is dependent upon the shield system mass. If the system mass is less than the allowable at a given condition, then a IMIEO reduction will result. Estimates of the Mars-transfer solar-shield-system mass were made for a number of cases. These estimates showed little variation with respect to any of the study parameters and yielded an average value of approximately 950 lb_m (430 kg). The shield itself accounts for almost 70% of the total system mass; the canister and associated subsystems were estimated to have a mass of 300 lb_m (136 kg). The 950-lb_m estimate of the solar-shield-system mass falls well below the allowable mass values presented in this section. Even with the highest-insulation performance and the partial-recondensation mode, the minimum allowable mass is 7700 lb_m (3490 kg). The difference is a measure of the savings achieved by use of the shield and can be expressed in terms of the IMIEO by multiplying by 1.98. This factor relates the IMIEO to mass which is jettisoned just prior to ignition of the Mars Braking Stage engine. Thus, the minimum savings in the IMIEO attributable to the Mars transfer solar

GENERAL DYNAMICS

Fort Worth Division

shield is approximately 13,400 lb_m (6060 kg). This amounts to roughly 0.6% of the vehicle IMIEO. At the other extreme, consider the low insulation performance, vent mode case with an allowable mass of 100,000 lb_m (45,360 kg). The IMIEO savings in this case would amount to 196,000 lb_m (88,900 kg), which is approximately 8% of the IMIEO.

5.4.2 Mars Orbit Solar Shield

The solar shield deployed during Mars orbit is designed to intercept only the direct solar component of the radiant energy incident upon the vehicle. This design follows the conclusion of the solar-shield feasibility study (Reference 5-2). There it was concluded that during orbital operation it was impossible to block all components of the incident radiation - direct solar and planetary emitted and albedo. The most effective shield-vehicle configuration was found to be a spherical shield deployed aft of the vehicle with the vehicle longitudinal axis oriented parallel to the solar vector. Figure 3.2-4 shows the spherical solar shield deployed from the Mars Departure Stage during the Mars orbit mission phase.

Figure 5.4-6 presents the allowable mass of the Mars orbit solar shield for the vent mode. The allowable mass of the shield and, thus, the effectiveness, is seen to be a strong function of altitude, increasing as the altitude increases. This is due to the smaller contribution of the planetary emitted and albedo radiation to the total incident energy at the higher altitudes. The allowable mass is also strongly influenced by the insulation performance. With the lowest-performance insulation, the allowable mass increases from 4950 lb_m (2245 kg) at the 216-n.mi (400 km) altitude to 25,140 lb_m (11405 kg) at the 9203-n.mi (17,053 km) synchronous altitude, an increase of 408%. With the intermediate performance insulation, the shield allowable mass drops roughly 50%. The allowable mass increases from 2560 lb_m (1160 kg) at the low altitude to 12,880 lb_m (5840 kg) at the synchronous altitude, a percentage increase of 403%. As the insulation performance improves to the low $k\rho$ value, the allowable mass drops only slightly, ranging from 2170 lb_m (980 kg) to 10,880 lb_m (4935 kg), a percentage increase of 402%.

GENERAL DYNAMICS

Fort Worth Division

The shield allowable mass for the partial-recondensation mode is shown in Figure 5.4-7. The overall trend of allowable mass increasing with increasing altitude and $k\rho$ value is similar to the vent mode results. However, the magnitude of the allowable mass is less than one-half that for the vent mode. With the lowest performance insulation, the allowable mass ranges from 2410 lb_m (1090 kg) at the low altitude to 11,410 lb_m (5170 kg), an increase of 373%. At the other extreme, the highest-performance insulation, the allowable mass ranges from 900 lb_m (410 kg) to 4590 lb_m (2080 kg), a 410% increase.

The effect of Earth orbit staytime on the Mars-orbit shield allowable mass is shown in Figure 5.4-8 for the vent mode at the synchronous altitude. The results show no influence of staytime, regardless of insulation performance. Increased staytime leads to additional boiloff and the attendant increases in tank and insulation mass. However, the increases are of the same order for both the shielded and the unshielded stages since a shield is not deployed during Earth orbit. Thus, the shield allowable mass is not affected by the longer staytime.

In order to estimate the actual savings in IMIEO, estimates of the Mars-orbit solar-shield-system mass were made at a number of conditions. Again, the variation of shield-system mass with the various study parameters was small, and an average value of 495 lb_m (225 kg) can be used as an estimate at all conditions. Comparing this value with the allowable mass data just discussed indicates that significant savings in the IMIEO result except at the low-altitude, high-insulation-performance condition. The maximum savings occur at the high-altitude, high- $k\rho$ -value case in the vent mode (Figure 5.4-6), with an allowable mass of 25,100 lb_m (11,400 kg). The factor relating the IMIEO to shield allowable mass at the 9203-n.mi altitude is 3.32. Thus, the savings in the IMIEO is 81,700 lb_m (37,000 kg). The other extreme is represented by the low-altitude, low- $k\rho$ -value condition for the partial-recondensation mode, where the allowable mass is 904 lb_m (410 kg) and the factor relating IMIEO to allowable mass is 3.18. With a shield system mass of 495 lb_m the savings in the IMIEO is only 1300 lb_m (590 kg).

GENERAL DYNAMICS
Fort Worth Division

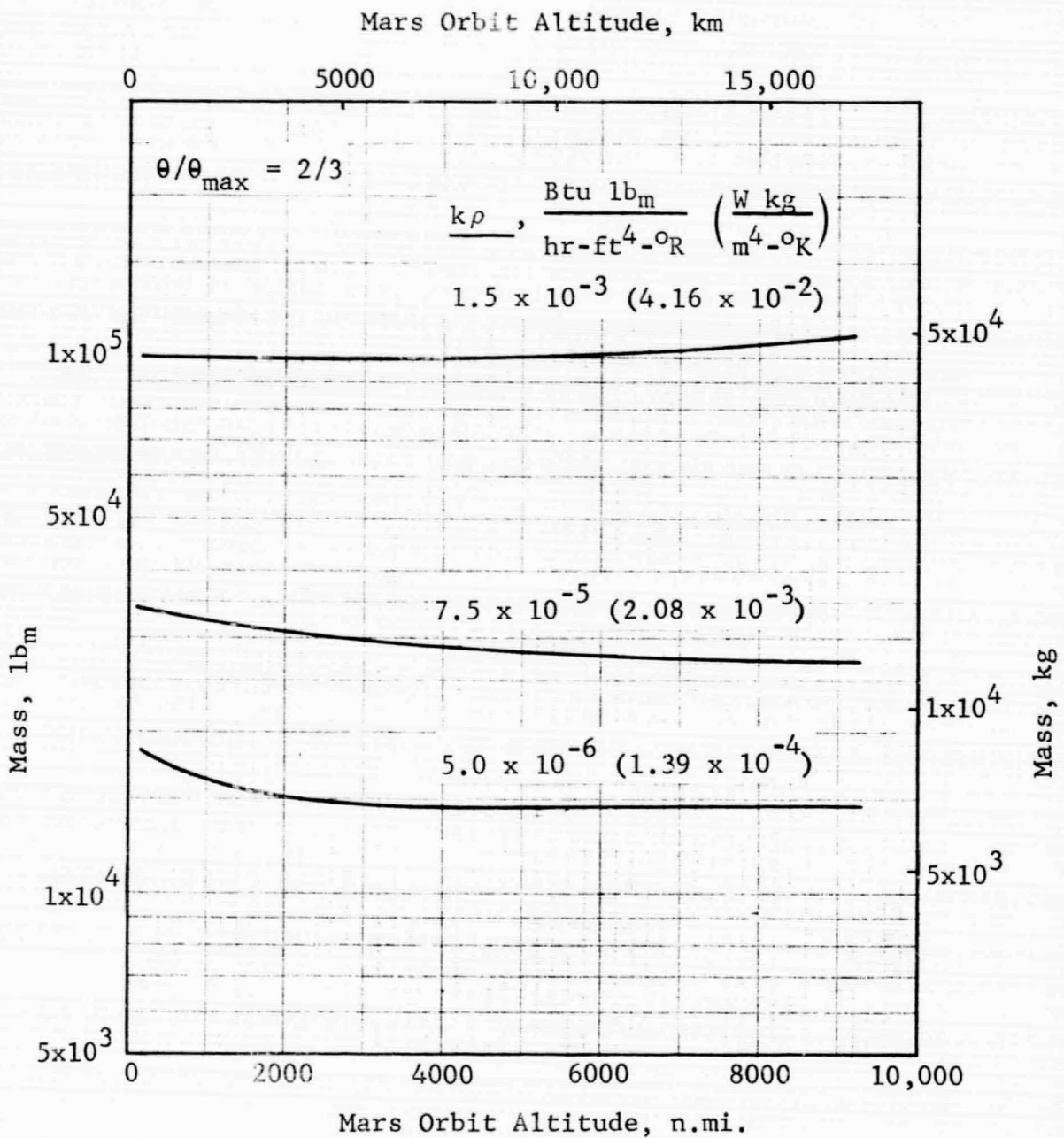


Figure 5.4-1 Mars Transfer Solar Shield
Allowable Mass vs Altitude:
Vent Mode

GENERAL DYNAMICS
Fort Worth Division

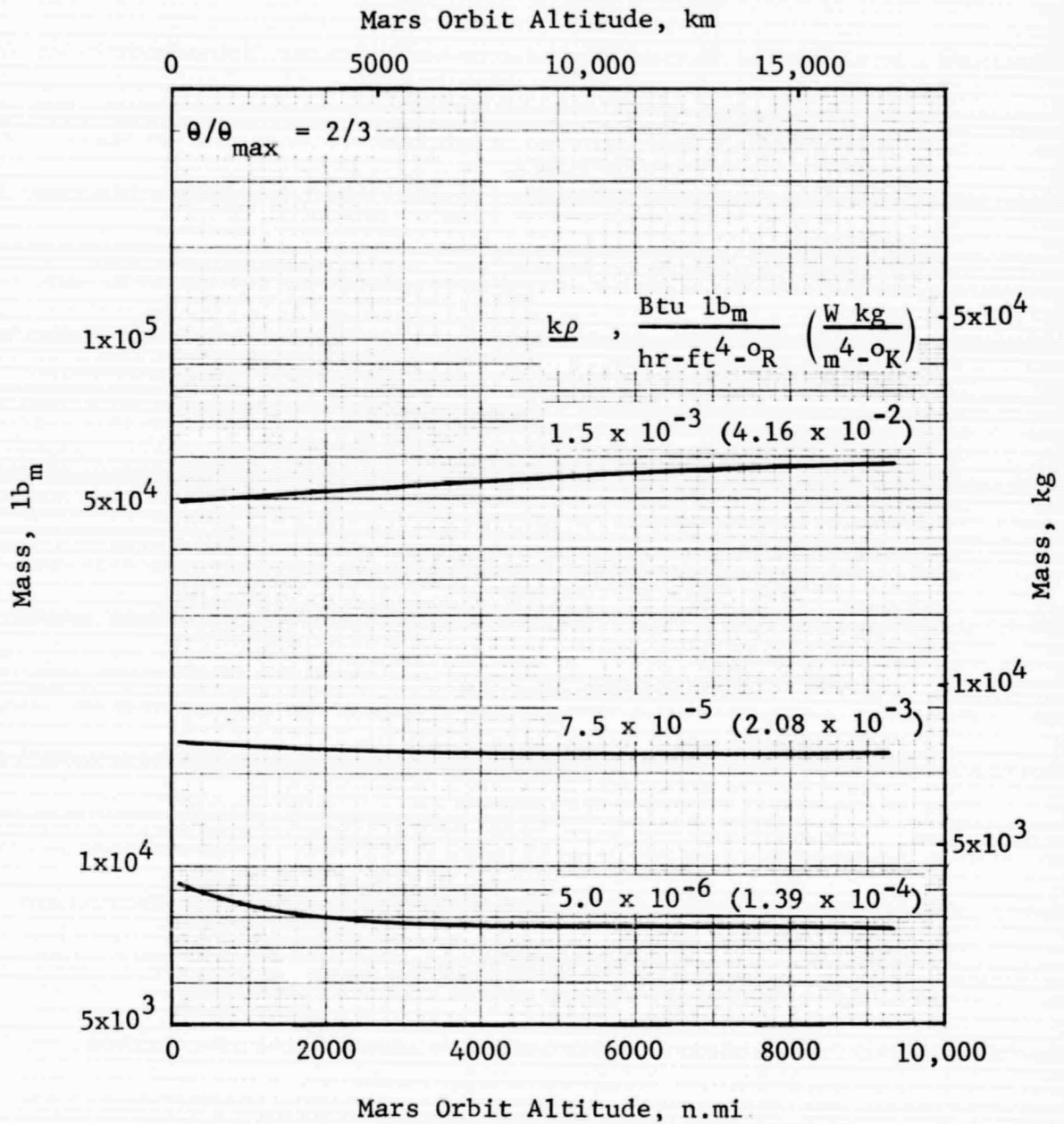


Figure 5.4-2 Mars Transfer Solar Shield Allowable Mass vs Altitude: Partial Recondensation Mode

GENERAL DYNAMICS
Fort Worth Division

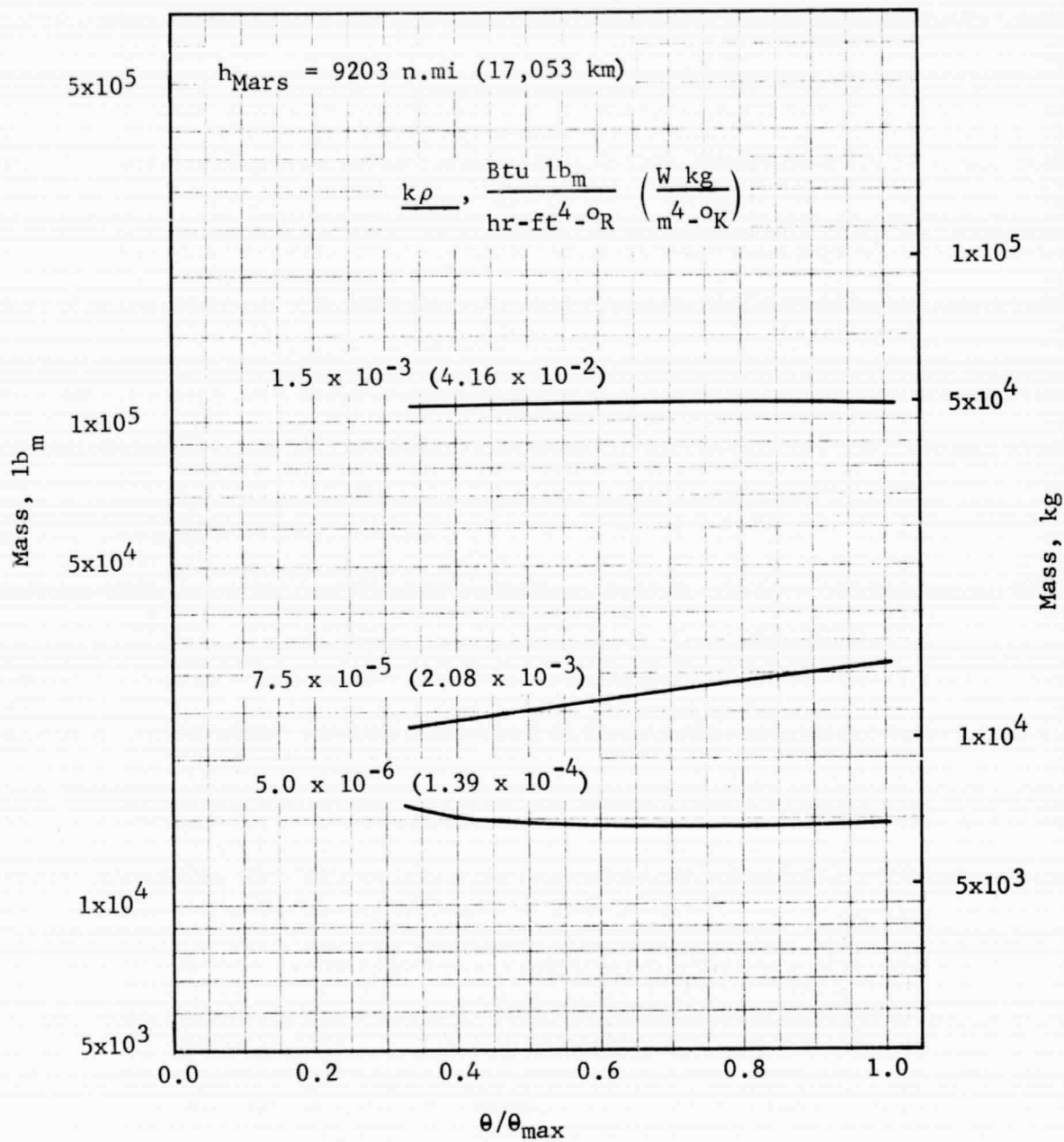


Figure 5.4-3 Mars Transfer Solar Shield
Allowable Mass vs Staytime:
Vent Mode

GENERAL DYNAMICS
Fort Worth Division

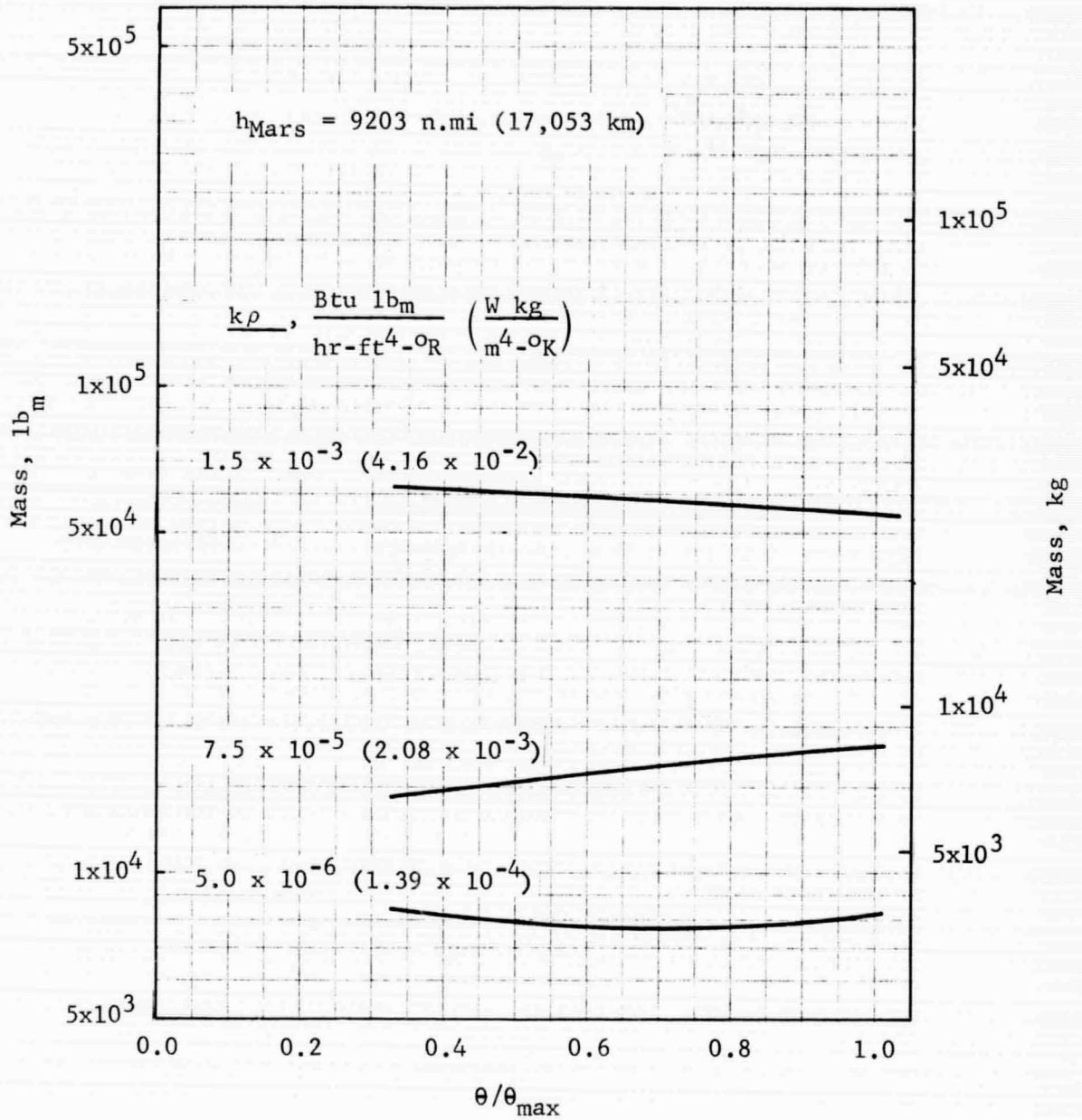


Figure 5.4-4 Mars Transfer Solar Shield
Allowable Mass vs Staytime:
Partial Recondensation Mode

GENERAL DYNAMICS
Fort Worth Division

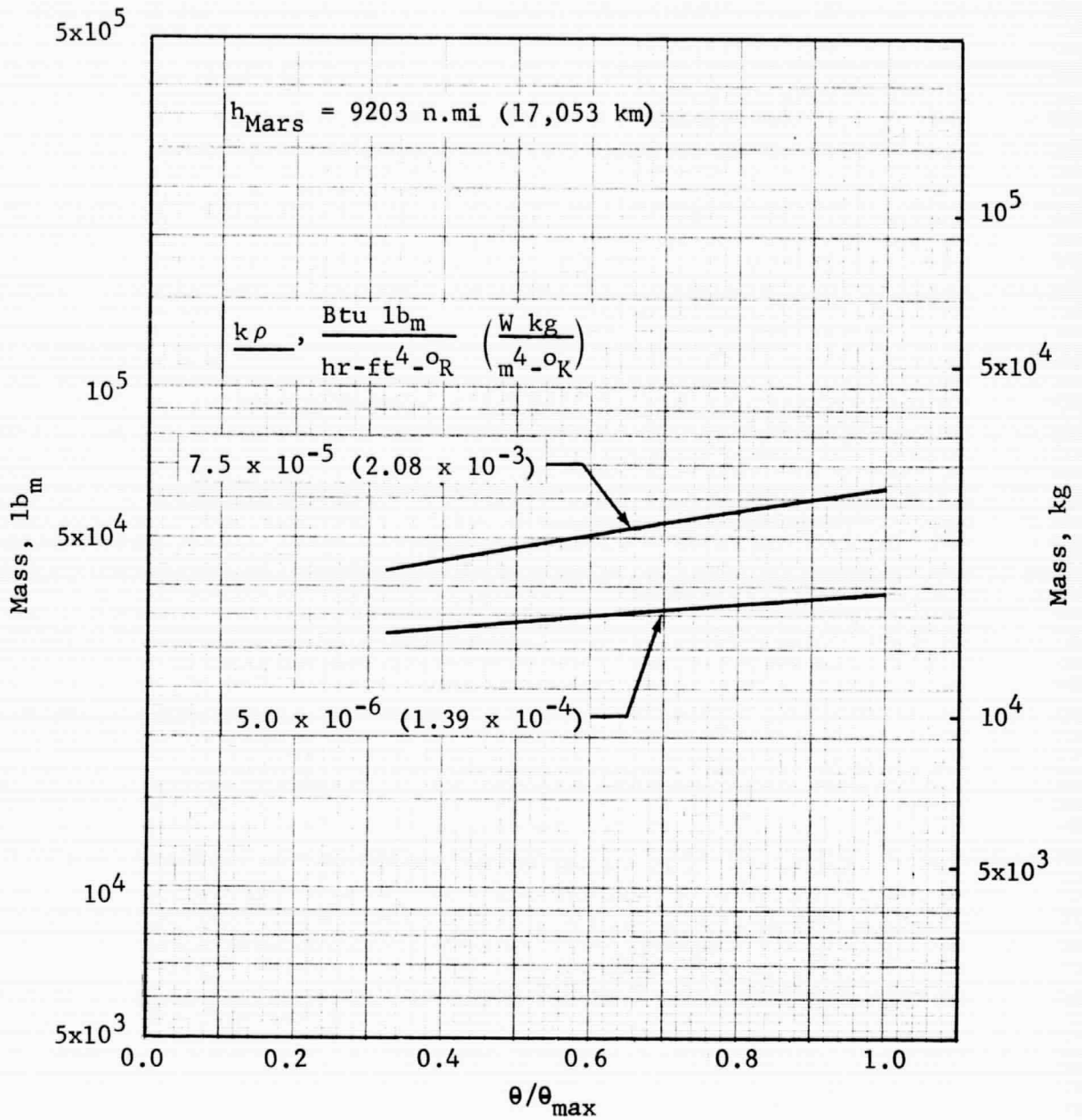


Figure 5.4-5 Mars Transfer Solar Shield
Allowable Mass vs Staytime:
Nonvent Mode

GENERAL DYNAMICS
Fort Worth Division

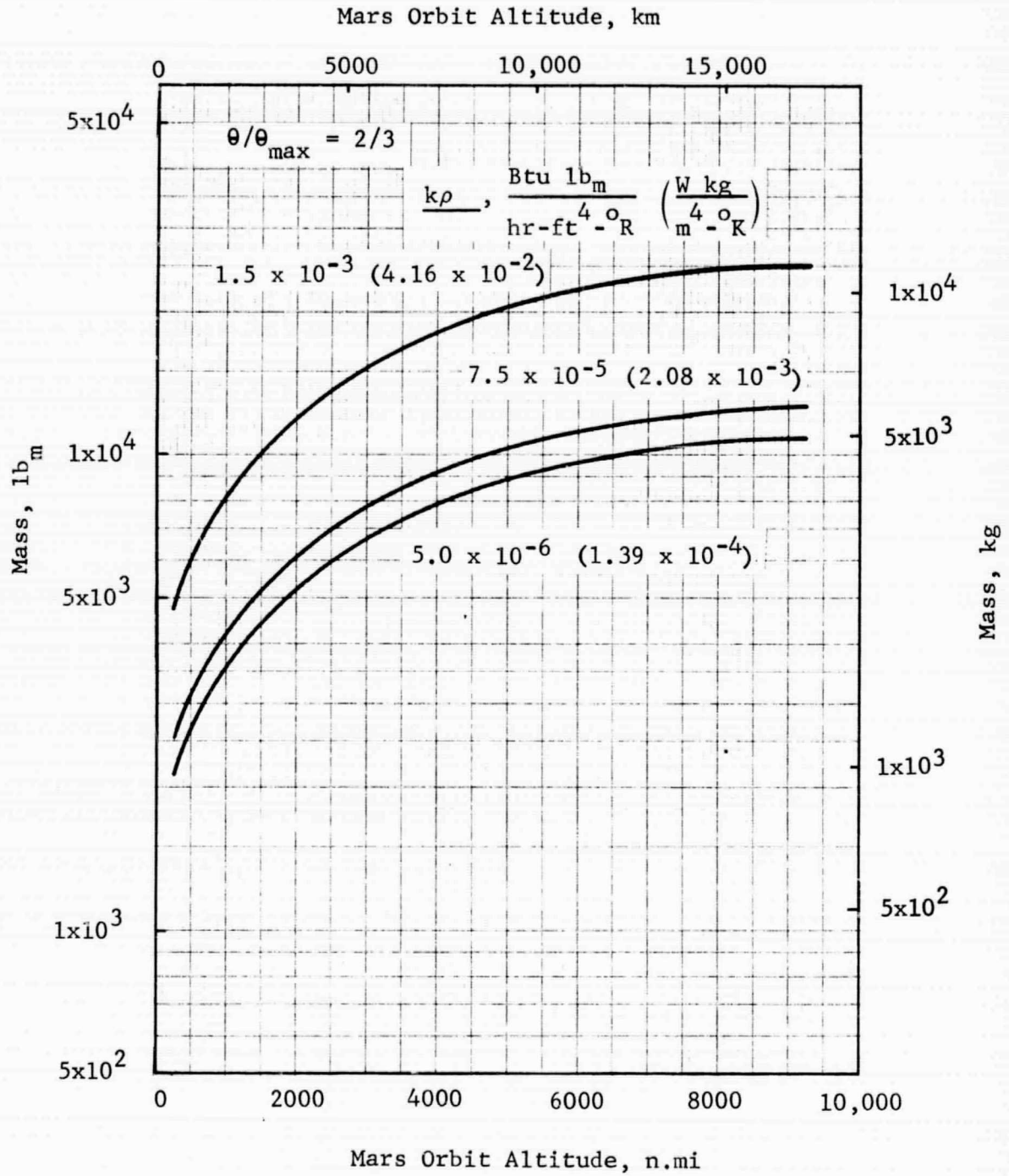


Figure 5.4-6 Mars Orbit Solar Shield
Allowable Mass vs Altitude:
Vent Mode

GENERAL DYNAMICS
Fort Worth Division

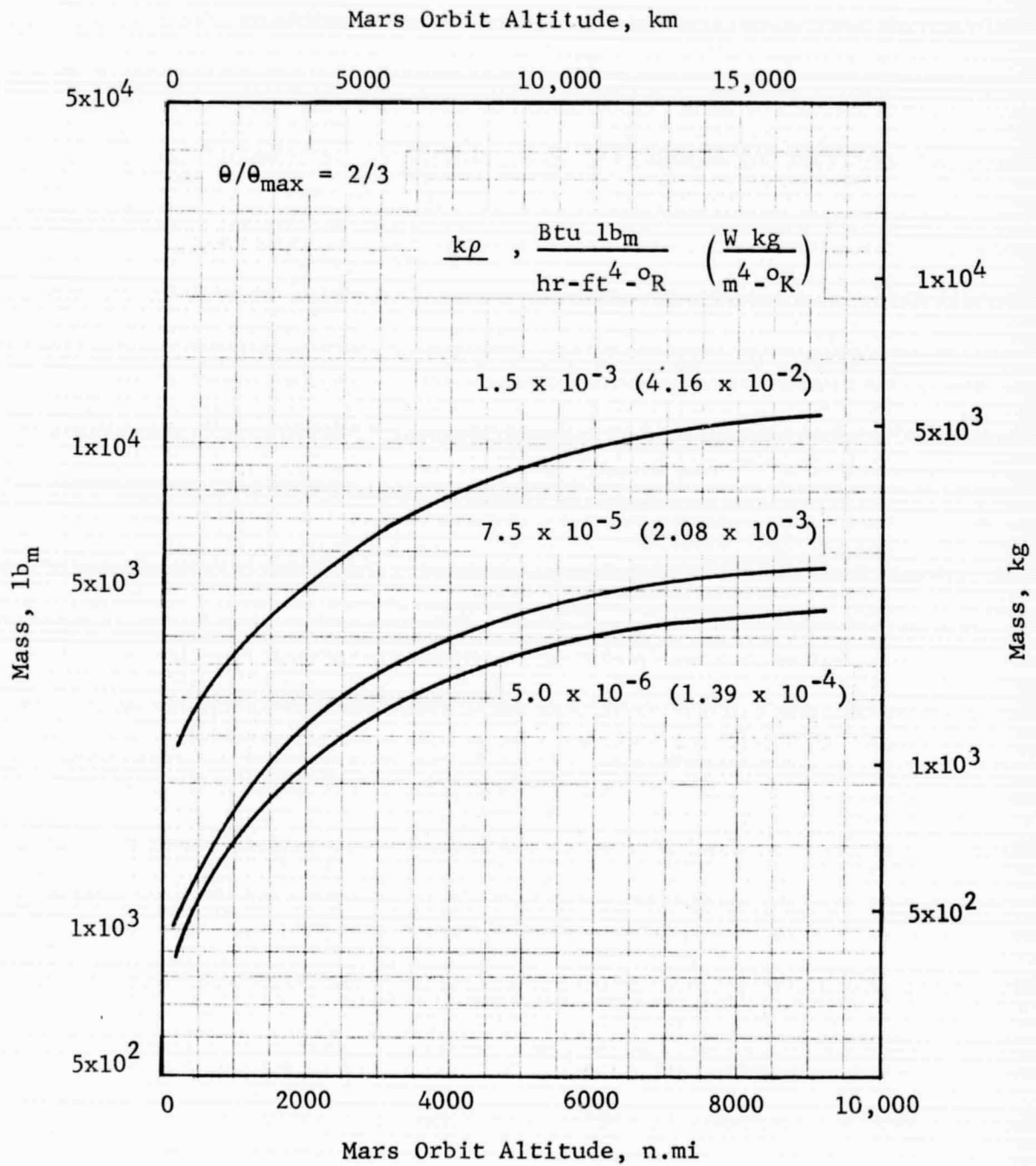


Figure 5.4-7 Mars Orbit Solar Shield
Allowable Mass vs Altitude:
Partial Recondensation Mode

GENERAL DYNAMICS
Fort Worth Division

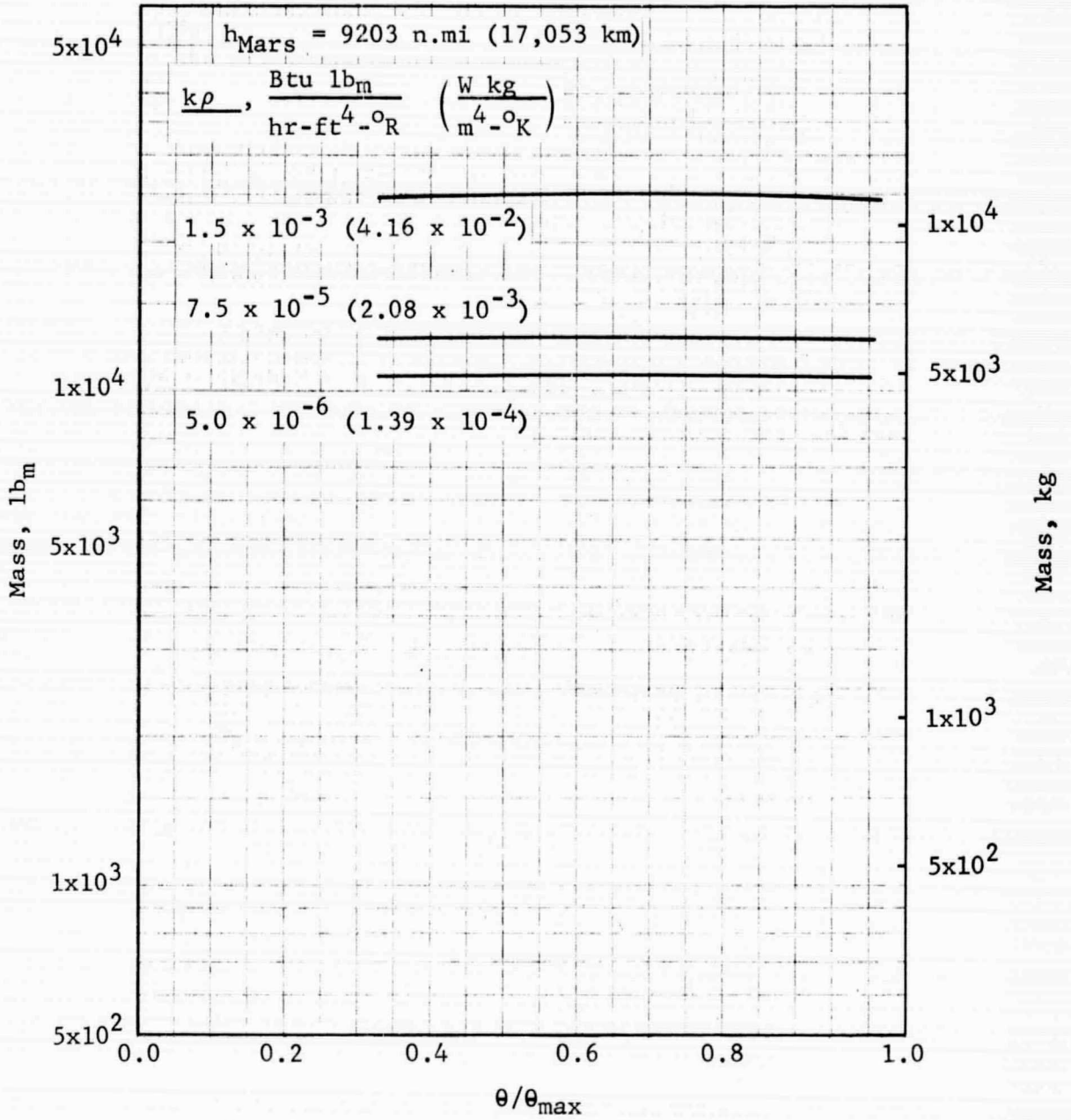


Figure 5.4-8 Effect of Earth Orbit Staytime on Mars Orbit Solar Shield Allowable Mass: Vent Mode

PRECEDING PAGE BLANK NOT FILMED.

GENERAL DYNAMICS

Fort Worth Division

S E C T I O N 6

S U M M A R Y O F R E S U L T S
A N D C O N C L U S I O N S

The main objectives of this study are an assessment of the problems associated with long-term storage of liquid hydrogen and the effects of the basic parameters, propellant storage modes, and systems on the stage thermal protection systems and the vehicle IMIEO. In the preceding sections the study results have been discussed with respect to optimized propellant storage systems and the important trends were noted. In this section the results are summarized and conclusions drawn from the data are presented.

Conclusions that relate directly to thermal protection are presented in Subsection 6.1. This area is the main concern of the study, but the results also have an impact on two related areas - the mission parameters and the structural concept. Implications of the results that relate to these areas are presented in Subsections 6.2 and 6.3, respectively.

An important general conclusion concerning the approach to this study should be noted here. The wide ranges in the basic parameters studied result in large variations in the mass of the propellant storage system. With increased storage system mass, the propellant loading must also increase, which itself increases the storage system mass since a larger tank is required. These mass increases also have an effect on the mass requirements of the lower stages and may have a large effect on the sensitivity of the vehicle IMIEO to the various subsystem masses. Thus, it is imperative that the mass-buildup and mass-sensitivity analyses correspond to the final propellant storage system definition. This approach was accomplished in the thermal protection system optimization computer program used in this study by an iteration between the mass-buildup-sensitivity analysis and the thermal protection system optimization analysis.

6.1 THERMAL PROTECTION FINDINGS

Each of the basic study parameters (Earth orbit stay-time, insulation thermal performance, and Mars orbit altitude), the propellant storage mode, and the solar shield

GENERAL DYNAMICS
Fort Worth Division

have significant effects on the stage thermal protection systems and the vehicle IMIEO. All of these variables are interrelated to some extent as to their effects, and the influence of each generally differs from stage to stage. Therefore, this subsection is organized to present first the conclusions with respect to the total Mars vehicle, and then the conclusions related to the individual stages.

6.1.1 Total Vehicle

The problems arising from an extended period in Earth orbit are an increase in the thermal protection system mass requirements and the attendant increase in the vehicle IMIEO. The severity of these problems is strongly dependent upon the insulation thermal performance and the propellant storage mode.

IMIEO increases over the range of staytime vary from 1 to 26% of the short-staytime IMIEO, with the higher increases associated with low-performance insulation. The largest absolute IMIEO values are also associated with low-performance insulation, ranging from 2.00 to 3.28 million lb_m (0.91 to 1.49 million kg) over the range of staytime. In Subsection 6.2.4 it is shown that an upper limit on the vehicle IMIEO can be established on the basis of a fixed number of modules (four-module Earth Departure Stage) and the payload capability of the uprated Saturn V launch vehicle. This upper limit ranges from 2.30 to 2.45 million lb_m (1.04 to 1.11 million kg), increasing with increasing altitude. Thus, in a number of cases at the high k_p value, the vehicle IMIEO exceeds this upper limit and at least one extra module is required in the Earth Departure Stage.

The problem of extended staytime can also be stated in terms of the propellant storage penalty, which represents the mass of the components necessary to contain and protect the propellant and the additional propellant required by virtue of this mass. With low-performance insulation, this penalty can reach 79% of the zero-mass-fraction vehicle IMIEO. In other words, a significant portion of the vehicle mass (in the above case, 44% of the actual vehicle IMIEO) is related to propellant storage. By reducing the staytime alone, this penalty can be reduced to 51% of the zero-mass-fraction vehicle IMIEO, a mass reduction of 444,500 lb_m (201,600 kg).

GENERAL DYNAMICS

Fort Worth Division

Improvement in the insulation thermal performance alone will reduce IMIEO below the limit mentioned above. With the highest currently quoted multilayer insulation performance (approximately 7.5×10^{-5} Btu lb_m/hr-ft⁴-°R or 2.08×10^{-3} W kg/m⁴-°K), the IMIEO is reduced to the range of 1.82 to 2.42 million lb_m (0.83 to 1.10 million kg), which is within the above-mentioned limits. The propellant storage penalty is also significantly reduced. For the same condition that yielded the 79% penalty with low-performance insulation, the penalty with intermediate performance is 28% of the zero-mass-fraction IMIEO. In addition, improved insulation performance reduces the effect of Earth orbit staytime. With the performance mentioned above, the percentage increase in IMIEO over the range of staytime is less than 6%. Further improvement in the insulation performance is, of course, beneficial, but the returns are limited. This trend was noticed throughout the study and is one of the most significant findings: limited mass savings are realized as the insulation performance is increased beyond the intermediate $k\rho$ value, which corresponds to the highest currently quoted multilayer insulation performance.

There is still a significant difference in IMIEO between even the highest performance insulation case and the adiabatic tank-wall case that represents the lower limit. However, this difference is due to heat transfer through penetrations and is not affected by the insulation performance. Penetration heat transfer can be decreased only through more effective design or reduction of the incident radiation by such means as solar shields.

Influence of the propellant storage mode on the vehicle IMIEO increases as the propellant heat transfer increases. At the highest $k\rho$ value, use of the partial-recondensation mode instead of the vent mode can, for the lower Mars orbit altitudes, reduce the IMIEO below the upper limit for a four-module Earth Departure Stage. The maximum difference in IMIEO between the vent and partial-recondensation modes is 519,000 lb_m (236,000 kg) or 18.3% of the vent-mode IMIEO. At the other extreme, high-performance insulation and a shielded vehicle, the IMIEO difference is as low as 7150 lb_m (3240 kg). Under these conditions, however, the partial-recondensation system is effective only on the Mars Departure Stage. The heat transfer to the propellant tanks of the lower stages is below that required to raise the propellant to the vent pressure, so boiloff does not occur from the

GENERAL DYNAMICS

Fort Worth Division

lower stages. Percentage increases in IMIEO over the range of staytime are also reduced by use of partial-recondensation systems. These increases are 25 to 50% less in the partial-recondensation mode than in the vent mode, with the larger reduction occurring at high $k\rho$ values.

The altitude of the Mars parking orbit affects the vehicle IMIEO in three different ways:

1. Mars Excursion Module Mass
2. Thermal environment
3. Energy requirements for the Mars braking and departure maneuvers

Results of the study show that the variation in the Mars Excursion Module mass dominates the other two factors with respect to the vehicle IMIEO. In all cases, the general trend of IMIEO follows that of the Excursion Module mass, increasing as the altitude increases; the magnitude of the increase ranges from 13 to 24% of the low-altitude value. The total propellant storage penalty for the Mars vehicle, however, decreases with increasing altitude, reflecting the less severe thermal environment of the Mars Departure Stage at the higher altitudes and larger propellant loadings on the lower stages.

Solar shields, deployed during Mars transfer and Mars orbit, yield significant reductions in the value of IMIEO, especially in combination with low-performance insulation. Mass savings range as high as 342,700 lb_m (155,400 kg), which includes shield system masses of 950 lb_m (430 kg) for the Mars transfer shield and 495 lb_m (225 kg) for the Mars orbit shield. The effectiveness of the Mars orbit shield is strongly dependent upon the Mars orbit altitude. At the lower altitudes, the planetary components of the incident radiation overshadow the beneficial aspects of the solar shield. However, with low-performance insulation, the savings in IMIEO attributable to the Mars orbit solar shield at the 216-n.mi (400 km) altitude is 14,200 lb_m (6440 kg), after accounting for the solar shield system mass.

One of the significant aspects of the solar shield is its effect on the heat transfer through penetrations. By

GENERAL DYNAMICS

Fort Worth Division

reducing the radiant energy incident upon the vehicle, the solar shield tends to eliminate this component of the total propellant heat transfer. During Mars transfer, for example, when only direct solar radiation is incident upon the vehicle, the spherical shield virtually eliminates the incident radiation and thus the penetration heat transfer. In an orbital environment, the shield is not effective against the planetary components of the incident radiation and its effect on the penetration heat transfer is reduced. This is demonstrated by examining the percentage reduction in the penetration heat transfer as a function of altitude for the Mars orbit mission phase. The values range from 7.1% at 216 n.mi (400 km) to 56.5% at 9203 n.mi (17,053 km). As the altitude increases, the planetary components of the incident radiation are reduced, thereby enhancing the effectiveness of the solar shield.

Estimates of the solar shield system masses showed little variation, even over the wide ranges of the variables investigated. Mass of the Mars transfer solar shield system was estimated at 950 lb_m (430 kg). For the Mars orbit shield, the system mass was estimated to be 495 lb_m (225 kg).

6.1.2 Earth Departure Stage

The Earth Departure Stage is affected to a greater degree by the Earth orbit staytime than the interplanetary stages because its mission is restricted to Earth orbit, where it encounters the most severe thermal environment of the mission. Propellant storage penalties for the stage increase with staytime; percent increases range from 8 to 143%, depending upon the insulation thermal performance, the propellant storage mode, and, to a small extent, the Mars orbit altitude.

The highest percentage increases are associated with low-performance insulation. With the nonvent storage mode, which yields the maximum 143% increase, the absolute value of the stage propellant storage penalty ranges from 12.6% to 30.6% of the zero-mass-fraction vehicle IMIEO. This penalty can be reduced by use of a vent or partial-recondensation thermal management system. However, greater benefit is gained by using higher-performance insulation. At the intermediate k_p value for example, the penalty is reduced

GENERAL DYNAMICS

Fort Worth Division

to the range of 6.0% to 9.3%, in the nonvent mode. With the highest insulation performance investigated during this study, the penalty can be reduced to the range of 5.5% to 6.1%. However, even under adiabatic conditions, which represents the lower limit, the propellant storage penalty would be 5.1%.

The influence of propellant storage mode increases as the insulation performance worsens. With the highest insulation performance (lowest $k\rho$ value), the vent pressure is not reached even at the maximum staytime and the vent and partial-recondensation modes cannot yield any benefit. Propellant storage mode effects are reflected in the performance criteria for the vent and the partial-recondensation thermal management systems. As mentioned, the vent and partial-recondensation modes are undefined at the lowest $k\rho$ value. Even at the intermediate $k\rho$ value, the allowable mass can be computed only at the 270-day staytime, where the value is only 390 lb_m (177 kg). For the low-performance insulation condition, the vent system allowable mass increases from only 450 lb_m (204 kg) to 8800 lb_m (3990 kg) as the staytime increases, on a per-tank basis. Allowable masses for the partial-recondensation system are generally higher, reaching a maximum of 27,900 lb_m (12,600 kg) at the highest $k\rho$ value. Again, intermediate $k\rho$ value results can be evaluated only at the maximum 270-day staytime where the allowable mass is 2000 lb_m (920 kg).

Data quoted in this subsection correspond to the 3238-n.mi (6000 km) Mars orbit altitude. However, the altitude has little effect on the propellant storage penalty of the Earth Departure Stage and the results are similar at the other altitudes. The general increase in \dot{M} IEO with altitude noted earlier in Subsection 6.1.1 affects the Earth Departure Stage mainly through increased propellant loadings and, consequently, larger tanks. Thus, the propellant storage component masses exhibit a small increase with altitude while the component mass fractions and the propellant storage penalty remain relatively unchanged.

Two methods of reducing the effect of the Earth orbit staytime, the combination propellant storage mode and orbital tanking, were examined during the study. However, neither of these methods is applicable to the Earth Departure Stage. The combination mode is equivalent functionally to either the vent or the partial-recondensation mode for this

GENERAL DYNAMICS

Fort Worth Division

stage since there is no nonvent period of operation beyond Earth orbit. In the orbital tanking case, the optimum case cannot be determined since there is no mission phase beyond Earth orbit over which to perform the optimization. Qualitatively, the optimum insulation thickness can be defined as zero, which corresponds to launching dry tanks. This appears to be incompatible with the pressure-stabilized tank concept, however.

6.1.3 Mars Braking Stage

Although Earth orbit staytime has less effect on the propellant storage penalty of the Mars Braking Stage than of the Earth Departure Stage, it remains a significant factor. Percentage increases in the storage penalty due to variations in the Braking Stage propellant storage system range up to 119% as the staytime increases from 60 to 180 days, depending upon the insulation thermal performance, the propellant storage mode, and whether the stage is shielded. The higher percentage increases occur for the shielded stage with low-performance insulation; the propellant heating history under these conditions is dominated by the Earth orbital storage period since the solar shield reduces the heat transfer during Mars transfer to a negligible amount.

For the unshielded stage, the propellant storage penalty ranges from a minimum of 3.9% of the zero-mass-fraction IMIEO to a maximum of 23.7%. This compares with the lower limit representing the adiabatic tank-wall case of 3.3%. Insulation thermal performance has a greater effect on the stage propellant storage penalty than any of the other study variables. The penalty is especially sensitive to insulation performance at the higher $k\rho$ values. Improving the insulation performance from the highest $k\rho$ value to the intermediate value of 7.5×10^{-5} Btu lb_m/hr-ft⁴-°R (2.08×10^{-3} W kg/m⁴-°K) reduces the penalty as much as 70%. Typical values range from 3.9 to 7.4%, which are comparable to the limiting values for the adiabatic case (3.3% to 3.9%, depending upon the Mars orbit altitude). Some further penalty reduction is obtained as the $k\rho$ value decreases to the lowest value investigated; typical storage penalties at this condition range from 3.9 to 5.5%.

GENERAL DYNAMICS
Fort Worth Division

The mode of propellant storage becomes a more important factor as the propellant heat transfer increases. With low-performance insulation, the propellant storage penalty for the vent mode is as much as 20% below that for the nonvent mode. The partial-recondensation mode offers even greater savings, up to 47% as compared to the nonvent mode. As the insulation performance improves, the mass savings gained through the vent and partial-recondensation modes is much reduced. At the lowest $k\rho$ value, these modes cannot be defined over the entire range of Earth orbit staytime since the vent pressure is not reached at the shorter staytimes. For the 9203-n.mi (17,053 km) altitude condition, the vent pressure is not reached even at the maximum staytime of 180 days.

Orbital tanking and the combination storage modes offer significant mass savings only when combined with the lowest-performance insulation. Tanking allows a substantial extension of the Earth orbit staytime; maximum staytimes of 885 and 1440 days were determined for the vent and partial-recondensation modes, respectively. However, these maxima correspond to boiloff of the complete propellant loading, which is probably not compatible with the pressure-stabilized tank concept. Nevertheless, partial tanking would effect considerable extension of the staytime.

Mars orbit altitude has very little effect on the propellant storage penalty for the unshielded Mars Braking Stage. Although the stage size increases as the altitude increases, the propellant storage penalty is little changed.

The Mars transfer solar shield has a substantial impact upon the Braking Stage propellant storage penalty and reduces the magnitude of the effects of the other study variables. Values of the propellant storage penalty are reduced as much as 57%, relative to the unshielded stage, and range from 3.6 to 14.8% of the zero-mass-fraction IMEO. The effect of the shield on insulation performance requirements is especially significant. Even with the lowest-performance insulation, storage penalties as low as 6% result. With higher-performance insulation, the penalty approaches the limiting value corresponding to the adiabatic tank wall quite closely.

GENERAL DYNAMICS

Fort Worth Division

Use of the solar shield may affect the choice of propellant storage mode. For example, with low-performance insulation the storage penalty for the shielded stage in the nonvent mode is comparable to that of the unshielded stage in the partial-recondensation mode. With improved insulation performance, the storage penalties for all modes are generally equal; the vent pressure is not reached and no boiloff results.

6.1.4 Mars Departure Stage

The length of the Earth orbital storage period has little effect on the propellant storage system of the Mars Departure Stage. Under the most extreme conditions, the percentage increase in storage penalty over the range of staytime is less than 10% of the zero-mass-fraction IMIEO value. Rather, the propellant heating history is dominated by the 510-day period in Mars orbit, for both the unshielded and the shielded stages. The long mission time and resulting high heat transfer make the propellant storage mode and the insulation thermal performance of equal importance with respect to propellant storage penalty. In fact, the nonvent storage mode is not feasible for this stage under any conditions. Even the least extreme case (shielded stage) yields a final tank pressure of 37 psia (25.5 N/cm^2).

In the unshielded case, the propellant storage penalty ranges from 2.3% to 19.3% of the zero-mass-fraction IMIEO. This compares with the penalty corresponding to the adiabatic tank-wall condition, which ranges from 1.1% to 0.8% as the altitude increases. The importance of the insulation performance is shown by the percentage increases in storage penalty over the range of insulation performance, which are of the magnitude of 150%. Again, the penalty is most sensitive to insulation performance in the upper range of $k\rho$ values. However, even with the highest insulation performance, the storage penalty is 45% greater than the penalty for the adiabatic case. This large difference is due to the combination of penetration heat transfer and long mission time, neither of which is affected by the insulation performance.

Propellant storage mode is an important consideration for the Mars Departure Stage under all conditions. As mentioned earlier, the nonvent mode results in a high tank pressure under the most favorable conditions and is not

GENERAL DYNAMICS

Fort Worth Division

considered a feasible storage mode for this stage. The partial-recondensation mode yields savings in the propellant storage penalty over the vent mode in all of the cases studied; the percentage decrease in storage penalty is roughly the same at all conditions for the unshielded stage, ranging from 45 to 49%. At the intermediate $k\rho$ value, a greater reduction in storage penalty can be achieved by changing the storage mode from vent to partial-recondensation than by improving the insulation performance to the lowest $k\rho$ value studied. This is another effect of the penetration heat transfer and the long mission time. The partial-recondensation system is effective with respect to heat transferred through penetrations as well as that transferred through the tank-wall insulation. Insulation performance, on the other hand, has no effect on the penetration heat transfer.

The altitude of the Mars parking orbit has considerable influence on the stage propellant storage penalty. At all $k\rho$ values, the penalty in both the vent and the partial-recondensation storage modes is reduced roughly 40% as the altitude increases from 216 n.mi (400 km) to 9203 n.mi (17,053 km). This is due to the less severe thermal environment at the higher altitudes.

In the same manner, the solar shields deployed during Mars transfer and Mars orbit have a strong impact on the propellant storage penalty of the Mars Departure Stage. Percentage reductions in the penalty are significant at all conditions; for the vent mode, they increase from 23% to 59% as the altitude increases, while showing little variation with insulation performance. For the partial-recondensation mode, the percentage reductions are somewhat lower, increasing from 18% to 46% as the altitude increases. Again, insulation performance has little effect. The effectiveness of the Mars orbit shield is dependent upon the altitude. At low altitudes, the bulk of the percentage reductions mentioned above are attributable to the Mars transfer shield. As the altitude increases, the Mars orbit shield becomes more effective, and at the higher altitudes, more than one-half of the penalty reduction is due to the Mars orbit shield.

Although the percentage reductions in storage penalty attributable to the shield are significant at all conditions, the small size of the Mars Departure Stage affects the

GENERAL DYNAMICS

Fort Worth Division

magnitude of the mass savings. The maximum savings occur in the high-altitude, low-performance-insulation case where the IMIEO is reduced 81,800 lb_m (37,100 kg) in the vent mode and 36,200 lb_m (16,400 kg) in the partial-recondensation mode. At the other extreme, the low-altitude, high-performance-insulation condition, the savings in IMIEO is only 5330 lb_m (2420 kg) and 1300 lb_m (590 kg), for the vent and the partial-recondensation modes, respectively.

6.2 MISSION PARAMETER IMPLICATIONS

The primary effort in this study concerns the stage thermal protection system. However, two of the basic parameters, Earth orbit staytime and Mars orbit altitude, are also mission parameters. In addition, the other variables may have an indirect effect on the mission parameters since they influence the stage and vehicle size. Thus it is important to examine the results of this study with respect to the mission parameters to ascertain the impact upon those parameters.

6.2.1 Earth Orbit

6.2.1.1 Orbit Staytime

From a mission viewpoint, the primary factors which influence orbit staytime are related to launch and orbit operations. Launch operations include such factors as ground assembly and facility turnaround time, which depend on the number of launches required and the available launch facilities. Orbital operations include vehicle assembly, checkout, and tanking. The launch operations, especially the turnaround time, is considered the dominant factor in establishing Earth orbit staytime.

Complex 39 is the launch facility being built for the Saturn V/Apollo lunar landing program. The facility includes a vertical assembly building (VAB) with three outfitted high bay areas, three mobile launchers, two launch pads, two transporters and one mobile service structure. A fourth high bay is available but is not outfitted. This launch facility can be modified for use with the uprated Saturn V launch vehicle assumed for this study. Estimated turnaround time for the present facility is three to four

GENERAL DYNAMICS

Fort Worth Division

months with the present ground equipment (Refs. 6-1 and 6-2). This includes assembly time in the VAB (about 9 weeks), time on the pad before launch (about 2 weeks), and time to refurbish the mobile launcher and the pad (2 to 3 weeks). With three high bay areas, this turnaround time implies a waiting period of three to four months between each group of three launches.

The order of launches assumed for this study begins with the modules of the Earth Departure Stage. The modules of the Mars Braking Stage are then launched, followed by the Mars Departure Stage module. This order minimizes the propellant storage time for the Mars Departure Stage. The vehicle has a total of seven modules. If the present three high bay areas are available, the first Earth Departure Stage module would be in orbit six to eight months longer than the Mars Departure Stage module. Therefore, the higher values of the Earth-orbit-staytime range investigated in this study are consistent with the present launch facility.

If the fourth high bay area is outfitted, the time span between the launch of the first Earth Departure Stage module and that of the Mars Departure Stage module could be reduced to 90 - 120 days. This corresponds to the intermediate values of Earth orbit staytime used in the study. The lower values in the range of Earth orbit staytime probably could be attained by extensive expansion of the launch facilities or by significantly reducing the turnaround time. If the turnaround time could not be reduced, an additional VAB with the associated equipment would have to be added.

In summary, a cursory study of the effects of launch and orbit operations on Earth orbit staytime indicates that the higher values of staytime are consistent with present launch facilities and that the lower values of staytime could be attained only by extensive expansion of the launch facilities or by significantly reducing the turnaround time. It is important to note that the turnaround time estimate is based on existing facilities and that some projected facility capabilities (Ref. 6-3) indicate that this time could be significantly reduced.

6.2.1.2 Orbit Geometry

The mission parameters related to Earth orbit geometry are the altitude and the inclination, both of which were

GENERAL DYNAMICS

Fort Worth Division

fixed in this study. The assembly orbit altitude of 262 n.mi (485 km) is commonly assumed for assembly of nuclear modules for interplanetary missions. The inclination was defined to be approximately equal to the absolute value of the declination of the departure asymptote for the mission (the inclination must be greater than or equal to the declination for coplanar departure).

From a mission viewpoint, the orbit geometry should also be selected on the basis of launch and orbit phasing requirements. The flight profile to the assembly orbit consists of a direct ascent to a low-altitude parking orbit followed by a Hohmann transfer to the assembly orbit. It is desirable to have two coplanar launch opportunities each day and to minimize the time in the low-altitude parking orbit by proper phasing. Also, it is necessary that the assembly orbit altitude have an adequate lifetime for vehicle assembly.

6.2.2 Mars Orbit

6.2.2.1 Orbit Altitude

One objective of this study was to determine the effect of Mars orbit altitude on IMIEO. The possibility of an optimum altitude existed since the altitude affects thermal protection requirements, Mars Excursion Module (MEM) mass requirements, and mission propellant requirements. The effects of Mars orbit altitude on thermal protection requirements have been discussed previously. The propellant heating and, hence, the thermal protection requirements of the Mars Departure Stage decrease as orbit altitude is increased. If all other factors were equal, this variation would cause IMIEO to decrease as the altitude increases.

The mission propellant loadings depend on the energy or ΔV requirements of the Mars Braking Stage and the Mars Departure Stage. The variation of the velocity change with altitude is presented in Figure 6.2-1 for both maneuvers. The ΔV requirement consists of an ideal ΔV based on the hyperbolic excess speed plus allowances for small plane changes, gravity losses, and performance reserves. For a given hyperbolic excess speed, the ideal ΔV requirements vary with altitude and, with direct entry into (or departure from) a circular orbit, reach a minimum at the radius for

GENERAL DYNAMICS

Fort Worth Division

which the escape speed equals the hyperbolic excess speed. The altitude where the sum of the ΔV 's is a minimum is approximately 3000 n.mi (5560 km). If all other factors were equal, IMIEO should be minimized at approximately the same altitude.

The effect of Mars orbit altitude on MEM mass is presented in Figure 3.2-5. The mass of the MEM increases as altitude is increased because of the increased propellant necessary to ascend and descend. If all other factors were equal, this MEM mass variation would cause IMIEO to increase as altitude is increased.

The variation of IMIEO with Mars orbit altitude is presented in the figures of Subsection 4.1. For a vehicle with a propellant storage system mass of zero, the variation is presented in Figure 4.1-13. These data show the effects of the mission ΔV requirements and the MEM mass on IMIEO without thermal effects. Since IMIEO increases as the altitude is increased, these data indicate that the MEM mass variation dominates the mission energy variation. The variation of IMIEO with Mars orbit altitude when the effects of the thermal environment are included is presented in other figures in Section 4. In all of the data presented, the trend is that IMIEO increases with altitude. This indicates that the MEM mass variation dominates the thermal environment effects as well as the mission ΔV requirements. Therefore, from a mission viewpoint, a low-altitude Mars orbit should be selected in order to minimize IMIEO.

6.2.2.2 Orbit Orientation

The equatorial inclinations of the Mars orbit were selected by the requirement that the resulting orbit precession during the staytime yielded the correct orientation for a coplanar departure from orbit. When more than one inclination satisfied this requirement, a high inclination posigrade orbit was selected to obtain more complete planet coverage for reconnaissance and to allow selection of a landing site over a wide range of latitudes.

The effect of orbit orientation on thermal protection requirements is a function of the inclination of the orbit to the terminator. A typical variation of the inclination to the terminator with staytime is presented in Figure 6.2-2. For long staytimes in Mars orbit, the variation is sinusoidal

GENERAL DYNAMICS

Fort Worth Division

and covers a wide range of inclinations. The net result is that the orbit orientation is of minor importance from a thermal protection viewpoint. For long staytimes then, the Mars orbit orientation should be selected from mission considerations rather than thermal considerations.

6.2.3 Interplanetary Legs

Factors classified as interplanetary mission parameters include (1) time during the outbound and inbound legs, (2) distance from the sun, (3) vehicle orientation requirements, and (4) guidance correction requirements. Only vehicle orientation requirements were varied in this study, while the other parameters were fixed by the selected mission. A broadside orientation with respect to the sun was assumed except when the Mars transfer solar shield would be deployed. With a shield, the vehicle is oriented with its longitudinal axis toward the sun except during periods of guidance correction. A broadside orientation is assumed for the total duration of each guidance correction.

For the reference mission (and most conjunction-class missions), the inbound phase of the mission is of minor importance with regard to vehicle mass and thermal protection requirements. The relatively low entry speeds at Earth arrival make it possible to use atmospheric braking and omit an Earth braking stage. When a solar shield is used during the outbound leg, the vehicle orientation and guidance correction requirements are more important considerations than the outbound time and distance from the sun. This is because (1) the longitudinal axis must be oriented toward the sun, and (2) a broadside orientation is assumed during periods of guidance corrections. Obviously, when a solar shield is not used, the outbound time and distance from the sun are important considerations.

6.2.4 Vehicle Mass Requirements

6.2.4.1 IMIEO

A parametric study of an interplanetary mission requires certain assumptions with regard to energy and payload requirements, and these assumptions can have considerable effect on IMIEO. For example, the energy requirements used

GENERAL DYNAMICS

Fort Worth Division

in this study are not the minimum values that could be assumed because allowances for plane changes, gravity losses, and performance reserves are included. If minimum ΔV requirements are assumed, the values of IMIEO are significantly reduced, as shown in Figure 6.2-3. Thus, in a parametric study, primary emphasis should be placed on the variations of IMIEO rather than on the absolute values of IMIEO. However, when a large quantity of parametric data is generated, it is desirable to determine where the data are most consistent with the study assumptions. Also, to make the data more useful, it is desirable to define some maximum value of IMIEO so that the least feasible systems can be noted.

For this study, the propellant requirements and the launch-vehicle payload capability dictated a four-module Earth Departure Stage. If the combined mass of the four modules for a given set of conditions exceeds the payload capability of four launch vehicles, an additional fifth nuclear module would be required. When an additional module is required, the fixed masses for the Earth Departure Stage used in the mass build-up should be increased to account for the additional clustering structure, piping, etc. Since all of the vehicles were sized assuming four modules, this implies that possibly some of the larger values of IMIEO, beyond some limiting value, are optimistic.

Ranges of IMIEO that are consistent with the assumption of a four-module Earth Departure Stage were obtained on the basis of an allowable mass for that stage that varies from 939,000 lb_m (426,000 kg) to 1,250,000 lb_m (568,000 kg). The upper limit represents the mass where the number of modules would have to be increased from four to five and the lower limit represents the mass where the number of modules could be decreased from four to three. Note that these limits are not even multiples of the payload capability of the up-rated Saturn V launch vehicle (330,000 lb_m). Each module has an ascent shell which has generally not been included in the IMIEO values presented in this report. Therefore, the allowable mass limits have been reduced by the mass of the ascent shell (17,000 lb_m or 7710 kg for the Earth Departure Stage modules). The resultant range of IMIEO is shown in Figure 6.2-4 as a function of Mars orbit altitude. The variation of the IMIEO range with altitude is caused mainly by the variation in the Mars Excursion Module mass.

GENERAL DYNAMICS

Fort Worth Division

6.2.4.2 Earth Launch Vehicles

A minimum number of Earth launches is desirable in order to minimize mission cost and operational requirements. The Earth Launch Vehicle (ELV) assumed for this study is an uprated Saturn V with a payload capability of 330,000 lb_m (150,000 kg) to a 262 n.mi (485 km) circular orbit. At least eight launches are required for the Mars vehicle considered in this study. In order to utilize the minimum number of ELV's, some components of the vehicle (mid-course systems, attitude control systems, payload) would have to be launched by the same ELV that launches one of the nuclear modules. Since this may be undesirable from an operational viewpoint, or the available volume may be exceeded, nine ELV's probably will be needed. These are enumerated, according to the major components of the Mars vehicle, below:

Earth Departure Stage - 4 ELV's

Mars Braking Stage - 2 ELV's

Mars Departure Stage - 1 ELV

Mars Excursion Module - 1 ELV

Other components - 1 ELV

Vehicle components such as mid-course correction systems, attitude control systems, the Mission Module, and the Earth Entry Module are included in the "other components" of the above breakdown. If the values of IMIEO exceed the upper limits of the ranges of IMIEO shown in Figure 6.2-4, another launch vehicle would be required for the Earth Departure Stage. In some of the cases examined in this study, particularly with low-performance insulation, the values of IMIEO do exceed these upper limits. Therefore, it can be concluded that the characteristics of the thermal protection system have an effect on launch vehicle requirements.

6.2.5 Other Planetary Missions

General results of this study should apply to other conjunction-class missions, mainly because the mission energy requirements do not have large variations from year to year. There is some variation in staytime in Mars orbit

GENERAL DYNAMICS

Fort Worth Division

which would change the thermal protection penalties for the Mars Departure Stage. However, the relative effects of the study parameters (Earth orbit staytime, Mars orbit altitude, and insulation thermal performance), the propellant storage mode, and the solar shields should not be significantly changed.

The other major class of Mars missions is the opposition class. The staytime at Mars is short (about 30 days) and the mission energy requirements are usually larger than the requirements for conjunction-class missions. In addition, there is a large variation in energy requirements over a synodic period. The results of this study with regard to the Mars Departure Stage are probably not applicable to opposition-class missions because of the large difference in staytime at Mars and in stage propellant loading. However, the effects of the study variables on the Earth Departure Stage and the Mars Braking Stage are applicable.

Other planetary missions where nuclear modules could be used include Mars flyby, Venus flyby, and Venus stopover missions. The relative effects of Earth orbit staytime, insulation thermal performance, and propellant storage mode on the Earth Departure Stage should also be applicable to these missions.

GENERAL DYNAMICS
Fort Worth Division

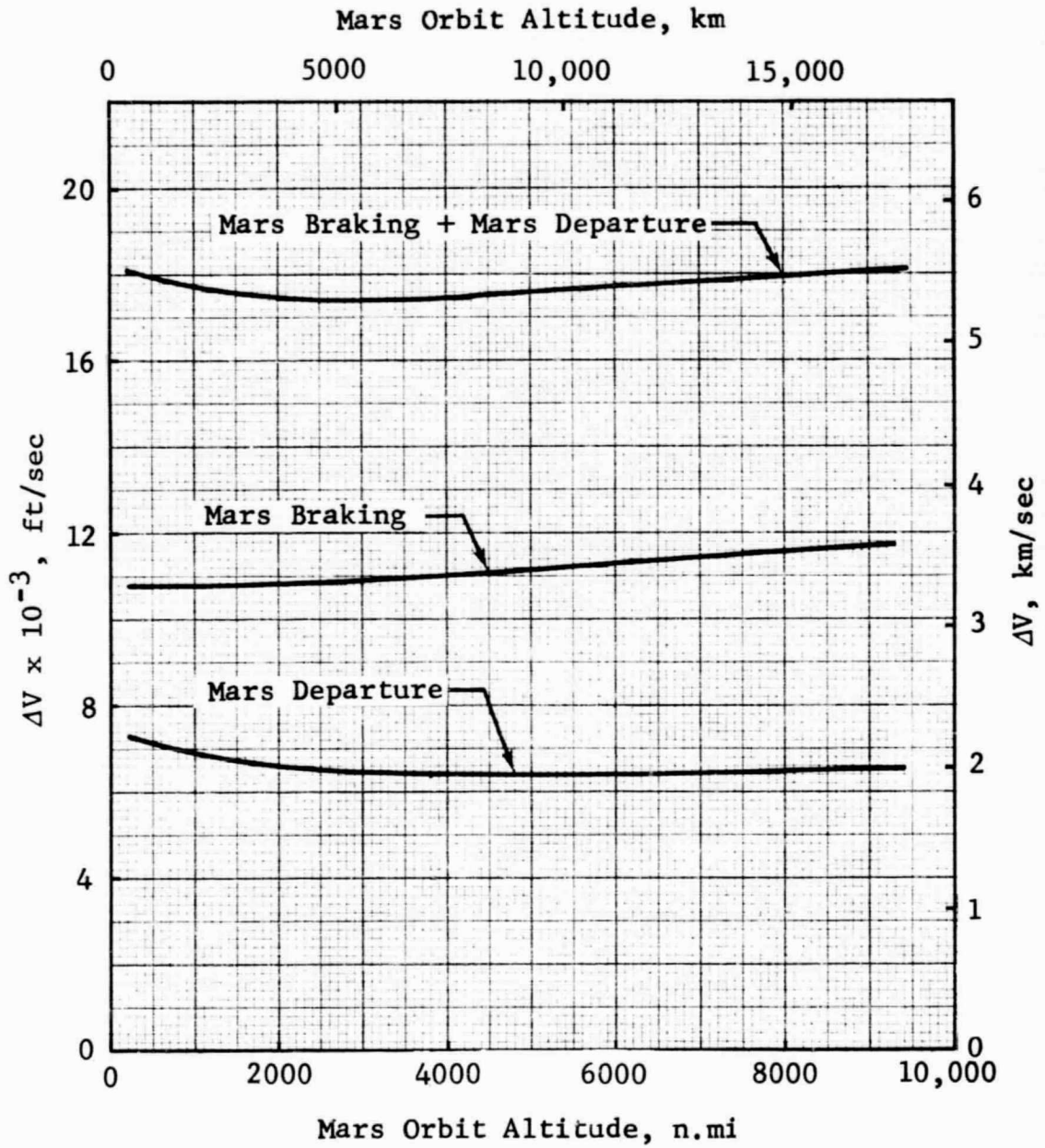


Figure 6.2-1 ΔV Requirements for Mars Braking and Departure vs Altitude

GENERAL DYNAMICS
Fort Worth Division

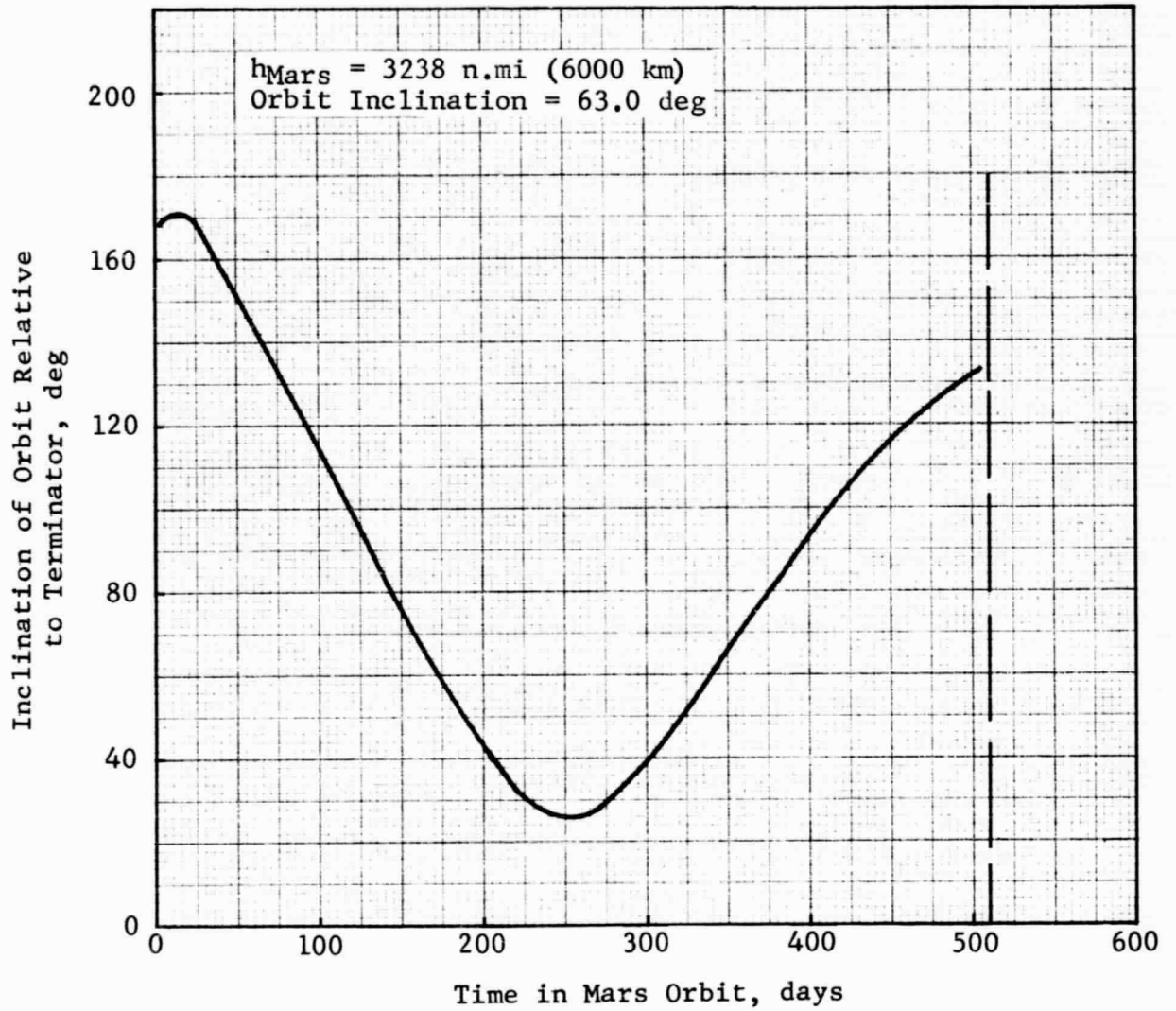


Figure 6.2-2 Mars Orbit Orientation History:
 $h_{\text{Mars}} = 3238 \text{ n.mi}$

GENERAL DYNAMICS
Fort Worth Division

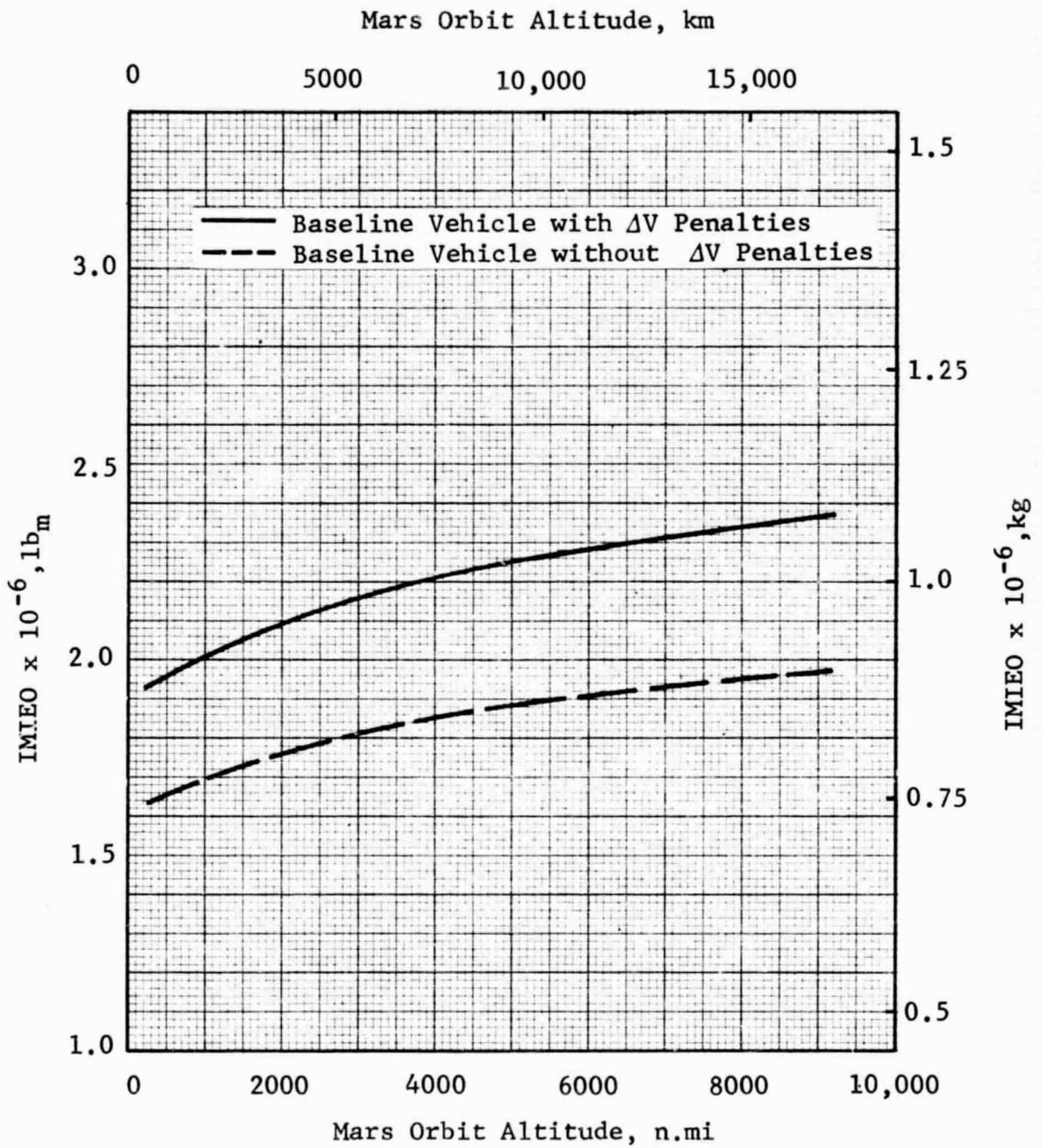


Figure 6.2-3 Effect of Mission Energy Requirements on IMIEO

GENERAL DYNAMICS
Fort Worth Division

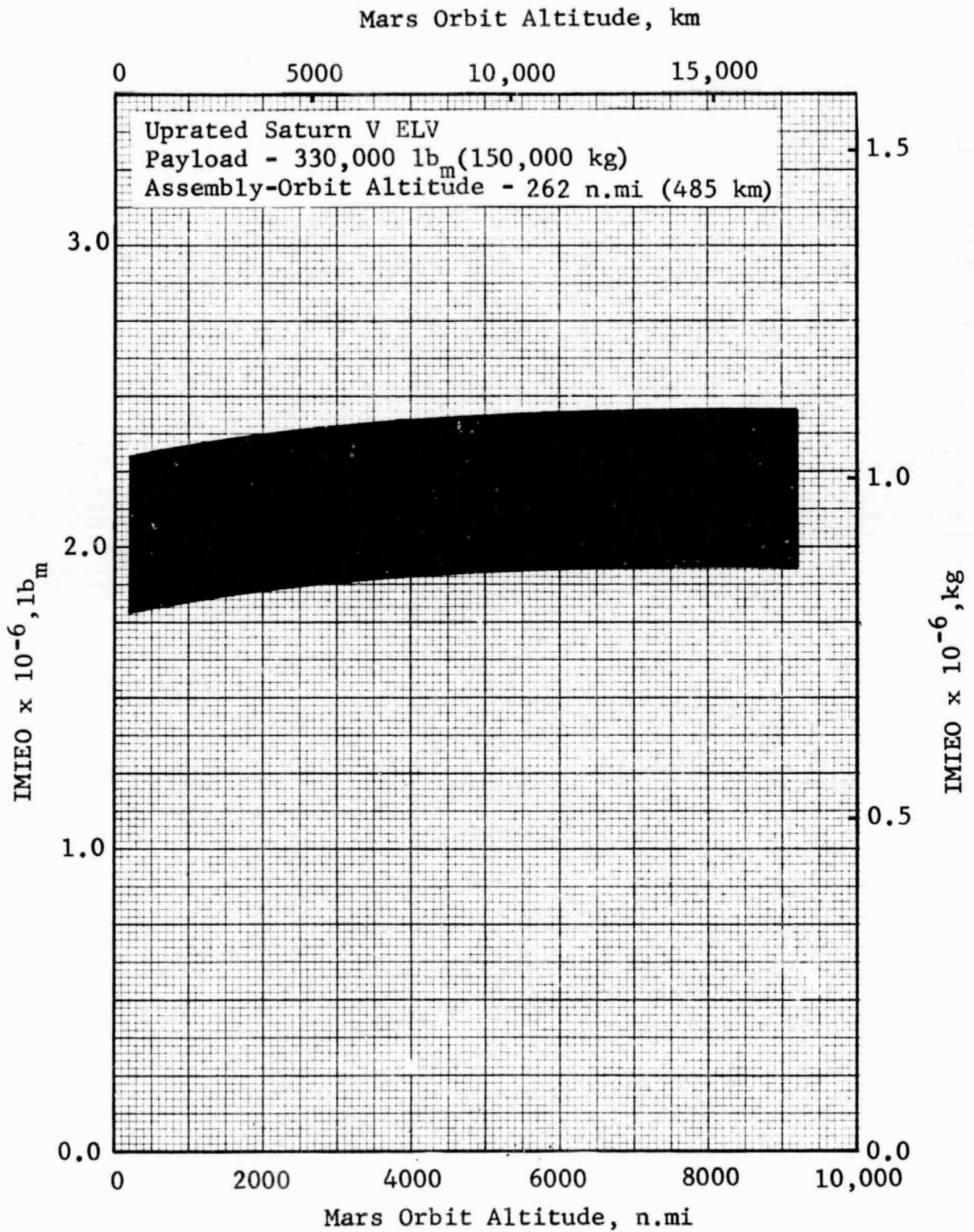


Figure 6.2-4 Approximate Range of IMIEO with a Four-Module Earth Departure Stage

GENERAL DYNAMICS

Fort Worth Division

6.3 STRUCTURAL IMPLICATIONS

Results of the parametric study have been reviewed to verify the structural integrity of the Mars vehicle. In all cases, the tank-wall thicknesses are of such magnitude that the tank diameter-to-wall-thickness ratio falls within the range appropriate to the membrane analogy. This confirms the assumption of a uniform stress distribution under pressure and/or axial loading.

A simplified stress analysis of the critical load conditions (Volume 2, Appendix B) showed that the expected loads can be sustained using the selected design concept of a load-carrying outer shell. The worst case corresponds to the unshielded vehicle with low-performance insulation in the vent mode (maximum staytime, high Mars orbit altitude). Of the three stages, the Earth Departure Stage modules sustain the highest loadings.

The highest tank-wall stress, with a margin-of-safety of approximately 42%, is produced by the Earth launch condition. Dynamic loads (attitude control, wind, sloshing, etc.) which are superimposed on the longitudinal acceleration effects were not taken into account. Fortunately, the maximum dynamic loadings do not occur simultaneously with the maximum accelerations. Thus, the 42% margin is considered to be sufficient to account for the combined loads.

In the interest of minimizing the vehicle mass, the tank wall has also been incorporated into the meteoroid protection system. Thickness requirements for meteoroid protection are, in all cases, well below those established by the minimum tank design pressure. This approach allows most of the mass associated with meteoroid protection to be jettisoned before the propulsive maneuvers, thereby reducing propellant requirements and the vehicle mass.

PRECEDING PAGE BLANK NOT FILMED.

GENERAL DYNAMICS

Fort Worth Division

S E C T I O N 7

R E C O M M E N D A T I O N S

Based on the results of the current study, the following recommendations should be considered in planning future programs related to manned interplanetary missions.

1. Development work on multilayer insulation systems should be aimed at achieving the highest currently quoted performance ($k\rho = 7.5 \times 10^{-5}$ Btu lb_m/hr-ft⁴-°R or 2.08×10^{-3} W kg/m⁴-°K) in the installed configuration.
2. Continued development of vent and partial-recondensation thermal management systems is necessary, since these systems will be required on the upper stages of manned interplanetary vehicles.
3. Vehicle orientation requirements and guidance correction requirements need to be defined to aid in the determination of the practicability of solar shields.
4. Effects of Earth orbit altitude should be investigated. Higher altitudes may reduce thermal protection system mass requirements, but the payload capability of the Earth launch vehicle is reduced and restrictions may be imposed on launch and orbit operations.
5. Detailed analyses of launch and orbit operations and their effects on Earth orbit staytime should be conducted, and the implications of changing the order of launches should be investigated (e.g., launching the Earth Departure Stage modules last rather than first).
6. The use of elliptical Mars orbits, rather than circular, should be studied, since they allow improved reconnaissance (i.e., observation of the planet over a range of altitudes) and reduced ΔV requirements for Mars braking and departure. However, the Mars Excursion Module mass requirements would be increased due to the increased ΔV

GENERAL DYNAMICS

Fort Worth Division

6. (Cont'd)
required to deorbit from and ascend to the higher-energy elliptical orbits.
7. The effects of cryogenic propulsion systems for the MEM should be investigated. Although the mass of the MEM could be reduced significantly, the problems associated with long-duration storage of cryogenic propellants on the surface of Mars may be formidable.
8. The Earth launch phase should be studied to establish the minimum acceptable ullage pressure to combine with the dynamic loads associated with ascent.
9. A study of the effects of meteoroid impingement on the structural integrity of tank walls should be made. This study should include the effects of pock-marking or cratering when the wall material is at cryogenic temperatures. Some attempt should be made at establishing acceptable cratering depths and diameters.

GENERAL DYNAMICS
Fort Worth Division

R E F E R E N C E S

- 3-1 Modular Nuclear Vehicle Study Phase II, Vol. III, Nuclear Propulsion Module-Vehicle Design, Lockheed Missiles and Space Company, LMSC-A830246, 1 March 1967.
- 3-2 McKay, L. M., et al., Study of Conjunction Class Manned Mars Trips, Douglas Missile and Space Division, SM-48662, June 1965.
- 4-1 Leonhard, K. E., et al., Superinsulation Research and Development Program, Convair Division of General Dynamics Corporation, GDC-ERR-AN-1037, December 1966.
- 4-2 Coston, R. M., High Performance Insulation Thermal Design Criteria, Vol. II, Handbook of Thermal Design Data for Multilayer Insulation Systems, Lockheed Missiles and Space Company, LMSC-A847882, 25 June 1967.
- 4-3 Cody, J. C., and Hyde, E. H., "Thermal Problems Associated with the Development of a Flight Configured Cryogenic Insulation System," Proceedings of the Conference on Long-Term Cryo-Propellant Storage in Space, George C. Marshall Space Flight Center, October 12 - 13, 1966 .
- 5-1 "Analytical and Experimental Development Program for Inflatable Solar Shields," NASA Contract NAS8-21132, presently being performed at the Fort Worth Division of General Dynamics Corporation.
- 5-2 Jones, L. R., and Barry, D. G., "Lightweight Inflatable Shadow Shields for Cryogenic Space Vehicles," J. Spacecraft and Rockets, Vol. 3, No. 5, (May 1966), 722 - 727.
- 6-1 Jones, A. L., Study of Manned Planetary Flyby Missions, Space Division of North American Aviation, Inc., SID 67-549-4, August 1967.
- 6-2 Macy, R. L., et al., Operations and Requirements for Manned Planetary Programs, Fort Worth Division of General Dynamics Corporation, MR-0-171, February 1967.

GENERAL DYNAMICS

Fort Worth Division

- 6-3 Harris, Ronald, J., "A Modular Nuclear Vehicle System with Multi-Mission Capability for Mars Stopover Missions," AIAA Paper No. 66-547, June 1967.